OULU 2021
C 790

ACTA UNIVERSITATIS OULUENSIS


*Mohammad Moltafet*

# INFORMATION FRESHNESS IN WIRELESS NETWORKS

*UNIVERSITY OF OULU GRADUATE SCHOOL;*
*UNIVERSITY OF OULU,*
*FACULTY OF INFORMATION TECHNOLOGY AND ELECTRICAL ENGINEERING*

ACTA UNIVERSITATIS OULUENSIS
C Technica 790

*MOHAMMAD MOLTAFET*

# INFORMATION FRESHNESS IN WIRELESS NETWORKS

Academic dissertation to be presented with the assent of the Doctoral Training Committee of Information Technology and Electrical Engineering of the University of Oulu for public defence in the OP auditorium (L10), Linnanmaa, on 29 June 2021, at 12 noon

UNIVERSITY OF OULU, OULU 2021

Acta Univ. Oul. C 790, 2021

Supervised by
Docent Marian Codreanu
Doctor Markus Leinonen

Reviewed by
Professor Sennur Ulukus
Assistant Professor Shirin Saeedi Bidokhti

Opponent
Associate Professor Sanjit Krishnan Kaul

ISBN 978-952-62-2990-4 (Paperback)
ISBN 978-952-62-2991-1 (PDF)

ISSN 0355-3213 (Printed)
ISSN 1796-2226 (Online)

Cover Design
Raimo Ahonen

PUNAMUSTA
TAMPERE 2021

**Moltafet, Mohammad, Information freshness in wireless networks.**
University of Oulu Graduate School; University of Oulu, Faculty of Information Technology and Electrical Engineering
*Acta Univ. Oul. C 790, 2021*
University of Oulu, P.O. Box 8000, FI-90014 University of Oulu, Finland

***Abstract***

With the advent of new services in 5G and beyond such as real-time Internet of things (IoT) applications, autonomous vehicles, and cyber-physical applications, the delivery of fresh status updates is gaining increasing interest. In these networks, various sensors transmit status updates about different monitored processes to a destination. Recently, the age of information (AoI) was proposed as a destination-centric metric to measure the information freshness. The objective of this thesis is to analyze the AoI and develop methods to improve the information freshness to enable emerging time-critical applications in future networks.

In the second chapter, the average AoI for multi-source queueing models under a first-come first-served (FCFS) serving policy is studied. For a multi-source M/M/1 queueing model, an exact expression for the average AoI is derived. Then, for an M/G/1 queueing model having a general service time distribution, three approximate average AoI expressions are calculated.

In the third chapter, a multi-source queueing model is considered and three source-aware packet management policies are introduced. The average AoI and the moment generating function (MGF) of the AoI are derived by using the stochastic hybrid systems (SHS) technique. The results show that the AoI can be significantly decreased through an appropriate packet management policy.

Fourth chapter considers a wireless sensor network (WSN), where the sensors can control the sampling process and they communicate timely information about random processes. The problem of jointly optimizing the sensors' sampling action, transmit power allocation, and sub-channel assignment to minimize the average total transmit power subject to a maximum average AoI constraint for each sensor is studied. By using the Lyapunov optimization method, a dynamic control algorithm is provided to solve the problem.

In the fifth chapter, a WSN application for the average and peak AoI expressions, derived in the second chapter, is presented. Sensors communicate status updates by contending for channel access based on a carrier sense multiple access with collision avoidance (CSMA/CA) method. Upper bounds for the average and peak AoI for each sensor are derived in a worst case scenario where all the other sensors continually send packets.

*Keywords:* age of information (AoI), information freshness, Lyapunov optimization, moment generating function (MGF), multi-access channel, multi-source queueing model, packet management, stochastic hybrid systems (SHS)

**Moltafet, Mohammad, Tiedon ajantasaisuus langattomissa verkoissa.**
Oulun yliopiston tutkijakoulu; Oulun yliopisto, Tieto- ja sähkötekniikan tiedekunta
*Acta Univ. Oul. C 790, 2021*
Oulun yliopisto, PL 8000, 90014 Oulun yliopisto

## *Tiivistelmä*

Uudet 5G-järjestelmien palvelut, kuten reaaliaikaiset esineiden internet -sovellukset, itsenäiset ajoneuvot sekä kyberfyysiset sovellukset, kasvattavat ajantasaisten tilapäivitysten toimittamisen kiinnostusta. Näissä verkoissa anturit lähettävät kohteelle tilapäivityksiä eri valvotuista prosesseista. Tiedon ikä (age of information, AoI) ehdotettiin hiljattain kohdekeskeiseksi tiedon ajantasaisuuden mittariksi. Väitöskirjan tarkoituksena on analysoida AoI:ta ja kehittää menetelmiä tiedon ajantasaisuuden parantamiseksi uusien aikakriittisten sovellusten mahdollistamiseksi tulevissa verkoissa.

Toisessa luvussa tutkitaan keskimääräistä AoI:ta monilähdejonomalleissa, joissa paketit palvellaan niiden saapumisjärjestyksessä. Työssä johdetaan keskimääräisen AoI:n tarkka lauseke monilähteiselle M/M/1-jonomallille. Lisäksi johdetaan yleisen palveluaikajakauman tapaukselle, eli M/G/1-jonomallille, kolme likimääräistä keskimääräisen AoI:n lauseketta.

Kolmannessa luvussa tarkastellaan monilähteistä jonotusmallia ja esitellään kolme pakettien lähteen huomioivaa palvelukurimenetelmää. Luvussa johdetaan keskimääräisen AoI:n ja momenttifunktion lausekkeet käyttäen SHS-menetelmää. Tulokset osoittavat, että asianmukainen palvelukuri pienentää AoI:ta merkittävästi.

Neljäs luku tutkii langatonta anturiverkkoa, jossa anturit voivat ohjata näytteenottoprosessiaan, välittäen kohteelle ajantasaista tietoa satunnaisprosesseista. Verkossa optimoidaan kunkin anturin näytteenotto, lähetysteho ja alikanavan valinta keskimääräisen kokonaislähetystehon minimoimiseksi, kun jokaiselle anturille on asetettu keskimääräisen AoI:n rajoite. Ratkaisuksi kehitetään dynaaminen ohjausalgoritmi Lyapunov-optimointia käyttäen.

Viidennessä luvussa esitetään kilpavarausmenetelmään pohjautuva anturiverkkosovellus toisessa luvussa johdetuille AoI:n lausekkeille. Järjestelmässä johdetaan anturille keskimääräisen sekä huippuarvoisen AoI:n ylärajat tilanteessa, jossa toiset kilpailevat anturit lähettävät alituisesti paketteja.

*Asiasanat:* Lyapunov-optimointi, momenttifunktio, monikäyttökanava, monilähdejonomalli, palvelukuri, stochastic hybrid systems (SHS) -menetelmä, tiedon ajantasaisuus, tiedon ikä (AoI)

*To my wife*

# Preface

The research work for this thesis was conducted at the Centre for Wireless Communications (CWC), at the University of Oulu, Finland between October 2018 and October 2020.

I would like to express my sincerest gratitude to my supervisor, Associate Professor Marian Codreanu, who gave me the opportunity to pursue doctoral studies at the Centre for Wireless Communications (CWC) at the University of Oulu in Finland. I have always been inspired by his rigorous approach towards research and the depth of his technical guidance. I will always remember his research standards and attitude towards science. I am also sincerely grateful to my co-supervisor, Dr. Markus Leinonen for his support from the very first days. I very much appreciate his insightful guidance, the countless discussions, and encouragement throughout my postgraduate research and studies. A special thank you goes to Associate Professor Nikolaos Pappas for the fruitful discussions, especially those related to the stochastic optimization. The special thanks extends to Professor Abolhassan Razminia and Dr. Mehrdad Fouladi for their advice and encouraging me towards ambitious goals in research. I wish to thank the reviewers of the thesis, Professor Sennur Ulukus from University of Maryland, College Park, United States, and Assistant Professor Shirin Saeedi Bidokhti from University of Pennsylvania, United States. Their comments significantly improved the quality of the thesis. I would also like to thank Professor Nandana Rajatheva and Dr. Satya Joshi for acting as my follow-up group members.

This research has been financially supported by Infotech Oulu, the Academy of Finland (grant 323698), and the Academy of Finland 6Genesis Flagship (grant 318927). I feel honored to have received several personal research grants from the following foundations: Finnish Foundation for Technology Promotion, HPY Research Foundation, Nokia Foundation Scholarship, Riitta ja Jorma J. Takanen Foundation, and Tauno Tönning Foundation.

I wish to thank all my past and present co-workers at CWC for providing a pleasant working environment. I would like to thank the research unit leader of CWC – Radio Technologies, Professor Markku Juntti, for giving me the opportunity to work in such a joyful research unit. I would also like to thank our administrative staff for helping me and making my life lot easier at CWC.

I would like to thank my dear friends Mohammad Dashtipour, Parsa Baseri, Hamid Niroomand, Hamed Fotoohi, Omid Hosseini, Milad Gohar, Amin Rafiee, and Mohammad Kazemian who have always been supportive throughout these years. I am also

grateful to my friends at the University of Oulu Mojtaba Jahandideh, Aram Baharmast, Mohammad Majidzadeh, Mohammad Hatami, Mohammad Javad Salehi, Shahab Khakpour, Saeid Sadeghi, Abolfazl Zakeri, Samad Ali, Ehsan Moeen Taghavi, Nariman Mahmoodi, Hossein Asgharimoghaddam, and Mostafa Jafari.

I would like to express my deepest appreciation to my parents for their invaluable support, love, and continuous encouragement throughout my life and education. I wish to thank my sisters Zahra and Hadis and my brother Milad for the motivation and love they always provide me. Also, I wish to thank my parents-in-law for their understanding and the motivation they gave me.

Last but not least, I am sincerely grateful to my lovely wife Saba for her unconditional love and support during these years. Without her understanding, continuous encouragement, and positive attitude towards life nothing would have been possible.

Oulu, December 4th, 2020 Mohammad Moltafet

# List of abbreviations

| | |
|---|---|
| 5G | *Fifth Generation* |
| AoI | *Age of Information* |
| ACK | *Acknowledgment* |
| CDF | *Cumulative Distribution Function* |
| CSMA/CA | *Carrier Sense Multiple Access with Collision Avoidance* |
| DIFS | *Distributed Interframe Space* |
| FCFS | *First-Come First-Served* |
| HARQ | *Hybrid Automatic Repeat Request* |
| IoT | *Internet of Things* |
| LCFS | *Last-Come First-Served* |
| LCFS-S | *LCFS with Preemption Under Service* |
| LCFS-W | *LCFS with Preemption Only in Waiting* |
| MGF | *Moment Generating Function* |
| PDF | *Probability Density Function* |
| SHS | *Stochastic Hybrid Systems* |
| SNR | *Signal-to-Noise Ratio* |
| WSN | *Wireless Sensor Network* |

**Mathematical symbols and operators:**

| | |
|---|---|
| $\max\{\cdot\}$ | *the maximum element inside* $\{\cdot\}$ |
| $\arg\max\{\cdot\}$ | *the argument that maximizes the term inside* $\{\cdot\}$ |
| $\min\{\cdot\}$ | *the minimum element inside* $\{\cdot\}$ |
| $\mathbb{E}\{\cdot\}$ | *the expectation operator* |
| $\mathrm{Var}\{\cdot\}$ | *the variance operator* |
| $\lvert y\rvert$ | *the absolute value of* $y$ |
| $\lvert\mathscr{A}\rvert$ | *the cardinality of set* $\mathscr{A}$ |
| $\Gamma(\cdot)$ | *the gamma function* |
| $\exp(\cdot)$ | *the natural exponential function* $\mathrm{e}^x$ |
| $I_m(\cdot)$ | *the modified Bessel function of the first kind of order* $m$ |
| $Q_m(\cdot,\cdot)$ | *the generalized Q-function* |
| $Y_1 \leftrightarrow Y_2 \leftrightarrow Y_3$ | *a Markov chain formed by random variables* $Y_1$, $Y_2$, *and* $Y_3$ |
| $Y_1 =^{\mathrm{st}} Y_2$ | *random variables* $Y_1$ *and* $Y_2$ *are stochastically identical, i.e., they have a same PDF* |

| | |
|---|---|
| $\log_a(\cdot)$ | *logarithm to base a* |
| $\succ$ | *component-wise inequality* |
| $\text{diag}\{\cdot\}$ | *a diagonal matrix with the argument values on its diagonal* |
| $\subseteq$ | *a subset* |
| $\|\cdot\|_0$ | *the operator that counts the number of non-zero entries of a vector* |
| $\triangleq$ | *defined as* |
| $\approx$ | *approximately equal* |
| $\frac{\mathrm{d}^m(f(a))}{\mathrm{d}a^m}$ | *the m–th derivative of $f(a)$* |
| $\frac{\partial f(\cdot)}{\partial a}$ | *the partial derivative of $f(\cdot)$ with respect to a* |
| $\mathbf{1}$ | *a row vector with all entries 1* |
| $\mathbf{0}$ | *a row vector with all entries 0* |
| $\emptyset$ | *an empty set* |
| $\Gamma(\kappa_1, \kappa_2)$ | *the gamma distribution with parameters $\kappa_1$ and $\kappa_2$* |

**Roman alphabet notations:**

| | |
|---|---|
| $\hat{A}$ | *a non-negative real value* |
| $\tilde{A}$ | *a non-negative real value* |
| $\bar{A}$ | *a non-negative real value* |
| $\underline{A}$ | *an event* |
| $A$ | *the average peak AoI* |
| $A_c$ | *the average peak AoI of source c in a multi-source queueing model* |
| $\mathbf{A}_l$ | *a binary transition reset map matrix associated with transition l* |
| $\hat{\mathbf{A}}_l$ | *a binary transition reset map matrix associated with transition l* |
| $\tilde{b}_k(t)$ | *the sampling action of sensor k at time slot t determined by the suboptimal solution* |
| $B$ | *a real value* |
| $b_k(t)$ | *the sampling action of sensor k at time slot t as $b_k(t) \in \{0,1\}$* |
| $\mathbf{b}(t)$ | *a vector containing all the sampling action variables* |
| $\dot{b}_k(t)$ | *a sub-optimal sampling action of sensor k at time slot t* |
| $\mathbb{B}$ | *the set of binary numbers* |
| $\bar{C}$ | *the contention window size* |
| $C$ | *number of sources in a multi-source queueing model* |
| $c$ | *source index in a multi-source queueing model* |
| $c_{k,n}(t)$ | *a Rayleigh distributed random coefficient associated with sensor k over sub-channel n in slot t* |
| $d_k$ | *the distance from sensor k to the sink* |
| $d_0$ | *the far field reference distance* |

| | |
|---|---|
| $D$ | *an integer number representing the number of exponentially distributed random variables in a hyper-exponential distribution* |
| $\bar{\mathbf{D}}$ | *a matrix with real elements* |
| $E^{\mathrm{B}}_{1,i}$ | *the event where the interarrival time of packet* $1,i$ *is brief, i.e., the interarrival time of packet* $1,i$ *is shorter than the system time of packet* $1,i-1$ *in an FCFS multi-source queueing model* |
| $E^{\mathrm{L}}_{1,i}$ | *the event where the interarrival time of packet* $1,i$ *is long, i.e., the interarrival time of packet* $1,i$ *is longer than the system time of packet* $1,i-1$ *in an FCFS multi-source queueing model* |
| $f_Y(y)$ | *the PDF of random variable* $Y$ |
| $f_{Y_1\|Y_2}(y_1)$ | *the conditional PDF of random variable* $Y_1$ *given* $Y_2$ |
| $f_{Y_1,Y_2\|Y_3}(y_1,y_2)$ | *the conditional joint PDF of random variables* $Y_1$ *and* $Y_2$ *given* $Y_3$ |
| $F_Y(y)$ | *the cumulative distribution function of random variable* $Y$ |
| $\hat{G}(\cdot)$ | *a positive real value* |
| $G^{\mathrm{opt}}$ | *the optimal value of the average total transmit power* |
| $h_{k,n}(t)$ | *the channel coefficient from sensor k to the sink over sub-channel n in slot t* |
| $J(\cdot,\cdot)$ | *the Jain's index* |
| $J^{\mathrm{L}}_{2,i}$ | *a random variable representing the number of source 2 packets in the system at the departure instant of packet* $1,i-1$ *for event* $E^{\mathrm{L}}_{1,i}$ *in an FCFS multi-source queueing model* |
| $K$ | *number of sensors in a WSN* |
| $L_Y(a)$ | *the Laplace transform of the PDF of the random variable* $Y$ *at* $a$ |
| $L'_Y(a)$ | *the first derivative of* $L_Y(a)$ *at* $a$ |
| $L''_Y(a)$ | *the second derivative of* $L_Y(a)$ *at* $a$ |
| $l$ | *a transition in the SHS technique* |
| $L(\mathbf{Q}(t))$ | *the quadratic Lyapunov function* |
| $M^{\mathrm{B}}_{2,i}$ | *a random variable representing the number of source 2 packets that must be served before packet* $1,i$ *under the event* $E^{\mathrm{B}}_{1,i}$ *in an FCFS multi-source queueing model* |
| $\hat{M}^{\mathrm{L}}_{2,i}$ | *a random variable representing the number of source 2 packets that must be served before packet* $1,i$ *under the event* $E^{\mathrm{L}}_{1,i}$ *in an FCFS multi-source queueing model* |
| $M_{\Delta_c}(s)$ | *the MGF of the AoI of source c* |
| $M$ | *a random variable representing the number of attempts in a CSMA/CA-based system* |

| | |
|---|---|
| $N$ | *number of orthogonal sub-channels in a WSN* |
| $N_0$ | *the noise power spectral density* |
| $\bar{N}(t)$ | *the index of the most recently received packet at time t* |
| $\bar{N}_c(t)$ | *the index of the most recently received packet of source c at time t* |
| $O$ | *a negative real value* |
| $\Pr(y)$ | *the probability associated with a random variable Y as* $\Pr(y) \triangleq \Pr(Y = y)$ |
| $\Pr(y_1 \mid y_2)$ | *the conditional probability associated with a random variable* $Y_1$ *given* $Y_2$ *as* $\Pr(Y_1 = y_1 \mid Y_2 = y_2)$ |
| $\bar{P}_{m\mid j}(\tau)$ | *the probability that a single-source M/M/1 queueing system with arrival rate* $\lambda_2$ *and which initially holds j packets (either in the queue or under service) ends up holding m packets after* $\tau = x - t$ *seconds* |
| $p_k$ | *the weight factor of k–th exponentially distributed random variable in the hyper-exponential distribution* |
| $p^*_{k,n}(t)$ | *the allocated power to sensor k over sub-channel n in slot t determined by a channel-only policy* |
| $\bar{p}_{k,n}(t)$ | *the allocated power to sensor k over sub-channel n in slot t as determined by the proposed dynamic control algorithm* |
| $\hat{p}_{k,n}(t)$ | *the allocated power to sensor k over sub-channel n in slot t determined by a channel-only policy* |
| $p_{k,n}(t)$ | *the transmit power of sensor k over sub-channel n in slot t* |
| $\tilde{p}_{k,n}(t)$ | *the allocated power to sensor k over sub-channel n in slot t determined by the suboptimal solution* |
| $\dot{p}_{k,n}(t)$ | *a sub-optimal allocated power to sensor k over sub-channel n in slot t* |
| $P^{\mathrm{tr}}_{j,i}$ | *the probability of having at least one transmission by the other sensors between two consecutive back-off counter states* $i$ *and* $i-1$ *at j–th attempt* |
| $P^{\mathrm{tr}}$ | *the probability of having at least one transmission by the other sensors between two consecutive back-off counters* |
| $P_{\mathrm{S}}$ | *the probability of having a successful transmission in each attempt* |
| $\hat{Q}_i$ | *a positive real value representing a specific area under the sawtooth AoI process* |
| $\underline{Q}$ | *a positive real value representing a specific area under the sawtooth AoI process* |
| $Q_{c,i}$ | *a positive real value representing a specific area under the sawtooth AoI process in a multi-source queueing model* |
| $Q_c$ | *a positive real value representing a specific area under the sawtooth AoI process in a multi-source queueing model* |

| | |
|---|---|
| $Q_k(t)$ | *the virtual queue associated with an AoI constraint of sensor k* |
| $\mathbf{Q}(t)$ | *a vector containing all the virtual queues associated with an AoI constraint in Chapter 4* |
| $\bar{\mathbf{Q}}$ | *a matrix with real elements* |
| $\bar{Q}_k(t)$ | *the virtual queue of sensor k in slot t as determined by the proposed dynamic control algorithm* |
| $\bar{\mathbf{Q}}(t)$ | *a vector containing all virtual queues* $\bar{Q}_k(t), \forall k$ |
| $q(t)$ | *the continuous-time finite-state Markov chain that describes the occupancy of the system in the SHS technique* |
| $r_{k,n}(t)$ | *the achievable rate for sensor k over sub-channel n in slot t* |
| $R_k(t)$ | *the achievable rate for sensor k in slot t* |
| $\mathbb{R}$ | *the set of real numbers* |
| $R^{\mathrm{B}}_{1,i}$ | *a random variable representing the residual system time to complete serving packet* $1,i-1$ *under the event* $E^{\mathrm{B}}_{1,i}$ *in an FCFS multi-source queueing model* |
| $S_{c,i}$ | *a random variable representing the service time of packet* $c,i$*, i.e., i–th packet of source c* |
| $S$ | *a random variable representing the stationary service time of a packet* |
| $S^{\mathrm{B}}_{1,i}$ | *a random variable representing the sum of service times of source 2 packets that arrived during* $X_{1,i}$ *under the event* $E^{\mathrm{B}}_{1,i}$ *in an FCFS multi-source queueing model* |
| $S^{\mathrm{L}}_{1,i}$ | *a random variable representing the sum of service times of source 2 packets that must be served before packet* $1,i$ *under the event* $E^{\mathrm{L}}_{1,i}$ *in an FCFS multi-source queueing model* |
| $S_m$ | *a random variable representing the service time conditioned on the event that the number of attempts is m in a CSMA/CA-based system* |
| $s$ | *a variable of the MGF function* |
| $\bar{s}$ | *a variable of the MGF function* |
| $S_k(\cdot,\cdot)$ | *a real tuple representing the coordinates of sensor k placed in a two-dimensional plane* |
| $t_i$ | *the time instant at which the i–th packet was generated* |
| $t'_i$ | *the time instant at which the i–th packet arrives at the destination* |
| $t_{c,i}$ | *the time instant at which the i–th packet of source c was generated* |
| $t'_{c,i}$ | *the time instant at which the i–th packet of source c arrives at the destination* |
| $T_{c,i}$ | *a random variable representing the system time of packet* $c,i$*, i.e., the time interval the packet spends in the system* |

| | |
|---|---|
| $T$ | *a random variable representing the stationary system time of a packet in Chapter 2 / the observation interval in Chapter 4* |
| $\bar{T}_{j,i}$ | *a random variable representing the time interval between two consecutive back-off counter states $i$ and $i-1$ at the $j$–th attempt* |
| $\bar{T}$ | *a random variable representing the time interval between two consecutive back-off counter states* |
| $T_{\mathrm{F}}$ | *a parameter of the CSMA/CA technique* |
| $T_{\mathrm{DIFS}}$ | *a parameter of the CSMA/CA technique* |
| $T_{\mathrm{P}}$ | *the required time to transmit a status update packet in a CSMA/CA-based system* |
| $\bar{U}$ | *an integer number* |
| $U(t)$ | *the time stamp of the most recently received packet* |
| $U_c(t)$ | *the time stamp of the most recently received packet of source $c$* |
| $\underline{\mathrm{U}}$ | *an integer random variable* |
| $V$ | *a parameter used to adjust the emphasis on the objective function in the drift-plus-penalty minimization method* |
| $\mathbf{v}_q(t)$ | *the correlation vector between the discrete state $q(t)$ and the continuous state $\mathbf{x}(t)$* |
| $\bar{\mathbf{v}}_q$ | *the value of correlation vector $\mathbf{v}_q(t)$ when $t \to \infty$* |
| $\mathbf{v}_q^s(t)$ | *the correlation vector between the discrete state $q(t)$ and the exponential function $e^{s\mathbf{x}(t)}$, $s \in \mathscr{R}$* |
| $\bar{\mathbf{v}}_q^s$ | *the value of correlation vector $\mathbf{v}_q^s(t)$ when $t \to \infty$* |
| $w$ | *a realization of the generated number in the contention interval in a CSMA/CA-based system* |
| $\bar{W}$ | *a random variable representing the generated number in the contention interval in a CSMA/CA-based system* |
| $\underline{W}$ | *bandwidth of a sub-channel in a WSN* |
| $W_{c,i}$ | *a random variable representing the waiting time of packet $c,i$* |
| $W$ | *a random variable representing the stationary waiting time of a packet* |
| $X_i$ | *a random variable representing the $i$–th interarrival time, i.e., the time elapsed between the generation of $i-1$–th packet and $i$–th packet* |
| $X_{c,i}$ | *a random variable representing the $i$–th interarrival time of source $c$, i.e., the time elapsed between the generation of $i-1$–th packet and $i$–th packet from source $c$* |
| $\mathbf{x}(t)$ | *a continuous process that describes the evolution of age-related processes at the sink in the SHS technique* |
| $\mathbf{x}'$ | *the updated value of $\mathbf{x}$ under a transition* |

| | |
|---|---|
| $\dot{\mathbf{x}}(t)$ | *the partial derivative of* $\mathbf{x}(t)$ *with respect to t, i.e.,* $\dot{\mathbf{x}}(t) = \dfrac{\partial \mathbf{x}(t)}{\partial t}$ |
| $x_i(t)$ | *the i–th element of* $\mathbf{x}(t)$ |

**Greek alphabet notations:**

| | |
|---|---|
| $\lambda_c$ | *the packet generation rate of source c* |
| $\lambda$ | *the overall packet generation rate in a queueing system* |
| $\rho_c$ | *the load of source c* |
| $\rho$ | *the overall load in a queueing system* |
| $\mu$ | *the service rate for each packet in the system* |
| $\Psi(\mu, \rho_1, \lambda_2)$ | *a function of* $\mu$, $\rho_1$, *and* $\lambda_2$ |
| $\kappa_1,\ \kappa_2$ | *parameters of the gamma distribution* |
| $\nu_1,\ \nu_2$ | *parameters of the log-normal distribution* |
| $\omega_1,\ \omega_2$ | *parameters of the Pareto distribution* |
| $\gamma_k$ | *a parameter of the hyper-exponential distribution* |
| $\pi_q(t)$ | *the probability of being in state q of a Markov chain in the SHS technique* |
| $\boldsymbol{\pi}(t)$ | *the state probability vector in the SHS technique* |
| $\bar{\boldsymbol{\pi}}$ | *the stationary state probability vector in the SHS technique* |
| $\lambda^{(l)}$ | *the rate of transition l in the SHS technique* |
| $\eta_i$ | *a function of* $\rho_2$ |
| $\tilde{\eta}_i$ | *a function of* $\rho_2$ |
| $\hat{\eta}_i$ | *a function of* $\rho_2$ |
| $\dot{\eta}_i$ | *a function of* $\rho_2$ |
| $\dot{\xi}_i$ | *a function of* $\rho_2$ |
| $\hat{\xi}_i$ | *a function of* $\rho_2$ |
| $\gamma_{i,j}$ | *a function of* $\rho_2$ |
| $\tilde{\xi}_i$ | *a function of* $\rho_2$ |
| $\bar{v}_{ij}$ | *a function of* $\rho_2$ |
| $\dot{\gamma}_i$ | *a function of* $\rho_2$ *and* $\bar{s}$ |
| $\bar{\gamma}_i$ | *a function of* $\rho_2$ *and* $\bar{s}$ |
| $\alpha_{i,j}$ | *a function of* $\rho_2$ *and* $\bar{s}$ |
| $\bar{v}^s_{ij}$ | *a function of* $\rho_2$ *and* $\bar{s}$ |
| $\sigma$ | *the standard deviation of the AoI* |
| $\rho_{k,n}(t)$ | *the sub-channel assignment at time slot t as* $\rho_{k,n}(t) \in \{0,1\}$ |
| $\gamma_{k,n}(t)$ | *the signal-to-noise ratio with respect to sensor k over sub-channel n in slot t* |
| $\underline{\eta}$ | *the size of each status update packet (in bits)* |
| $\delta_k(t)$ | *the AoI of sensor k at the beginning of slot t in a WSN* |

| | |
|---|---|
| $\hat{\delta}_k(t)$ | *the value of the AoI of sensor k in slot t determined by a channel-only policy* |
| $\Delta(t)$ | *the AoI at the destination at time instant t* |
| $\Delta_\tau$ | *the time average AoI at the destination over the time interval* $(0,\tau)$ |
| $\Delta$ | *the average AoI* |
| $\Delta_c(t)$ | *the AoI of source c at the destination at time instant t* |
| $\Delta_{\tau,c}$ | *the time average AoI of the source c at the destination over the time interval* $(0,\tau)$ |
| $\Delta_c$ | *the average AoI of source c in a multi-source queueing model* |
| $\Delta_1^{\text{app}_i}$ | *the i–th approximate expression for the average AoI of source 1 in an FCFS multi-source queueing model* |
| $\Delta_c^{(m)}$ | *the m–th moment of the AoI of source c* |
| $\Delta_k^{\max}$ | *the maximum acceptable average AoI of sensor k* |
| $\varepsilon$ | *a positive real value* |
| $\nu$ | *a positive real value* |
| $\alpha(\cdot)$ | *the conditional Lyapunov drift* |
| $\delta_k^*(t)$ | *the value of the AoI of sensor k in slot t determined by a channel-only policy* |
| $\delta^{\max}$ | *the maximum value of the AoI of each sensor in each slot* |
| $\bar{\alpha}(\cdot)$ | *the conditional Lyapunov drift determined by the proposed dynamic control algorithm* |
| $\tilde{\rho}_{k,n}(t)$ | *sub-channel assignment at time slot t determined by the sub-optimal solution* |
| $\dot{\rho}_{k,n}(t)$ | *a sub-optimal sub-channel assignment at time slot t* |
| $\Delta^{\max}$ | *the maximum acceptable average AoI of each sensor in a WSN* |
| $\underline{\xi}$ | *the path loss exponent* |
| $\xi_m$ | *a random variable representing the elapsed time of a successful transmission of a sensor at the m–th attempt* |
| $\zeta_j$ | *a random variable representing the elapsed time of an unsuccessful transmission of a sensor at the j–th attempt* |
| $\xi_{j,w}$ | *a random variable representing the elapsed time of a successful transmission of a sensor at the j–th attempt conditioned on the event that the generated number in the back-off rule is* $\bar{W}=w$ *in a CSMA/CA-based system* |
| $\zeta_{j,w}$ | *a random variable representing the elapsed time of an unsuccessful transmission of a sensor at the j–th attempt conditioned on the event that* |

| | |
|---|---|
| | *the generated number in the back-off rule is $\bar{W} = w$ in a CSMA/CA-based system* |
| $\bar{\xi}_1$ | *the expectation of the elapsed time of a successful transmission of a sensor at an attempt in a CSMA/CA-based system* |
| $\bar{\xi}_2$ | *the second moment of the elapsed time of a successful transmission of a sensor at an attempt in a CSMA/CA-based system* |
| $\bar{\xi}_3$ | *the Laplace transform of the elapsed time of a successful transmission of a sensor at an attempt in a CSMA/CA-based system* |
| $\bar{\alpha}$ | *a positive real value* |
| $\Theta_1$ | *a notation representing interarrival time distribution in Kendall notation* |
| $\Theta_2$ | *a notation representing service time distribution in Kendall notation* |
| $\Theta_3$ | *a positive integer number representing the number of servers in a queueing system in Kendall notation* |
| $\Theta_4$ | *a positive integer number representing total capacity of a queueing system in Kendall notation* |

**Calligraphy letter notations:**

| | |
|---|---|
| $\mathscr{C}$ | *a set of independent sources in a multi-source queueing model* |
| $\mathscr{M}_{2,i}^{\mathrm{B}}$ | *the set of indices of queued packets of source 2 that must be served before packet $1,i$ under the event $E_{1,i}^{\mathrm{B}}$* |
| $\hat{\mathscr{M}}_{2,i}^{\mathrm{L}}$ | *the set of indices of queued packets of source 2 that must be served before packet $1,i$ under the event $E_{1,i}^{\mathrm{L}}$* |
| $\mathscr{Q}$ | *the state space of the Markov chain in the SHS technique* |
| $\mathscr{L}$ | *a set of transitions in the SHS technique* |
| $\mathscr{L}'_q$ | *the set of incoming transitions for state $q$* |
| $\mathscr{L}_q$ | *the set of outgoing transitions for state $q$* |
| $\mathscr{N}$ | *a set of sub-channels* |
| $\mathscr{K}$ | *a set of sensors* |
| $\mathscr{S}(t)$ | *the network state at slot $t$* |
| $\mathscr{B}$ | *the set of all possible values of binary vector $\mathbf{b}(t)$* |
| $\tilde{\mathscr{B}}$ | *a set of values of binary vector $\mathbf{b}(t)$* |
| $\mathscr{N}'$ | *a set of sub-channels* |
| $\mathscr{K}'$ | *a set of sensors* |

# Contents

**Abstract**
**Tiivistelmä**
**Preface** **9**
**List of abbreviations** **11**
**Contents** **21**
**1 Introduction** **25**
1.1 Motivation . . . . . 25
1.2 Scope and objectives of the thesis . . . . . 26
1.3 Outline of the thesis . . . . . 27
1.4 Basics of the AoI analysis . . . . . 28
1.4.1 Kendall notation in queueing models . . . . . 31
1.5 Literature review . . . . . 32
1.5.1 AoI analysis in various queueing models . . . . . 32
1.5.2 AoI analysis using the SHS technique . . . . . 34
1.5.3 Optimization and control in relation to AoI . . . . . 35
1.6 Contributions of the thesis . . . . . 37
1.6.1 Key contributions . . . . . 37
1.6.2 Author's contribution to the publications . . . . . 39
**2 AoI in multi-source FCFS queueing models** **41**
2.1 System model and summary of results . . . . . 41
2.1.1 Average AoI in a multi-source queueing model . . . . . 42
2.1.2 Summary of the main results . . . . . 44
2.2 AoI in a multi-source M/G/1 queueing model . . . . . 45
2.2.1 The first conditional expectation in (20) . . . . . 48
2.2.2 The second conditional expectation in (20) . . . . . 50
2.2.3 The third conditional expectation in (20) . . . . . 51
2.3 Exact expression for the average AoI in a multi-source M/M/1 queueing model . . . . . 53
2.4 Approximate expressions for the average AoI in a multi-source M/G/1 queueing model . . . . . 57
2.4.1 Single-source M/G/1 queueing model . . . . . 61
2.5 Average peak AoI expression for a multi-source M/G/1 queueing model . . . . . 62

2.6 Validation and simulation results . . . . . 62
2.6.1 Multi-source M/M/1 queueing model . . . . . 62
2.6.2 Multi-source M/G/1 queueing model . . . . . 64
2.7 Summary and discussion . . . . . 70
**3 AoI in multi-source queueing models with packet management 73**
3.1 System model and summary of the main results . . . . . 74
3.2 Average AoI . . . . . 78
3.2.1 A brief introduction to the SHS technique for calculating average AoI . . . . . 78
3.2.2 Average AoI under policy 1 . . . . . 80
3.2.3 Average AoI under policy 2 . . . . . 86
3.2.4 Average AoI under policy 3 . . . . . 90
3.3 MGF of the AoI . . . . . 91
3.3.1 The SHS technique to calculate MGF . . . . . 91
3.3.2 The MGF of the AoI under policy 2 and policy 3 . . . . . 92
3.3.3 Deriving the first and second moments of the AoI using the MGF . . . . . 95
3.4 Numerical results . . . . . 96
3.4.1 Average AoI . . . . . 97
3.4.2 Sum average AoI . . . . . 97
3.4.3 Fairness . . . . . 98
3.4.4 Standard deviation of the AoI . . . . . 102
3.5 Summary and discussion . . . . . 102
**4 Power minimization for AoI constrained dynamic control in wireless sensor networks 105**
4.1 System model and problem formulation . . . . . 106
4.1.1 System model . . . . . 106
4.1.2 Problem formulation . . . . . 108
4.2 Dynamic control algorithm . . . . . 110
4.3 Optimality analysis of the solution . . . . . 114
4.4 A sub-optimal solution for the per-slot problem (118) . . . . . 119
4.4.1 Solution algorithm . . . . . 120
4.4.2 Complexity of the sub-optimal solution . . . . . 122
4.5 Numerical and simulation results . . . . . 123
4.5.1 Simulation setup . . . . . 123
4.5.2 Performance of the dynamic control algorithm . . . . . 124
4.5.3 Performance of the sub-optimal solution . . . . . 127

4.6 Summary and discussion . . . . . 128
**5 AoI in wireless sensor networks: A multi-access channel 133**
5.1 System model and AoI metrics . . . . . 133
5.1.1 CSMA/CA mechanism . . . . . 134
5.1.2 Average AoI and peak AoI . . . . . 134
5.2 Worst case average AoI and average peak AoI of the simplified CSMA/CA-based system . . . . . 135
5.2.1 Calculation of the first moment of $S_m$ . . . . . 136
5.2.2 Calculation of the second moment of $S_m$ . . . . . 139
5.2.3 Calculation of the Laplace transform of $S_m$ at $\lambda$ . . . . . 140
5.2.4 Calculation of probability $\Pr(M = m)$ . . . . . 141
5.3 Numerical results . . . . . 142
5.4 Summary and discussion . . . . . 143
**6 Conclusions and future work 147**
6.1 Conclusions . . . . . 147
6.2 Future work . . . . . 148
**References 151**
**Appendices 157**

# 1 Introduction

## 1.1 Motivation

The freshness of status information of various physical processes e.g., temperature of a specific environment (room, greenhouse, etc.) [1] or a vehicular status (position, acceleration, etc.) [2] is a key performance enabler in many time-critical applications of wireless sensor networks (WSNs), e.g., surveillance in smart home systems, remote surgery, intelligent transportation systems, and drone control. In these networks, low power sensors may be assigned to send status updates about a random process to intended destinations [1–7].

The traditional metrics, such as throughput and delay, can not fully characterize the information freshness [5–9]. The age of information (AoI) was first introduced in the seminal work [10] as a destination-centric metric to measure the information freshness in status update systems. A status update packet contains the measured value of a monitored process and a time stamp representing the time at which the sample was generated. Due to wireless channel access, channel errors, and fading etc., communicating a status update packet through the network experiences a random delay. If at a time instant $t$, the most recently received status update packet contains the time stamp $U(t)$, AoI is defined as the random process $\Delta(t) = t - U(t)$. Thus, for each sensor, the AoI measures the time elapsed since the last received status update packet was generated at the sensor.

Besides the requirement of high information freshness, low energy consumption is vital for maintaining a status update WSN operational. Namely, the wireless sensors are typically battery limited and thus, it may not be feasible to recharge or replace batteries during the operation. The main contributors to the sensors' energy resources are the wireless access [11], and also, the sensing/sampling part [12]. Consequently, it is crucial to minimize the amount of information (e.g., the number of data packets) that must be communicated from each sensor to the sink to meet the application requirements. This engenders the need for joint optimization of the information freshness, sensors' sampling policies, and radio resource allocation (transmit power, bandwidth etc.) for designing energy-efficient status update WSNs.

## 1.2 Scope and objectives of the thesis

**Objectives:** The aim of the thesis is to analyze the information freshness and propose some novel methods to improve it in the upcoming WSNs. The AoI metric is used to measure the information freshness. The main activities regarding the thesis can be summarized into two categories: i) analyzing the AoI when we cannot control the sampling process in the system and ii) optimizing the AoI when we can control the sampling process in the system. In the first category, the AoI for various queueing models are analyzed and some novel packet management policies are introduced to improve the information freshness. Moreover, an application of the derived results is studied. In the second category, the problem of optimizing the sampling action and radio resources to improve the system energy efficiency subject to AoI constraints is studied. The main research questions are as follows:

**Q1:** How can the average AoI be characterized in multi-source queueing models with a general service time distribution?

**Q2:** How can the information freshness be improved by applying appropriate packet management policies in multi-source status update systems?

**Q3:** Can fairness among sources be improved by applying appropriate packet management policies in multi-source status update systems?

**Q4:** How do the radio resources need to be allocated to maximize the performance of a status update system subject to freshness constraints?

**Q5:** How do the sampling actions of each sensor need to be designed to maximize the performance of a status update system subject to freshness constraints?

**Q6:** What is the applicability of the derived results for various queueing models?

**Methodology:** Mathematical modeling and analysis using well-established tools, namely, i) queueing theory, ii) stochastic hybrid systems (SHS) technique, iii) stochastic optimization, and iv) convex optimization techniques. Queueing theory and the SHS technique are used for mathematical modeling and performance analysis of the status update systems. Stochastic optimization is used for performance optimization in the status update systems, and convex optimization is used for algorithm derivation. Validation of the derived theoretical results and performance evaluation of the devised methods and algorithms are performed via MATLAB simulations.

**Significance:** The research work is expected to influence the development and implementation of ultra-reliable low-latency communication services in WSNs where freshness of sensor information at destinations is important. Information freshness and energy efficiency are key enablers for these services. This thesis analyzes information freshness in various scenarios and proposes various solutions to improve the information

freshness and system energy efficiency. The derived theoretical results have particular significance in establishing performance limits for practical methods and can, thus, be used for benchmarking. Moreover, the proposed schemes, novel ideas, and possible extensions are expected to influence the development of new and more sophisticated strategies in related research fields.

## 1.3 Outline of the thesis

Chapter 2 of this thesis, the results of which have been presented in [13–15], studies the average AoI of single-server multi-source queueing models under a first-come first-served (FCFS) serving policy. In the considered model, each source independently generates status update packets according to a Poisson process and the packets are served according to a service time with general distribution. An exact expression for the average AoI for a multi-source M/M/1 queueing model is derived and three approximate expressions for the average AoI in a multi-source M/G/1 queueing model are derived.

Chapter 3, the results of which have been presented in [16–20], studies the AoI under three novel source-aware packet management policies in a status update system consisting of two independent sources and one server. The packets of each source are generated according to a Poisson process and the packets are served according to an exponentially distributed service time. The average AoI and the moment generating function (MGF) of the AoI under the introduced policies are derived.

Chapter 4, the results of which have been presented in [21, 22], considers a WSN where multiple sensors communicate timely information about various random processes to a sink. The sensors share orthogonal sub-channels to transmit such information in the form of status update packets. The problem of jointly optimizing the sampling action of each sensor, the transmit power allocation, and the sub-channel assignment to minimize the average total transmit power of all sensors subject to a maximum average AoI constraint for each sensor is studied. To solve the proposed problem, the Lyapunov drift-plus-penalty method is used.

Chapter 5, the results of which have been presented in [23, 24], considers a WSN where sensors communicate status updates to a sink by contending for the channel access based on a carrier sense multiple access with collision avoidance (CSMA/CA) method. The worst case average AoI and average peak AoI are analyzed.

Chapter 6 concludes the thesis where the main results are summarized and some open problems for future research are presented.

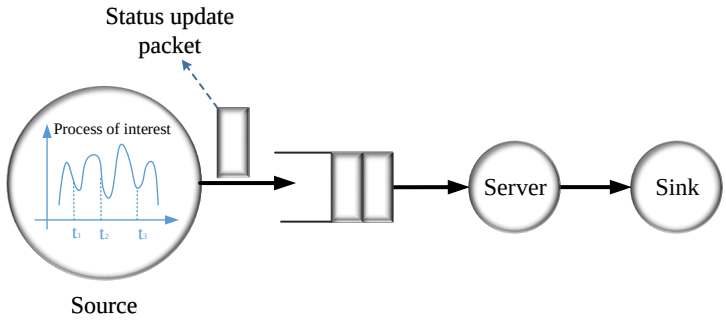


**Fig. 1. The basic status update system.**

## 1.4 Basics of the AoI analysis

In this section, the basics and formal definitions related to the AoI are presented. Consider a simple status update system consisting of a source that generates status updates of a random process, a queue, a server, and a sink, as depicted in Fig. 1. The generated updates are stored in the queue as status update packets. Due to wireless channel access, channel errors, and fading etc., the server delivers each packet to the sink with a random delay. Awareness of the source's state at the sink needs to be as timely as possible. Next, we introduce the AoI and the most commonly used metrics for evaluating this timeliness, i.e., the average AoI and average peak AoI.

Let $t_i$ denote the time instant at which the $i$th status update packet was generated, and $t_i'$ denote the time instant at which this packet arrives at the destination. At a time instant $\tau$, the index of the most recently received packet is given by

$$\bar{N}(\tau) = \max\{i' | t_{i'}' \leq \tau\}, \tag{1}$$

and the time stamp of the most recently received packet is $U(\tau) = t_{\bar{N}(\tau)}$. The AoI at the destination is defined as the random process $\Delta(t) = t - U(t)$.

An example of the AoI evolution is shown in Fig. 2. As can be seen, $\Delta(t)$ increases linearly with time, until the reception of a new status update, when the AoI is reset to the age of the newly received status update, i.e., the difference of the current time instant and the time stamp of the newly received update. Thus, two parameters that influence AoI are packet delay and inter-delivery time.

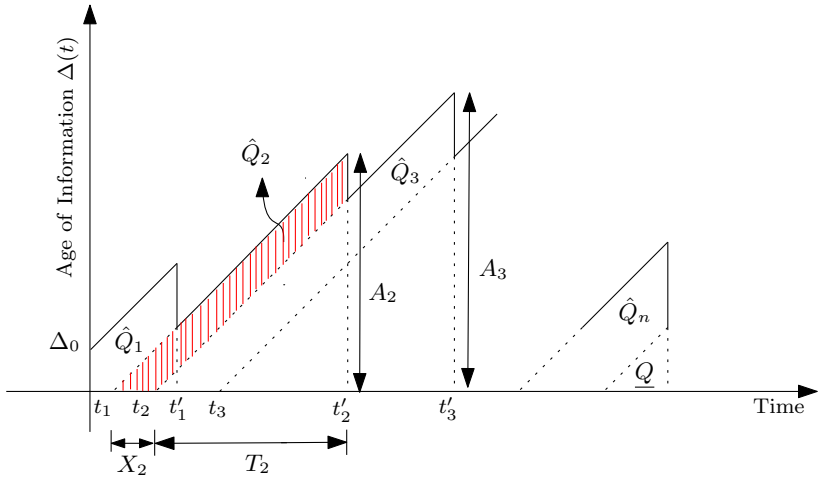


**Fig. 2. Age of information as a function of time.**

The most commonly used metrics for evaluating the AoI of a source at the destination are the average AoI and average peak AoI [5, 7–9, 25–27], which are used in this thesis. Next, these metrics are introduced.

### *Average AoI*

Let $(0,\tau)$ denote an observation interval. Accordingly, the time average AoI at the destination, denoted as $\Delta_\tau$, is defined as

$$\Delta_\tau = \frac{1}{\tau}\int_0^\tau \Delta(t)\mathrm{d}t. \tag{2}$$

The integral in (2) is equal to the area under $\Delta(t)$ which can be expressed as a sum of disjoint areas determined by a polygon $\hat{Q}_1$, $\bar{N}(\tau)-1$ trapezoids $\hat{Q}_i, i=2,\ldots,\bar{N}(\tau)$, and a triangle $\underline{Q}$, as illustrated in Fig. 2. Following the definition of $\bar{N}(\tau)$ in (1), $\Delta_\tau$ can be calculated as

$$\begin{aligned}\Delta_\tau &= \frac{1}{\tau}\left(\hat{Q}_1 + \sum_{i=2}^{\bar{N}(\tau)}\hat{Q}_i + \underline{Q}\right) \\ &= \frac{\hat{Q}_1+\underline{Q}}{\tau} + \frac{\bar{N}(\tau)-1}{\tau}\frac{1}{\bar{N}(\tau)-1}\sum_{i=2}^{\bar{N}(\tau)}\hat{Q}_i.\end{aligned} \tag{3}$$

The average AoI, denoted by $\Delta$, is defined as

$$\Delta = \lim_{\tau\to\infty} \Delta_\tau.$$

The term $\dfrac{\hat{Q}_1 + Q}{\tau}$ in (3) goes to zero as $\tau \to \infty$. The rate of generating the status update packets is defined by $\lambda = \lim_{\tau\to\infty} \dfrac{\bar{N}(\tau)}{\tau}$, and thus the term $\dfrac{\bar{N}(\tau)-1}{\tau}$ in (3) converges to $\lambda$ as $\tau \to \infty$, i.e.,

$$\lim_{\tau\to\infty} \frac{\bar{N}(\tau)-1}{\tau} = \lim_{\tau\to\infty} \frac{\bar{N}(\tau)}{\tau} = \lambda.$$

Moreover, as $\tau \to \infty$, the number of transmitted packets grows to infinity, i.e., $\bar{N}(\tau) \to \infty$. Thus, assuming that the random process $\{\hat{Q}_i\}_{i>1}$ is (mean) ergodic [7–9], the sample average term $\dfrac{1}{\bar{N}(\tau)-1}\sum_{i=2}^{\bar{N}(\tau)} \hat{Q}_i$ in (3) converges to the stochastic average $\mathbb{E}[\hat{Q}_i]$. Consequently, $\Delta$ is given by

$$\Delta = \lambda \mathbb{E}[\hat{Q}_i].$$

As shown in Fig. 2, $\hat{Q}_i$ can be calculated by subtracting the area of the isosceles triangle with sides $(t_i' - t_i)$ from the area of the isosceles triangle with sides $(t_i' - t_{i-1})$. Let the random variable

$$X_i = t_i - t_{i-1} \tag{4}$$

represent the $i$th interarrival time, i.e., the time elapsed between the generation of $i-1$th packet and $i$th packet. Moreover, let the random variable

$$T_i = t_i' - t_i \tag{5}$$

represent the system time of packet $i$, i.e., the time interval the packet spends in the system which consists of the sum of the waiting time and the service time. By using (4) and (5), $\hat{Q}_i$ can be calculated by subtracting the area of the isosceles triangle with sides $X_i$ from the area of the isosceles triangle with sides $X_i + T_i$ (see Fig. 2), and thus, the average AoI is given as [28]

$$\begin{aligned}\Delta = \lambda \mathbb{E}[\hat{Q}_i] &= \lambda\left(\frac{1}{2}\mathbb{E}[(X_i+T_i)^2] - \frac{1}{2}\mathbb{E}[T_i^2]\right) \\ &= \lambda\left(\frac{\mathbb{E}[X_i^2]}{2} + \mathbb{E}[X_i T_i]\right).\end{aligned} \tag{6}$$

In general, in any system, the most challenging part of calculating the average AoI (6) is the correlation term $\mathbb{E}[X_i T_i]$. This is because the interarrival time $X_i$ and the system time $T_i$ are statistically dependent (i.e., they are usually negatively correlated).

#### *Average peak AoI*

The peak AoI provides a more tractable metric than the average AoI for the analysis of freshness. This metric can be used in applications where we need a threshold restriction on the AoI. Moreover, it can be exploited when we are interested in the worst case AoI [26, 27].

The peak AoI at the destination is defined as the value of the AoI immediately before receiving an update packet. Accordingly, the peak AoI with respect to the $i$th successfully received packet, denoted by $A_i$ (see Fig. 2), is given by

$$A_i = X_i + T_i. \tag{7}$$

For the observation interval $(0, \tau)$, the time average peak AoI, denoted by $A_\tau$, is defined as

$$A_\tau = \frac{1}{\bar{N}(\tau)} \sum_{i=1}^{\bar{N}(\tau)} A_i.$$

The average peak AoI, denoted by $A$, is given by

$$A = \lim_{\tau \to \infty} A_\tau.$$

Consequently, considering the ergodicity assumption, the average peak AoI is given by [26, 27]

$$A = \mathbb{E}[A_i] = \mathbb{E}[X_i] + \mathbb{E}[T_i]. \tag{8}$$

### 1.4.1 Kendall notation in queueing models

Kendall notation is a system used to describe and classify different queueing models [29]. Using Kendall notation, a general queueing model is denoted by $\Theta_1/\Theta_2/\Theta_3$, where $\Theta_1$ refers to the distribution of interarrival time, $\Theta_2$ refers to the distribution of service time, and $\Theta_3$ is a positive integer number that refers to the number of servers in the queueing system. In Table 1, some symbols used for $\Theta_1$ and $\Theta_2$ in Kendall notation are presented. Note that Kendall notation has been extended to $\Theta_1/\Theta_2/\Theta_3/\Theta_4$, where $\Theta_4$ is a positive integer number that refers to the total capacity of a queueing system, i.e., the number of

packets in both the waiting queue and the server. For example, $\Theta_4 = 1$ indicates that there can be one packet under service whereas the queue holds zero packets. Note that by convention, when $\Theta_4$ is missing, it is assumed that the waiting queue has infinite capacity.

**Table 1. Symbols used in Kendall notation.**

| Symbol used for $\Theta_1$ and $\Theta_2$ | Distribution | Example |
|---|---|---|
| M | Exponential distribution | M/M/1 queueing model |
| D | Deterministic | M/D/1 queueing model |
| G | General distribution | M/G/1 queueing model |
| PH | Phase-type distribution [30] | PH/PH/1 queueing model |
| $E_k$ | Erlang distribution | M/$E_k$/1 queueing model |

## 1.5 Literature review

In this section, the earlier and parallel works to the thesis research are presented; the author's contributions are not included herein. The related works are categorized into three groups, namely, i) AoI analysis in various queueing models, ii) AoI analysis using the SHS technique, and iii) optimization and control in relation to AoI.

### *1.5.1 AoI analysis in various queueing models*

#### *Single-source queueing models*

The first queueing theoretic work on AoI is [8] where the authors derived the average AoI for M/M/1, D/M/1, and M/D/1 FCFS queueing models. In [26], the authors proposed peak AoI as an alternative metric to evaluate information freshness. In [31], the authors derived the average peak AoI expression in an M/M/1 queueing system for both FCFS and LCFS policies with packet delivery errors.

It has been shown that, with an appropriate packet management policy, we can improve the information freshness in status update systems [27, 32]. The average AoI for an M/M/1 last-come first-served (LCFS) queueing model with preemption was analyzed in [32]. The average AoI and average peak AoI for three packet management policies named M/M/1/1, M/M/1/2, and M/M/1/2$^*$ were derived in [27]. Under the M/M/1/1 model, when the server is busy, new arrivals are blocked and cleared. Under the M/M/1/2 model, there is a waiting queue of size one in the system and when the waiting queue is occupied, new arrivals are blocked and cleared. Under the M/M/1/2$^*$ model, there is a waiting queue of size one in the system and if at arrival instant of a

new packet the waiting queue is occupied, the fresh packet preempts the packet in the waiting queue. The work in [33] derived the average AoI expression in an M/M/1/2 queueing model considering a deadline for packets in the system. The authors of [34] derived the average AoI for the M/M/2 queueing model and provided upper and lower bounds for the average AoI for the M/M/$\infty$ queueing model.

Besides exponentially distributed service time and Poisson process arrivals, AoI has also been studied under various arrival processes and service time distributions. The work in [30] derived the distribution of the AoI and peak AoI for the PH/PH/1/1 and M/PH/1/2 queueing models. The authors of [35] analyzed the AoI in a D/G/1 FCFS queueing model. The authors of [36] derived a closed-form expression for the average AoI of an M/G/1/1 preemptive queueing model with hybrid automatic repeat request (HARQ). In [37], the authors derived a general formula for the stationary distribution of the AoI. They showed that the stationary distribution of the AoI is given in terms of the stationary distributions of the delay and peak AoI. The stationary distributions of the AoI and peak AoI of M/G/1/1 and G/M/1/1 queueing models were derived in [38]. The work in [39] considered an LCFS queueing model where the packets arrive according to a Poisson process and the service time follows a gamma distribution. They derived the average AoI and average peak AoI for two packet management policies, LCFS with and without preemption. The work in [33, 40] derived the average AoI expression for an G/G/1/1 queueing model under two packet management policies. In the first policy, if a new update arrives when the service is busy, it is blocked and cleared; in the second policy, a new update preempts the current update under service. The authors of [41] considered a status update system consisting of one source node that sends multiple update streams to multiple receiver nodes and derived the average AoI of each stream.

### *Multi-source queueing models*

The work in [28] was the first to investigate the AoI in a multi-source setup in which the authors derived an approximate expression for the average AoI in a multi-source M/M/1 FCFS queueing model. The authors of [42] considered an M/G/1 queueing system and optimized the arrival rates of each source to minimize the peak AoI. The closed-form expressions for the average AoI and average peak AoI in an M/G/1/1 preemptive queueing model were derived in [43]. In [44], the authors derived the average AoI for a queueing system with two classes of Poisson arrivals with different priorities and a service time with general distribution. They assumed that the system can contain at most one packet and a new arriving packet replaces the possible currently-in-service packet with a same or lower priority.

### 1.5.2 AoI analysis using the SHS technique

The seminal work [9] introduced a powerful technique, called stochastic hybrid systems (SHS), to calculate the average AoI. In [45], the authors extended the SHS analysis to calculate the MGF of the AoI. In this section, the works in which the SHS technique has been used to analyze the AoI are presented.

In [46], the authors derived the average AoI for a single-source status update system in which the updates follow a route through a series of network nodes where each node has an LCFS queue that supports preemption in service. The work in [47] derived the average AoI in a single-source queueing model with multiple servers with preemption in service.

The work in [9] considered a multi-source queueing model in which the packets of different sources are generated according to the Poisson process and served according to an exponentially distributed service time. The authors derived the average AoI for two packet management policies: 1) LCFS with preemption under service (LCFS-S), and 2) LCFS with preemption only in waiting (LCFS-W). Under the LCFS-S policy, a new arriving packet preempts any packet that is currently under service (regardless of the source index). Under the LCFS-W policy, a new arriving packet replaces any older packet waiting in the queue (regardless of the source index); however, the new packet has to wait for any packet under service to finish. The results showed that if arrival rates of the sources can be controlled, the LCFS-S policy minimizes the sum AoI. The authors of [48] considered a multi-source queueing model in which sources have different priorities and derived the average AoI for two priority based packet management policies. In [49], the authors derived the average AoI in a multi-source LCFS queueing model with multiple servers that employ preemption in service. The work in [50] derived the average AoI in a multi-source system with preemption in service and packet delivery errors.

As mentioned in Section 1.5.1, an approximate expression for the average AoI in a multi-source M/M/1 FCFS queueing model was derived in [28]. However, the authors revisited this problem recently in [51], which is the parallel work to the author's original article [13], and provided an exact expression for the average AoI by using the SHS technique.

The work in [52] considered a WSN with an unslotted, uncoordinated, unreliable multiple access collision channel. They assumed that the sensors generate status updates as a Poisson process and each update has an independent exponentially distributed transmission time. They analyzed the AoI by using the SHS technique. The authors of [53] analyzed the AoI in a CSMA/CA-based system using the SHS technique. To

make the analysis tractable, they assumed that there are no collisions in the system by considering that the channel sensing delay is zero and the back-off time is continuous. They considered a system without queueing time where the total capacity of the queueing system is one packet under service. They optimized the average AoI by calibrating the back-off time of each link.

### 1.5.3 Optimization and control in relation to AoI

Resource management to improve the information freshness has been studied in various works. In [54], the authors considered a status update system in which the updates of different sensors are generated at a fixed rate and proposed a power control algorithm to minimize the average AoI. The work in [55] considered a single-user fading channel system and studied the problem of long-term average throughput maximization subject to average AoI and power constraints. In [56], the authors studied the problem of minimizing the average AoI for status updates sent by an energy harvesting source with a finite-capacity battery. The authors of [57] considered an energy harvesting sensor with a Poisson energy arrival process and minimized the average AoI by determining the sequence of update epochs subject to an energy constraint. In [58, 59], the authors studied the problem of minimizing total transmit power subject to probabilistic AoI constraints. They solved the optimization problem using the Lyapunov optimization method. In [60], the authors considered a wireless power transfer powered sensor network and studied the performance of the system in terms of the average AoI. The authors of [61, 62] studied the problem of average AoI and peak AoI minimization in a status update system, consisting of a set of source-destination links, subject to general interference constraints. In [63], the authors studied the performance of a massive machine type communications in status update systems. They derived a closed-form expression for the average AoI and studied the problem of average AoI minimization. The work in [64] considered a status update system consisting of multiple sources and multiple sensors and investigated sensor scheduling to minimize average AoI. The work in [65] considered a two-hop status update system consisting of one source, one relay, and one sink and studied the problem of average AoI minimization subject to a constraint on the average number of forwarding operations at the relay. The authors of [66] studied the average AoI minimization problem in multi-channel status update systems.

Optimizing the sampling action of each sensor plays a critical role in the performance of status update systems. The work in [67] proposed the mutual information between the real-time source value and the delivered samples at the receiver as a new metric to

quantify the information freshness. They considered a sampling problem, where samples of a Markov source are taken and sent through a queue to the sink. The authors proved that the optimal sampling policy is a threshold policy and found the optimal threshold. In [68], the authors studied the problem of how to take samples in a status update system to optimize information freshness under various non-linear functions of AoI. The work in [69] considered an energy harvesting sensor and derived the optimal threshold, in terms of remaining energy, to trigger a new sample to minimize the average AoI. The authors of [70, 71] considered a multi-source status update system in which different sources send their updates through a shared channel with random delay. They studied the joint sampling and transmission scheduling problem in order to optimize the information freshness. The authors of [72] considered two source nodes generating heterogeneous traffic with different power supplies and studied the peak-age-optimal status update scheduling. In [73], the authors considered a status update system consisting of an energy harvesting source with a noisy channel and investigated the optimal status updating policy to minimize the average AoI. The work in [74] considered a status update system with multiple users, multiple energy harvesting sensors, and a wireless edge node. Users send requests to the edge node where a cache contains the most recently received measurements from each sensor. The authors optimized the action of the edge node to minimize the average AoI [74], or a weighted combination of the average AoI and energy consumption [75], by determining whether the edge node commands the sensor to send a status update or retrieves the aged measurement from the cache. In [76–78], the authors studied the transmission scheduling of status updates over an error-prone communication channel to minimize the average AoI subject to the constraint of the average number of transmissions. The authors of [79, 80] studied the transmission scheduling of status updates for energy harvesting sensors with finite batteries.

AoI has been widely studied for status update systems in which multiple sensors share wireless channels. In the seminal work on the AoI [10], the authors investigated the AoI in a CSMA/CA-based vehicular network using simulation. The work in [81] studied AoI and throughput in a shared access network that consists of one primary and several secondary transmitter and receiver pairs. They investigated the AoI of the primary pair. In [82], the authors investigated the ALOHA and scheduled-based access techniques in WSNs and minimized the average AoI by optimizing the probability of transmission in each node. The work in [83] investigated various decentralized age-efficient transmission policies for random access channels. In [84], the authors considered a slotted time system and derived the average AoI with and without packet management for various access methods. The work in [85] considered a WSN in

which sensors share one unreliable sub-channel in each slot. They minimized the expected weighted sum average AoI of the network by determining the transmission scheduling policy. The authors of [86] considered a wireless broadcast network with a base station sending time-sensitive information to a number of clients over an unreliable channel. They studied the problem of optimizing scheduling decisions to minimize the weighted sum AoI of the clients in the network. In [87], the authors considered a broadcast network where many clients are interested in different pieces of information that should be delivered by a base station. They studied the problem of average AoI minimization subject to the constraint that only one user can be served at a time. In [88], the authors considered a system where a base station serves multiple traffic streams arriving according to a Bernoulli process and the packets of different streams are enqueued in separate queues. They minimized the expected weighted sum AoI of the network by optimizing the transmission scheduling policy. The authors of [89] considered a multi-user system in which users share one unreliable sub-channel in each slot. They proposed an optimization problem to minimize the cost of sampling and transmitting status updates in the system under an average AoI constraint for each user in the system. They proposed a solution algorithm for the problem by using the Lyapunov drift-plus-penalty method.

## 1.6 Contributions of the thesis

In this section, the main contributions of the thesis and the author's contribution to the publications are presented.

### *1.6.1 Key contributions*

In **Chapter 2**, the average AoI of different sources in single-server multi-source queueing models under an FCFS service policy with Poisson packet arrivals is analyzed. An *exact* expression for the average AoI for a multi-source M/M/1 queueing model is derived. The setup was earlier addressed in [9, 28], where the authors derived an approximate expression for the average AoI by neglecting the statistical dependency between certain random variables; this will be elaborated upon in Chapter 2. The difficulties in an M/G/1 case are pointed out and three *approximate* expressions for the average AoI in a multi-source M/G/1 queueing model are derived. The simulation results are presented to 1) validate the derived exact average AoI in a multi-source M/M/1 queueing model, 2) show that the proposed approximations are relatively tight in the M/G/1 case where the

service time follows different distributions, and 3) exemplify the AoI behavior under different system parameters.

In **Chapter 3**, three different source-aware packet management policies are introduced and the AoI is studied under the proposed policies in a status update system consisting of two independent sources and one server. In all policies, when the system is empty, any arriving packet immediately enters the server. However, the policies differ in how they handle the arriving packets when the server is busy. In Policy 1, the waiting queue can contain at most two waiting packets at the same time (in addition to the packet under service), one packet of source 1 and one packet of source 2. When the server is busy and a new packet arrives, the possible packet of the same source waiting in the queue (not being served) is replaced by the fresh packet. In Policy 2, the system (i.e., the waiting queue and the server) can contain at most two packets, one from each source; when the server is busy and a new packet arrives, the possible packet of the same source either waiting in the queue or being served is replaced by the fresh packet. Policy 3 is similar to Policy 2 but it does not permit preemption in service, i.e., while a packet is under service all new arrivals from the same source are blocked and cleared. The SHS technique is used to derive the average AoI of each source under Policy 1, Policy 2, and Policy 3 and the MGF of the AoI under Policy 2 and Policy 3. Numerical results are provided to assess the fairness between sources, the sum average AoI, and the importance of higher moments of AoI of the proposed policies.

In **Chapter 4**, a WSN consisting of a set of sensors and a sink that is interested in time-sensitive information from the sensors is considered. The problem of optimizing the sensors sampling action and radio resources allocation to minimize the average total transmit power of all sensors subject to an AoI constraint for each sensor is studied. To solve the proposed problem, a dynamic control algorithm using the Lyapunov drift-plus-penalty method is developed. In addition, optimality analysis of the proposed dynamic control algorithm is provided. According to the Lyapunov drift-plus-penalty method, to solve the main problem, we need to solve an optimization problem in each time slot which is a mixed integer non-convex optimization problem. A low-complexity sub-optimal solution for this per-slot optimization problem is proposed that provides near-optimal performance and the computational complexity of the solution is evaluated. Numerical results show the performance of the proposed dynamic control algorithm in terms of transmit power consumption and AoI of the sensors versus different system parameters. In addition, they show that the sub-optimal solution for the per-slot optimization problems is near-optimal.

In **Chapter 5**, the worst case average AoI and average peak AoI of a sensor in a simplified CSMA/CA-based WSN under the FCFS policy and infinite queue size

are derived. The worst case analysis is carried out by considering that when a sensor contends for the channel to transmit its status update packet, all the other sensors have a packet to transmit and thus, the probability of collisions has the highest value.

### 1.6.2 Author's contribution to the publications

This thesis is written as a monograph based on the following thirteen original publications: four published journal articles [13, 16, 17, 23], one under revision journal article [21], and seven published conference papers [14, 15, 18–20, 22, 24]. The author has had the main responsibility in performing the analysis, developing the simulation software, generating the numerical results, and writing all the papers. Other co-authors provided valuable guidance for research directions, ideas on developed methods, and comments during the preparation of the manuscripts to improve their quality.

# 2 AoI in multi-source FCFS queueing models

In this chapter, the average AoI of different sources in single-server multi-source queueing models under an FCFS service policy with Poisson packet arrivals is analyzed. Analyzing the FCFS policy is important because we might have a system in which packet management policies cannot be applied, or all the generated packets in the system are useful and it is necessary to be delivered to the destination in the order in which they were generated. In Chapter 3, various packet management policies are studied which can improve the AoI.

In this chapter, first, an *exact* expression for the average AoI for a multi-source M/M/1 queueing model is derived. Second, the difficulties in an M/G/1 case are pointed out and three *approximate* expressions for the average AoI in a multi-source M/G/1 queueing model are derived. Finally, the simulation results are presented to validate the results.

The remainder of this chapter is organized as follows. The system model, AoI definition, and a summary of the main results are presented in Section 2.1. The main steps required to derive the average AoI for a multi-source M/G/1 queueing model are presented in Section 2.2. The exact expression for the average AoI in a multi-source M/M/1 queueing model is derived in Section 2.3. Three approximate expressions for the average AoI in a multi-source M/G/1 queueing model are derived in Section 2.4. Numerical validation and results are presented in Section 2.6. Finally, concluding remarks are expressed in Section 2.7.

## 2.1 System model and summary of results

Consider a system consisting of a set of independent sources denoted by $\mathscr{C} = \{1, \ldots, C\}$ and one server, as depicted in Fig. 3. Each source observes a random process, representing, e.g., temperature, vehicular speed or location at random time instants. A sink is interested in timely information about the status of these random processes. Status updates are transmitted as packets, containing the measured value of the monitored process and a time stamp representing the time when the sample was generated. The packets of source $c$ are assumed to be generated according to the Poisson process with rate $\lambda_c$, $c \in \mathscr{C}$.

For each source, the AoI at the sink is defined as the time elapsed since the last successfully received packet was generated. Formal definition of the AoI is given next.

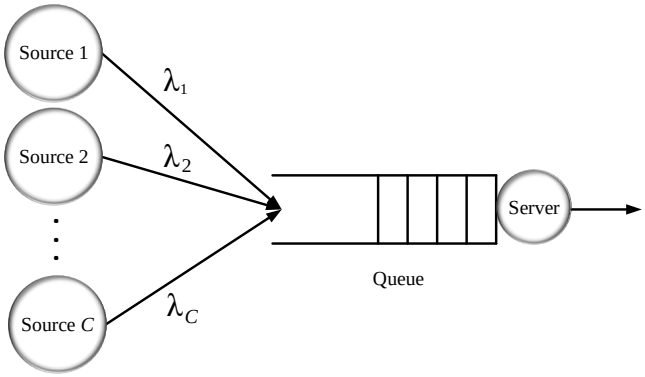


**Fig. 3. The considered status update system modeled as a multi-source M/G/1 queueing model (Reprinted by permission [13] © 2020, IEEE).**

### 2.1.1 Average AoI in a multi-source queueing model

Let $t_{c,i}$ denote the time instant at which the $i$th status update packet of source $c$ was generated, and $t'_{c,i}$ denote the time instant at which this packet arrives at the destination. At a time instant $\tau$, the index of the most recently received packet of source $c$ is given by

$$\bar{N}_c(\tau) = \max\{i' | t'_{c,i'} \leq \tau\}, \tag{9}$$

and the time stamp of the most recently received packet of source $c$ is $U_c(\tau) = t_{c,\bar{N}_c(\tau)}$. The AoI of source $c$ at the destination is defined as the random process $\Delta_c(t) = t - U_c(t)$.

The sawtooth AoI process of source $c$ at the sink in a multi-source queueing model is illustrated in Fig. 4. Following the same steps presented in Section 1.4, the average AoI of source $c$, $\Delta_c$, is given by

$$\Delta_c = \lambda_c \mathbb{E}[Q_{c,i}].$$

As shown in Fig. 4, $Q_{c,i}$ can be calculated by subtracting the area of the isosceles triangle with sides $(t'_{c,i} - t_{c,i})$ from the area of the isosceles triangle with sides $(t'_{c,i} - t_{c,i-1})$. Let the random variable

$$X_{c,i} = t_{c,i} - t_{c,i-1} \tag{10}$$

represent the $i$th interarrival time of source $c$, i.e., the time elapsed between the generation of $i-1$th packet and $i$th packet from source $c$. From here onwards, the $i$th packet from

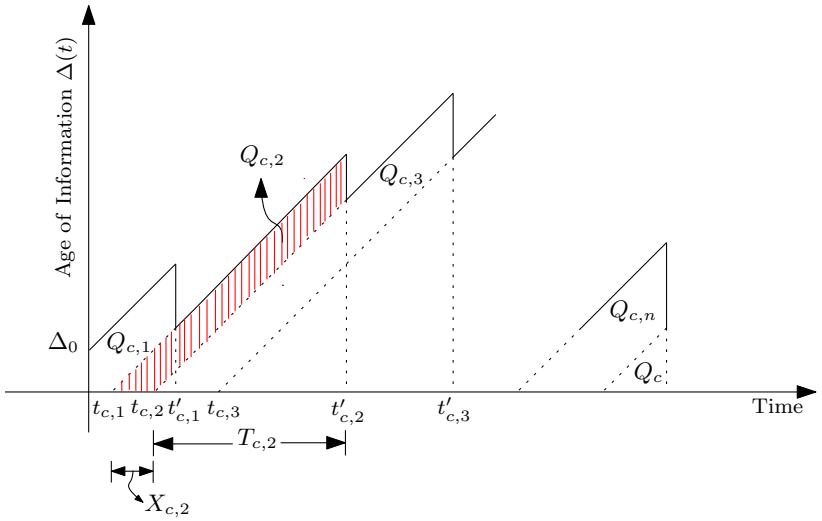


**Fig. 4. Age of information of source $c$ as a function of time (Reprinted by permission [13] © 2020, IEEE).**

source $c$ is simply referred as packet $c,i$. Moreover, let the random variable

$$T_{c,i} = t'_{c,i} - t_{c,i} \tag{11}$$

represent the system time of packet $c,i$, i.e., the time interval the packet spends in the system which consists of the sum of the waiting time and the service time. By using (10) and (11), $Q_{c,i}$ can be calculated by subtracting the area of the isosceles triangle with sides $X_{c,i}$ from the area of the isosceles triangle with sides $X_{c,i}+T_{c,i}$ (see Fig. 4), and thus, the average AoI of source $c$ is given as [28]

$$\begin{aligned}\Delta_c &= \lambda_c \mathbb{E}[Q_{c,i}] = \lambda_c \left( \frac{1}{2}\mathbb{E}[(X_{c,i}+T_{c,i})^2] - \frac{1}{2}\mathbb{E}[T_{c,i}^2] \right) \\ &= \lambda_c \left( \frac{\mathbb{E}[X_{c,i}^2]}{2} + \mathbb{E}[X_{c,i}T_{c,i}] \right).\end{aligned} \tag{12}$$

Let $W_{c,i}$ be the random variable representing the waiting time of packet $c,i$, and $S_{c,i}$ the random variable representing the service time of packet $c,i$. Consequently, the system time $T_{c,i}$ is given as the sum $T_{c,i} = W_{c,i} + S_{c,i}$, and the average AoI in (12) can be written as

$$\Delta_c = \lambda_c \left( \frac{\mathbb{E}[X_{c,i}^2]}{2} + \mathbb{E}[X_{c,i}(W_{c,i}+S_{c,i})] \right). \tag{13}$$

### 2.1.2 Summary of the main results

Here, the main results of this chapter are briefly summarized. To evaluate the AoI of one source in a queueing model with multiple sources of Poisson arrivals, two sources without loss of generality can be considered. Thus, the AoI of source 1 is evaluated by aggregating the other $C-1$ sources into source 2 having the Poisson arrival rate $\lambda_2 = \sum_{c' \in \mathscr{C} \setminus \{1\}} \lambda_{c'}$. The mean service time for each packet in the system is equal, given as $\mathbb{E}[S_{1,i}] = \mathbb{E}[S_{2,i}] = 1/\mu$, $\forall i$. Let $\rho_1 = \lambda_1/\mu$ and $\rho_2 = \lambda_2/\mu$ be the load of source 1 and 2, respectively. Since packets of each source are generated according to the Poisson process and the sources are independent, the packet generation in the system follows the Poisson process with rate $\lambda = \lambda_1 + \lambda_2$, and the overall load in the system is $\rho = \rho_1 + \rho_2 = \lambda/\mu$. Since there is no assumption on the probability density function (PDF) of the service time, the considered model is referred to a multi-source M/G/1 queueing model.

The main contributions of this chapter are twofold: 1) an *exact* expression for the average AoI for a multi-source M/M/1 queueing model is derived and 2) three *approximate* expressions for the average AoI in a multi-source M/G/1 queueing model are proposed. The derived results are summarized as follows.

**Theorem 1.** *The exact expression for the average AoI of source 1 for a multi-source M/M/1 queueing model is given in* (50) *and has the following form:*

$$\Delta_1 = \lambda_1^2(1-\rho)\Psi(\mu,\rho_1,\lambda_2) + \frac{1}{\mu}\left(\frac{1}{\rho_1} + \frac{\rho}{1-\rho} + \frac{(2\rho_2-1)(\rho-1)}{(1-\rho_2)^2} + \frac{2\rho_1\rho_2(\rho-1)}{(1-\rho_2)^3}\right),$$

*where* $\Psi(\mu,\rho_1,\lambda_2)$ *is a function that is characterized by transient behavior of an M/M/1 queue which is presented in* (42)*.*

*Proof:* The proof of Theorem 1 appears in parts in Sections 2.2 and 2.3.

The three approximate expressions for the average AoI of source 1 for a multi-source M/G/1 queueing model, denoted by $\Delta_1^{\text{app}_1}, \Delta_1^{\text{app}_2}$, and $\Delta_1^{\text{app}_3}$, are given in (56), (59), and (62), and are of the following form:

$$\Delta_1^{\text{app}_1} \approx \mathbb{E}[W] + \frac{2}{\mu} + \frac{2\rho_2-1}{\lambda_1} + \frac{2(1-\rho_2)}{\lambda_1} L_T(\lambda_1) + (\rho_2-1)L_T'(\lambda_1).$$

$$\Delta_1^{\text{app}_2} \approx \mathbb{E}[W] + \frac{2}{\mu} + \frac{2\rho_2-1}{\lambda_1} + \left(\frac{1}{\mu} + \frac{2(1-\rho_2)}{\lambda_1}\right) L_T(\lambda_1) + \left(\rho_2 - 1 - \frac{\lambda_1}{\mu}\right) L_T'(\lambda_1).$$

$$\Delta_1^{\text{app}_3} \approx \mathbb{E}[W] + \frac{2}{\mu} + \frac{2\rho_2 - 1}{\lambda_1} + \left( \frac{\lambda_2 \mathbb{E}[S^2]}{2(1-\rho_2)} + \frac{2(1-\rho_2)}{\lambda_1} \right) L_T(\lambda_1) + \left( 2\rho_2 - 1 - \frac{\lambda_1 \lambda_2 \mathbb{E}[S^2]}{2(1-\rho_2)} \right) L_T'(\lambda_1) - \lambda_1 \rho_2 L_T''(\lambda_1),$$

where $\mathbb{E}[W]$ is the average waiting time of each packet in the system (which is given in (46)), $L_T(\lambda_1)$ is the Laplace transform of the PDF of the system time (which is given in (47)), and $L_T'(\lambda_1)$ and $L_T''(\lambda_1)$ are the first and second derivative of $L_T(\cdot)$ at $\lambda_1$. The calculations to derive the approximate expressions are presented in Sections 2.2 and 2.4.

For the completeness of presentation, we also address the average peak AoI of a multi-source M/G/1 FCFS queueing model which was earlier derived in [42].

## 2.2 AoI in a multi-source M/G/1 queueing model

In this section, the main steps required to derive the average AoI in (12) for the considered multi-source M/G/1 queueing model are presented and the main difficulties regarding the average AoI calculation are pointed out. Then, in Section 2.3, the exact expression for the M/M/1 case is derived and in Section 2.4, the approximate expressions for the M/G/1 case with a general service time distribution are derived.

The first term in (13) is easy to compute. Namely, since the interarrival time of source 1 follows the exponential distribution with parameter $\lambda_1$, we have $\mathbb{E}[X_{1,i}^2] = 2/\lambda_1^2$. The second term in (13) can be written as

$$\begin{aligned} \mathbb{E}[X_{1,i}(W_{1,i} + S_{1,i})] &\overset{(a)}{=} \mathbb{E}[X_{1,i} W_{1,i}] + \mathbb{E}[X_{1,i}]\mathbb{E}[S_{1,i}] \\ &= \mathbb{E}[X_{1,i} W_{1,i}] + \frac{1}{\lambda_1 \mu}, \end{aligned} \tag{14}$$

where equality $(a)$ follows because the interarrival time and service time of the packet $1,i$ are independent. Since the random variables $X_{1,i}$ and $W_{1,i}$ are dependent, the most challenging part in calculating (13) is $\mathbb{E}[X_{1,i} W_{1,i}]$ which is derived in the following.

In order to calculate $\mathbb{E}[X_{1,i} W_{1,i}]$, the approach of [28] is followed and the waiting time $W_{1,i}$ is characterized by means of two events $E_{1,i}^{\mathrm{B}}$ and $E_{1,i}^{\mathrm{L}}$ as

$$\begin{aligned} E_{1,i}^{\mathrm{B}} &= \left\{ T_{1,i-1} \geq X_{1,i} \right\}, \\ E_{1,i}^{\mathrm{L}} &= \left\{ T_{1,i-1} < X_{1,i} \right\}. \end{aligned} \tag{15}$$

Here, *brief event* $E_{1,i}^{\mathrm{B}}$ is the event where the interarrival time of packet $1,i$ is brief, i.e., the interarrival time of packet $1,i$ is shorter than the system time of packet $1,i-1$. On

the contrary, *long event* $E^{\mathrm{L}}_{1,i}$ refers to the complementary event where the interarrival time of packet $1,i$ is long, i.e., the interarrival time of packet $1,i$ is longer than the system time of packet $1,i-1$.

Next, the waiting time for packet $1,i$ is characterized. Under the event $E^{\mathrm{B}}_{1,i}$, the waiting time of packet $1,i$ ($W_{1,i}$) contains two terms: 1) the residual system time to complete serving packet $1,i-1$, and 2) the sum of service times of the source 2 packets that arrived during $X_{1,i}$ and must be served before packet $1,i$ according to the FCFS policy (see Fig. 5(a)). Under the event $E^{\mathrm{L}}_{1,i}$, the waiting time of packet $1,i$ contains two terms: 1) the possible residual service time of a source 2 packet that is under service at the arrival instant of packet $1,i$, and 2) the sum of service times of source 2 packets in the queue that must be served before packet $1,i$ according to the FCFS policy (see Fig. 5(b)). For the event $E^{\mathrm{B}}_{1,i}$, let

$$R^{\mathrm{B}}_{1,i} = T_{1,i-1} - X_{1,i} \tag{16}$$

represent the residual system time to complete serving packet $1,i-1$ and let

$$S^{\mathrm{B}}_{1,i} = \sum_{i' \in \mathscr{M}^{\mathrm{B}}_{2,i}} S_{2,i'} \tag{17}$$

represent the sum of service times of source 2 packets that arrived during $X_{1,i}$ and must be served before packet $1,i$, where $\mathscr{M}^{\mathrm{B}}_{2,i}$ is the set of indices of queued packets of source 2 that must be served before packet $1,i$ under the event $E^{\mathrm{B}}_{1,i}$, where $|\mathscr{M}^{\mathrm{B}}_{2,i}| = M^{\mathrm{B}}_{2,i}$. Similarly for the event $E^{\mathrm{L}}_{1,i}$, let

$$S^{\mathrm{L}}_{1,i} = \sum_{i' \in \mathscr{M}^{\mathrm{L}}_{2,i}} S_{2,i'} \tag{18}$$

represent the sum of service times of source 2 packets that must be served before packet $1,i$ where $\mathscr{M}^{\mathrm{L}}_{2,i}$ is the set of indices of packets of source 2 that are in the queue (but not under service) at the arrival instant of packet $1,i$ conditioned on the event $E^{\mathrm{L}}_{1,i}$ and thus, must be served before packet $1,i$, where $|\mathscr{M}^{\mathrm{L}}_{2,i}| = M^{\mathrm{L}}_{2,i}$. Thus, by means of the two events in (15) and definitions (16), (17), and (18), the waiting time for packet $1,i$ can be expressed as

$$W_{1,i} = \begin{cases} S^{\mathrm{B}}_{1,i} + R^{\mathrm{B}}_{1,i}, & E^{\mathrm{B}}_{1,i} \\ S^{\mathrm{L}}_{1,i} + R^{\mathrm{L}}_{2,i}, & E^{\mathrm{L}}_{1,i}, \end{cases} \tag{19}$$

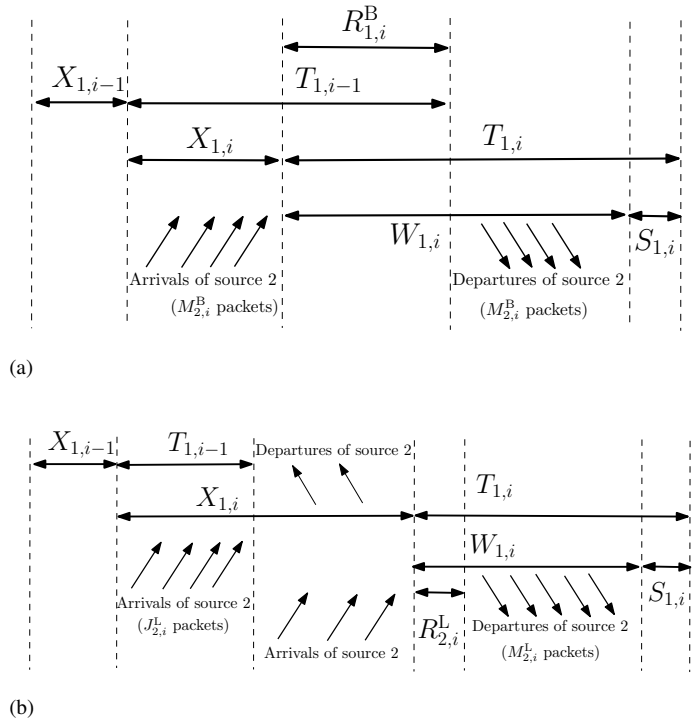


**Fig. 5. Illustration of the key quantities in characterizing the waiting time in** (19) **under (a) brief event $E^{\mathrm{B}}_{1,i}$ and (b) long event $E^{\mathrm{L}}_{1,i}$ (Reprinted by permission [13] © 2020, IEEE).**

where $R^{\mathrm{L}}_{2,i}$ is a random variable that represents the possible residual service time of the packet of source 2 that is under service at the arrival instant of packet $1,i$ conditioned on the event $E^{\mathrm{L}}_{1,i}$.

Based on (19), $\mathbb{E}[X_{1,i}W_{1,i}]$ in (14) can be expressed as

$$\begin{aligned}\mathbb{E}[X_{1,i}W_{1,i}] = &\left(\mathbb{E}[R^{\mathrm{B}}_{1,i}X_{1,i}|E^{\mathrm{B}}_{1,i}] + \mathbb{E}[S^{\mathrm{B}}_{1,i}X_{1,i}|E^{\mathrm{B}}_{1,i}]\right)\Pr(E^{\mathrm{B}}_{1,i}) \\ &+ \mathbb{E}[(S^{\mathrm{L}}_{1,i} + R^{\mathrm{L}}_{2,i})X_{1,i}|E^{\mathrm{L}}_{1,i}]\Pr(E^{\mathrm{L}}_{1,i}),\end{aligned} \tag{20}$$

where $\Pr(E^{\mathrm{B}}_{1,i})$ and $\Pr(E^{\mathrm{L}}_{1,i})$ denote the probabilities of the events $E^{\mathrm{B}}_{1,i}$ and $E^{\mathrm{L}}_{1,i}$, respectively.

Next, the expressions for $\Pr(E^{\mathrm{B}}_{1,i})$ and $\Pr(E^{\mathrm{L}}_{1,i})$ in (20) are derived. Then, by referring to $\mathbb{E}[R^{\mathrm{B}}_{1,i}X_{1,i}|E^{\mathrm{B}}_{1,i}]$, $\mathbb{E}[S^{\mathrm{B}}_{1,i}X_{1,i}|E^{\mathrm{B}}_{1,i}]$, and $\mathbb{E}[(S^{\mathrm{L}}_{1,i} + R^{\mathrm{L}}_{2,i})X_{1,i}|E^{\mathrm{L}}_{1,i}]$ in (20) as the first, second, and third conditional expectation terms of (20), the elaborate derivations of the first and second terms are presented in Sections 2.2.1 and 2.2.2, respectively, and in Section

2.2.3, the difficulties involved in computing the third term for a generic service time distribution are pointed out.

The following lemma gives the expressions for $\Pr(E^{\mathrm{B}}_{1,i})$ and $\Pr(E^{\mathrm{L}}_{1,i})$ in (20).

**Lemma 1.** *The probabilities of the events $E^{\mathrm{B}}_{1,i}$ and $E^{\mathrm{L}}_{1,i}$ in* (15) *are calculated as follows:*

$$\Pr(E^{\mathrm{B}}_{1,i}) = \frac{L_S(\lambda_1)(\lambda + (\rho-1)\lambda_1) - \lambda_2}{\lambda L_S(\lambda_1) - \lambda_2}, \tag{21}$$

$$\Pr(E^{\mathrm{L}}_{1,i}) = \frac{(1-\rho)\lambda_1 L_S(\lambda_1)}{\lambda L_S(\lambda_1) - \lambda_2}, \tag{22}$$

*where $L_S(\lambda_1)$ is the Laplace transform of the PDF of the service time $S$ at $\lambda_1$; note that the service times of all packets are stochastically identical as $S_{1,i} =^{\mathrm{st}} S_{2,i} =^{\mathrm{st}} S$, $\forall i$.*

*Proof.* See Appendix 1.1.1. □

### 2.2.1 The first conditional expectation in (20)

Let the focus now be on the first conditional expectation term $\mathbb{E}[R^{\mathrm{B}}_{1,i} X_{1,i} | E^{\mathrm{B}}_{1,i}]$ in (20). According to (16), this term is expressed as follows:

$$\begin{aligned}\mathbb{E}[R^{\mathrm{B}}_{1,i} X_{1,i} | E^{\mathrm{B}}_{1,i}] &= \mathbb{E}[T_{1,i-1} X_{1,i} | E^{\mathrm{B}}_{1,i}] - \mathbb{E}[X^2_{1,i} | E^{\mathrm{B}}_{1,i}] \\ &= \int_0^\infty \int_0^\infty xt f_{X_{1,i}, T_{1,i-1} | E^{\mathrm{B}}_{1,i}}(x,t)\mathrm{d}x\mathrm{d}t - \int_0^\infty x^2 f_{X_{1,i}|E^{\mathrm{B}}_{1,i}}(x)\mathrm{d}x,\end{aligned} \tag{23}$$

where $f_{X_{1,i}|E^{\mathrm{B}}_{1,i}}(x)$ is the conditional PDF of the interarrival time $X_{1,i}$ given the event $E^{\mathrm{B}}_{1,i}$ and $f_{X_{1,i},T_{1,i-1}|E^{\mathrm{B}}_{1,i}}(x,t)$ is the conditional joint PDF of the interarrival time $X_{1,i}$ and system time $T_{1,i-1}$ given the event $E^{\mathrm{B}}_{1,i}$. They are given by the following lemma and corollary.

**Lemma 2.** *The conditional PDF $f_{X_{1,i},T_{1,i-1}|E^{\mathrm{B}}_{1,i}}(x,t)$ is given by*

$$f_{X_{1,i},T_{1,i-1}|E^{\mathrm{B}}_{1,i}}(x,t) = \begin{cases} 0 & x > t \\ \dfrac{\lambda_1 e^{-\lambda_1 x} f_{T_{1,i-1}}(t)}{\Pr(E^{\mathrm{B}}_{1,i})} & x \le t. \end{cases} \tag{24}$$

*Proof.* See Appendix 1.1.2. □

The conditional PDF $f_{X_{1,i}|E^{\mathrm{B}}_{1,i}}(x)$ is determined by the following corollary, which is an immediate consequence of Lemma 2.

**Corollary 1.** *The conditional PDF $f_{X_{1,i}|E^{\mathrm{B}}_{1,i}}(x)$ is given by*

$$f_{X_{1,i}|E^{\mathrm{B}}_{1,i}}(x) = \frac{\lambda_1 e^{-\lambda_1 x}(1 - F_{T_{1,i-1}}(x))}{\Pr(E^{\mathrm{B}}_{1,i})}, \tag{25}$$

*where $F_{T_{1,i-1}}(x)$ is the cumulative distribution function (CDF) of $T_{1,i-1}$.*

Now, having introduced the conditional PDFs in Lemma 2 and Corollary 1, the conditional expectation $\mathbb{E}[R^{\mathrm{B}}_{1,i}X_{1,i}|E^{\mathrm{B}}_{1,i}]$ in (23) can be computed. Using Lemma 2, the first term in (23) is calculated as

$$\begin{aligned}
\mathbb{E}[T_{1,i-1}X_{1,i}|E^{\mathrm{B}}_{1,i}] &= \int_0^\infty \int_0^\infty xt f_{X_{1,i},T_{1,i-1}|E^{\mathrm{B}}_{1,i}}(x,t)\mathrm{d}x\mathrm{d}t \\
&= \frac{1}{\Pr(E^{\mathrm{B}}_{1,i})} \int_0^\infty \int_0^t tx\lambda_1 e^{-\lambda_1 x} f_{T_{1,i-1}}(t)\mathrm{d}x\mathrm{d}t \\
&= \frac{1}{\Pr(E^{\mathrm{B}}_{1,i})} \int_0^\infty \left( -t^2 e^{-\lambda_1 t} - \frac{t}{\lambda_1} e^{-\lambda_1 t} + \frac{t}{\lambda_1} \right) f_{T_{1,i-1}}(t)\mathrm{d}t \\
&= \frac{1}{\Pr(E^{\mathrm{B}}_{1,i})} \left( -\mathbb{E}[T^2 e^{-\lambda_1 T}] - \frac{\mathbb{E}[Te^{-\lambda_1 T}]}{\lambda_1} + \frac{\mathbb{E}[T]}{\lambda_1} \right) \\
&\overset{(a)}{=} \frac{1}{\Pr(E^{\mathrm{B}}_{1,i})} \left( -L''_T(\lambda_1) + \frac{L'_T(\lambda_1)}{\lambda_1} + \frac{\mathbb{E}[W] + 1/\mu}{\lambda_1} \right),
\end{aligned} \tag{26}$$

where in equality $(a)$ the first and second derivative of the Laplace transform of the PDF of the system time, $L'_T$ and $L''_T$ at $\lambda_1$, respectively, were obtained using the feature of the Laplace transform that for any function $f(y), y \geq 0$, we have [90, Sect. 13.5]

$$L_{y^n f(y)}(a) = (-1)^n \frac{\mathrm{d}^n (L_{f(y)}(a))}{\mathrm{d}a^n}, \tag{27}$$

and consequently,

$$\mathbb{E}[T^n e^{-aT}] = (-1)^n \frac{\mathrm{d}^n (L_T(a))}{\mathrm{d}a^n}. \tag{28}$$

Using Corollary 1, the second term $\mathbb{E}[X_{1,i}^2|E_{1,i}^{\mathrm{B}}]$ in (23) is calculated as

$$\begin{aligned}\mathbb{E}[X_{1,i}^2|E_{1,i}^{\mathrm{B}}] &= \int_0^\infty x^2 f_{X_{1,i}|E_{1,i}^{\mathrm{B}}}(x)\mathrm{d}x \\ &= \frac{1}{\Pr(E_{1,i}^{\mathrm{B}})}\int_0^\infty x^2\lambda_1 e^{-\lambda_1 x}\big(1-F_{T_{1,i-1}}(x)\big)\mathrm{d}x \\ &= \frac{1}{\Pr(E_{1,i}^{\mathrm{B}})}\left(\int_0^\infty x^2\lambda_1 e^{-\lambda_1 x}\mathrm{d}x - \lambda_1\int_0^\infty e^{-\lambda_1 x}\big(x^2 F_{T_{1,i-1}}(x)\big)\mathrm{d}x\right) \\ &= \frac{1}{\Pr(E_{1,i}^{\mathrm{B}})}\left(\frac{2}{\lambda_1^2} - \lambda_1 L_{x^2F_{T_1}(x)}(\lambda_1)\right).\end{aligned} \tag{29}$$

The Laplace transform $L_{x^2F_{T_1}(x)}(\lambda_1)$ in (29) is given by the following lemma.

**Lemma 3.** *$L_{x^2F_{T_1}(x)}(\lambda_1)$ is given as follows:*

$$L_{x^2F_{T_1}(x)}(a)\Big|_{a=\lambda_1} = \frac{\lambda_1 L_T''(\lambda_1) - 2L_T'(\lambda_1)}{\lambda_1^2} + \frac{2L_T(\lambda_1)}{\lambda_1^3}. \tag{30}$$

*Proof.* See Appendix 1.1.3. □

Thus, applying Lemma 3, the conditional expectation in (29) is given as

$$\mathbb{E}[X_{1,i}^2|E_{1,i}^{\mathrm{B}}] = \frac{1}{\Pr(E_{1,i}^{\mathrm{B}})}\left(\frac{2}{\lambda_1^2} - L_T''(\lambda_1) + \frac{2L_T'(\lambda_1)}{\lambda_1} - \frac{2L_T(\lambda_1)}{\lambda_1^2}\right). \tag{31}$$

Finally, substituting (26) and (31) in (23), the first conditional expectation in (20) is given by

$$\mathbb{E}[R_{1,i}^{\mathrm{B}}X_{1,i}|E_{1,i}^{\mathrm{B}}] = \frac{1}{\Pr(E_{1,i}^{\mathrm{B}})}\left(\frac{\mathbb{E}[W]+1/\mu}{\lambda_1} - \frac{L_T'(\lambda_1)}{\lambda_1} + \frac{2L_T(\lambda_1)}{\lambda_1^2} - \frac{2}{\lambda_1^2}\right). \tag{32}$$

### 2.2.2 The second conditional expectation in (20)

Next, the second term $\mathbb{E}[S_{1,i}^{\mathrm{B}}X_{1,i}|E_{1,i}^{\mathrm{B}}]$ in (20) is derived. First, let us elaborate the quantity $M_{2,i}^{\mathrm{B}}$ which is an integral part of calculating (20). Recall that $M_{2,i}^{\mathrm{B}}$ is defined as the number of queued packets of source 2 that must be served before packet $1,i$ according to the FCFS policy under the event $E_{1,i}^{\mathrm{B}} = \{T_{1,i-1} \geq X_{1,i}\}$. Thus, $M_{2,i}^{\mathrm{B}}$ is equal to the number of arrived (and thus, queued) packets of source 2 during the (brief) interarrival time $X_{1,i}$. Consequently, we have a Markov chain $T_{1,i-1} \leftrightarrow X_{1,i} \leftrightarrow M_{2,i}^{\mathrm{B}}$ conditioned on the event $E_{1,i}^{\mathrm{B}}$, i.e., $M_{2,i}^{\mathrm{B}}$ is independent of $T_{1,i-1}$ given $X_{1,i}$ under the event $E_{1,i}^{\mathrm{B}}$.

Accordingly, the conditional expectation $\mathbb{E}[S^{\mathrm{B}}_{1,i}X_{1,i}|E^{\mathrm{B}}_{1,i}]$ in (20) can be expressed as

$$\begin{aligned}\mathbb{E}[S^{\mathrm{B}}_{1,i}X_{1,i}|E^{\mathrm{B}}_{1,i}] &= \int_0^\infty x\mathbb{E}\left[\sum_{i'\in\mathscr{M}^{\mathrm{B}}_{2,i}} S_{2,i'}|E^{\mathrm{B}}_{1,i}, X_{1,i}=x\right] f_{X_{1,i}|E^{\mathrm{B}}_{1,i}}(x)\mathrm{d}x \\ &\overset{(a)}{=} \frac{1}{\mu}\int_0^\infty x\mathbb{E}\left[M^{\mathrm{B}}_{2,i}|X_{1,i}=x\right] f_{X_{1,i}|E^{\mathrm{B}}_{1,i}}(x)\mathrm{d}x \\ &\overset{(b)}{=} \frac{\rho_2}{\Pr(E^{\mathrm{B}}_{1,i})}\int_0^\infty x^2\lambda_1 e^{-\lambda_1 x}(1-F_{T_{1,i-1}}(x))\mathrm{d}x \\ &= \frac{\rho_2}{\Pr(E^{\mathrm{B}}_{1,i})}\left(\int_0^\infty x^2\lambda_1 e^{-\lambda_1 x}\mathrm{d}x - \int_0^\infty x^2\lambda_1 e^{-\lambda_1 t}F_{T_{1,i-1}}(x)\mathrm{d}x\right) \\ &\overset{(c)}{=} \frac{\rho_2}{\Pr(E^{\mathrm{B}}_{1,i})}\left(\frac{2}{\lambda_1^2} - L''_T(\lambda_1) + \frac{2L'_T(\lambda_1)}{\lambda_1} - \frac{2L_T(\lambda_1)}{\lambda_1^2}\right),\end{aligned} \tag{33}$$

where equality $(a)$ follows because (i) the service time $S_{2,i'}$ is independent of all other random variables in the system and (ii) by the Markov chain property $T_{1,i-1}\leftrightarrow X_{1,i}\leftrightarrow M^{\mathrm{B}}_{2,i}$ conditioned on $E^{\mathrm{B}}_{1,i}$, $M^{\mathrm{B}}_{2,i}$ is independent of $T_{1,i-1}$ given $X_{1,i}=x$ under the event $E^{\mathrm{B}}_{1,i}$; equality $(b)$ comes from Corollary 1 and the fact that $\mathbb{E}[M^{\mathrm{B}}_{2,i}|X_{1,i}=x]=\lambda_2 x$; equality $(c)$ comes from Lemma 3.

### 2.2.3 The third conditional expectation in (20)

The third term $\mathbb{E}[(S^{\mathrm{L}}_{1,i}+R^{\mathrm{L}}_{2,i})X_{1,i}|E^{\mathrm{L}}_{1,i}]$ in (20) can be calculated as

$$\begin{aligned}&\mathbb{E}[(S^{\mathrm{L}}_{1,i}+R^{\mathrm{L}}_{2,i})X_{1,i}|E^{\mathrm{L}}_{1,i}]= \\ &\int_0^\infty\int_0^\infty x\mathbb{E}\left[\sum_{i'\in\mathscr{M}^{\mathrm{L}}_{2,i}} S_{2,i'}|X_{1,i}=x, T_{1,i-1}=t, E^{\mathrm{L}}_{1,i}\right] f_{X_{1,i},T_{1,i-1}|E^{\mathrm{L}}_{1,i}}(x,t)\mathrm{d}x\mathrm{d}t \\ &+\int_0^\infty\int_0^\infty x\mathbb{E}\left[R^{\mathrm{L}}_{2,i}|X_{1,i}=x, T_{1,i-1}=t, E^{\mathrm{L}}_{1,i}\right] f_{X_{1,i},T_{1,i-1}|E^{\mathrm{L}}_{1,i}}(x,t)\mathrm{d}x\mathrm{d}t,\end{aligned} \tag{34}$$

where the first term on the right hand side can be calculated as

$$\begin{aligned}
&\int_0^\infty \int_0^\infty x\mathbb{E}\left[\sum_{i'\in\mathscr{M}_{2,i}^{\mathrm{L}}} S_{2,i'}|X_{1,i}=x,T_{1,i-1}=t,E_{1,i}^{\mathrm{L}}\right] f_{X_{1,i},T_{1,i-1}|E_{1,i}^{\mathrm{L}}}(x,t)\mathrm{d}x\mathrm{d}t \\
&\overset{(a)}{=} \frac{1}{\mu}\int_0^\infty \int_0^\infty x\mathbb{E}\left[M_{2,i}^{\mathrm{L}}|X_{1,i}=x,T_{1,i-1}=t,E_{1,i}^{\mathrm{L}}\right] f_{X_{1,i},T_{1,i-1}|E_{1,i}^{\mathrm{L}}}(x,t)\mathrm{d}x\mathrm{d}t \qquad (35)\\
&= \frac{1}{\mu}\int_0^\infty \int_0^\infty x\sum_{m=0}^{\infty} m\mathrm{Pr}[M_{2,i}^{\mathrm{L}}=m|X_{1,i}=x,T_{1,i-1}=t,E_{1,i}^{\mathrm{L}}] f_{X_{1,i},T_{1,i-1}|E_{1,i}^{\mathrm{L}}}(x,t)\mathrm{d}x\mathrm{d}t,
\end{aligned}$$

where equality $(a)$ follows because (i) the service time $S_{2,i'}$ is independent of all other random variables in the system and (ii) the expectation of a sum of random number $\underline{U}$ independent and identically distributed random variables $Y_u, u = 1,\ldots,\underline{U}$, is equal to the expectation of the random number $\mathbb{E}[\underline{U}]$ times the expectation of a random variable $\mathbb{E}[Y_u]$ [91, Sect. 11.2], i.e.,

$$\mathbb{E}\left[\sum_{u=1}^{\underline{U}} Y_u\right] = \mathbb{E}[\underline{U}]E[Y_u].$$

**Remark 1.** The second term on the right hand side of (34) and the final expression in (35) reveal two critical issues in deriving the third conditional expectation term of (20). The second term on the right hand side of (34) contains the possible residual service time of the packet of source 2 that is under service at the arrival instant of packet $1,i$, $R_{2,i}^{\mathrm{L}}$, which cannot be further simplified. In the final expression of (35), we need to calculate the time-dependent probability of the number of packets in an M/G/1 queue with source 2 packet arrivals, i.e., $\mathrm{Pr}[M_{2,i}^{\mathrm{L}}=m|X_{1,i}=x,T_{1,i-1}=t,E_{1,i}^{\mathrm{L}}]$. Computing this time-dependent probability in an M/G/1 queueing model is complicated and needs the transient analysis of an M/G/1 queueing model. While characterizations of the transient behavior of an M/G/1 queue are investigated in some works, such as [92], such a time-dependent probability has not been derived before in closed form so that it could be used in deriving the conditional expectation in (35).

Fortunately, these difficulties can be overcome when the service time is exponential, i.e., in an M/M/1 queueing model. Thus, the next two sections are organized as follows. An *exact* expression of the average AoI in a multi-source M/M/1 queueing model is derived in Section 2.3. In Section 2.4, three approximations for (34) are proposed and three *approximate* expressions for the average AoI in a multi-source M/G/1 queueing model are derived.

## 2.3 Exact expression for the average AoI in a multi-source M/M/1 queueing model

In this section, the *exact* expression of the average AoI in (13) for a multi-source M/M/1 queueing model that was stated in Theorem 1 in Section 2.1.2 is derived. Recall that in Section 2.2, the general expressions (for an M/G/1 case) for the key terms needed to describe the average AoI were derived, i.e., the three conditional expectation terms of (20), which are given in (32), (33), and (34), respectively. Next, these three terms are specified to the case with exponentially distributed service time. First, an exact expression for the most challenging term, i.e., the third term (34) is derived, followed by the calculation of (32) and (33).

Focus now on (34). Due to the memoryless property of the exponentially distributed service time, the possible residual service time of the packet of source 2 that is under service at the arrival instant of packet $1,i$ for event $E^{\mathrm{L}}_{1,i}$ is also exponentially distributed; thus, the waiting time is the sum of $\hat{M}^{\mathrm{L}}_{2,i}$ exponentially distributed random variables, where $\hat{M}^{\mathrm{L}}_{2,i}$ is the total number of source 2 packets in the *system* (either in the queue or under service) at the arrival instant of packet $1,i$ conditioned on the event $E^{\mathrm{L}}_{1,i}$ [93, p. 168]. Therefore, the waiting time in (34) can be expressed as

$$W_{1,i} = S^{\mathrm{L}}_{1,i} + R^{\mathrm{L}}_{2,i} = \sum_{i' \in \mathscr{M}^{\mathrm{L}}_{2,i}} S_{2,i'}, \tag{36}$$

where $\mathscr{M}^{\mathrm{L}}_{2,i}$ is the set of indices of packets of source 2 that are in the system at the arrival instant of packet $1,i$ for event $E^{\mathrm{L}}_{1,i}$, with $|\mathscr{M}^{\mathrm{L}}_{2,i}| = \hat{M}^{\mathrm{L}}_{2,i}$.

By (36), $\mathbb{E}[W_{1,i}X_{1,i}|E^{\mathrm{L}}_{1,i}]$ (cf. (34)) can be calculated as

$$\begin{aligned}
&\mathbb{E}[W_{1,i}X_{1,i}|E^{\mathrm{L}}_{1,i}] = \qquad (37)\\
&\int_0^\infty \int_0^\infty x\mathbb{E}\left[\sum_{i' \in \mathscr{M}^{\mathrm{L}}_{2,i}} S_{2,i'} | X_{1,i} = x, T_{1,i-1} = t, E^{\mathrm{L}}_{1,i}\right] f_{X_{1,i}T_{1,i-1}|E^{\mathrm{L}}_{1,i}}(x,t)\mathrm{d}x\mathrm{d}t\\
&= \frac{1}{\mu}\int_0^\infty \int_0^\infty x\mathbb{E}\left[\hat{M}^{\mathrm{L}}_{2,i} | X_{1,i} = x, T_{1,i-1} = t, E^{\mathrm{L}}_{1,i}\right] f_{X_{1,i}T_{1,i-1}|E^{\mathrm{L}}_{1,i}}(x,t)\mathrm{d}x\mathrm{d}t \qquad (38)\\
&= \frac{1}{\mu}\int_0^\infty \int_0^\infty x \sum_{m=0}^{\infty} m\Pr[\hat{M}^{\mathrm{L}}_{2,i} = m | X_{1,i} = x, T_{1,i-1} = t, E^{\mathrm{L}}_{1,i}] f_{X_{1,i}T_{1,i-1}|E^{\mathrm{L}}_{1,i}}(x,t)\mathrm{d}x\mathrm{d}t.
\end{aligned}$$

Next, $\Pr[\hat{M}^{\mathrm{L}}_{2,i} = m | X_{1,i} = x, T_{1,i-1} = t, E^{\mathrm{L}}_{1,i}]$ in (37) is calculated by introducing an *auxiliary* random variable $J^{\mathrm{L}}_{2,i}$ that represents the number of source 2 packets in the system at the departure instant of packet $1, i-1$ for event $E^{\mathrm{L}}_{1,i}$ (see Fig. 5(b)). Using the

law of total expectation, $\Pr[\hat{M}^{\mathrm{L}}_{2,i} = m | X_{1,i} = x, T_{1,i-1} = t, E^{\mathrm{L}}_{1,i}]$ in (37) is written as

$$\Pr[\hat{M}^{\mathrm{L}}_{2,i} = m | X_{1,i} = x, T_{1,i-1} = t, E^{\mathrm{L}}_{1,i}] = \tag{39}$$
$$\sum_{j=0}^{\infty} \Pr[\hat{M}^{\mathrm{L}}_{2,i} = m | J^{\mathrm{L}}_{2,i} = j, X_{1,i} = x, T_{1,i-1} = t, E^{\mathrm{L}}_{1,i}] \Pr[J^{\mathrm{L}}_{2,i} = j | X_{1,i} = x, T_{1,i-1} = t, E^{\mathrm{L}}_{1,i}],$$

where

$$\Pr[J^{\mathrm{L}}_{2,i} = j | X_{1,i} = x, T_{1,i-1} = t, E^{\mathrm{L}}_{1,i}] \overset{(a)}{=} \Pr[J^{\mathrm{L}}_{2,i} = j | T_{1,i-1} = t, E^{\mathrm{L}}_{1,i}] \overset{(b)}{=} e^{-\lambda_2 t} \frac{(\lambda_2 t)^j}{j!}, \tag{40}$$

where equality $(a)$ follows because $J^{\mathrm{L}}_{2,i}$ is conditionally independent of $X_{1,i}$ given $T_{1,i-1}$ and $E^{\mathrm{L}}_{1,i}$; equality $(b)$ follows because (i) under the long event $E^{\mathrm{L}}_{1,i}$, all $J^{\mathrm{L}}_{2,i}$ source 2 packets that are in the system at the departure instant of packet $1,i-1$ must have arrived during the system time $T_{1,i-1}$ (see Fig. 5(b)), and (ii) the probability of having $j$ Poisson arrivals of rate $\lambda_2$ during the time interval $T_{1,i-1} = t$ is $e^{-\lambda_2 t} \frac{(\lambda_2 t)^j}{j!}$ [93, Eq. (2.119)].

Focus now on the term $\Pr[\hat{M}^{\mathrm{L}}_{2,i} = m | J^{\mathrm{L}}_{2,i} = j, X_{1,i} = x, T_{1,i-1} = t, E^{\mathrm{L}}_{1,i}]$ in (39). Note that during the time interval between the departure of packet $1,i-1$ and the arrival of packet $1,i$ (i.e., $(t'_{1,i-1}, t_{1,i})$ in Fig. 2), the queue receives packets only from source 2 and therefore, the system behaves as a single-source M/M/1 queue. Thus, $\Pr[\hat{M}^{\mathrm{L}}_{2,i} = m | J^{\mathrm{L}}_{2,i} = j, X_{1,i} = x, T_{1,i-1} = t, E^{\mathrm{L}}_{1,i}]$ in (39) represents the probability that a single-source M/M/1 queueing system with arrival rate $\lambda_2$ and which initially holds $j$ packets (either in the queue or under service) ends up holding $m$ packets after $\tau = x - t$ seconds. This probability is compactly denoted by $\bar{P}_{m|j}(\tau)$ and it is given by the transient analysis of an M/M/1 queueing system as [94, Eq. (6)], [93, Eq. (2.163)]

$$\bar{P}_{m|j}(\tau) = e^{-(\lambda_2+\mu)\tau} \left[ \rho_2^{(m-1)/2} I_{m-1}(2\sqrt{\mu\lambda_2}\tau) + \rho_2^{(m-j-1)/2} I_{m+j+1}(2\sqrt{\mu\lambda_2}\tau) \right] \tag{41}$$
$$+ \rho_2^m (1-\rho_2) \left(1 - Q_{m+j+2}(\sqrt{2\lambda_2\tau}, \sqrt{2\mu\tau})\right).$$

where $I_k(\cdot)$ represents the modified Bessel function of the first kind of order $k$, and $Q_k(a,b)$ is the generalized Q-function.

Substituting (39), (40), and (41) into (37), we have

$$\begin{aligned}\mathbb{E}[W_{1,i}X_{1,i}|E_{1,i}^{\mathrm{L}}] &= \frac{1}{\mu}\int_0^\infty\int_0^\infty x\sum_{m=0}^{\infty}\sum_{j=0}^{\infty} m\bar{P}_{m|j}(x-t)e^{-\lambda_2 t}\frac{(\lambda_2 t)^j}{j!}f_{X_{1,i}T_{1,i-1}|E_{1,i}^{\mathrm{L}}}(x,t)\mathrm{d}x\mathrm{d}t \\ &\overset{(a)}{=} \frac{\lambda_1(1-\rho)}{\Pr(E_{1,i}^{\mathrm{L}})}\int_0^\infty\int_0^\infty (t+\tau)e^{-\mu(t+\rho_1\tau)}\left(\sum_{m=0}^{\infty}\sum_{j=0}^{\infty} m\bar{P}_{m|j}(\tau)\frac{(\lambda_2 t)^j}{j!}\right)\mathrm{d}\tau\mathrm{d}t \\ &\triangleq \frac{\lambda_1(1-\rho)}{\Pr(E_{1,i}^{\mathrm{L}})}\Psi(\mu,\rho_1,\lambda_2), \end{aligned} \tag{42}$$

where $(a)$ follows from the substitution $\tau = x-t$ and Lemma 4 (below) which derives the conditional PDF $f_{X_{1,i},T_{1,i-1}|E_{1,i}^{\mathrm{L}}}(x,t)$. Note that the double integral in $\Psi(\mu,\rho_1,\lambda_2)$ needs to be in general numerically calculated.

**Lemma 4.** *The conditional PDF $f_{X_{1,i},T_{1,i-1}|E_{1,i}^{\mathrm{L}}}(x,t)$ is given by*

$$f_{X_{1,i},T_{1,i-1}|E_{1,i}^{\mathrm{L}}}(x,t) = \begin{cases} 0 & x < t \\ \dfrac{\lambda_1 e^{-\lambda_1 x} f_{T_{1,i-1}}(t)}{\Pr(E_{1,i}^{\mathrm{L}})} & x \geq t. \end{cases} \tag{43}$$

*Proof.* The proof of Lemma 4 follows from the similar steps as used for Lemma 2. □

By substituting the probabilities $\Pr(E_{1,i}^{\mathrm{B}})$ and $\Pr(E_{1,i}^{\mathrm{L}})$ given by Lemma 1 and the three derived conditional expectation terms (32), (33), and (42) into (20), $\mathbb{E}[X_{1,i}W_{1,i}]$ can be expressed as

$$\begin{aligned}\mathbb{E}[X_{1,i}W_{1,i}] = \frac{\mathbb{E}[W]}{\lambda_1} &+ \lambda_1(1-\rho)\Psi(\mu,\rho_1,\lambda_2) + \frac{2(\rho_2-1)}{\lambda_1^2} + \frac{1}{\lambda_1\mu} \\ &+ \frac{2(1-\rho_2)}{\lambda_1^2}L_T(\lambda_1) + \frac{2\rho_2-1}{\lambda_1}L_T'(\lambda_1) - \rho_2 L_T''(\lambda_1). \end{aligned} \tag{44}$$

Finally, by substituting (44) and (14) into (13), the average AoI of source 1 for a multi-source M/M/1 queueing model is expressed as:

$$\begin{aligned}\Delta_1 =& \mathbb{E}[W] + \lambda_1^2(1-\rho)\Psi(\mu,\rho_1,\lambda_2) + \frac{2}{\mu}\left(\frac{\lambda_2}{\lambda_1}+1\right) - 1/\lambda_1 + \frac{2(1-\rho_2)}{\lambda_1}L_T(\lambda_1) \\ &+ (2\rho_2-1)L_T'(\lambda_1) - \lambda_1\rho_2 L_T''(\lambda_1), \end{aligned} \tag{45}$$

where the average waiting time of each packet in the system, $\mathbb{E}[W]$, is given as [95, Sect. 3]

$$\mathbb{E}[W] = \frac{\mathbb{E}[S^2]\lambda}{2(1-\rho)}, \tag{46}$$

where $\mathbb{E}[S^2] = 2/\mu^2$ is the second moment of the service time, $L_T(\lambda_1)$ is a function of the Laplace transform of the PDF of the service time given by [96, Sect. 5.1.2]

$$L_T(\lambda_1) = \frac{(1-\rho)\lambda_1 L_S(\lambda_1)}{\lambda_1 - \lambda\left(1-L_S(\lambda_1)\right)}, \tag{47}$$

and $L'_T(\lambda_1)$ and $L''_T(\lambda_1)$ are the first and second derivatives of $L_T(\cdot)$ at $\lambda_1$, respectively, as

$$L'_T(\lambda_1) = \left.\frac{\mathrm{d}(L_T(a))}{\mathrm{d}a}\right|_{a=\lambda_1} = (1-\rho)\frac{\lambda L_S^2(\lambda_1) + \left(\lambda_1^2 - \lambda_1\lambda\right)L'_S(\lambda_1) - \lambda L_S(\lambda_1)}{\left(\lambda_1 - \lambda\left(1-L_S(\lambda_1)\right)\right)^2}, \tag{48}$$

$$L''_T(\lambda_1) = \left.\frac{\mathrm{d}^2(L_T(a))}{\mathrm{d}a^2}\right|_{a=\lambda_1} =$$
$$(1-\rho)\Bigg(\frac{\lambda L''_S(\lambda_1)\left(\lambda_1^2 - \lambda_1\lambda\right) + 2L'_S(\lambda_1)\left(\lambda_1 - \lambda + \lambda L_S(\lambda_1)\right)}{\left(\lambda_1 - \lambda\left(1-L_S(\lambda_1)\right)\right)^2} -$$
$$\frac{2(\lambda L_S^2(\lambda_1) + \left(\lambda_1^2 - \lambda_1\lambda\right)L'_S(\lambda_1) - \lambda L_S(\lambda_1))(1+\lambda L'_S(\lambda_1))}{\left(\lambda_1 - \lambda\left(1-L_S(\lambda_1)\right)\right)^3}\Bigg),$$

where $L'_S(\lambda_1)$ and $L''_S(\lambda_1)$ for the exponential service time are computed according to (27) as

$$\begin{aligned} L_S(\lambda_1) &= \int_0^\infty \mu e^{-(\mu+\lambda_1)s}\mathrm{d}s = \frac{\mu}{\mu+\lambda_1}, \\ L'_S(\lambda_1) &= -\int_0^\infty s\mu e^{-(\mu+\lambda_1)s}\mathrm{d}s = -\frac{\mu}{(\mu+\lambda_1)^2}, \\ L''_S(\lambda_1) &= \int_0^\infty s^2\mu e^{-(\mu+\lambda_1)s}\mathrm{d}s = \frac{2\mu}{(\mu+\lambda_1)^3}. \end{aligned} \tag{49}$$

Finally, by substituting $\mathbb{E}[W]$, $L_T(\lambda_1)$, $L'_T(\lambda_1)$, and $L''_T(\lambda_1)$ into (45) we get the result in Theorem 1 in Section 2.1.2, i.e., the average AoI of source 1 for a multi-source M/M/1

queueing model is given as

$$\Delta_1 = \lambda_1^2(1-\rho)\Psi(\mu,\rho_1,\lambda_2) + \frac{1}{\mu}\left(\frac{1}{\rho_1} + \frac{\rho}{1-\rho} + \frac{(2\rho_2-1)(\rho-1)}{(1-\rho_2)^2} + \frac{2\rho_1\rho_2(\rho-1)}{(1-\rho_2)^3}\right). \tag{50}$$

**Remark 2.** It is worth noting that (50) does not coincide with the prior result [9, Theorem 1] and [28, Eq. (16)]. The dissimilarity is explained in the following. The authors of [9, 28] considered a similar two-source FCFS M/M/1 queueing model, with the aim of deriving a closed-form expression for the average AoI of source 1 ($\Delta_1$). Let the focus be on [28, Eq. (33)] where the authors compute a conditional expectation equivalent to our $\mathbb{E}[W_{1,i}X_{1,i}|E_{1,i}^{\mathrm{L}}]$ given by (42), which by (36) can be expressed as

$$\mathbb{E}[W_{1,i}X_{1,i}|E_{1,i}^{\mathrm{L}}] = \mathbb{E}\Big[\sum_{i'\in\mathscr{M}_{2,i}^{\mathrm{L}}} S_{2,i'}X_{1,i}|E_{1,i}^{\mathrm{L}}\Big]. \tag{51}$$

The authors of [28] tacitly assumed conditional independency between $\sum_{i'\in\mathscr{M}_{2,i}^{\mathrm{L}}} S_{2,i'}$ and $X_{1,i}$ under the event $E_{1,i}^{\mathrm{L}} = \{T_{1,i-1} < X_{1,i}\}$, and calculated (51) as a multiplication of two expectations as

$$\mathbb{E}[W_{1,i}X_{1,i}|E_{1,i}^{\mathrm{L}}] = \mathbb{E}\Big[\sum_{i'\in\mathscr{M}_{2,i}^{\mathrm{L}}} S_{2,i'}|T_{1,i-1} < X_{1,i}\Big]\mathbb{E}\Big[X_{1,i}|T_{1,i-1} < X_{1,i}\Big]. \tag{52}$$

The critical point is that even if $X_{1,i}$ is independent of $T_{1,i-1}$, they become dependent when conditioned on the event $E_{1,i}^{\mathrm{L}} = \{T_{1,i-1} < X_{1,i}\}$, as in (51). This conditional dependency is violated by the separation of the expectations in (52) because the quantity $\hat{M}_{2,i}^{\mathrm{L}}$ in general depends on both $T_{1,i-1}$ and $X_{1,i}$, and thus, the multiplicative quantities $\sum_{i'\in\mathscr{M}_{2,i}^{\mathrm{L}}} S_{2,i'}$ and $X_{1,i}$ are dependent under the event $E_{1,i}^{\mathrm{L}}$. Note that this conditional dependency in calculating $\mathbb{E}[W_{1,i}X_{1,i}|E_{1,i}^{\mathrm{L}}]$ is incorporated by using the conditional joint PDF $f_{X_{1,i},T_{1,i-1}|E_{1,i}^{\mathrm{L}}}(x,t)$.

## 2.4 Approximate expressions for the average AoI in a multi-source M/G/1 queueing model

In this section, the three *approximate* expressions of the average AoI in (13) for a multi-source M/G/1 queueing model that were presented in Section 2.1.2 are derived. Recall that the exact expressions for the first and second conditional expectation terms of (20) are given by (32) and (33), respectively. From (34) and (35), the third conditional

expectation is given as

$$\begin{aligned}
&\mathbb{E}[(S^{\mathrm{L}}_{1,i}+R^{\mathrm{L}}_{2,i})X_{1,i}|E^{\mathrm{L}}_{1,i}] = \\
&\frac{1}{\mu}\int_0^\infty\int_0^\infty x\mathbb{E}\left[M^{\mathrm{L}}_{2,i}|X_{1,i}=x,T_{1,i-1}=t,E^{\mathrm{L}}_{1,i}\right] f_{X_{1,i},T_{1,i-1}|E^{\mathrm{L}}_{1,i}}(x,t)\mathrm{d}x\mathrm{d}t \\
&+\int_0^\infty\int_0^\infty x\mathbb{E}\left[R^{\mathrm{L}}_{2,i}|X_{1,i}=x,T_{1,i-1}=t,E^{\mathrm{L}}_{1,i}\right] f_{X_{1,i},T_{1,i-1}|E^{\mathrm{L}}_{1,i}}(x,t)\mathrm{d}x\mathrm{d}t. \qquad (53)
\end{aligned}$$

Next, three approximate calculations for the third conditional expectation term of (20), given by (53), are proposed differing in the way that the following two terms are approximated

$$\mathbb{E}\left[M^{\mathrm{L}}_{2,i}|X_{1,i}=x,T_{1,i-1}=t,E^{\mathrm{L}}_{1,i}\right],$$
$$\mathbb{E}\left[R^{\mathrm{L}}_{2,i}|X_{1,i}=x,T_{1,i-1}=t,E^{\mathrm{L}}_{1,i}\right].$$

**Approximation 1:** First, the possible residual service time of source 2 packet that is under service at the arrival instant of packet $1,i$ is neglected. Second, it is assumed that the average number of packets of source 2 that must be served before packet $1,i$ is equal to the average number of packets of source 2 that are queued during the system time of packet $1,i-1$ ($T_{1,i-1}$). Thus, it is assumed

$$\mathbb{E}\left[M^{\mathrm{L}}_{2,i}|X_{1,i}=x,T_{1,i-1}=t,E^{\mathrm{L}}_{1,i}\right] = \mathbb{E}\left[J^{\mathrm{L}}_{2,i}|X_{1,i}=x,T_{1,i-1}=t,E^{\mathrm{L}}_{1,i}\right],$$

where, as defined previously, the random variable $J^{\mathrm{L}}_{2,i}$ represents the number of source 2 packets in the system at the departure instant of packet $1,i-1$ for the long event $E^{\mathrm{L}}_{1,i}$. With the simplifications above, (53) can be approximated as

$$\begin{aligned}
&\mathbb{E}[(S^{\mathrm{L}}_{1,i}+R^{\mathrm{L}}_{2,i})X_{1,i}|E^{\mathrm{L}}_{1,i}] \\
&\approx\frac{1}{\mu}\int_0^\infty\int_0^\infty x\mathbb{E}\left[J^{\mathrm{L}}_{2,i}|X_{1,i}=x,T_{1,i-1}=t,E^{\mathrm{L}}_{1,i}\right] f_{X_{1,i},T_{1,i-1}|E^{\mathrm{L}}_{1,i}}(x,t)\mathrm{d}x\mathrm{d}t \\
&\overset{(a)}{=}\rho_2\int_0^\infty\int_0^\infty txf_{X_{1,i},T_{1,i-1}|E^{\mathrm{L}}_{1,i}}(x,t)\mathrm{d}x\mathrm{d}t \qquad (54) \\
&\overset{(b)}{=}\frac{\rho_2}{\Pr(E^{\mathrm{L}}_{1,i})}\int_0^\infty\int_t^\infty xt\lambda_1 e^{-\lambda_1 x}f_{T_{1,i-1}}(t)\mathrm{d}x\mathrm{d}t \\
&=\frac{\rho_2}{\Pr(E^{\mathrm{L}}_{1,i})}\int_0^\infty\left(t^2e^{-\lambda_1 t}f_{T_{1,i-1}}(t)+\frac{te^{-\lambda_1 t}}{\lambda_1}f_{T_{1,i-1}}(t)\right)\mathrm{d}t \\
&\overset{(c)}{=}\frac{\rho_2}{\Pr(E^{\mathrm{L}}_{1,i})}\left(L''_T(\lambda_1)-\frac{L'_T(\lambda_1)}{\lambda_1}\right),
\end{aligned}$$

where $(a)$ comes from the fact that $\mathbb{E}\left[J_{2,i}^{\mathrm{L}}|X_{1,i}=x,T_{1,i-1}=t,E_{1,i}^{\mathrm{L}}\right]=\lambda_2 t$, $(b)$ follows from Lemma 4, and $(c)$ follows from (28).

By substituting the probabilities $\Pr(E_{1,i}^{\mathrm{B}})$ and $\Pr(E_{1,i}^{\mathrm{L}})$ given by Lemma 1 and the three derived conditional expectation terms (32), (33), and (54) into (20), an approximation for $\mathbb{E}[X_{1,i}W_{1,i}]$ can be expressed as

$$\mathbb{E}[X_{1,i}W_{1,i}]\approx\frac{1}{\lambda_1}\left(\mathbb{E}[W]+\frac{1}{\mu}+\frac{2(\rho_2-1)}{\lambda_1}+\frac{2(1-\rho_2)}{\lambda_1}L_T(\lambda_1)+(\rho_2-1)L_T'(\lambda_1)\right). \tag{55}$$

By substituting (55) and (14) into (13), an approximation for the average AoI of source 1 in a multi-source M/G/1 queueing model is given as

$$\Delta_1^{\mathrm{app}_1}\approx\mathbb{E}[W]+\frac{2}{\mu}+\frac{2\rho_2-1}{\lambda_1}+\frac{2(1-\rho_2)}{\lambda_1}L_T(\lambda_1)+(\rho_2-1)L_T'(\lambda_1), \tag{56}$$

where the quantities $\mathbb{E}[W]$, $L_T(\lambda_1)$, and $L_T'(\lambda_1)$ are calculated by (46)–(49) for a specific service time distribution.

**Approximation 2:** First, it is assumed that the average residual service time of the source 2 packet that is under service at the arrival instant of packet $1,i$ is equal to the average service time of one packet in the system. Thus, it is assumed that

$$\mathbb{E}\left[R_{2,i}^{\mathrm{L}}|X_{1,i}=x,T_{1,i-1}=t,E_{1,i}^{\mathrm{L}}\right]=\frac{1}{\mu}.$$

Second, for the term $\mathbb{E}\left[M_{2,i}^{\mathrm{L}}|X_{1,i}=x,T_{1,i-1}=t,E_{1,i}^{\mathrm{L}}\right]$, the same approximation as used for Approximation 1 is considered, i.e.,

$$\mathbb{E}\left[M_{2,i}^{\mathrm{L}}|X_{1,i}=x,T_{1,i-1}=t,E_{1,i}^{\mathrm{L}}\right]=\mathbb{E}\left[J_{2,i}^{\mathrm{L}}|X_{1,i}=x,T_{1,i-1}=t,E_{1,i}^{\mathrm{L}}\right].$$

Based on these simplifications, (53) can be approximated as

$$\begin{aligned}
&\mathbb{E}[(S_{1,i}^{\mathrm{L}}+R_{2,i}^{\mathrm{L}})X_{1,i}|E_{1,i}^{\mathrm{L}}]\approx\frac{1}{\mu}\int_0^\infty\int_0^\infty x\mathbb{E}\left[J_{2,i}^{\mathrm{L}}|X_{1,i}=x,T_{1,i-1}=t,E_{1,i}^{\mathrm{L}}\right]f_{X_{1,i},T_{1,i-1}|E_{1,i}^{\mathrm{L}}}(x,t)\mathrm{d}x\mathrm{d}t\\
&+\frac{1}{\mu}\int_0^\infty\int_0^\infty xf_{X_{1,i},T_{1,i-1}|E_{1,i}^{\mathrm{L}}}(x,t)\mathrm{d}x\mathrm{d}t \qquad (57)\\
&=\rho_2\int_0^\infty\int_0^\infty txf_{X_{1,i},T_{1,i-1}|E_{1,i}^{\mathrm{L}}}(x,t)\mathrm{d}x\mathrm{d}t+\frac{1}{\mu}\int_0^\infty\int_0^\infty xf_{X_{1,i},T_{1,i-1}|E_{1,i}^{\mathrm{L}}}(x,t)\mathrm{d}x\mathrm{d}t\\
&=\frac{1}{\Pr(E_{1,i}^{\mathrm{L}})}\left(\rho_2L_T''(\lambda_1)-\left(\frac{\rho_2}{\lambda_1}+\frac{1}{\mu}\right)L_T'(\lambda_1)+\frac{L_T(\lambda_1)}{\mu\lambda_1}\right).
\end{aligned}$$

Using (57) and following the steps used to derive (55), an approximation for $\mathbb{E}[X_{1,i}W_{1,i}]$ under Approximation 2 is given as

$$\mathbb{E}[X_{1,i}W_{1,i}] \approx \frac{1}{\lambda_1}\left(\mathbb{E}[W]+\frac{1}{\mu}+\frac{2(\rho_2-1)}{\lambda_1}+\left(\frac{1}{\mu}+\frac{2(1-\rho_2)}{\lambda_1}\right)L_T(\lambda_1)\right. \\ \left.+\left(\rho_2-1-\frac{\lambda_1}{\mu}\right)L_T'(\lambda_1)\right). \tag{58}$$

By substituting (58) and (14) into (13), an approximation for the average AoI of source 1 in a multi-source M/G/1 queueing model is given as

$$\Delta_1^{\text{app}_2} \approx \mathbb{E}[W]+\frac{2}{\mu}+\frac{2\rho_2-1}{\lambda_1}+\left(\frac{1}{\mu}+\frac{2(1-\rho_2)}{\lambda_1}\right)L_T(\lambda_1)+\left(\rho_2-1-\frac{\lambda_1}{\mu}\right)L_T'(\lambda_1). \tag{59}$$

**Approximation 3:** It is assumed that the queue is in the stationary state. In other words, first, it is assumed that the average residual service time of the source 2 packet that is under service at the arrival instant of packet $1,i$ is equal to the average residual service time of a stationary M/G/1 queue that has only source 2 packet arrivals. Thus, it is assumed that [95, Eq. (3.52)]

$$\mathbb{E}\left[R_{2,i}^{\text{L}}|X_{1,i}=x,T_{1,i-1}=t,E_{1,i}^{\text{L}}\right]=\frac{\lambda_2\mathbb{E}[S^2]}{2}.$$

Second, it is assumed that the average number of source 2 packets that must be served before packet $1,i$ is equal to the average number of packets in a stationary M/G/1 queue with only source 2 packet arrivals. Thus, it is assumed [95, Eq. (3.43)]

$$\mathbb{E}\left[M_{2,i}^{\text{L}}|X_{1,i}=x,T_{1,i-1}=t,E_{1,i}^{\text{L}}\right]=\frac{\lambda_2^2\mathbb{E}[S^2]}{2(1-\rho_2)}.$$

Thus, the third conditional expectation in (53) is approximated as follows:

$$\begin{aligned}\mathbb{E}[(S_{1,i}^{\text{L}}+R_{2,i}^{\text{L}})X_{1,i}|E_{1,i}^{\text{L}}] &\approx \frac{\lambda_2^2\mathbb{E}[S^2]}{2\mu(1-\rho_2)}\int_0^\infty\int_0^\infty x f_{X_{1,i},T_{1,i-1}|E_{1,i}^{\text{L}}}(x,t)\mathrm{d}x\mathrm{d}t \\ &\quad+\frac{\lambda_2\mathbb{E}[S^2]}{2}\int_0^\infty\int_0^\infty x f_{X_{1,i},T_{1,i-1}|E_{1,i}^{\text{L}}}(x,t)\mathrm{d}x\mathrm{d}t \\ &=\frac{\lambda_2\mathbb{E}[S^2]}{2(1-\rho_2)\Pr(E_{1,i}^{\text{L}})}\left(\frac{L_T(\lambda_1)}{\lambda_1}-L_T'(\lambda_1)\right).\end{aligned} \tag{60}$$

Using (60) and following the steps used to derive (55), an approximation for $\mathbb{E}[X_{1,i}W_{1,i}]$ under Approximation 3 is given as

$$\mathbb{E}[X_{1,i}W_{1,i}] \approx \frac{1}{\lambda_1}\left(\mathbb{E}[W]+\frac{1}{\mu}+\frac{2(\rho_2-1)}{\lambda_1}+\left(\frac{\lambda_2\mathbb{E}[S^2]}{2(1-\rho_2)}+\frac{2(1-\rho_2)}{\lambda_1}\right)L_T(\lambda_1)\right. \quad (61)$$
$$\left.+\left(2\rho_2-1-\frac{\lambda_1\lambda_2\mathbb{E}[S^2]}{2(1-\rho_2)}\right)L_T'(\lambda_1)-\lambda_1\rho_2 L_T''(\lambda_1)\right).$$

By substituting (61) and (14) into (13), an approximation for the average AoI of source 1 in a multi-source M/G/1 queueing model is given as

$$\Delta_1^{\text{app}_3} \approx \mathbb{E}[W]+\frac{2}{\mu}+\frac{2\rho_2-1}{\lambda_1}+\left(\frac{\lambda_2\mathbb{E}[S^2]}{2(1-\rho_2)}+\frac{2(1-\rho_2)}{\lambda_1}\right)L_T(\lambda_1) \quad (62)$$
$$+\left(2\rho_2-1-\frac{\lambda_1\lambda_2\mathbb{E}[S^2]}{2(1-\rho_2)}\right)L_T'(\lambda_1)-\lambda_1\rho_2 L_T''(\lambda_1).$$

### 2.4.1 Single-source M/G/1 queueing model

For $\lambda_2 \to 0$, we have a single-source M/G/1 queueing model. In this case, it can be shown that (56) and (62) provide the following expression for the average AoI:

$$\Delta = \mathbb{E}[W]+\frac{2}{\mu}+\frac{2L_T(\lambda_1)}{\lambda_1}-L_T'(\lambda_1)-\frac{1}{\lambda_1}. \quad (63)$$

Using (46), (47), and (48), the quantities $\mathbb{E}[W]$, $L_T(\lambda)$, and $L_T'(\lambda)$ are calculated as

$$\mathbb{E}[W] = \frac{\mathbb{E}[S^2]\lambda}{2(1-\rho)}, \quad (64)$$
$$L_T(\lambda) = 1-\rho,$$
$$L_T'(\lambda) = \frac{(1-\rho)(L_S(\lambda)-1)}{\lambda L_S(\lambda)}.$$

By substituting $\mathbb{E}[W]$, $L_T(\lambda)$, and $L_T'(\lambda)$ into (63), we have

$$\Delta = \frac{1}{\mu}+\frac{\lambda\mathbb{E}[S^2]}{2(1-\rho)}+\frac{1-\rho}{\lambda L_S(\lambda)}, \quad (65)$$

which is an *exact* expression for the average AoI of the single-source M/G/1 queueing case derived in [38, Eq. (22)].

## 2.5 Average peak AoI expression for a multi-source M/G/1 queueing model

For completeness of presentation, the average peak AoI of a multi-source M/G/1 FCFS queueing model which was earlier derived in [42] is addressed.

Following the steps presented in Section 1.4, the average peak AoI of source 1 is given by

$$A_1 = \mathbb{E}[X] + \mathbb{E}[S] + \mathbb{E}[W]. \tag{66}$$

By substituting the average waiting time presented in (64) into the average peak AoI expression in (66), the average peak AoI of source 1 is given by

$$A_1 = \frac{1}{\lambda_1} + \frac{1}{\mu} + \frac{\mathbb{E}[S^2]\lambda}{2\big(1-\rho\big)}. \tag{67}$$

## 2.6 Validation and simulation results

In this section, first, the average AoI in a multi-source M/M/1 queueing model is evaluated and the exact expression in (50) is compared with the results in existing work [28]. Then, the accuracy of the proposed three approximate expressions for the M/G/1 queueing model in (56), (59), and (62) are evaluated under various service time distributions.

### *2.6.1 Multi-source M/M/1 queueing model*

Fig. 6 depicts the average AoI of source 1 ($\Delta_1$) as a function of $\lambda_1$ with $\lambda_2 = 0.6$ and $\mu = 1$. As can be seen, the simulation result and the proposed solution in this chapter overlap perfectly. The *"integral2"* command in MATLAB software is used to calculate the double integral in (42). Due to the calculation errors in [28], the curve has a gap to the correct average AoI value.

The effect of $\lambda_2$ on the average AoI of source 1 is shown in Fig. 7. When $\lambda_2$ increases, the increased overall load in the system results in longer waiting time for packets of source 1 (and source 2), which increases $\Delta_1$. Note, however, that when $\lambda_2$ increases, the optimal value of $\lambda_1$ that minimizes $\Delta_1$ decreases. The figures illustrate that generating the status update packets too frequently or too rarely does not minimize the average AoI. Moreover, Fig. 7 depicts the gap between the exact and approximate

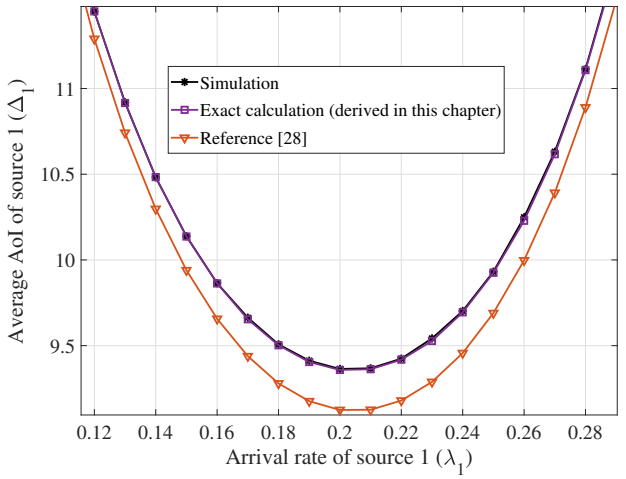


**Fig. 6. The average AoI of source 1 as a function of $\lambda_1$ with $\lambda_2 = 0.6$ and $\mu = 1$ (Reprinted by permission [13] © 2020, IEEE).**

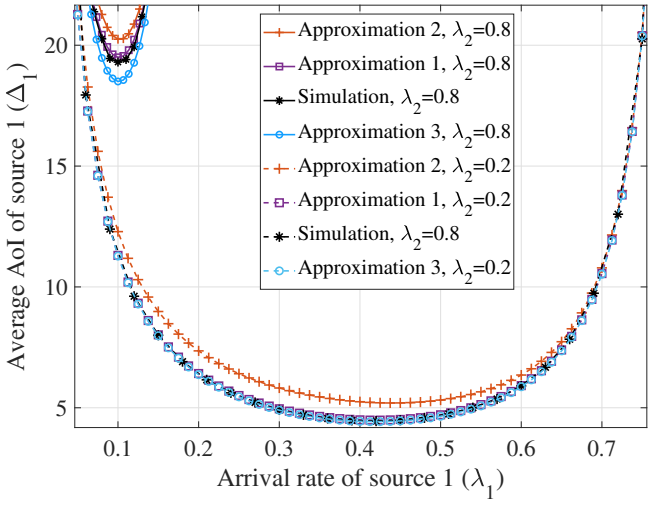


**Fig. 7. The average AoI of source 1 as a function of $\lambda_1$ for different values of $\lambda_2$ with $\mu = 1$ (Reprinted by permission [13] © 2020, IEEE).**

average AoI expressions. As can be seen, the proposed approximations are relatively close to the exact one in the M/M/1 queueing model.

Fig. 8 depicts the average delay of source 1 as a function of $\lambda_1$ for different values of $\lambda_2$ with $\mu = 1$. The average delay is defined as the summation of the average waiting

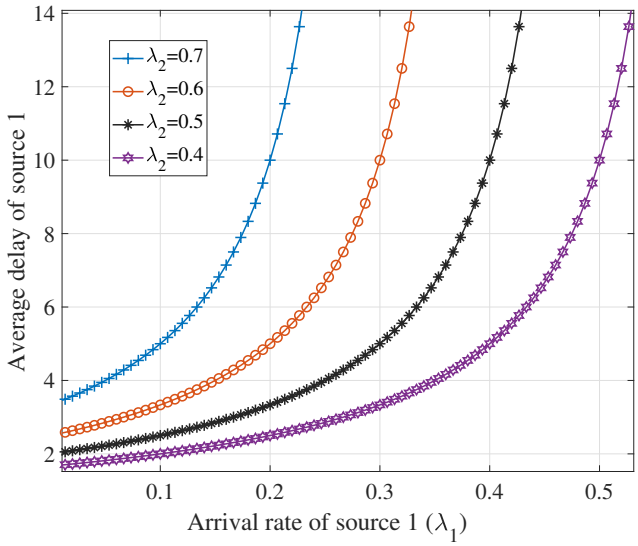


**Fig. 8. The average delay of source 1 as a function of $\lambda_1$ for different values of $\lambda_2$ with $\mu = 1$ (Reprinted by permission [13] © 2020, IEEE).**

time and average service time i.e., $\mathbb{E}[W] + 1/\mu$. As the number of arrivals of source 2 packets increases, the queue becomes more congested and the average delay of source 1 increases. By comparing Figs. 7 and 8, one can see that the delay does not fully capture the information freshness, i.e., minimizing the average system delay does not necessarily lead to good performance in terms of AoI and, reciprocally, minimizing the average AoI does not minimize the average system delay.

### *2.6.2 Multi-source M/G/1 queueing model*

In this section, the accuracy of the proposed three approximations using the following service time distributions is examined: i) gamma distribution, ii) hyper-exponential distribution, iii) log-normal distribution, and iv) Pareto distribution. In the following, first, the distributions are defined and then the accuracy of the proposed approximations is shown for each distribution.

**Definition 1.** *(Gamma distribution).* The PDF of a random variable $S$ following a gamma distribution is defined as

$$f_S(s) = \Gamma(\kappa_1, \kappa_2) = \frac{\kappa_2^{\kappa_1} s^{\kappa_1 - 1} \exp(-\kappa_2 s)}{\Gamma(\kappa_1)}, \text{ for } s > 0,\ \kappa_1 > 0,\ \kappa_2 > 0,$$

where $\Gamma(\kappa_1)$ is the gamma function at $\kappa_1$. The mean and variance of this random variable are $\mathbb{E}[S] = \kappa_1/\kappa_2$ and $\mathrm{Var}[S] = \dfrac{\kappa_1}{\kappa_2^2}$, respectively.

**Definition 2.** *(Hyper-exponential distribution).* The PDF of a random variable $S$ following a hyper-exponential distribution is defined as

$$f_S(s) = \sum_{k=1}^{D} f_{Y_k}(s) p_k,$$

where $Y_k$ is an exponentially distributed random variable with parameter $\gamma_k$, and $p_k$ is the weight factor of random variable $Y_k$ such that $\sum_{k=1}^{D} p_k = 1$. The mean and variance of this random variable are

$$\mathbb{E}[S] = \sum_{k=1}^{D} \frac{p_k}{\gamma_k}, \ \ \mathrm{Var}[S] = \sum_{k=1}^{D} \frac{2p_k}{\gamma_k^2} - \left( \sum_{k=1}^{D} \frac{p_k}{\gamma_k} \right)^2.$$

**Definition 3.** *(Log-normal distribution).* The PDF of a random variable $S$ following a log-normal distribution is defined as

$$f_S(s) = \frac{1}{s\nu_1\sqrt{2\pi}} \exp\left( -\frac{(\ln(s) - \nu_2)^2}{2\nu_1^2} \right), \text{ for } s > 0, \ \nu_1 > 0, \ \nu_2 \in (-\infty, +\infty).$$

The mean and variance of this random variable are

$$\mathbb{E}[S] = \exp\left( \nu_2 + \frac{\nu_1^2}{2} \right), \ \ \mathrm{Var}[S] = \exp(2\nu_2 + \nu_1^2)\left( \exp(\nu_1^2) - 1 \right).$$

**Definition 4.** *(Pareto distribution).* The PDF of a random variable $S$ following a Pareto distribution is defined as

$$f_S(s) = \frac{\omega_2 {\omega_1}^{\omega_2}}{s^{\omega_2+1}}, \ \ \text{for } s \in [\omega_1, \infty], \ \omega_1 > 0, \ \omega_2 > 0.$$

The mean and variance of this random variable are

$$\mathbb{E}[S] = \begin{cases} \infty & \omega_2 \leq 1 \\ \dfrac{\omega_2 \omega_1}{\omega_2 - 1} & \omega_2 > 1, \end{cases}$$

$$\mathrm{Var}[S] = \begin{cases} \infty & \omega_2 \leq 2 \\ \dfrac{\omega_2 \omega_1^2}{(\omega_2 - 1)^2(\omega_2 - 2)} & \omega_2 > 2. \end{cases}$$

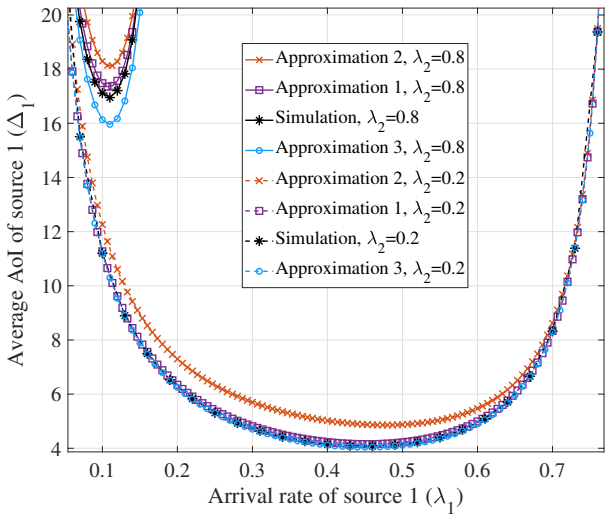


(a)

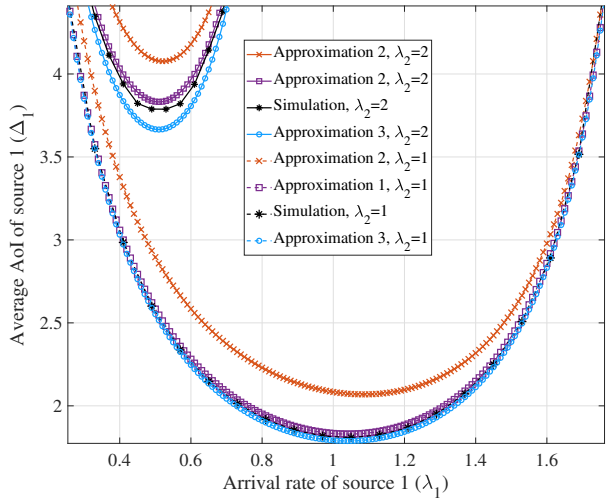


(b)

**Fig. 9. The average AoI of source 1 as a function of $\lambda_1$ for different values of $\lambda_2$ with the service time following a gamma distribution with parameters (a) $\kappa_1 = 2,\ \kappa_2 = 2$, and $\mu = 1$, and (b) $\kappa_1 = 1,\ \kappa_2 = 3$, and $\mu = 3$ (Reprinted by permission [13] © 2020, IEEE).**

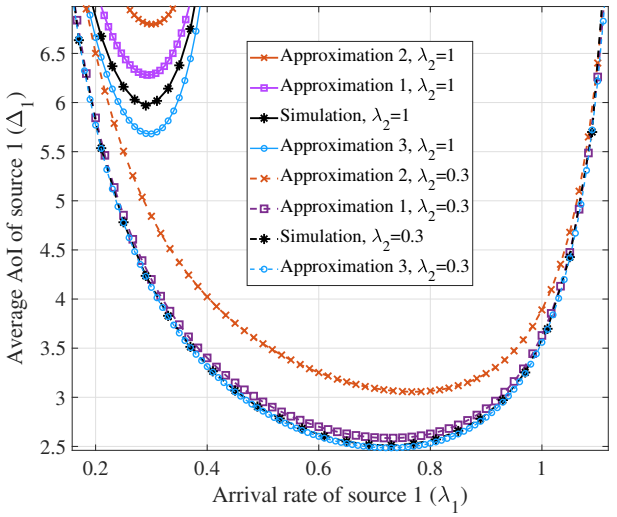


(a)

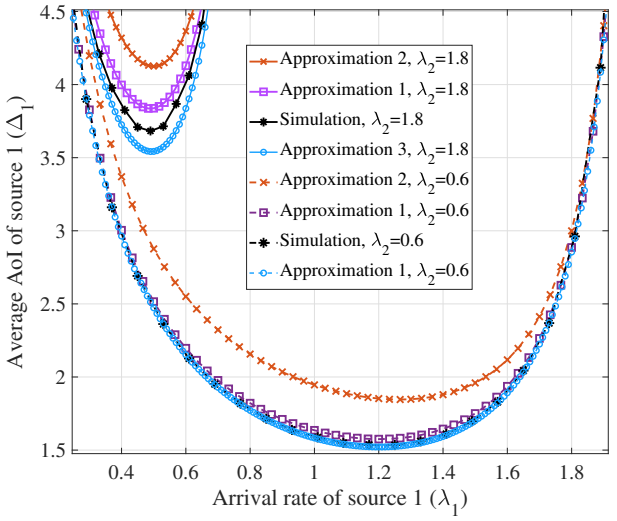


(b)

**Fig. 10. The average AoI of source 1 as a function of $\lambda_1$ for different values of $\lambda_2$ with the service time following a Pareto distribution with parameters (a) $\omega_1 = 0.5,\ \omega_2 = 4$, and $\mu = 1.5$, and (b) $\omega_1 = 0.25,\ \omega_2 = 3$, and $\mu = 8/3$ (Reprinted by permission [13] © 2020, IEEE).**

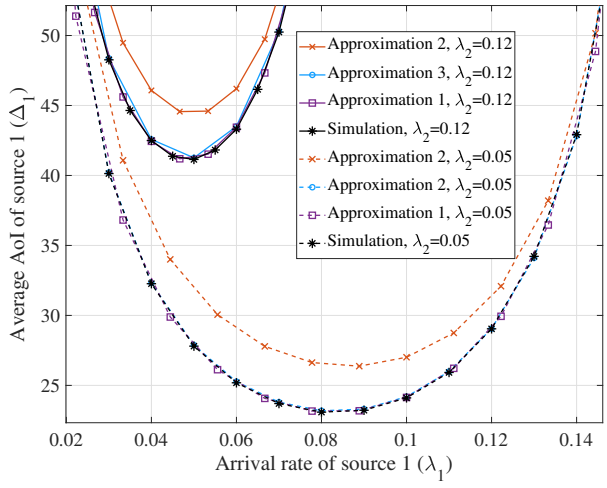


(a)

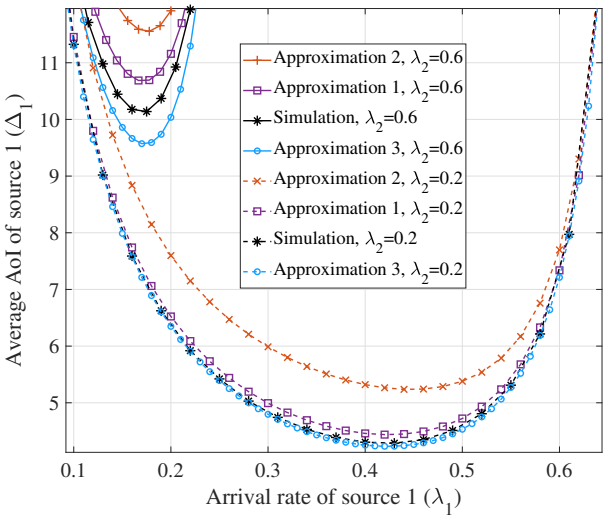


(b)

**Fig. 11. The average AoI of source 1 as a function of $\lambda_1$ for different values of $\lambda_2$ with the service time following a log-normal distribution with parameters (a) $\nu_2 = 1,\ \nu_1 = 1$, and $\mu = 0.2231$, and (b) $\nu_2 = 0.1,\ \nu_1 = 0.2$, and $\mu = 0.8869$ (Reprinted by permission [13] © 2020, IEEE).**

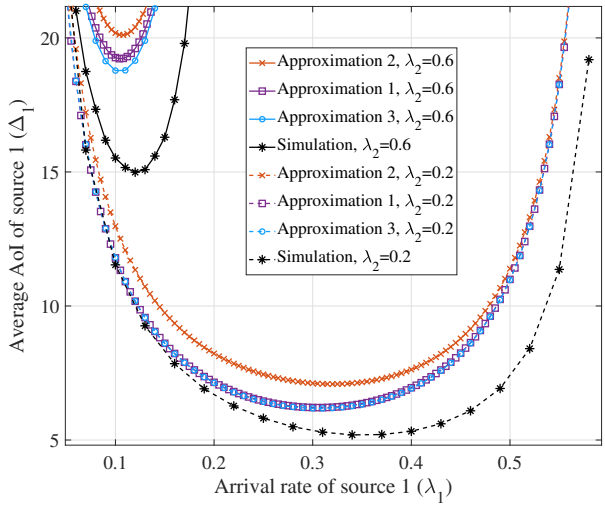


(a)

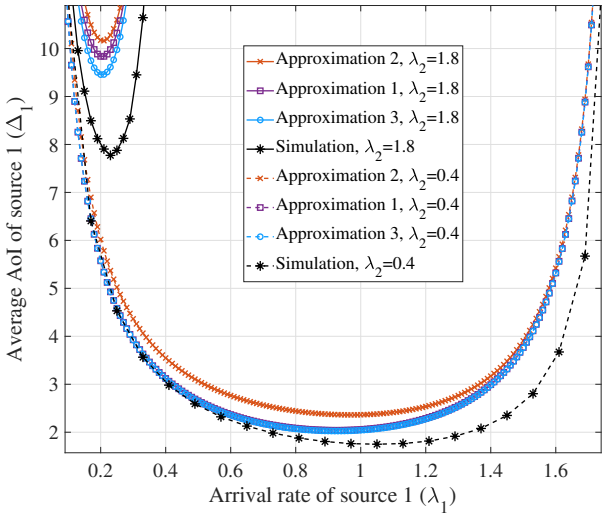


(b)

**Fig. 12. The average AoI of source 1 as a function of $\lambda_1$ for different values of $\lambda_2$ with the service time following a hyper-exponential distribution with parameters (a)** $D = 3,\ \gamma_1 = 0.5,\ \gamma_2 = 1,\ \gamma_3 = 1.5, p_k = 1/D,\ \forall k \in \{1,2,3\}$, **and** $\mu = 0.8182$**, and (b)** $D = 3,\ \gamma_1 = 1.5,\ \gamma_2 = 2.5,\ \gamma_3 = 3.5,\ p_k = 1/D,\ \forall k \in \{1,2,3\}$, **and** $\mu = 2.2183$ **(Reprinted by permission [13] © 2020, IEEE).**

Figs. 9, 10, 11, and 12 depict the average AoI of source 1 as a function of $\lambda_1$ for different service time distributions under both heavy (a larger value of $\lambda_2$) and light (a smaller value of $\lambda_2$) traffic conditions of source 2. Fig. 9 illustrates the average AoI of source 1 for different values of $\lambda_2$ with the service time following a gamma distribution with parameters $\kappa_1 = 2,\ \kappa_2 = 2$, and $\mu = 1$ in Fig. 9(a) and $\kappa_1 = 1,\ \kappa_2 = 3$, and $\mu = 3$ in Fig. 9(b). Fig. 10 illustrates the average AoI of source 1 for different values of $\lambda_2$ with the service time following a Pareto distribution with parameters $\omega_1 = 0.5,\ \omega_2 = 4$, and $\mu = 1.5$ in Fig. 10(a) and $\omega_1 = 0.25,\ \omega_2 = 3$, and $\mu = 8/3$ in Fig. 10(b). Fig. 11 illustrates the average AoI of source 1 for different values of $\lambda_2$ with the service time following a log-normal distribution with parameters $\nu_2 = 1,\ \nu_1 = 1$, and $\mu = 0.2231$ in Fig. 11(a) and $\nu_2 = 0.1,\ \nu_1 = 0.2$, and $\mu = 0.8869$ in Fig. 11(b). Fig. 12 illustrates the average AoI of source 1 for different values of $\lambda_2$ with the service time following a hyper-exponential distribution with parameters $D = 3,\ \gamma_1 = 0.5,\ \gamma_2 = 1,\ \gamma_3 = 1.5, p_k = 1/D,\ \forall k \in \{1,2,3\}$, and $\mu = 0.8182$ in Fig. 12(a) and $D = 3,\ \gamma_1 = 1.5,\ \gamma_2 = 2.5,\ \gamma_3 = 3.5, p_k = 1/D,\ \forall k \in \{1,2,3\}$, and $\mu = 2.2183$ in Fig. 12(b). As can be seen, Approximation 1 and Approximation 3 are relatively tight for both the heavy and light traffic conditions under the gamma, Pareto, and log-normal distributions. By comparing the curves of Approximation 1 and Approximation 2, we can see the effect of approximating the residual service time of source 2 packet that is under service at the arrival instant of packet $1,i$ by the average service time of one packet in the system as compared to completely ignoring it. Finally, as expected, the average AoI provided by Approximation 2 is always higher than that of Approximation 1.

## 2.7 Summary and discussion

In this chapter, a single-server multi-source FCFS queueing model with Poisson arrivals was considered and the average AoI of each source was analyzed. An exact expression for the average AoI for a multi-source M/M/1 queueing model was derived and three approximate expressions for the average AoI for a multi-source M/G/1 queueing model were also derived. The simulation results showed that the approximate expressions for the average AoI are relatively accurate for different service time distributions.

The results showed that generating the status update packets too frequently or too rarely does not minimize the average AoI. This is because generating the status update packets too frequently causes congestion on the transmitter side which results in long waiting time in the queue. On the other hand, generating the status update packets too rarely causes infrequent updates on the sink side which results in stale information. In

addition, the results pointed out the significance of the AoI as a metric in time-sensitive control applications: minimizing merely the average delay does not minimize the AoI.

As discussed in Remark 1, deriving an exact expression for the average AoI in a multi-source M/G/1 queueing model with FCFS serving policy is very complicated and needs the transient analysis of an M/G/1 queueing model. While some accurate approximations can be derived for the average AoI expression, deriving an exact expression for the average AoI in a multi-source FCFS M/G/1 queueing model is an open problem.

It is worth noting that the work in [51], which is the parallel work to the author's original article [13], derived an exact expression for the average AoI for a multi-source M/M/1 FCFS queueing model by using the SHS technique.

In the next chapter, various packet management policies in multi-source status update systems are studied. As it will be shown, by applying appropriate packet management policies, the information freshness can be improved as compared to the FCFS serving policy discussed in this chapter. However, in some situations there is no possibility of applying packet management or all the generated packets are needed to be delivered to the sink. Thus, it is necessary to study queueing models under the FCFS serving policy as well.

# 3 AoI in multi-source queueing models with packet management

In Chapter 2, the average AoI in multi-source queueing models with an FCFS policy was studied. In this chapter, the effectiveness of applying various packet management policies on the AoI is studied. In this regard, a status update system is considered in which two independent sources generate packets according to the Poisson process and the packets are served according to an exponentially distributed service time. Three different source-aware packet management policies are introduced and their AoI performance is analyzed.

In all policies, when the system is empty, any arriving packet immediately enters the server. However, the policies differ in how they handle the arriving packets when the server is busy. In Policy 1, the waiting queue can contain at most two waiting packets at the same time (in addition to the packet under service), one packet of source 1 and one packet of source 2; when the server is busy and a new packet arrives, the possible packet of the same source waiting in the queue (not being served) is replaced by the fresh packet. In Policy 2, the system (i.e., the waiting queue and the server) can contain at most two packets, one from each source; when the server is busy and a new packet arrives, the possible packet of the same source either waiting in the queue or being served is replaced by the fresh packet. Policy 3 is similar to Policy 2 but it does not permit preemption in service, i.e., while a packet is under service all new arrivals from the same source are blocked and cleared.

The average AoI expression under the proposed packet management policies is derived and the MGF of the AoI under Policy 2 and Policy 3 is derived using the SHS technique. By numerical experiments, the effectiveness of the proposed packet management policies in terms of the sum average AoI and fairness between different sources is investigated. The results show that the proposed policies provide better fairness than that of the existing policies. In addition, Policy 2 outperforms the existing policies in terms of the sum average AoI.

The remainder of this chapter is organized as follows. The system model and summary of the main results are presented in Section 3.1. The average AoI analysis by using the SHS technique is presented in Section 3.2. The MGF of the AoI analysis by using the SHS technique is presented in Section 3.3. Numerical results are presented in Section 3.4. Finally, concluding remarks are expressed in Section 3.5.

## 3.1 System model and summary of the main results

Consider a status update system consisting of two independent sources[1], one server, and one sink, as depicted in Fig. 13. Each source observes a random process at random time instants. The sink is interested in timely information about the status of these random processes. Status updates are transmitted as packets, containing the measured value of the monitored process and a time stamp representing the time when the sample was generated. It is assumed that the packets of sources 1 and 2 are generated according to the Poisson process with rates $\lambda_1$ and $\lambda_2$, respectively, and the packets are served according to an exponentially distributed service time with mean $1/\mu$. Let $\rho_1 = \lambda_1/\mu$ and $\rho_2 = \lambda_2/\mu$ be the load of sources 1 and 2, respectively. Since packets of the sources are generated according to the Poisson process and the sources are independent, the packet generation in the system follows the Poisson process with rate $\lambda = \lambda_1 + \lambda_2$. The overall load in the system is $\rho = \rho_1 + \rho_2 = \lambda/\mu$.

In the next subsections, first, each packet management policy is explained, and then, a summary of the main results is presented.

### *Packet management policies*

The structure of the queueing system for all considered policies is illustrated in Fig. 13. In all policies, when the system is empty, any arriving packet immediately enters the server. However, the policies differ in how they handle the arriving packets when the server is busy.

In Policy 1 (see Fig. 13(a)), when the server is busy and a new packet arrives, the possible packet of the same source waiting in the queue (not being served) is replaced by the fresh packet.

In Policy 2 (see Fig. 13(b)), when the server is busy and a new packet arrives, the possible packet of the same source either waiting in the queue or being served (called *self-preemption*) is replaced by the fresh packet.

Policy 3 is similar to Policy 2 but it does not permit preemption in service (see Fig. 13(b)). While a packet is under service, all new arrivals from the same source are blocked and cleared. However, the packet waiting in the queue is replaced upon the arrival of a newer one from the same source. It is also interesting to remark that this policy is also similar to Policy 1 but it has a waiting queue one unit shorter.

[1]Two sources is considered for the sake of clarity of the presentation; the same methodology as used in this chapter can be applied for more than two sources. However, the complexity of the calculations increases exponentially with the number of sources.

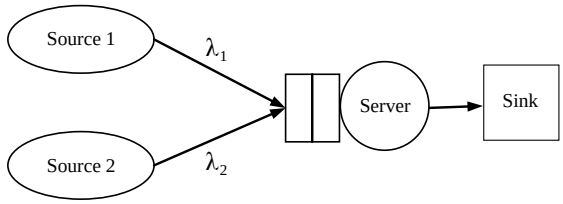


(a) Policy 1: The queue can contain at most two waiting packets at the same time (in addition to the packet under service), one packet of source 1 and one packet of source 2; when the server is busy and a new packet arrives, the possible packet of the same source waiting in the queue (not being served) is replaced by the fresh packet.

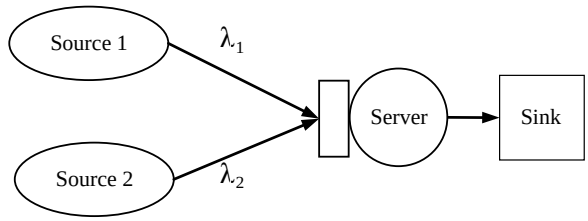


(b) Policies 2 and 3: The system (i.e., the waiting queue and the server) can contain at most two packets, one from each source. In Policy 2, when the server is busy and a new packet arrives, the possible packet of the same source either waiting in the queue or being served is replaced by the fresh packet. Policy 3 is similar to Policy 2 but it does not permit preemption in service.

**Fig. 13. The packet management policies (Reprinted by permission [16] © 2021, IEEE).**

### *Summary of the main results*

In this chapter, the average AoI for each source under Policy 1, Policy 2, and Policy 3 is derived. In addition, the MGF of the AoI for each source under Policy 2 and Policy 3 is derived. The derived results are summarized by the following five theorems.

**Theorem 2.** *The average AoI of source 1 under Policy 1 is given as*

$$\Delta_1 = \frac{\sum_{k=0}^{7} \rho_1^k \eta_k}{\mu \rho_1 (1+\rho_1)^2 \sum_{j=0}^{4} \rho_1^j \hat{\xi}_j},$$

*where*

$$
\begin{aligned}
\eta_0 &= \rho_2^4 + 2\rho_2^3 + 3\rho_2^2 + 2\rho_2 + 1,\\
\eta_1 &= 7\rho_2^4 + 15\rho_2^3 + 21\rho_2^2 + 14\rho_2 + 6,\\
\eta_2 &= 17\rho_2^4 + 46\rho_2^3 + 64\rho_2^2 + 42\rho_2 + 16,\\
\eta_3 &= 15\rho_2^4 + 73\rho_2^3 + 118\rho_2^2 + 78\rho_2 + 26,\\
\eta_4 &= 5\rho_2^4 + 52\rho_2^3 + 124\rho_2^2 + 102\rho_2 + 30,\\
\eta_5 &= 15\rho_2^3 + 66\rho_2^2 + 79\rho_2 + 24,\\
\eta_6 &= 15\rho_2^2 + 31\rho_2 + 11,\\
\eta_7 &= 5\rho_2 + 2,\\
\hat{\xi}_0 &= \rho_2^4 + 2\rho_2^3 + 3\rho_2^2 + 2\rho_2 + 1,\\
\hat{\xi}_1 &= 2\rho_2^4 + 6\rho_2^3 + 9\rho_2^2 + 7\rho_2 + 3,\\
\hat{\xi}_2 &= 6\rho_2^3 + 12\rho_2^2 + 10\rho_2 + 4,\\
\hat{\xi}_3 &= 6\rho_2^2 + 8\rho_2 + 3,\\
\hat{\xi}_4 &= 2\rho_2 + 1.
\end{aligned}
$$

*Proof.* The proof of Theorem 2 appears in Section 3.2.2. □

**Theorem 3.** *The average AoI of source 1 under Policy 2 is given as*

$$
\Delta_1 = \frac{(\rho_2+1)^2 + \sum_{k=1}^{5} \rho_1^k \tilde{\eta}_k}{\mu\rho_1 (1+\rho_1)^2 \left(\rho_1^2(2\rho_2+1) + (\rho_2+1)^2(2\rho_1+1)\right)},
$$

*where*

$$
\begin{aligned}
\tilde{\eta}_1 &= 6\rho_2^2 + 11\rho_2 + 5,\\
\tilde{\eta}_2 &= 13\rho_2^2 + 24\rho_2 + 10,\\
\tilde{\eta}_3 &= 10\rho_2^2 + 27\rho_2 + 10,\\
\tilde{\eta}_4 &= 3\rho_2^2 + 14\rho_2 + 5,\\
\tilde{\eta}_5 &= 3\rho_2 + 1.
\end{aligned}
$$

*Proof.* The proof of Theorem 3 appears in Section 3.2.3. □

**Theorem 4.** *The average AoI of source 1 under Policy 3 is given as*

$$\Delta_1 = \frac{(\rho_2+1)^3 + \sum_{k=1}^{4} \rho_1^k \hat{\eta}_k}{\mu\rho_1(1+\rho_1)(1+\rho_2)\left(\rho_1^2(2\rho_2+1)+(\rho_2+1)^2(2\rho_1+1)\right)},$$

*where*

$$\begin{aligned}
\hat{\eta}_1 &= 5\rho_2^3 + 14\rho_2^2 + 13\rho_2 + 4,\\
\hat{\eta}_2 &= 10\rho_2^3 + 28\rho_2^2 + 25\rho_2 + 7,\\
\hat{\eta}_3 &= 5\rho_2^3 + 22\rho_2^2 + 23\rho_2 + 6,\\
\hat{\eta}_4 &= 5\rho_2^2 + 8\rho_2 + 2.
\end{aligned}$$

*Proof.* The proof of Theorem 4 appears in Section 3.2.4. □

**Theorem 5.** *The MGF of the AoI of source 1 under Policy 2 is given as*

$$M_{\Delta_1}(s) = \frac{\rho_1}{2\rho_1\rho_2+\rho+1}\left[\frac{\rho_2^2(1-\bar{s})^2 + 2\rho_2(1-\bar{s})^3 + (1-\bar{s})^4 + \sum_{k=1}^{4}\rho_1^k\dot{\gamma}_k}{(\rho_1-\bar{s})(1-\bar{s})^2(1+\rho_1-\bar{s})^2(1+\rho-\bar{s})^2}\right], \quad (68)$$

*where* $\bar{s} = \dfrac{s}{\mu}$ *and*

$$\begin{aligned}
\dot{\gamma}_1 &= \rho_2^2(4-6\bar{s}+4\bar{s}^2-\bar{s}^3)+\rho_2(8-20\bar{s}+16\bar{s}^2-6\bar{s}^3+\bar{s}^4)+(1-\bar{s})^3(4-\bar{s}),\\
\dot{\gamma}_2 &= \rho_2^2(5-6\bar{s}+2\bar{s}^2)+\rho_2(12-22\bar{s}+14\bar{s}^2-3\bar{s}^3)+3(1-\bar{s})^2(2-\bar{s}),\\
\dot{\gamma}_3 &= \rho_2^2(2-\bar{s})+\rho_2(8-10\bar{s}+3\bar{s}^2)+3\bar{s}^2-7\bar{s}+4,\\
\dot{\gamma}_4 &= \rho_2(2-\bar{s})+1-\bar{s}.
\end{aligned}$$

*Proof.* The proof of Theorem 5 appears in Section 3.3.2. □

**Theorem 6.** *The MGF of the AoI of source 1 under Policy 3 is given as*

$$M_{\Delta_1}(s) = \frac{\rho_1}{2\rho_1\rho_2+\rho+1}\left[\frac{\rho_2^3(1-\bar{s})^2+3\rho_2^2(1-\bar{s})^3+3\rho_2(1-\bar{s})^4+(1-\bar{s})^5+\sum_{k=1}^{3}\rho_1^k\bar{\gamma}_k}{(\rho_1-\bar{s})(1-\bar{s})^3(1+\rho_1-\bar{s})(1+\rho-\bar{s})}\right] \quad (69)$$

*where* $\bar{s} = \dfrac{s}{\mu}$ *and*

$$\begin{aligned}
\bar{\gamma}_1 &= \rho_2^3(3-3\bar{s}+\bar{s}^2)+\rho_2^2(9-19\bar{s}+11\bar{s}^2-2\bar{s}^3)+\\
&\quad \rho_2(9-28\bar{s}+29\bar{s}^2-11\bar{s}^3+\bar{s}^4)+3(1-\bar{s})^4,\\
\bar{\gamma}_2 &= \rho_2^3(2-\bar{s})+\rho_2^2(8-10\bar{s}+3\bar{s}^2)+\rho_2(9-19\bar{s}+11\bar{s}^2-2\bar{s}^3)+(1-\bar{s})^3,\\
\bar{\gamma}_3 &= \rho_2^2(2-\bar{s})+\rho_2(3-3\bar{s}+\bar{s}^2)+(1-\bar{s})^2.
\end{aligned}$$

*Proof.* The proof of Theorem 6 appears in Section 3.3.2. □

## 3.2 Average AoI

In this section, first, the main idea behind the SHS technique as the key tool to calculate average AoI is briefly presented, then the average AoI of each source under the proposed packet management policies is derived. The readers are referred to [9] for more details of the SHS technique.

### *3.2.1 A brief introduction to the SHS technique for calculating average AoI*

The SHS technique models a queueing system through the states $(q(t),\mathbf{x}(t))$, where $q(t) \in \mathscr{Q} = \{0,1,\ldots,m\}$ is a continuous-time finite-state Markov chain that describes the occupancy of the system and $\mathbf{x}(t) = [x_0(t)\ x_1(t)\cdots x_n(t)] \in \mathbb{R}^{1\times(n+1)}$ is a continuous process that describes the evolution of age-related processes at the sink. Following the approach in [9], the source of interest is labeled as source 1 and the continuous process $\mathbf{x}(t)$ is employed to track the age of source 1 status updates at the sink.

The Markov chain $q(t)$ can be presented as a graph $(\mathscr{Q},\mathscr{L})$ where each discrete state $q(t) \in \mathscr{Q}$ is a node of the chain and a (directed) link $l \in \mathscr{L}$ from node $q_l$ to node $q'_l$ indicates a transition from state $q_l \in \mathscr{Q}$ to state $q'_l \in \mathscr{Q}$.

A transition occurs when a packet arrives or departs in the system. Since the time elapsed between departures and arrivals is exponentially distributed, transition $l \in \mathscr{L}$ from state $q_l$ to state $q'_l$ occurs with the exponential rate $\lambda^{(l)}\delta_{q_l,q(t)}$[2], where the Kronecker delta function $\delta_{q_l,q(t)}$ ensures that the transition $l$ occurs only when the discrete state $q(t)$ is equal to $q_l$. When a transition $l$ occurs, the discrete state $q_l$ changes to state $q'_l$, and the continuous state $\mathbf{x}$ is reset to $\mathbf{x}'$ according to a binary transition

[2] In the considered system model, $\lambda^{(l)}$ can represent three quantities: arrival rate of source 1 ($\lambda_1$), arrival rate of source 2 ($\lambda_2$), and the service rate ($\mu$).

reset map matrix $\mathbf{A}_l \in \mathbb{B}^{(n+1)\times(n+1)}$ as $\mathbf{x}' = \mathbf{x}\mathbf{A}_l$. In addition, at each state $q(t) = q \in \mathscr{Q}$, the continuous state $\mathbf{x}$ evolves as a piece-wise linear function through the differential equation $\dot{\mathbf{x}}(t) \triangleq \dfrac{\partial \mathbf{x}(t)}{\partial t} = \mathbf{1}$, where $\mathbf{1}$ is the row vector $[1 \cdots 1] \in \mathbb{R}^{1\times(n+1)}$

Note that unlike in a typical continuous-time Markov chain, a transition from a state to itself (i.e., a self-transition) is possible in $q(t) \in \mathscr{Q}$. In the case of a self-transition, a reset of the continuous state $\mathbf{x}$ takes place, but the discrete state remains the same. In addition, for a given pair of states $\bar{q}, \hat{q} \in \mathscr{Q}$, there may be multiple transitions $l$ and $l'$ such that the discrete state changes from $\bar{q}$ to $\hat{q}$ but the transition reset maps $\mathbf{A}_l$ and $\mathbf{A}_{l'}$ are different (for more details, see [9, Sect. III]).

To calculate the average AoI using the SHS technique, the state probabilities of the Markov chain and the correlation vector between the discrete state $q(t)$ and the continuous state $\mathbf{x}(t)$ need to be calculated. Let $\pi_q(t)$ denote the probability of being in state $q$ of the Markov chain and $\mathbf{v}_q(t) = [v_{q0}(t) \cdots v_{qn}(t)] \in \mathbb{R}^{1\times(n+1)}$ denote the correlation vector between the discrete state $q(t)$ and the continuous state $\mathbf{x}(t)$. Accordingly, we have

$$\pi_q(t) = \Pr(q(t) = q) = \mathbb{E}[\delta_{q,q(t)}],\ \forall q \in \mathscr{Q}, \tag{70}$$

$$\mathbf{v}_q(t) = [v_{q0}(t) \cdots v_{qn}(t)] = \mathbb{E}[\mathbf{x}(t)\delta_{q,q(t)}],\ \forall q \in \mathscr{Q}. \tag{71}$$

Let $\mathscr{L}'_q$ denote the set of incoming transitions and $\mathscr{L}_q$ denote the set of outgoing transitions for state $q$, defined as

$$\mathscr{L}'_q = \{l \in \mathscr{L} : q'_l = q\},\ \forall q \in \mathscr{Q},$$
$$\mathscr{L}_q = \{l \in \mathscr{L} : q_l = q\},\ \forall q \in \mathscr{Q}.$$

Following the ergodicity assumption of the Markov chain $q(t)$ in the AoI analysis [9, 45, 53], the state probability vector $\boldsymbol{\pi}(t) = [\pi_0(t) \cdots \pi_m(t)]$ converges uniquely to the stationary vector $\bar{\boldsymbol{\pi}} = [\bar{\pi}_0 \cdots \bar{\pi}_m]$ satisfying [9]

$$\bar{\pi}_q \sum_{l\in\mathscr{L}_q} \lambda^{(l)} = \sum_{l\in\mathscr{L}'_q} \lambda^{(l)} \bar{\pi}_{q_l},\ \forall q \in \mathscr{Q}, \tag{72}$$

$$\sum_{q\in\mathscr{Q}} \bar{\pi}_q = 1. \tag{73}$$

Further, it has been shown in [9, Theorem 4] that under the ergodicity assumption of the Markov chain $q(t)$ with stationary distribution $\bar{\boldsymbol{\pi}} \succ \mathbf{0}$, the existence of a non-negative

solution, $\bar{\mathbf{v}}_q = [\bar{v}_{q0} \cdots \bar{v}_{qn}], \forall q \in \mathscr{Q}$, for the following system of linear equations

$$\bar{\mathbf{v}}_q \sum_{l \in \mathscr{L}_q} \lambda^{(l)} = \mathbf{1}\bar{\pi}_q + \sum_{l \in \mathscr{L}'_q} \lambda^{(l)} \bar{\mathbf{v}}_{q_l} \mathbf{A}_l, \ \forall q \in \mathscr{Q}, \tag{74}$$

implies that the correlation vector $\mathbf{v}_q(t)$ converges to $\bar{\mathbf{v}}_q = [\bar{v}_{q0} \cdots \bar{v}_{qn}], \forall q \in \mathscr{Q}$ as $t \to \infty$. Finally, the average AoI of source 1 is calculated by [9, Theorem 4]

$$\Delta_1 = \sum_{q \in \mathscr{Q}} \bar{v}_{q0}. \tag{75}$$

As (75) implies, the main challenge in calculating the average AoI of a source using the SHS technique reduces to deriving the first elements of each correlation vector $\bar{\mathbf{v}}_q$, i.e., $\bar{v}_{q0}$, $\forall q \in \mathscr{Q}$. Note that these quantities are, in general, different for each particular queueing model.

The SHS technique is used to calculate the average AoI of each source under the considered packet management policies described in Section 3.1. Recall from (75) that the characterization of the average AoI in each of our queueing setup is accomplished by deriving the quantities $\bar{v}_{q0}$, $\forall q \in \mathscr{Q}$. The next three sections are devoted to elaborate derivations of these quantities.

### 3.2.2 Average AoI under policy 1

In Policy 1, the state space of the Markov chain is $\mathscr{Q} = \{0, 1, \ldots, 5\}$, with each state presented in Table 2. For example, $q = 0$ indicates that the server is idle which is shown by I; $q = 1$ indicates that a packet is under service, i.e., the queue is empty and the server is busy which is shown by B; and $q = 5$ indicates that server is busy, the first packet in the queue (i.e., the packet that is at the head of the queue as depicted in Fig. 13(a)) is a source 2 packet, and the second packet in the queue is a source 1 packet.

The continuous process is $\mathbf{x}(t) = [x_0(t)\ x_1(t)\ x_2(t)\ x_3(t)]$, where $x_0(t)$ is the current AoI of source 1 at time instant $t$, $\Delta_1(t)$; $x_1(t)$ encodes what $\Delta_1(t)$ would become if the packet that is under service is delivered to the sink at time instant $t$; $x_2(t)$ encodes what $\Delta_1(t)$ would become if the first packet in the queue is delivered to the sink at time instant $t$; $x_3(t)$ encodes what $\Delta_1(t)$ would become if the second packet in the queue is delivered to the sink at time instant $t$.

Recall that our goal is to find $\bar{v}_{q0}, \forall q \in \mathscr{Q}$, to calculate the average AoI of source 1 in (75). To this end, we need to solve the system of linear equations (74) with variables $\bar{\mathbf{v}}_q, \forall q \in \mathscr{Q}$. To form the system of linear equations (74) for each state $\forall q \in \mathscr{Q}$, we

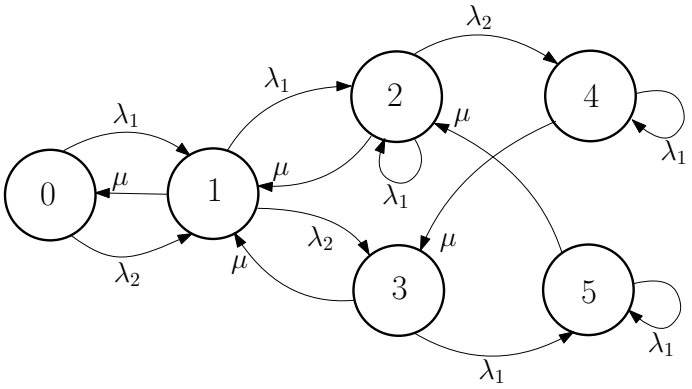


**Fig. 14. The SHS Markov chain for Policy 1 (Reprinted by permission [16] © 2021, IEEE).**

**Table 2. SHS Markov chain states for Policy 1.**

| State | Source index of the second packet in the queue | Source index of the first packet in the queue | Server |
|---|---|---|---|
| 0 | - | - | I |
| 1 | - | - | B |
| 2 | - | 1 | B |
| 3 | - | 2 | B |
| 4 | 2 | 1 | B |
| 5 | 1 | 2 | B |

need to determine $\mathbf{b}_q$, $\bar{\pi}_q$, and $\bar{\mathbf{v}}_{q_l}\mathbf{A}_l$ for each incoming transition $l \in \mathscr{L}'_q$. Next, these quantities are derived for Policy 1.

### *Determining the value of $\bar{\mathbf{v}}_{q_l}\mathbf{A}_l$ for incoming transitions for each state $q \in \mathscr{Q}$*

The Markov chain for the discrete state $q(t)$ with the incoming and outgoing transitions for each state $q \in \mathscr{Q}$ is shown in Fig. 14. The transitions between the discrete states $q_l \to q'_l$, $\forall l \in \mathscr{L}$, and their effects on the continuous state $\mathbf{x}(t)$ are summarized in Table 3. In the following, the transitions presented in Table 3 are explained:

– *l=1*: A source 1 packet arrives at an empty system. With this arrival/transition, the AoI of source 1 does not change, i.e., $x'_0 = x_0$. This is because the arrival of source 1 packet does not yield an age reduction until it is delivered to the sink. Since the arriving source 1 packet is fresh and its age is zero, we have $x'_1 = 0$. Since with this arrival the queue is still empty, $x_2$ and $x_3$ become irrelevant to the AoI of source 1, and thus, $x'_2 = x_2$ and $x'_3 = x_3$. Note that if the system moves into a new state where $x_j$ is irrelevant, we set $x'_j = x_j$, $j \in \{1,2,3\}$. An interpretation of this assignment is

**Table 3. Table of transitions for the Markov chain of Policy 1 in Fig. 14.**

| $l$ | $q_l \to q_l'$ | $\lambda^{(l)}$ | $\mathbf{A}_l$ | $\mathbf{xA}_l$ | $\bar{\mathbf{v}}_{q_l}\mathbf{A}_l$ |
|---|---|---|---|---|---|
| 1 | $0 \to 1$ | $\lambda_1$ | $[x_0\ 0\ x_2\ x_3]$ | $\begin{bmatrix}1&0&0&0\\0&0&0&0\\0&0&1&0\\0&0&0&1\end{bmatrix}$ | $[\bar{v}_{00}\ 0\ \bar{v}_{02}\ \bar{v}_{03}]$ |
| 2 | $0 \to 1$ | $\lambda_2$ | $[x_0\ x_0\ x_2\ x_3]$ | $\begin{bmatrix}1&1&0&0\\0&0&0&0\\0&0&1&0\\0&0&0&1\end{bmatrix}$ | $[\bar{v}_{00}\ \bar{v}_{00}\ \bar{v}_{02}\ \bar{v}_{03}]$ |
| 3 | $1 \to 0$ | $\mu$ | $[x_1\ x_1\ x_2\ x_3]$ | $\begin{bmatrix}0&0&0&0\\1&1&0&0\\0&0&1&0\\0&0&0&1\end{bmatrix}$ | $[\bar{v}_{11}\ \bar{v}_{11}\ \bar{v}_{12}\ \bar{v}_{13}]$ |
| 4 | $1 \to 2$ | $\lambda_1$ | $[x_0\ x_1\ 0\ x_3]$ | $\begin{bmatrix}1&0&0&0\\0&1&0&0\\0&0&0&0\\0&0&0&1\end{bmatrix}$ | $[\bar{v}_{10}\ \bar{v}_{11}\ 0\ \bar{v}_{13}]$ |
| 5 | $1 \to 3$ | $\lambda_2$ | $[x_0\ x_1\ x_1\ x_3]$ | $\begin{bmatrix}1&0&0&0\\0&1&1&0\\0&0&0&0\\0&0&0&1\end{bmatrix}$ | $[\bar{v}_{10}\ \bar{v}_{11}\ \bar{v}_{11}\ \bar{v}_{13}]$ |
| 6 | $2 \to 1$ | $\mu$ | $[x_1\ x_2\ x_2\ x_3]$ | $\begin{bmatrix}0&0&0&0\\1&0&0&0\\0&1&1&0\\0&0&0&1\end{bmatrix}$ | $[\bar{v}_{21}\ \bar{v}_{22}\ \bar{v}_{22}\ \bar{v}_{23}]$ |
| 7 | $3 \to 1$ | $\mu$ | $[x_1\ x_1\ x_2\ x_3]$ | $\begin{bmatrix}0&0&0&0\\1&1&0&0\\0&0&1&0\\0&0&0&1\end{bmatrix}$ | $[\bar{v}_{31}\ \bar{v}_{31}\ \bar{v}_{32}\ \bar{v}_{33}]$ |
| 8 | $2 \to 2$ | $\lambda_1$ | $[x_0\ x_1\ 0\ x_3]$ | $\begin{bmatrix}1&0&0&0\\0&1&0&0\\0&0&0&0\\0&0&0&1\end{bmatrix}$ | $[\bar{v}_{20}\ \bar{v}_{21}\ 0\ \bar{v}_{23}]$ |
| 9 | $2 \to 4$ | $\lambda_2$ | $[x_0\ x_1\ x_2\ x_2]$ | $\begin{bmatrix}1&0&0&0\\0&1&0&0\\0&0&1&0\\0&0&0&1\end{bmatrix}$ | $[\bar{v}_{20}\ \bar{v}_{21}\ \bar{v}_{22}\ \bar{v}_{22}]$ |
| 10 | $3 \to 5$ | $\lambda_1$ | $[x_0\ x_1\ x_1\ 0]$ | $\begin{bmatrix}1&0&0&0\\0&1&1&0\\0&0&0&0\\0&0&0&0\end{bmatrix}$ | $[\bar{v}_{30}\ \bar{v}_{31}\ \bar{v}_{31}\ 0]$ |
| 11 | $4 \to 4$ | $\lambda_1$ | $[x_0\ x_1\ 0\ 0]$ | $\begin{bmatrix}1&0&0&0\\0&1&0&0\\0&0&0&0\\0&0&0&0\end{bmatrix}$ | $[\bar{v}_{40}\ \bar{v}_{41}\ 0\ 0]$ |
| 12 | $5 \to 5$ | $\lambda_1$ | $[x_0\ x_1\ x_1\ 0]$ | $\begin{bmatrix}1&0&0&0\\0&1&1&0\\0&0&0&0\\0&0&0&0\end{bmatrix}$ | $[\bar{v}_{50}\ \bar{v}_{51}\ \bar{v}_{51}\ 0]$ |
| 13 | $4 \to 3$ | $\mu$ | $[x_1\ x_2\ x_2\ x_3]$ | $\begin{bmatrix}0&0&0&0\\1&0&0&0\\0&1&1&0\\0&0&0&1\end{bmatrix}$ | $[\bar{v}_{41}\ \bar{v}_{42}\ \bar{v}_{42}\ \bar{v}_{43}]$ |
| 14 | $5 \to 2$ | $\mu$ | $[x_1\ x_1\ x_3\ x_3]$ | $\begin{bmatrix}0&0&0&0\\1&1&0&0\\0&0&0&0\\0&0&1&1\end{bmatrix}$ | $[\bar{v}_{51}\ \bar{v}_{51}\ \bar{v}_{53}\ \bar{v}_{53}]$ |

that $x_j$ has not changed in the transition to the new state. Finally, we have

$$\mathbf{x}' = [x_0\ x_1\ x_2\ x_3]\mathbf{A}_1 = [x_0\ 0\ x_2\ x_3]. \tag{76}$$

According to (76), it can be shown that the binary matrix $\mathbf{A}_1$ is given by

$$\mathbf{A}_1 = \begin{bmatrix} 1 & 0 & 0 & 0 \\ 0 & 0 & 0 & 0 \\ 0 & 0 & 1 & 0 \\ 0 & 0 & 0 & 1 \end{bmatrix}. \tag{77}$$

Then, by using (77), $\bar{\mathbf{v}}_0\mathbf{A}_1$ is calculated as

$$\bar{\mathbf{v}}_0\mathbf{A}_1 = [\bar{v}_{00}\ \bar{v}_{01}\ \bar{v}_{02}\ \bar{v}_{03}]\mathbf{A}_1 = [\bar{v}_{00}\ 0\ \bar{v}_{02}\ \bar{v}_{03}]. \tag{78}$$

It can be seen from (76)-(78) that when we have $\mathbf{x}'$ for a transition $l \in \mathscr{L}$, it is easy to calculate $\bar{\mathbf{v}}_{q_l}\mathbf{A}_l$. Thus, for the rest of the transitions, the calculation of $\mathbf{x}'$ is just explained and the final expressions of $\mathbf{A}_l$ and $\bar{\mathbf{v}}_{q_l}\mathbf{A}_l$ are presented.

- *l=2*: A source 2 packet arrives at an empty system. We have $x_0' = x_0$, because this arrival does not change the AoI at the sink. Since the arriving packet is a source 2 packet, its delivery does not change the AoI of source 1, thus we have $x_1' = x_0$. Moreover, since the queue is empty, $x_2$ and $x_3$ become irrelevant, and we have $x_2' = x_2$ and $x_3' = x_3$.
- *l=3*: A packet is under service and it completes service and is delivered to the sink. With this transition, the AoI at the sink is reset to the age of the packet that just completed service, and thus, $x_0' = x_1$. Since the system enters state $q = 0$, we have $x_1' = x_1$, $x_2' = x_2$, and $x_3' = x_3$.
- *l=4*: A packet is under service and a source 1 packet arrives. In this transition, we have $x_0' = x_0$ because there is no departure. The delivery of the packet under service reduces the AoI to $x_1$ and thus, $x_1' = x_1$. Since the arriving source 1 packet is fresh and its age is zero, we have $x_2' = 0$. Since there is only one packet in the queue, $x_3$ becomes irrelevant, and we have $x_3' = x_3$.
- *l=5*: A packet is under service and a source 2 packet arrives. In this transition, we have $x_0' = x_0$ because there is no departure. The delivery of the packet under service reduces the AoI to $x_1$ and thus, $x_1' = x_1$. Since the arriving source 2 packet, its delivery does not change the AoI of source 1, and thus, we have $x_2' = x_1$. Since there is only one packet in the queue, $x_3$ becomes irrelevant, and we have $x_3' = x_3$.

– *l=6*: A source 1 packet is in the queue, a packet is under service and it completes service and is delivered to the sink. With this transition, the AoI at the sink is reset to the age of the packet that just completed service, and thus, $x'_0 = x_1$. Since the source 1 packet in the queue goes to the server, we have $x'_1 = x_2$. In addition, since with this departure the queue becomes empty, we have $x'_2 = x_2$ and $x'_3 = x_3$.
– *l=7*: A source 2 packet is in the queue, a packet is under service and it completes service and is delivered to the sink. With this transition, the AoI at the sink is reset to the age of the packet that just completed service, and thus, $x'_0 = x_1$. Since the source 2 packet in the queue goes to the server and its delivery does not change the AoI of source 1, we have $x'_1 = x_1$. In addition, since with this departure the queue becomes empty, we have $x'_2 = x_2$ and $x'_3 = x_3$.
– *l=8*: A packet is under service, a source 1 packet is in the queue, and a source 1 packet arrives. According to Policy 1, the source 1 packet in the queue is replaced by the fresh source 1 packet. In this transition, we have $x'_0 = x_0$ because there is no departure. The delivery of the packet under service reduces the AoI to $x_1$, and thus, $x'_1 = x_1$. Since the arriving source 1 packet is fresh and its age is zero, we have $x_2 = 0$. Since there is only one packet in the queue, we have $x'_3 = x_3$.
– *l=9*: A packet is under service, a source 1 packet is in the queue, and a source 2 packet arrives. In this transition, $x'_0 = x_0$ because there is no departure. The delivery of the packet under service reduces the AoI to $x_1$, and thus, $x'_1 = x_1$. The delivery of the first packet in the queue reduces the AoI to $x_2$, and thus, $x'_2 = x_2$. Since the second packet in the queue is a source 2 packet, its delivery does not change the AoI of source 1, and thus, we have $x'_3 = x_2$.
– *l=10*: A packet is under service, a source 2 packet is in the queue, and a source 1 packet arrives. In this transition, $x'_0 = x_0$ because there is no departure. The delivery of the packet under service reduces the AoI to $x_1$, and thus, $x'_1 = x_1$. Since the first packet in the queue is a source 2 packet, its delivery does not change the AoI of source 1, and thus we have $x'_1 = x_1$. Since the arriving source 1 packet is fresh and its age is zero, we have $x_3 = 0$.
– *l=11*: A packet is under service, the first packet in the queue is a source 1 packet, the second packet in the queue is a source 2 packet, and a source 1 packet arrives. According to Policy 1, the source 1 packet in the queue is replaced by the fresh source 1 packet. In this transition, we have $x'_0 = x_0$ because there is no departure. The delivery of the packet under service reduces the AoI to $x_1$, thus, $x'_1 = x_1$. Since the arriving source 1 packet is fresh and its age is zero, we have $x'_2 = 0$. Since the second packet in the queue is a source 2 packet, its delivery does not change the AoI

of source 1, and thus, we have $x_3' = 0$. The reset maps of transition $l = 12$ can be derived similarly.

– *l=13*: The first packet in the queue is a source 1 packet, the second packet in the queue is a source 2 packet, and the packet under service completes service and is delivered to the sink. With this transition, the AoI at the sink is reset to the age of the source 1 packet that just completed service, and thus, $x_0' = x_1$. Since the first packet in the queue goes to the server, we have $x_1' = x_2$. In addition, since with this departure the queue holds the source 2 packet and its delivery does not change the AoI of source 1, we have $x_2' = x_2$ and $x_3' = x_3$. The reset maps of transition $l = 14$ can be derived similarly.

Having defined the sets of incoming and outgoing transitions, and the value of $\bar{\mathbf{v}}_{q_l}\mathbf{A}_l$ for each incoming transition for each state $q \in \mathscr{Q}$, the remaining task is to derive the stationary probability vector $\bar{\boldsymbol{\pi}}$. This is carried out next.

### *Calculation of $\bar{\pi}_q$ for each state $q \in \mathscr{Q}$*

To calculate the stationary probability vector $\bar{\boldsymbol{\pi}}$, (72) and (73) are used. Using (72) and the transitions between the different states presented in Table 3, it can be shown that the stationary probability vector $\bar{\boldsymbol{\pi}}$ satisfies $\bar{\boldsymbol{\pi}}\bar{\mathbf{D}} = \bar{\boldsymbol{\pi}}\bar{\mathbf{Q}}$ where the diagonal matrix $\bar{\mathbf{D}} \in \mathbb{R}^{(n+1)\times(n+1)}$ and matrix $\bar{\mathbf{Q}} \in \mathbb{R}^{(n+1)\times(n+1)}$ are given as

$$\bar{\mathbf{D}} = \text{diag}[\lambda, \lambda+\mu, \lambda+\mu, \lambda_1+\mu, \lambda_1+\mu, \lambda_1+\mu],$$

$$\bar{\mathbf{Q}} = \begin{bmatrix} \mu & \lambda & 0 & 0 & 0 & 0 \\ 0 & 0 & \lambda_1 & \lambda_2 & \lambda_2 & 0 \\ 0 & \mu & \lambda_1 & 0 & 0 & 0 \\ 0 & \mu & 0 & 0 & 0 & \lambda_1 \\ 0 & 0 & 0 & \mu & \lambda_1 & 0 \\ 0 & 0 & \mu & 0 & 0 & \lambda_1 \end{bmatrix},$$

where $\text{diag}[a_1, a_2, \ldots, a_n]$ denotes a diagonal matrix with elements $a_1, a_2, \ldots, a_n$ on its main diagonal. Using the above $\bar{\boldsymbol{\pi}}\bar{\mathbf{D}} = \bar{\boldsymbol{\pi}}\bar{\mathbf{Q}}$ and $\sum_{q\in\mathscr{Q}} \bar{\pi}_q = 1$ in (73), the stationary probabilities are given as

$$\bar{\boldsymbol{\pi}} = \frac{1}{\rho^2 + \rho(2\rho_1\rho_2 + 1) + 1} \left[1 \;\; \rho \;\; \rho_1\rho \;\; \rho_2\rho \;\; \rho_1\rho_2\rho \;\; \rho_1\rho_2\rho\right]. \tag{79}$$

*Average AoI calculation*

By substituting (79) into (74) and solving the corresponding system of linear equations, the values of $\bar{v}_{q0}$, $\forall q \in \mathscr{Q}$, are calculated as presented in Appendix 1.2. Finally, substituting the values of $\bar{v}_{q0}$, $\forall q \in \mathscr{Q}$, into (75) results in the average AoI of source 1 under Policy 1, given in Theorem 2. Note that the expression is *exact*; it characterizes the average AoI in the considered queueing model in *closed form*.

### 3.2.3 Average AoI under policy 2

Recall from Section 3.1 that the main difference of Policy 2 compared to Policy 1 treated above is that *the system* can contain only two packets, one packet of source 1 and one packet of source 2. Accordingly for Policy 2, the state space of the Markov chain is $\mathscr{Q} = \{0,1,2,3,4\}$, where $q = 0$ indicates that the server is idle, i.e., the system is empty; $q = 1$ indicates that a source 1 packet is under service and the queue is empty; $q = 2$ indicates that a source 2 packet is under service and the queue is empty; $q = 3$ indicates that a source 1 packet is under service, and a source 2 packet is in the queue; and $q = 4$ indicates that a source 2 packet is under service, and a source 1 packet is in the queue.

The continuous process is $\mathbf{x}(t) = [x_0(t)\ x_1(t)\ x_2(t)]$, where $x_0(t)$ is the current AoI of source 1 at time instant $t$, $\Delta_1(t)$; $x_1(t)$ encodes what $\Delta_1(t)$ would become if the packet that is under service is delivered to the sink at time instant $t$; $x_2(t)$ encodes what $\Delta_1(t)$ would become if the packet in the queue is delivered to the sink at time instant $t$. Next, the required quantities to form the system of linear equations in (74) under Policy 2 are determined.

*Determining the value of $\bar{\mathbf{v}}_{q_l}\mathbf{A}_l$ for incoming transitions for each state $q \in \mathscr{Q}$*

The Markov chain for the discrete state $q(t)$ is shown in Fig. 15. The transitions between the discrete states $q_l \to q'_l$, $\forall l \in \mathscr{L}$, and their effects on the continuous state $\mathbf{x}(t)$ are summarized in Table 4. In the following, the transitions presented in Table 4 are explained:

- *l=1*: A source 1 packet arrives at an empty system. With this transition we have $x'_0 = x_0$ because there is no departure. Since with this arrival the queue is still empty, $x_2$ becomes irrelevant to the AoI of source 1, and thus, $x'_2 = x_2$.
- *l=2*: A source 2 packet arrives at an empty system. We have $x'_0 = x_0$, because this arrival does not change the AoI at the sink. Since the arriving packet is a source 2

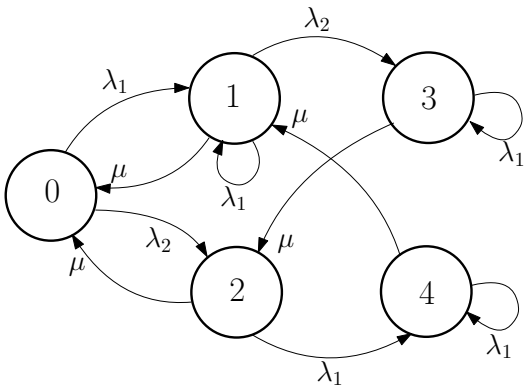


**Fig. 15. The SHS Markov chain for Policy 2 (Reprinted by permission [16] © 2021, IEEE).**

**Table 4. Table of transitions for the Markov chain of Policy 2 in Fig. 15 to calculate the average AoI.**

| $l$ | $q_l \to q_l'$ | $\lambda^{(l)}$ | $\mathbf{x}\mathbf{A}_l$ | $\mathbf{A}_l$ | $\bar{\mathbf{v}}_{q_l}\mathbf{A}_l$ |
|---|---|---|---|---|---|
| 1 | $0 \to 1$ | $\lambda_1$ | $[x_0\ 0\ x_2]$ | $\begin{bmatrix}1&0&0\\0&0&0\\0&0&1\end{bmatrix}$ | $[\bar{v}_{00}\ 0\ \bar{v}_{02}]$ |
| 2 | $0 \to 2$ | $\lambda_2$ | $[x_0\ x_0\ x_2]$ | $\begin{bmatrix}1&1&0\\0&0&0\\0&0&1\end{bmatrix}$ | $[\bar{v}_{00}\ \bar{v}_{00}\ \bar{v}_{02}]$ |
| 3 | $1 \to 1$ | $\lambda_1$ | $[x_0\ 0\ x_2]$ | $\begin{bmatrix}1&0&0\\0&0&0\\0&0&1\end{bmatrix}$ | $[\bar{v}_{10}\ 0\ \bar{v}_{12}]$ |
| 4 | $1 \to 3$ | $\lambda_2$ | $[x_0\ x_1\ x_1]$ | $\begin{bmatrix}1&0&0\\0&1&1\\0&0&0\end{bmatrix}$ | $[\bar{v}_{10}\ \bar{v}_{11}\ \bar{v}_{11}]$ |
| 5 | $2 \to 4$ | $\lambda_1$ | $[x_0\ x_0\ 0]$ | $\begin{bmatrix}1&1&0\\0&0&0\\0&0&0\end{bmatrix}$ | $[\bar{v}_{20}\ \bar{v}_{20}\ 0]$ |
| 6 | $3 \to 3$ | $\lambda_1$ | $[x_0\ 0\ 0]$ | $\begin{bmatrix}1&0&0\\0&0&0\\0&0&0\end{bmatrix}$ | $[\bar{v}_{30}\ 0\ 0]$ |
| 7 | $4 \to 4$ | $\lambda_1$ | $[x_0\ x_0\ 0]$ | $\begin{bmatrix}1&1&0\\0&0&0\\0&0&0\end{bmatrix}$ | $[\bar{v}_{40}\ \bar{v}_{40}\ 0]$ |
| 8 | $1 \to 0$ | $\mu$ | $[x_1\ x_1\ x_2]$ | $\begin{bmatrix}0&0&0\\1&1&0\\0&0&1\end{bmatrix}$ | $[\bar{v}_{11}\ \bar{v}_{11}\ \bar{v}_{12}]$ |
| 9 | $2 \to 0$ | $\mu$ | $[x_0\ x_1\ x_2]$ | $\begin{bmatrix}1&0&0\\0&1&0\\0&0&1\end{bmatrix}$ | $[\bar{v}_{20}\ \bar{v}_{21}\ \bar{v}_{22}]$ |
| 10 | $3 \to 2$ | $\mu$ | $[x_1\ x_1\ x_2]$ | $\begin{bmatrix}0&0&0\\1&1&0\\0&0&1\end{bmatrix}$ | $[\bar{v}_{31}\ \bar{v}_{31}\ \bar{v}_{32}]$ |
| 11 | $4 \to 1$ | $\mu$ | $[x_0\ x_2\ x_2]$ | $\begin{bmatrix}1&0&0\\0&0&0\\0&1&1\end{bmatrix}$ | $[\bar{v}_{40}\ \bar{v}_{42}\ \bar{v}_{42}]$ |

packet, its delivery does not change the AoI of source 1, and thus we have $x_1' = x_0$. Moreover, since the queue is empty, $x_2$ becomes irrelevant, and thus, we have $x_2' = x_2$.

- *l=3*: A source 1 packet is under service and a source 1 packet arrives. According to the self-preemptive service of Policy 2, the source 1 packet that is under service is preempted by the arriving source 1 packet. In this transition, we have $x_0' = x_0$ because there is no departure. Since the arrived source 1 packet that entered the server through the preemption is fresh and its age is zero, we have $x_1' = 0$. Since the queue is empty, $x_2$ becomes irrelevant, and thus, we have $x_2' = x_2$.
- *l=4*: A source 1 packet is under service and a source 2 packet arrives. In this transition, we have $x_0' = x_0$ because there is no departure. The delivery of the packet under service reduces the AoI to $x_1$, and thus, we have $x_1' = x_1$. Since the packet in the queue is a source 2 packet, its delivery does not change the AoI of source 1, and thus we have $x_2' = x_1$. The reset map of transition $l = 6$ can be derived similarly.
- *l=5*: A source 2 packet is under service and a source 1 packet arrives. In this transition, we have $x_0' = x_0$ because there is no departure. Since the packet under service is a source 2 packet, its delivery does not change the AoI of source 1, and thus we have $x_1' = x_0$. Since the arriving source 1 packet is fresh and its age is zero, we have $x_2 = 0$.
- *l=6*: A source 1 packet is under service, the packet in the queue is a source 2 packet, and a source 1 packet arrives. According to the self-preemptive policy, the source 1 packet that is under service is preempted by the arriving source 1 packet. In this transition, we have $x_0' = x_0$ because there is no departure. Since the arrived source 1 packet that entered the server through the preemption is fresh and its age is zero, we have $x_1' = 0$. Since the packet in the queue is a source 2 packet, its delivery does not change the AoI of source 1, and thus we have $x_2' = 0$. The reset maps of transition $l = 7$ can be derived similarly.
- *l=8*: A source 1 packet is under service and it completes service and is delivered to the sink. With this transition, the AoI at the sink is reset to the age of the source 1 packet that just completed service, and thus, $x_0' = x_1$. Since the system enters state $q = 0$, we have $x_1' = x_1$, and $x_2' = x_2$. The reset map of transition $l = 9$ can be derived similarly.
- *l=10*: The packet in the queue is a source 2 packet and the source 1 packet in the server completes service and is delivered to the sink. With this transition, the AoI at the sink is reset to the age of the source 1 packet that just completed service, i.e., $x_0' = x_1$. Since the packet that goes to the server is a source 2 packet, its delivery does not change the AoI of source 1, and thus we have $x_1' = x_1$. In addition, since with this transition the queue becomes empty, we have $x_2' = x_2$. The reset map of transition $l = 11$ can be derived similarly.

*Calculation of $\bar{\pi}_q$ for each state $q \in \mathscr{Q}$*

Using (72) and the transition rates among the different states presented in Table 4, it can be shown that the stationary probability vector $\bar{\boldsymbol{\pi}}$ satisfies $\bar{\boldsymbol{\pi}}\bar{\mathbf{D}} = \bar{\boldsymbol{\pi}}\bar{\mathbf{Q}}$ with

$$\bar{\mathbf{D}} = \text{diag}[\lambda, \lambda+\mu, \lambda_1+\mu, \lambda_1+\mu, \lambda_1+\mu],$$
$$\bar{\mathbf{Q}} = \begin{bmatrix} 0 & \lambda_1 & \lambda_2 & 0 & 0 \\ \mu & \lambda_1 & 0 & \lambda_2 & 0 \\ \mu & 0 & 0 & 0 & \lambda_1 \\ 0 & 0 & \mu & \lambda_1 & 0 \\ 0 & \mu & 0 & 0 & \lambda_1 \end{bmatrix}.$$

Using the above $\bar{\boldsymbol{\pi}}\bar{\mathbf{D}} = \bar{\boldsymbol{\pi}}\bar{\mathbf{Q}}$ and $\sum_{q\in\mathscr{Q}} \bar{\pi}_q = 1$ in (73), the stationary probabilities are given as

$$\bar{\boldsymbol{\pi}} = \frac{1}{2\rho_1\rho_2+\rho+1}\left[1 \;\; \rho_1 \;\; \rho_2 \;\; \rho_1\rho_2 \;\; \rho_1\rho_2\right]. \tag{80}$$

*Average AoI calculation*

By substituting (80) into (74) and solving the corresponding system of linear equations, the values of $\bar{v}_{q0}$, $\forall q \in \mathscr{Q}$, are calculated as

$$\begin{aligned}
\bar{v}_{00} &= \frac{\rho_1^2(2\rho+5)+(4\rho_1+1)(\rho_2+1)}{\mu\rho_1(1+\rho_1)^2(1+\rho)(1+\rho+2\rho_1\rho_2)}, \\
\bar{v}_{10} &= \frac{(1+\rho_2)(\rho_1^3+4\rho_1^2+1)+\rho_1(5\rho_2+4)}{\mu(1+\rho_2)(1+\rho_1)^2(1+\rho+2\rho_1\rho_2)}, \\
\bar{v}_{20} &= \frac{\rho_2\big(\rho_1^2(2\rho+6)+(4\rho_1+1)(\rho_2+1)\big)}{\mu\rho_1(1+\rho_1)^2(1+\rho)(1+\rho+2\rho_1\rho_2)}, \\
\bar{v}_{30} &= \frac{\rho_2\big((1+\rho_2)(2\rho_1^3+6\rho_1^2+1)+\rho_1(6\rho_2+5)\big)}{\mu(1+\rho_2)(1+\rho_1)^2(1+\rho+2\rho_1\rho_2)}, \\
\bar{v}_{40} &= \frac{\rho_2\big(\rho_1^2(\rho_1^2+5\rho_1+\rho_1\rho_2+4\rho_2+9)+(5\rho_1+1)(1+\rho_2)\big)}{\mu(1+\rho_1)^2(1+\rho)(1+\rho+2\rho_1\rho_2)}.
\end{aligned} \tag{81}$$

Finally, substituting the values of $\bar{v}_{q0}$, $\forall q \in \mathscr{Q}$, in (81) into (75) results in the average AoI of source 1 under Policy 2, given in Theorem 3.

**Table 5. Table of transitions for the Markov chain of Policy 3 to calculate the average AoI.**

| $l$ | $q_l \to q_l'$ | $\lambda^{(l)}$ | $\mathbf{x}\mathbf{A}_l$ | $\mathbf{A}_l$ | $\bar{\mathbf{v}}_{q_l}\mathbf{A}_l$ |
|---|---|---|---|---|---|
| 1 | $0 \to 1$ | $\lambda_1$ | $[x_0\ 0\ x_2]$ | $\begin{bmatrix}1&0&0\\0&0&0\\0&0&1\end{bmatrix}$ | $[\bar{v}_{00}\ 0\ \bar{v}_{02}]$ |
| 2 | $0 \to 2$ | $\lambda_2$ | $[x_0\ x_0\ x_2]$ | $\begin{bmatrix}1&1&0\\0&0&0\\0&0&1\end{bmatrix}$ | $[\bar{v}_{00}\ \bar{v}_{00}\ \bar{v}_{02}]$ |
| 3 | $1 \to 1$ | $\lambda_1$ | $[x_0\ x_1\ x_2]$ | $\begin{bmatrix}1&0&0\\0&1&0\\0&0&1\end{bmatrix}$ | $[\bar{v}_{10}\ \bar{v}_{11}\ \bar{v}_{12}]$ |
| 4 | $1 \to 3$ | $\lambda_2$ | $[x_0\ x_1\ x_1]$ | $\begin{bmatrix}1&0&0\\0&1&1\\0&0&0\end{bmatrix}$ | $[\bar{v}_{10}\ \bar{v}_{11}\ \bar{v}_{11}]$ |
| 5 | $2 \to 4$ | $\lambda_1$ | $[x_0\ x_0\ 0]$ | $\begin{bmatrix}1&1&0\\0&0&0\\0&0&0\end{bmatrix}$ | $[\bar{v}_{20}\ \bar{v}_{20}\ 0]$ |
| 6 | $3 \to 3$ | $\lambda_1$ | $[x_0\ x_1\ x_1]$ | $\begin{bmatrix}1&0&0\\0&1&1\\0&0&0\end{bmatrix}$ | $[\bar{v}_{30}\ \bar{v}_{31}\ \bar{v}_{31}]$ |
| 7 | $4 \to 4$ | $\lambda_1$ | $[x_0\ x_0\ 0]$ | $\begin{bmatrix}1&1&0\\0&0&0\\0&0&0\end{bmatrix}$ | $[\bar{v}_{40}\ \bar{v}_{40}\ 0]$ |
| 8 | $1 \to 0$ | $\mu$ | $[x_1\ x_1\ x_2]$ | $\begin{bmatrix}0&0&0\\1&1&0\\0&0&1\end{bmatrix}$ | $[\bar{v}_{11}\ \bar{v}_{11}\ \bar{v}_{12}]$ |
| 9 | $2 \to 0$ | $\mu$ | $[x_0\ x_1\ x_2]$ | $\begin{bmatrix}1&0&0\\0&1&0\\0&0&1\end{bmatrix}$ | $[\bar{v}_{20}\ \bar{v}_{21}\ \bar{v}_{22}]$ |
| 10 | $3 \to 2$ | $\mu$ | $[x_1\ x_1\ x_2]$ | $\begin{bmatrix}0&0&0\\1&1&0\\0&0&1\end{bmatrix}$ | $[\bar{v}_{31}\ \bar{v}_{31}\ \bar{v}_{32}]$ |
| 11 | $4 \to 1$ | $\mu$ | $[x_0\ x_2\ x_2]$ | $\begin{bmatrix}1&0&0\\0&0&0\\0&1&1\end{bmatrix}$ | $[\bar{v}_{40}\ \bar{v}_{42}\ \bar{v}_{42}]$ |

### 3.2.4 Average AoI under policy 3

The main difference of Policy 3 compared to Policy 2 is that it does not permit preemption in service. The Markov chain and the continuous process of Policy 3 are the same as those for Policy 2. Thus, the stationary probability vector $\bar{\boldsymbol{\pi}}$ of Policy 3 is given in (80). The transitions between the discrete states $q_l \to q_l'$, $\forall l \in \mathscr{L}$, and their effects on the continuous state $\mathbf{x}(t)$ are summarized in Table 5. The reset maps of transitions $l \in \{1,2,4,5,7,8,9,10,11\}$ are the same as those for Policy 2. Thus, transitions $l = 3$ and $l = 6$ are only explained (see Table 5).

- *l=3*: A source 1 packet is under service and a source 1 packet arrives. According to Policy 3, the arrived source 1 packet is blocked and cleared. In this transition, we have $x_0' = x_0$ because there is no departure. The delivery of the packet under service reduces the AoI to $x_1$, and thus, we have $x_1' = x_1$. Since the queue is empty, $x_2$ becomes irrelevant, and thus, we have $x_2' = x_2$.
- *l=6*: A source 1 packet is under service, the packet in the queue is a source 2 packet, and a source 1 packet arrives. The arrived source 1 packet is blocked and cleared. In this transition, we have $x_0' = x_0$ because there is no departure. The delivery of

the packet under service reduces the AoI to $x_1$, and thus, we have $x_1' = x_1$. Since the packet in the queue is a source 2 packet, its delivery does not change the AoI of source 1, and thus we have $x_2' = x_1$.

Having the stationary probability vector $\bar{\boldsymbol{\pi}}$ (given in (80)) and the table of transitions (Table 5), the system of linear equations (74) can be formed. By solving the system of linear equations, the values of $\bar{v}_{q0},\ \forall q \in \mathscr{Q}$, are calculated as

$$\begin{aligned}
\bar{v}_{00} &= \frac{\rho_1^3+\rho_1^2((\rho_2+2)^2-1)+(\rho_2+1)^2(3\rho_1+1)}{\mu\rho_1(1+\rho_1)(1+\rho_2)(1+\rho)(1+\rho+2\rho_1\rho_2)}, \\
\bar{v}_{10} &= \frac{(1+\rho_2)(2\rho_1^2+1)+\rho_1(4\rho_2+3)}{\mu(1+\rho_2)(1+\rho_1)(1+\rho+2\rho_1\rho_2)}, \\
\bar{v}_{20} &= \frac{\rho_2\big(\rho_1^3(\rho_2+2)+\rho_1^2(\rho_2^2+5\rho_2+4)+(3\rho_1+1)(\rho_2+1)^2\big)}{\mu\rho_1(1+\rho_1)(1+\rho_2)(1+\rho)(1+\rho+2\rho_1\rho_2)}, \\
\bar{v}_{30} &= \frac{\rho_2\big((\rho_2+1)(3\rho_1^2+1)+\rho_1(5\rho_2+4)\big)}{\mu(1+\rho_1)(1+\rho_2)(1+\rho+2\rho_1\rho_2)}, \\
\bar{v}_{40} &= \frac{\rho_2\big(\rho_1^3(2\rho_2+3)+2\rho_1^2((\rho_2+2)^2-1)+(4\rho_1+1)(\rho_2+1)^2\big)}{\mu(1+\rho_1)(1+\rho_2)(1+\rho)(1+\rho+2\rho_1\rho_2)}.
\end{aligned} \tag{82}$$

Finally, substituting the values of $\bar{v}_{q0},\ \forall q \in \mathscr{Q}$, in (82) into (75) results in the average AoI of source 1 under Policy 3, given in Theorem 4.

## 3.3 MGF of the AoI

In this section, first, it is briefly explained how to extend the SHS technique presented in Section 3.2.1 for the MGF analysis in Section 3.3.2. Then, the MGF of the AoI under Policy 2 and Policy 3 is derived.

### *3.3.1 The SHS technique to calculate MGF*

To calculate the MGF of the AoI using the SHS technique in addition to the state probabilities of the Markov chain and the correlation vector between the discrete state $q(t)$ and the continuous state $\mathbf{x}(t)$, the correlation vector between the discrete state $q(t)$ and the exponential function $e^{s\mathbf{x}(t)},\ s \in \mathbb{R}$, needs to be defined. Let $\mathbf{v}_q^s(t) = [v_{q0}^s(t)\cdots v_{qn}^s(t)] \in \mathbb{R}^{1\times(n+1)}$ denote the correlation vector between the discrete state $q(t)$ and the exponential function $e^{s\mathbf{x}(t)}$. Accordingly, we have

$$\mathbf{v}_q^s(t) = [v_{q0}^s(t)\cdots v_{qn}^s(t)] = \mathbb{E}[e^{s\mathbf{x}(t)}\boldsymbol{\delta}_{q,q(t)}],\ \forall q \in \mathscr{Q}. \tag{83}$$

Following the ergodicity assumption of the Markov chain $q(t)$ in the AoI analysis [9, 45], it has been shown in [45, Theorem 1] that if we can find a non-negative limit, $\bar{\mathbf{v}}_q = [\bar{v}_{q0} \cdots \bar{v}_{qn}], \forall q \in \mathscr{Q}$, for the correlation vector $\mathbf{v}_q(t)$ satisfying

$$\bar{\mathbf{v}}_q \sum_{l \in \mathscr{L}_q} \lambda^{(l)} = \bar{\pi}_q \mathbf{1} + \sum_{l \in \mathscr{L}'_q} \lambda^{(l)} \bar{\mathbf{v}}_{q_l} \mathbf{A}_l, \ \forall q \in \mathscr{Q}, \tag{84}$$

there exists $s_0 > 0$ such that for all $s < s_0$, $\mathbf{v}_q^s(t), \forall q \in \mathscr{Q}$, converges to $\bar{\mathbf{v}}_q^s$ that satisfies

$$\bar{\mathbf{v}}_q^s \sum_{l \in \mathscr{L}_q} \lambda^{(l)} = s \bar{\mathbf{v}}_q^s + \sum_{l \in \mathscr{L}'_q} \lambda^{(l)} [\bar{\mathbf{v}}_{q_l}^s \mathbf{A}_l + \bar{\pi}_{q_l} \mathbf{1} \hat{\mathbf{A}}_l], \ \forall q \in \mathscr{Q}, \tag{85}$$

where $\hat{\mathbf{A}}_l \in \mathbb{B}^{(n+1)\times(n+1)}$ is a binary matrix whose $k, j$th element, $\hat{\mathbf{A}}_l(k, j)$, is given as

$$\hat{\mathbf{A}}_l(k, j) = \begin{cases} 1, & k = j, \text{ and } j\text{th column of } \mathbf{A}_l \text{ is a zero vector,} \\ 0, & \text{otherwise.} \end{cases}$$

Finally, the MGF of the continuous state $\mathbf{x}(t)$, which is calculated by $\mathbb{E}[e^{s\mathbf{x}(t)}]$, converges to the stationary vector [45, Theorem 1]

$$\mathbb{E}[e^{s\mathbf{x}}] = \sum_{q \in \mathscr{Q}} \bar{\mathbf{v}}_q^s. \tag{86}$$

As (86) implies, if the first element of continuous state $\mathbf{x}(t)$ represents the AoI of source 1 at the sink, the MGF of the AoI of source 1 at the sink converges to

$$M_{\Delta_1}(s) = \sum_{q \in \mathscr{Q}} \bar{v}_{q0}^s. \tag{87}$$

From (87), the main challenge in calculating the MGF of the AoI of source 1 using the SHS technique reduces to deriving the first elements of correlation vectors $\bar{\mathbf{v}}_q^s$, $\forall q \in \mathscr{Q}$.

### 3.3.2 The MGF of the AoI under policy 2 and policy 3

In this section, the SHS technique is used to calculate the MGF of the AoI of source 1 in (87) under Policy 2 and Policy 3. The discrete state space $\mathscr{Q}$ and the continuous process $\mathbf{x}(t)$ for Policy 2 and Policy 3 are described in Sections 3.2.3 and 3.2.4, respectively.

Recall that to calculate the MGF of the AoI of source 1 in (87) we need to find $\bar{v}_{q0}^s, \forall q \in \mathscr{Q}$, which are the solutions of the system of linear equations (85) with variables

**Table 6. Table of transitions for Policy 2 to calculate the MGF of the AoI.**

| $l$ | $q_l \to q_l'$ | $\lambda^{(l)}$ | $\mathbf{x}\mathbf{A}_l$ | $\mathbf{A}_l$ | $\hat{\mathbf{A}}_l$ |
|---|---|---|---|---|---|
| 1 | $0 \to 1$ | $\lambda_1$ | $[x_0\ 0\ x_2]$ | $\begin{bmatrix}1&0&0\\0&0&0\\0&0&1\end{bmatrix}$ | $\begin{bmatrix}0&0&0\\0&1&0\\0&0&0\end{bmatrix}$ |
| 2 | $0 \to 2$ | $\lambda_2$ | $[x_0\ x_0\ x_2]$ | $\begin{bmatrix}1&1&0\\0&0&0\\0&0&1\end{bmatrix}$ | $\begin{bmatrix}0&0&0\\0&0&0\\0&0&0\end{bmatrix}$ |
| 3 | $1 \to 1$ | $\lambda_1$ | $[x_0\ 0\ x_2]$ | $\begin{bmatrix}1&0&0\\0&0&0\\0&0&1\end{bmatrix}$ | $\begin{bmatrix}0&0&0\\0&1&0\\0&0&0\end{bmatrix}$ |
| 4 | $1 \to 3$ | $\lambda_2$ | $[x_0\ x_1\ x_1]$ | $\begin{bmatrix}1&0&0\\0&1&1\\0&0&0\end{bmatrix}$ | $\begin{bmatrix}0&0&0\\0&0&0\\0&0&0\end{bmatrix}$ |
| 5 | $2 \to 4$ | $\lambda_1$ | $[x_0\ x_0\ 0]$ | $\begin{bmatrix}1&1&0\\0&0&0\\0&0&0\end{bmatrix}$ | $\begin{bmatrix}0&0&0\\0&0&0\\0&0&1\end{bmatrix}$ |
| 6 | $3 \to 3$ | $\lambda_1$ | $[x_0\ 0\ 0]$ | $\begin{bmatrix}1&0&0\\0&0&0\\0&0&0\end{bmatrix}$ | $\begin{bmatrix}0&0&0\\0&1&0\\0&0&1\end{bmatrix}$ |
| 7 | $4 \to 4$ | $\lambda_1$ | $[x_0\ x_0\ 0]$ | $\begin{bmatrix}1&1&0\\0&0&0\\0&0&0\end{bmatrix}$ | $\begin{bmatrix}0&0&0\\0&0&0\\0&0&1\end{bmatrix}$ |
| 8 | $1 \to 0$ | $\mu$ | $[x_1\ x_1\ x_2]$ | $\begin{bmatrix}0&0&0\\1&1&0\\0&0&1\end{bmatrix}$ | $\begin{bmatrix}0&0&0\\0&0&0\\0&0&0\end{bmatrix}$ |
| 9 | $2 \to 0$ | $\mu$ | $[x_0\ x_1\ x_2]$ | $\begin{bmatrix}1&0&0\\0&1&0\\0&0&1\end{bmatrix}$ | $\begin{bmatrix}0&0&0\\0&0&0\\0&0&0\end{bmatrix}$ |
| 10 | $3 \to 2$ | $\mu$ | $[x_1\ x_1\ x_2]$ | $\begin{bmatrix}0&0&0\\1&1&0\\0&0&1\end{bmatrix}$ | $\begin{bmatrix}0&0&0\\0&0&0\\0&0&0\end{bmatrix}$ |
| 11 | $4 \to 1$ | $\mu$ | $[x_0\ x_2\ x_2]$ | $\begin{bmatrix}1&0&0\\0&0&0\\0&1&1\end{bmatrix}$ | $\begin{bmatrix}0&0&0\\0&0&0\\0&0&0\end{bmatrix}$ |

$\bar{\mathbf{v}}_q^s, \forall q \in \mathscr{Q}$. To form the system of linear equations (85), we need to determine $\bar{\boldsymbol{\pi}}_q$, $\mathbf{A}_l$, and $\hat{\mathbf{A}}_l$ for each state $\forall q \in \mathscr{Q}$, and transition $l \in \mathscr{L}_q'$. Next, these are derived under Policy 2 and Policy 3.

### *MGF of the AoI under policy 2*

The transitions between the discrete states $q_l \to q_l'$, $\forall l \in \mathscr{L}$, and their effects on the continuous state $\mathbf{x}(t)$ are summarized in Table 6. The explanations of the transitions can be found in Section 3.3.2.

As it has been shown in Section 3.3.2, the stationary probabilities are given as

$$\bar{\boldsymbol{\pi}} = \frac{1}{2\rho_1\rho_2 + \rho + 1} [1 \ \ \rho_1 \ \ \rho_2 \ \ \rho_1\rho_2 \ \ \rho_1\rho_2]. \tag{88}$$

Recall from Section 3.3.1 that to calculate the MGF of the AoI, first, we need to make sure whether we can find non-negative vectors $\bar{\mathbf{v}}_q = [\bar{v}_{q0} \cdots \bar{v}_{qn}], \forall q \in \mathscr{Q}$, satisfying (84). As it is shown in (81), the system of linear equations in (84) has a non-negative solution. Thus, the MGF of the AoI can be calculated by solving the system of linear

**Table 7. Table of transitions for Policy 3 to calculate the MGF of the AoI.**

| $l$ | $q_l \to q'_l$ | $\lambda^{(l)}$ | $\mathbf{x}\mathbf{A}_l$ | $\mathbf{A}_l$ | $\hat{\mathbf{A}}_l$ |
|---|---|---|---|---|---|
| 3 | $1 \to 1$ | $\lambda_1$ | $[x_0\ x_1\ x_2]$ | $\begin{bmatrix} 1 & 0 & 0 \\ 0 & 1 & 0 \\ 0 & 0 & 1 \end{bmatrix}$ | $\begin{bmatrix} 0 & 0 & 0 \\ 0 & 0 & 0 \\ 0 & 0 & 0 \end{bmatrix}$ |
| 6 | $3 \to 3$ | $\lambda_1$ | $[x_0\ x_1\ x_1]$ | $\begin{bmatrix} 1 & 0 & 0 \\ 0 & 1 & 1 \\ 0 & 0 & 0 \end{bmatrix}$ | $\begin{bmatrix} 0 & 0 & 0 \\ 0 & 0 & 0 \\ 0 & 0 & 0 \end{bmatrix}$ |

equations in (85). The system of linear equations (85) is formed by substituting the values of $\mathbf{A}_l$ and $\hat{\mathbf{A}}_l$ presented in Table 6 and the vector $\bar{\boldsymbol{\pi}}$ in (88). By solving the formed system of linear equations, the values of $\bar{v}^s_{q0}$, $\forall q \in \mathscr{Q}$, under Policy 2 are calculated as presented in Appendix 1.3.

Finally, substituting the values of $\bar{v}^s_{q0}$, $\forall q \in \mathscr{Q}$, into (87), the MGF of the AoI of source 1 under Policy 2 is obtained, as given in Theorem 5.

### *MGF of the AoI under policy 3*

The Markov chain of Policy 3 is the same as that for the Policy 2. Thus, the stationary probability vector $\bar{\boldsymbol{\pi}}$ of Policy 3 is given in (88). The transitions between the discrete states $q_l \to q'_l$, and their effects on the continuous state $\mathbf{x}(t)$ for $l \in \{1,2,4,5,7,8,9,10,11\}$ are same as those fo the Policy 2. The transitions $l \in \{3,6\}$ and their effects on the continuous state $\mathbf{x}(t)$ are summarized in Table 7. The explanations of the transitions can be found in Section 3.2.4.

As it is shown in (82), the system of linear equations in (84) has a non-negative solution. Thus, the MGF of the AoI can be calculated by solving the system of linear equations in (85). The system of linear equations (85) is formed by substituting the values of $\mathbf{A}_l$ and $\hat{\mathbf{A}}_l$ presented in Tables 6 and 7 and the vector $\bar{\boldsymbol{\pi}}$ in (88). By solving the formed system of linear equations, the values of $\bar{v}^s_{q0}$, $\forall q \in \mathscr{Q}$, under Policy 3 are calculated as presented in Appendix 1.4.

Finally, substituting the values of $\bar{v}^s_{q0}$, $\forall q \in \mathscr{Q}$, into (87) results in the MGF of the AoI of source 1 under Policy 3, given in Theorem 6.

The following remark presents how different moments of the AoI can be derived by using the MGF.

**Remark 3.** The $\underline{m}$th moment of the AoI of source 1, $\Delta_1^{(\underline{m})}$, is calculated as

$$\Delta_1^{(\underline{m})} = \frac{\mathrm{d}^{\underline{m}}(M_{\Delta_1}(s))}{\mathrm{d}s^{\underline{m}}}\Big|_{s=0}. \tag{89}$$

### 3.3.3 Deriving the first and second moments of the AoI using the MGF

Having derived the MGF of the AoI presented in Theorems 5 and 6, Remark 3 is applied to derive the first and second moments of the AoI of source 1.

The first moment of the AoI of source 1 under Policy 2 is given as

$$\Delta_1 = \frac{(\rho_2+1)^2 + \sum_{k=1}^{5} \rho_1^k \tilde{\eta}_k}{\mu\rho_1 (1+\rho_1)^2 \left(\rho_1^2(2\rho_2+1)+(\rho_2+1)^2(2\rho_1+1)\right)}, \tag{90}$$

where

$$\begin{aligned} \tilde{\eta}_1 &= 6\rho_2^2 + 11\rho_2 + 5, \\ \tilde{\eta}_2 &= 13\rho_2^2 + 24\rho_2 + 10, \\ \tilde{\eta}_3 &= 10\rho_2^2 + 27\rho_2 + 10, \\ \tilde{\eta}_4 &= 3\rho_2^2 + 14\rho_2 + 5, \\ \tilde{\eta}_5 &= 3\rho_2 + 1. \end{aligned} \tag{91}$$

The first moment of the AoI of source 1 under Policy 3 is given as

$$\Delta_1 = \frac{(\rho_2+1)^3 + \sum_{k=1}^{4} \rho_1^k \hat{\eta}_k}{\mu\rho_1 (1+\rho_1)(1+\rho_2)\left(\rho_1^2(2\rho_2+1)+(\rho_2+1)^2(2\rho_1+1)\right)}, \tag{92}$$

where

$$\begin{aligned} \hat{\eta}_1 &= 5\rho_2^3 + 14\rho_2^2 + 13\rho_2 + 4, \\ \hat{\eta}_2 &= 10\rho_2^3 + 28\rho_2^2 + 25\rho_2 + 7, \\ \hat{\eta}_3 &= 5\rho_2^3 + 22\rho_2^2 + 23\rho_2 + 6, \\ \hat{\eta}_4 &= 5\rho_2^2 + 8\rho_2 + 2. \end{aligned} \tag{93}$$

It is worth noting that (90) and (92) coincide with the results in Theorems 3 and 4, as expected.

The second moment of the AoI of source 1 under Policy 2 is given as

$$\Delta_1^{(2)} = \frac{2(\rho_2+1)^3 + 2\sum_{k=1}^{8} \rho_1^k \tilde{\xi}_k}{\mu\rho_1^2 (1+\rho_1)^3 (1+\rho)^2 (2\rho_1\rho_2+\rho+1)}, \tag{94}$$

where

$$\begin{aligned}
\tilde{\xi}_1 &= 7\rho_2^3 + 21\rho_2^2 + 21\rho_2 + 7, \\
\tilde{\xi}_2 &= 22\rho_2^3 + 68\rho_2^2 + 68\rho_2 + 22, \\
\tilde{\xi}_3 &= 40\rho_2^3 + 113\rho_2^2 + 134\rho_2 + 41, \\
\tilde{\xi}_4 &= 36\rho_2^3 + 161\rho_2^2 + 180\rho_2 + 50, \\
\tilde{\xi}_5 &= 18\rho_2^3 + 113\rho_2^2 + 160\rho_2 + 41, \\
\tilde{\xi}_6 &= 4\rho_2^3 + 45\rho_2^2 + 88\rho_2 + 22, \\
\tilde{\xi}_7 &= 8\rho_2^2 + 28\rho_2 + 7, \\
\tilde{\xi}_8 &= 4\rho_2 + 1.
\end{aligned} \tag{95}$$

The second moment of the AoI of source 1 under Policy 3 is

$$\Delta_1^{(2)} = \frac{2(\rho_2+1)^5 + 2\sum_{k=1}^{7} \rho_1^k \dot{\eta}_k}{\mu\rho_1^2(1+\rho_1)^2(1+\rho_2)^2(1+\rho)^2(2\rho_1\rho_2+\rho+1)}, \tag{96}$$

where

$$\begin{aligned}
\dot{\eta}_1 &= 6\rho_2^5 + 30\rho_2^4 + 60\rho_2^3 + 60\rho_2^2 + 30\rho_2 + 6, \\
\dot{\eta}_2 &= 18\rho_2^5 + 91\rho_2^4 + 182\rho_2^3 + 180\rho_2^2 + 88\rho_2 + 17, \\
\dot{\eta}_3 &= 34\rho_2^5 + 178\rho_2^4 + 361\rho_2^3 + 355\rho_2^2 + 169\rho_2 + 31, \\
\dot{\eta}_4 &= 29\rho_2^5 + 190\rho_2^4 + 439\rho_2^3 + 463\rho_2^2 + 224\rho_2 + 39, \\
\dot{\eta}_5 &= 9\rho_2^5 + 97\rho_2^4 + 293\rho_2^3 + 365\rho_2^2 + 192\rho_2 + 32, \\
\dot{\eta}_6 &= 18\rho_2^4 + 92\rho_2^3 + 151\rho_2^2 + 93\rho_2 + 15, \\
\dot{\eta}_7 &= 9\rho_2^3 + 24\rho_2^2 + 19\rho_2 + 3.
\end{aligned}$$

### 3.4 Numerical results

In this section, the effectiveness of the proposed packet management policies in terms of the sum average AoI and fairness between the different sources in the system are shown. In addition, the importance of higher moments of AoI is investigated. The proposed policies are compared against the following existing policies: the source-agnostic packet management policies LCFS-S and LCFS-W proposed in [9], and the priority based packet management policies proposed in [48], which are termed PP-NW and PP-WW. Under the LCFS-S policy, a new arriving packet preempts any packet that is currently

under service (regardless of the source index). Under the LCFS-W policy, a new arriving packet replaces any older packet waiting in the queue (regardless of the source index); however, the new packet has to wait for any packet under service to finish. Under the PP-NW policy, there is no waiting room and an update under service is preempted on arrival of an equal or higher priority update. Under the PP-WW policy, there is a waiting room for at most one update and preemption is allowed in waiting but not in service. Without loss of generality, for the PP-NW and PP-WW policies, it is assumed that source 2 has higher priority than source 1; for the opposite case, the results are symmetric.

### 3.4.1 Average AoI

Fig. 16 depicts the contours of achievable average AoI pairs $(\Delta_1, \Delta_2)$ under the introduced packet management policies and the FCFS policy for $\mu = 1$ with $\rho = \rho_1 + \rho_2 = 0.9$. As can be seen, by applying an appropriate packet management policy the average AoI can be significantly improved.

Fig. 17 depicts the contours of achievable average AoI pairs $(\Delta_1, \Delta_2)$ for fixed values of system load $\rho = \rho_1 + \rho_2$ under different packet management policies with normalized service rate $\mu = 1$; in Fig. 17(a), $\rho = 1$ and in Fig. 17(b), $\rho = 6$. This figure shows that under an appropriate packet management policy in the system (either in the queue or server), by increasing the load of the system the average AoI decreases. Besides that, it shows that Policy 2 provides the lowest average AoI as compared to the other policies.

### 3.4.2 Sum average AoI

Fig. 18 depicts sum average AoI as a function of $\rho_1$ under different packet management policies with $\mu = 1$; in Fig. 18(a), $\rho = \rho_1 + \rho_2 = 1$ and in Fig. 18(b), $\rho = \rho_1 + \rho_2 = 6$. This figure shows that Policy 2 provides the lowest average AoI for all values of $\rho_1$ as compared to the other policies. In addition, it can be observed that among Policy 1, Policy 3, PP-NW, PP-WW, LCFS-S, and LCFS-W policies, the policy that achieves the lowest value of the sum average AoI depends on the system parameters. Moreover, it can be observed that under the PP-NW and PP-WW policies the minimum value of sum average AoI is achieved for a high value of $\rho_1$. This is because when priority is with source 2, a high value of $\rho_1$ is needed to compensate for the priority. In addition, it can be seen that for a high value of total load, i.e., $\rho = 6$, the range of values of $\rho_1$ for which PP-NW and PP-WW policies operate well becomes narrow.

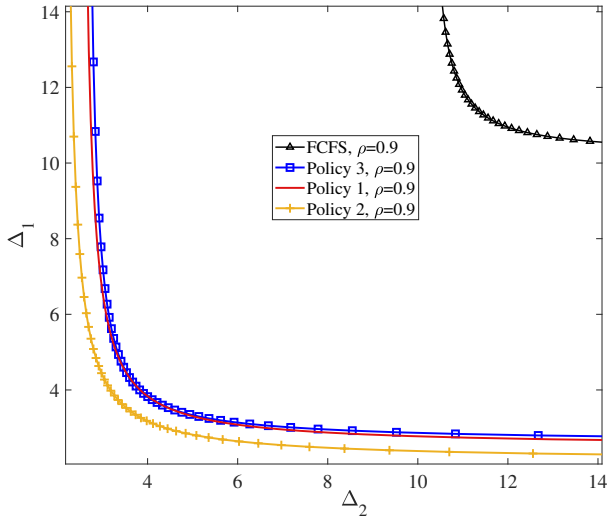


**Fig. 16. The average AoI of sources 1 and 2 under the introduced packet management policies and the FCFS policy for $\mu = 1$ with $\rho = \rho_1 + \rho_2 = 0.9$.**

### *3.4.3 Fairness*

For some applications, besides the sum average AoI, the individual average AoI of each source is critical. In this case, fairness between different sources becomes important to be taken into account. To compare the fairness between different sources under the different packet management policies, the Jain's fairness index [97] is used. For the average AoI of sources 1 and 2, the Jain's fairness index $J(\Delta_1, \Delta_2)$ is defined as [97, Definition 1] [98, Sect. 3]

$$J(\Delta_1, \Delta_2) = \frac{(\Delta_1 + \Delta_2)^2}{2(\Delta_1^2 + \Delta_2^2)}. \tag{97}$$

The Jain's index $J(\Delta_1, \Delta_2)$ is continuous and lies in $[0.5, 1]$, where $J(\Delta_1, \Delta_2) = 1$ indicates the fairest situation in the system.

Fig. 19 depicts the Jain's fairness index for the average AoI of sources 1 and 2 as a function of $\rho_1$ under different packet management policies with $\mu = 1$; in Fig. 19(a), $\rho = \rho_1 + \rho_2 = 1$ and in Fig. 19(b), $\rho = \rho_1 + \rho_2 = 6$. As can be seen, among Policy 1, Policy 2, Policy 3, LCFS-S, and LCFS-W policies, the LCFS-S policy provides the lowest fairness in the system. This is because the packets of a source with a lower packet arrival rate are most of the time preempted by the packets of the other source having a

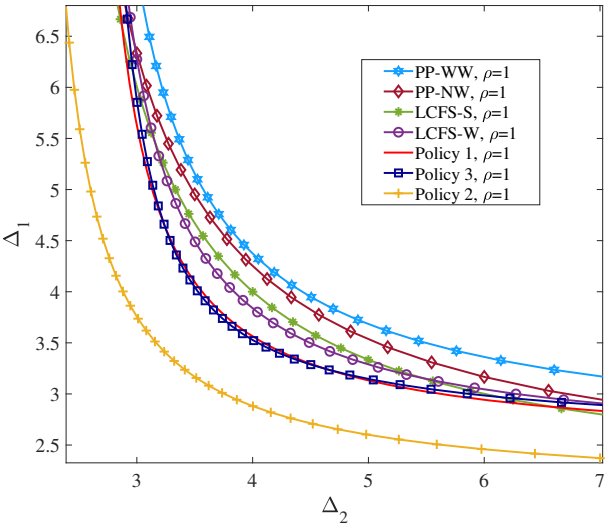


(a)

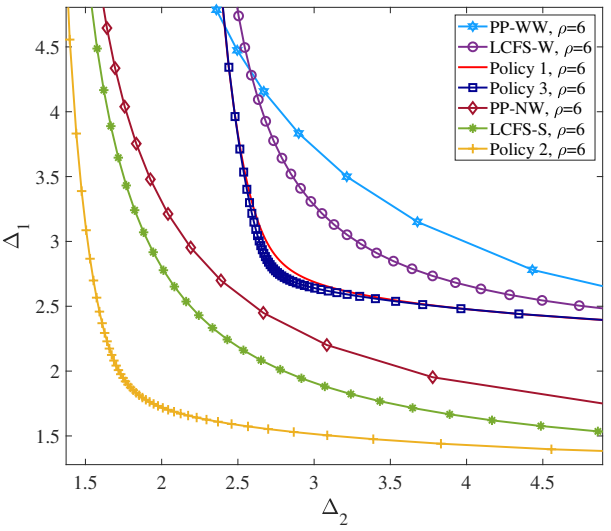


(b)

**Fig. 17. The average AoI of sources 1 and 2 under different packet management policies for $\mu = 1$ with (a) $\rho = \rho_1 + \rho_2 = 1$, and (b) $\rho = \rho_1 + \rho_2 = 6$ (Reprinted by permission [16] © 2021, IEEE).**

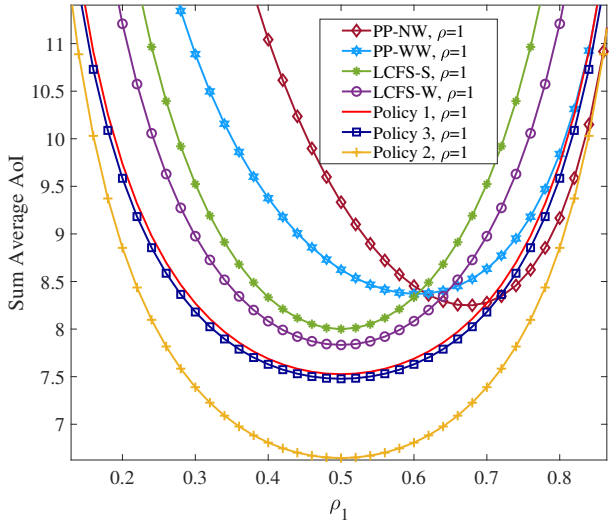


(a)

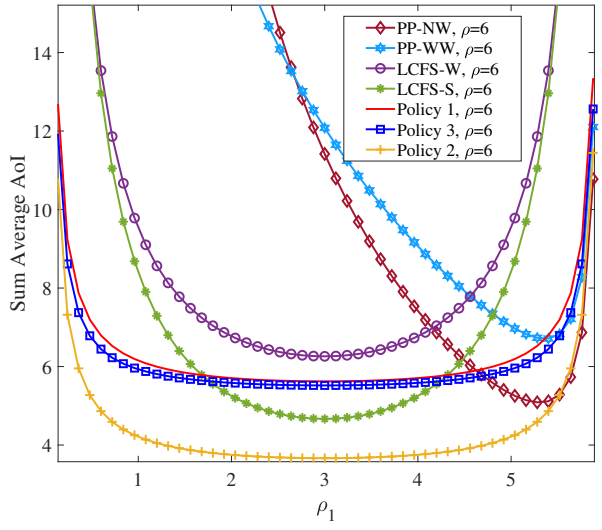


(b)

**Fig. 18. Sum average AoI as a function of $\rho_1$ under different packet management policies for $\mu = 1$ with (a) $\rho = \rho_1 + \rho_2 = 1$, and (b) $\rho = \rho_1 + \rho_2 = 6$ (Reprinted by permission [16] © 2021, IEEE).**

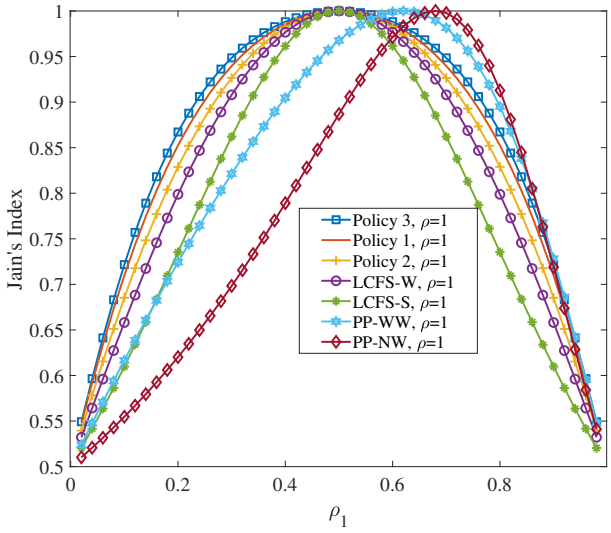


(a)

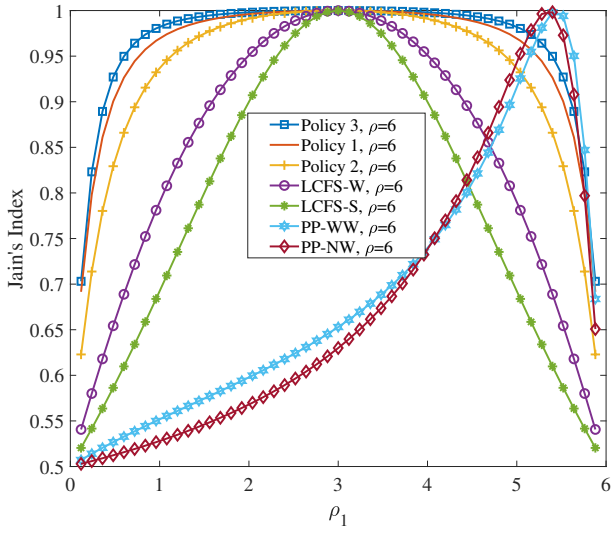


(b)

**Fig. 19. The Jain's fairness index for the average AoI of sources 1 and 2 as a function of $\rho_1$ under different packet management policies for $\mu = 1$ with (a) $\rho = \rho_1 + \rho_2 = 1$, and (b) $\rho = \rho_1 + \rho_2 = 6$ (Reprinted by permission [16] © 2021, IEEE).**

higher packet arrival rate. In addition, it is observed that the proposed source-aware policies (i.e., Policy 1, Policy 2, and Policy 3) in general provide better fairness than that of the other policies and Policy 3 provides the fairest situation in the system. This is because under these policies, a packet in the queue or server can be preempted *only* by a packet with the same source index. Similarly as in Fig. 18(b), for the high load case, the range of values of $\rho_1$ for which PP-NW and PP-WW policies provide a good fairness becomes narrow.

### *3.4.4 Standard deviation of the AoI*

Fig. 20 depicts the average AoI of source 1 and its standard deviation ($\sigma$) as a function of $\rho_1$ under Policy 2 and Policy 3 for $\mu = 1$ with (a) $\rho = \rho_1 + \rho_2 = 1$, and (b) $\rho = \rho_1 + \rho_2 = 6$. This figure shows that in a status update system, the standard deviation of the AoI might have a large value. Thus, to have a reliable system, in addition to optimizing the average AoI, we need to take the higher moments of the AoI into account.

## 3.5 Summary and discussion

A status update system consisting of two independent sources, one server, and one sink was considered. Three source-aware packet management policies where a packet in the system can be preempted only by a packet with the same source index were introduced and analyzed. The average AoI for each source under the proposed packet management policies was derived using the SHS technique. The numerical results showed that Policy 2 results in a lower sum average AoI in the system compared to the existing policies. In addition, the experiments showed that in general the proposed source-aware policies result in higher fairness in the system than that of the existing policies and, in particular, Policy 3 provides the fairest situation in the system.

Since Policy 2 provides the lowest sum average AoI and Policy 3 provides the fairest situation in the system, the results under these two policies were generalized by deriving the MGF of the AoI for each source in the system. By using the MGF in the numerical results section, it was shown that to have a reliable system, in addition to optimizing the average AoI, we need to take the higher moments of the AoI into account.

As numerically shown in this chapter, by applying an appropriate packet management policy the information freshness and fairness between different sources can be significantly improved.

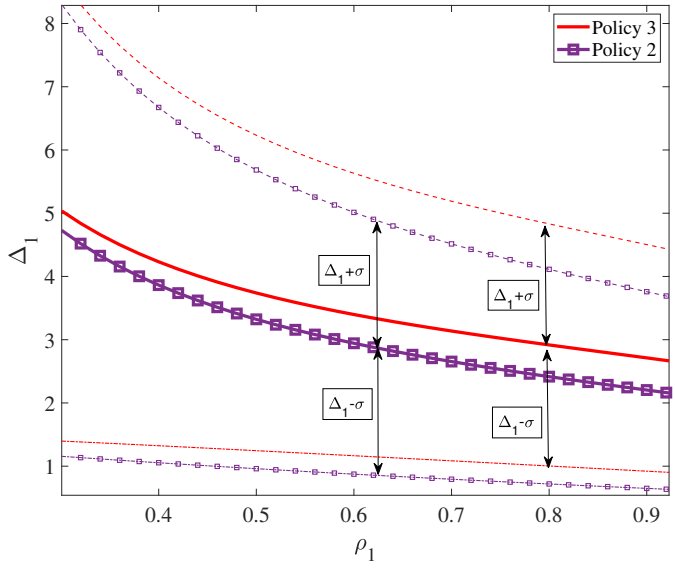


(a)

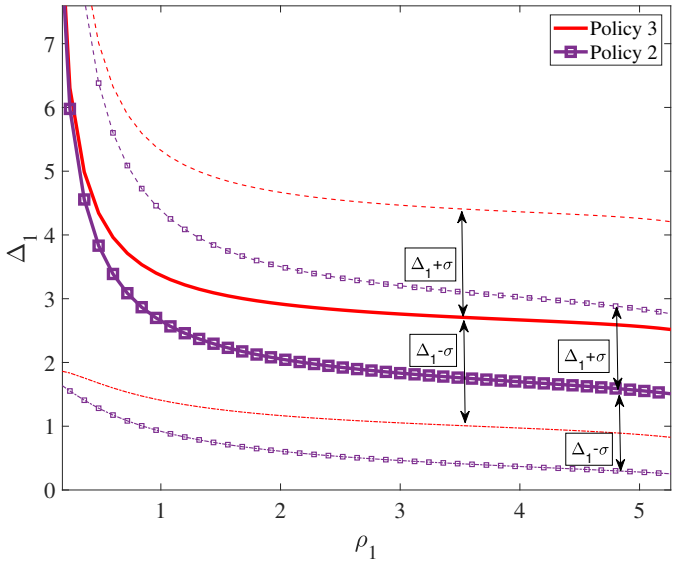


(b)

**Fig. 20. The average AoI of source 1 and its standard deviation as a function of $\rho_1$ under Policy 2 and Policy 3 for $\mu = 1$ with (a) $\rho = \rho_1 + \rho_2 = 1$, and (b) $\rho = \rho_1 + \rho_2 = 6$.**

# 4 Power minimization for AoI constrained dynamic control in wireless sensor networks

In Chapters 2 and 3, the AoI was analyzed in systems where we cannot control the sampling process on the transmitter side, i.e., packet arrivals follow a Poisson process and there was a queueing system on the transmitter side. In this chapter, it is assumed that the sampling process in a WSN can be controlled and the radio resources need to be efficiently assigned to meet an information freshness constraint for each sensor. A WSN consisting of a set of sensors and a sink that is interested in time-sensitive information from the sensors is considered. The problem of optimizing the sensors' sampling action and radio resource allocation to minimize the average total transmit power of all sensors subject to an AoI constraint for each sensor is studied.

To solve the proposed problem, a dynamic control algorithm using the Lyapunov drift-plus-penalty method is developed. In addition, optimality analysis of the proposed dynamic control algorithm is provided. According to the Lyapunov drift-plus-penalty method, to solve the main problem, we need to solve an optimization problem in each time slot which is a mixed integer non-convex optimization problem. A low-complexity sub-optimal solution for this per-slot optimization problem that provides near-optimal performance is proposed and the computational complexity of the solution is evaluated. Numerical results show the performance of the proposed dynamic control algorithm in terms of transmit power consumption and AoI of the sensors versus different system parameters. In addition, they show that the sub-optimal solution for the per-slot optimization problems is near-optimal.

The rest of this chapter is organized as follows. The system model and problem formulation are presented in Section 4.1. The Lyapunov drift-plus-penalty method to solve the proposed problem is presented in Section 4.2. The optimality analysis of the proposed dynamic control algorithm to solve the main problem is provided in Section 4.3. The proposed sub-optimal solution for the mixed integer non-convex optimization problem in each slot is presented in Section 4.4. Numerical results are presented in Section 4.5. Finally, concluding remarks are made in Section 4.6.

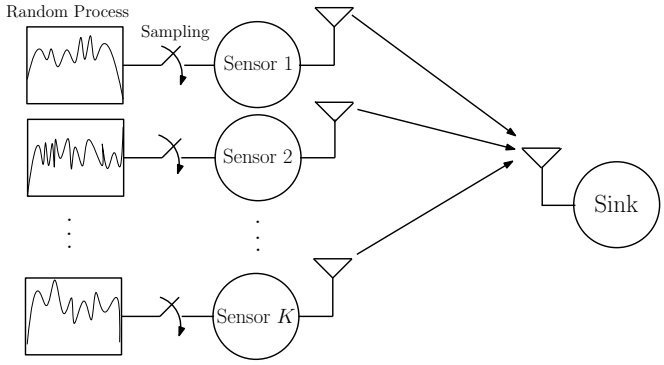


**Fig. 21. A WSN consisting of $K$ sensors and one sink that is interested in time-sensitive information from the sensors (Reprinted by permission [22] © 2019, IEEE).**

## 4.1 System model and problem formulation

### *4.1.1 System model*

Consider a WSN consisting of a set $\mathscr{K}$ of $K$ sensors and one sink, as depicted in Fig. 21. The sink is interested in time-sensitive information from the sensors which measure physical phenomena. A slotted communication with normalized slots $t \in \{0,1,\dots\}$, is assumed where in each slot, the sensors share a set $\mathscr{N}$ of $N$ orthogonal sub-channels with bandwidth $\underline{W}$ Hz per sub-channel. It is assumed that a central controller controls the sampling process of sensors in such a way that it decides whether each sensor takes a sample or not at the beginning of each slot $t$.

It is assumed that the perfect channel state information of all sub-channels is available at the central controller at the beginning of each slot. Let $h_{k,n}(t)$ denote the channel coefficient from sensor $k$ to the sink over sub-channel $n$ in slot $t$. It is assumed that $h_{k,n}(t)$ is a stationary process and is independent and identically distributed (i.i.d) over slots.

Let $\rho_{k,n}(t)$ denote the sub-channel assignment at time slot $t$ as $\rho_{k,n}(t) \in \{0,1\}$, $\forall k \in \mathscr{K}, n \in \mathscr{N}$, where $\rho_{k,n}(t) = 1$ indicates that sub-channel $n$ is assigned to sensor $k$ at time slot $t$, and $\rho_{k,n}(t) = 0$ otherwise. To ensure that at any given time slot $t$, each sub-channel can be assigned to at most one sensor, the following constraint is used

$$\sum_{k \in \mathscr{K}} \rho_{k,n}(t) \leq 1, \forall n \in \mathscr{N}, t. \tag{98}$$

Let $p_{k,n}(t)$ denote the transmit power of sensor $k$ over sub-channel $n$ in slot $t$. Then, the signal-to-noise ratio (SNR) with respect to sensor $k$ over sub-channel $n$ in slot $t$ is

given by

$$\gamma_{k,n}(t) = \frac{p_{k,n}(t)|h_{k,n}(t)|^2}{\underline{W}N_0}, \tag{99}$$

where $N_0$ is the noise power spectral density. The achievable rate for sensor $k$ over sub-channel $n$ in slot $t$ is given by

$$r_{k,n}(t) = \underline{W}\log_2\left(1+\gamma_{k,n}(t)\right). \tag{100}$$

The achievable data rate of sensor $k$ in slot $t$ is the sum of the achievable data rates over all the assigned sub-channels at slot $t$, expressed as

$$R_k(t) = \sum_{n\in\mathcal{N}} \rho_{k,n}(t) r_{k,n}(t).$$

Let $b_k(t)$ denote the sampling action of sensor $k$ at time slot $t$ as $b_k(t) \in \{0,1\}$, $\forall k \in \mathcal{K}$, where $b_k(t) = 1$ indicates that sensor $k$ takes a sample at the beginning of time slot $t$, and $b_k(t) = 0$ otherwise. It is assumed that sampling time (i.e., the time needed to acquire a sample) is negligible. It is considered that the central controller decides that sensor $k$ takes a sample at the beginning of slot $t$ only if there are enough resources to guarantee that the sample is successfully transmitted during the same slot $t$. Thus, if sensor $k$ takes a sample at the beginning of slot $t$ (i.e., $b_k(t) = 1$), the sample will be transmitted during the same slot $t$ successfully. To this end, the following constraint is used

$$R_k(t) = \underline{\eta} b_k(t), \forall k \in \mathcal{K}, t, \tag{101}$$

where $\underline{\eta}$ is the size of each status update packet (in bits). This constraint ensures that when sensor $k$ takes a sample at the beginning of slot $t$ (i.e., $b_k(t) = 1$), the achievable rate for sensor $k$ in slot $t$ is $R_k(t) = \underline{\eta}$, guaranteeing that the sample is transmitted during the slot.

Let $\delta_k(t)$ denote the AoI of sensor $k$ at the beginning of slot $t$. If sensor $k$ takes a sample at the beginning of slot $t$ (i.e., $b_k(t) = 1$), the AoI at the beginning of slot $t+1$ drops to one, and otherwise (i.e., $b_k(t) = 0$), the AoI increases by one. Thus, the evolution of $\delta_k(t)$ is characterized as

$$\delta_k(t+1) = \begin{cases} 1, & \text{if } b_k(t) = 1; \\ \delta_k(t)+1, & \text{otherwise.} \end{cases} \tag{102}$$

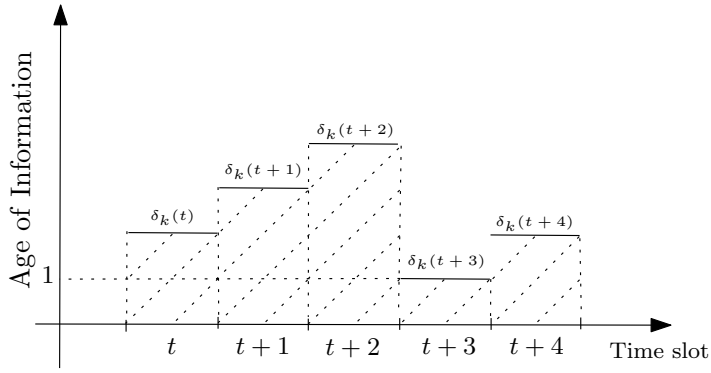


**Fig. 22. The evolution of the AoI of sensor $k$. Without status updates, the AoI increases by one unit during each slot; a status update received during slot $t+2$ caused the AoI to drop to one at the beginning of slot $t+3$.**

The evolution of the AoI of sensor $k$ is illustrated in Fig. 22.

Following a commonly used approach [6, 85, 88, 99], the average AoI of sensor $k$ is defined as the time average of the expected value of the AoI given as

$$\Delta_k = \lim_{T\to\infty} \frac{1}{T} \sum_{t=0}^{T-1} \mathbb{E}[\delta_k(t)], \tag{103}$$

where the expectation is with respect to the random wireless channel states and control actions made in reaction to the channel states[3]. Without loss of generality, it is considered that the initial value of the AoI of all sensors is $\delta_k(0) = 0$, $\forall k \in \mathscr{K}$.

### *4.1.2 Problem formulation*

The objective is to minimize the average total transmit power of sensors by jointly optimizing the sampling action, the transmit power allocation, and the sub-channel assignment in each slot subject to the maximum average AoI constraint for each sensor.

[3]In this work, all expectations are taken with respect to the randomness of the wireless channel states and control actions made in reaction to the channel states.

Thus, the problem is formulated as follows

$$\text{minimize} \lim_{T\to\infty} \frac{1}{T} \sum_{t=0}^{T-1} \sum_{k\in\mathscr{K}} \sum_{n\in\mathscr{N}} \mathbb{E}[p_{k,n}(t)] \tag{104a}$$

$$\text{subject to} \lim_{T\to\infty} \frac{1}{T} \sum_{t=0}^{T-1} \mathbb{E}[\delta_k(t)] \leq \Delta_k^{\max},\ \forall k \in \mathscr{K} \tag{104b}$$

$$\sum_{n\in\mathscr{N}} \rho_{k,n}(t) \underline{W} \log_2 \left(1 + \frac{p_{k,n}(t)|h_{k,n}(t)|^2}{\underline{W} N_0}\right) = \underline{\eta} b_k(t),\ \forall k \in \mathscr{K},\ t \tag{104c}$$

$$\sum_{k\in\mathscr{K}} \rho_{k,n}(t) \leq 1,\ \forall n \in \mathscr{N}, t \tag{104d}$$

$$p_{k,n}(t) \geq 0,\ \forall k \in \mathscr{K}, n \in \mathscr{N},\ t \tag{104e}$$

$$\rho_{k,n}(t) \in \{0,1\},\ \forall k \in \mathscr{K}, n \in \mathscr{N},\ t \tag{104f}$$

$$b_k(t) \in \{0,1\},\ \forall k \in \mathscr{K},\ t, \tag{104g}$$

with variables $\{p_{k,n}(t), \rho_{k,n}(t)\}_{k\in\mathscr{K}, n\in\mathscr{N}}$ and $\{b_k(t)\}_{k\in\mathscr{K}}$ for all $t \in \{0,1,\dots\}$, where $\Delta_k^{\max}$ is the maximum acceptable average AoI of sensor $k$. The constraints of problem (104) are as follows. The inequality (104b) is the maximum acceptable average AoI constraint for each sensor; the equality (104c) ensures that each sample is transmitted during one slot; the inequality (104d) constrains that each sub-channel can be assigned to at most one sensor in each slot; (104e), (104f), and (104g) represent the feasible values for the transmit power, sub-channel assignment, and sampling policy variables, respectively.

Problem (104) is a mixed integer non-convex problem where the constraints and the objective function both contain averages over the optimization variables. In the next section, a dynamic control algorithm is proposed to solve problem (104).

Prior to that, the definitions of feasibility of problem (104), channel-only policies, and the Slater's condition for problem (104) are introduced. These definitions are needed in the optimality analysis in Section 4.3.

**Definition 5.** Problem (104) is *feasible* if there exists a policy that satisfies constraints (104b)–(104g) [100, Sect. 4.3].

**Definition 6.** The *channel-only* policies are a class of policies that make decisions for sampling action, power allocation and sub-channel assignment of each sensor independently at every slot $t$ based only on the observed channel state [100, Sect. 3.1].

Note that since a channel-only policy does not consider any other information about the system, such as the AoI of the sensors, it might be difficult to devise a feasible

channel-only policy. We would like to emphasize that our proposed solution (presented in Section 4.2) is not a channel-only policy and we use the channel-only policies only to prove the optimality of the proposed dynamic algorithm.

**Assumption 1.** It is assumed that problem (104) satisfies Slater's condition [100, Sect. 4.3], i.e., there are values $\varepsilon > 0$, $\hat{G}(\varepsilon) \geq 0$, and a channel-only policy that satisfy in each slot

$$\sum_{k\in\mathscr{K}} \sum_{n\in\mathscr{N}} \mathbb{E}\left[\hat{p}_{k,n}(t)\right] = \hat{G}(\varepsilon), \tag{105}$$

$$\mathbb{E}[\hat{\delta}_k(t)] + \varepsilon \leq \Delta_k^{\max}, \ \forall k \in \mathscr{K}, \tag{106}$$

where $\hat{p}_{k,n}(t)$ and $\hat{\delta}_k(t)$ denote the allocated power to sensor $k$ over sub-channel $n$ in slot $t$ and the value of the AoI of sensor $k$ in slot $t$ determined by the channel-only policy, respectively.

## 4.2 Dynamic control algorithm

In this section, a dynamic control algorithm is developed to solve problem (104). To this end, the Lyapunov drift-plus-penalty method [100], [101] is used. According to the drift-plus-penalty method, the average AoI constraints (104b) are enforced by transforming them into queue stability constraints. For each inequality constraint (104b), a virtual queue is associated in such a way that the stability of these virtual queues implies the feasibility of the average AoI constraint (104b).

Let $\{Q_k(t)\}_{k\in\mathscr{K}}$ denote the virtual queues associated with AoI constraint (104b). The virtual queues are updated in each time slot as

$$Q_k(t+1) = \max\left[Q_k(t) - \Delta_k^{\max} + \delta_k(t+1), 0\right], \ \forall k \in \mathscr{K}. \tag{107}$$

Here, the notion of strong stability is used; the virtual queues are strongly stable if [100, Ch. 2]

$$\lim_{T\to\infty} \frac{1}{T} \sum_{t=0}^{T-1} \mathbb{E}[Q_k(t)] < \infty, \ \forall k \in \mathscr{K}. \tag{108}$$

According to (108), a queue is strongly stable if its average mean backlog is finite. Note that the strong stability of the virtual queues in (107) implies that the average AoI constraint (104b) is satisfied. Next, the Lyapunov function and its drift which are needed to define the queue stability problem are introduced.

Let $\mathscr{S}(t) = \{Q_k(t), \delta_k(t)\}_{k\in\mathscr{K}}$ denote the network state at slot $t$, and $\mathbf{Q}(t)$ denote a vector containing all the virtual queues, i.e., $\mathbf{Q}(t) = [Q_1(t), Q_2(t), \ldots, Q_K(t)] \in \mathbb{R}^{1\times K}$. Then, a quadratic Lyapunov function $L(\mathbf{Q}(t))$ is defined by [100, Ch. 3]

$$L(\mathbf{Q}(t)) = \frac{1}{2}\sum_{k\in\mathscr{K}} Q_k^2(t). \tag{109}$$

The Lyapunov function measures the network congestion: if the Lyapunov function is small, then all the queues are small, and if the Lyapunov function is large, then at least one queue is large. Therefore, by minimizing the expected change of the Lyapunov function from one slot to the next slot, queues $\{Q_k(t)\}_{k\in\mathscr{K}}$ can be stabilized [100, Ch. 4].

**Definition 7.** The conditional Lyapunov drift $\alpha(\mathscr{S}(t))$ is defined as the expected change in the Lyapunov function over one slot given that the current network state in slot $t$ is $\mathscr{S}(t)$. Thus, $\alpha(\mathscr{S}(t))$ is given by

$$\alpha(\mathscr{S}(t)) = \mathbb{E}\left[L(\mathbf{Q}(t+1)) - L(\mathbf{Q}(t)) \mid \mathscr{S}(t)\right]. \tag{110}$$

According to the drift-plus-penalty minimization method, a control policy that minimizes the objective function of problem (104) with constraints (104b)–(104g) is obtained by solving the following problem [100, Ch. 3]

$$\text{minimize } \alpha(\mathscr{S}(t)) + V\sum_{k\in\mathscr{K}}\sum_{n\in\mathscr{N}} \mathbb{E}[p_{k,n}(t) \mid \mathscr{S}(t)] \tag{111a}$$

$$\text{subject to } (104c) - (104g) \tag{111b}$$

with variables $\{p_{k,n}(t), \rho_{k,n}(t)\}_{k\in\mathscr{K},n\in\mathscr{N}}$ and $\{b_k(t)\}_{k\in\mathscr{K}}$, where a parameter $V \geq 0$ is used to adjust the emphasis on the objective function (i.e., power minimization). Therefore, by varying $V$, a desired trade-off between the sizes of the queue backlogs and the objective function value can be obtained.

Because of the presence of the $\max[\cdot]$ function in the virtual queue evolution in (107), working with the conditional Lyapunov drift $\alpha(\mathscr{S}(t))$ is difficult. Therefore, following the standard procedure of the drift-plus-penalty method, we provide an upper bound for the drift part that can be readily used in the optimization procedure [100, Ch. 4]; note that the penalty part (i.e., the original objective function) will remain unchanged. We would like to point out that when the conditional Lyapunov drift is replaced with the upper bound we have that: i) by minimizing the upper-bound of the conditional Lyapunov drift, the same logic for stabilizing the virtual queues mentioned above holds

true, and ii) the asymptotic optimality (as $V \to \infty$) of the proposed dynamic control algorithm is preserved, as shown in the optimality analysis in Section 4.3. To find the upper bound of the conditional Lyapunov drift $\alpha(\mathscr{S}(t))$, the following inequality is used in which, for any $\hat{A} \geq 0$, $\tilde{A} \geq 0$, and $\bar{A} \geq 0$, we have [100, Ch. 3]

$$\left(\max\left[\hat{A}-\tilde{A}+\bar{A},0\right]\right)^2 \leq \hat{A}^2+\tilde{A}^2+\bar{A}^2+2\hat{A}(\bar{A}-\tilde{A}). \tag{112}$$

By applying (112) to (107), an upper bound for $Q_k^2(t+1)$ is given as

$$Q_k^2(t+1) \leq Q_k^2(t)+(\Delta_k^{\max})^2+\delta_k^2(t+1)+2Q_k(t)\left(\delta_k(t+1)-\Delta_k^{\max}\right),\ \forall k \in \mathscr{K}. \tag{113}$$

By applying (113) to the conditional Lyapunov drift $\alpha(\mathscr{S}(t))$, an upper bound to (110) is obtained as

$$\alpha(\mathscr{S}(t)) \leq \frac{1}{2}\mathbb{E}\left[\sum_{k\in\mathscr{K}}\left((\Delta_k^{\max})^2+\delta_k^2(t+1)+2Q_k(t)\big(\delta_k(t+1)-\Delta_k^{\max}\big)\right)\middle|\mathscr{S}(t)\right] =$$
$$\frac{1}{2}\sum_{k\in\mathscr{K}}\left((\Delta_k^{\max})^2+\mathbb{E}[\delta_k^2(t+1)\mid\mathscr{S}(t)]+2Q_k(t)\big(\mathbb{E}[\delta_k(t+1)\mid\mathscr{S}(t)]-\Delta_k^{\max}\big)\right). \tag{114}$$

To characterize the upper bound in (114), we need to determine $\mathbb{E}[\delta_k(t+1)\mid\mathscr{S}(t)]$ and $\mathbb{E}[\delta_k^2(t+1)\mid\mathscr{S}(t)]$ in (114). To this end, by using the evolution of the AoI in (102), $\delta_k(t+1)$ and $\delta_k^2(t+1)$ are calculated as

$$\begin{aligned}\delta_k(t+1) &= b_k(t)+(1-b_k(t))\left(\delta_k(t)+1\right),\ \forall k\in\mathscr{K}\\ \delta_k^2(t+1) &= b_k(t)+(1-b_k(t))\left(\delta_k(t)+1\right)^2,\ \forall k\in\mathscr{K}.\end{aligned} \tag{115}$$

By using the expressions in (115), $\mathbb{E}[\delta_k(t+1)\mid\mathscr{S}(t)]$ and $\mathbb{E}[\delta_k^2(t+1)\mid\mathscr{S}(t)]$ in (114) are given as

$$\begin{aligned}\mathbb{E}[\delta_k(t+1)\mid\mathscr{S}(t)] &= \mathbb{E}[b_k(t)\mid\mathscr{S}(t)]+(1-\mathbb{E}[b_k(t)\mid\mathscr{S}(t)])(\delta_k(t)+1),\ \forall k\in\mathscr{K}\\ \mathbb{E}[\delta_k^2(t+1)\mid\mathscr{S}(t)] &= \mathbb{E}[b_k(t)\mid\mathscr{S}(t)]+(1-\mathbb{E}[b_k(t)\mid\mathscr{S}(t)])(\delta_k(t)+1)^2,\ \forall k\in\mathscr{K}.\end{aligned} \tag{116}$$

By substituting (116) into the right hand side of (114), and adding the term

$$V\sum_{k\in\mathscr{K}}\sum_{n\in\mathscr{N}}\mathbb{E}[p_{k,n}(t)\mid\mathscr{S}(t)]$$

to both sides of (114), the upper bound for (111a) is given as

$$\alpha(\mathscr{S}(t))+V\sum_{k\in\mathscr{K}}\sum_{n\in\mathscr{N}}\mathbb{E}[p_{k,n}(t)\mid\mathscr{S}(t)]\leq \tag{117}$$
$$\mathbb{E}\left[V\sum_{k\in\mathscr{K}}\sum_{n\in\mathscr{N}}p_{k,n}(t)+\frac{1}{2}\sum_{k\in\mathscr{K}}b_k(t)\big(1-(\delta_k(t)+1)^2-2Q_k(t)\delta_k(t)\big)\Big|\mathscr{S}(t)\right]$$
$$+\frac{1}{2}\sum_{k\in\mathscr{K}}\Big((\Delta_k^{\max})^2+(\delta_k(t)+1)^2+2Q_k(t)(\delta_k(t)+1)-2Q_k(t)\Delta_k^{\max}\Big).$$

Having defined the upper bound (117), instead of minimizing (111a), (117) is minimized subject to the constraints (104c)–(104g) with variables $\{p_{k,n}(t),\rho_{k,n}(t)\}_{k\in\mathscr{K},n\in\mathscr{N}}$ and $\{b_k(t)\}_{k\in\mathscr{K}}$. Given that we observe the channel states $\{h_{k,n}(t)\}_{k\in\mathscr{K},n\in\mathscr{N}}$ at the beginning of each slot, the approach of *opportunistically minimizing an expectation*[4] is used to solve the optimization problem. According to this approach, (117) is minimized by ignoring the expectations in each slot. Note that the approach of opportunistically minimizing an expectation provides the optimal control policy [100, Sect. 1.8].

The main steps of the proposed dynamic control algorithm are summarized in Algorithm 1. The controller observes the channel states $\{h_{k,n}(t)\}_{k\in\mathscr{K},n\in\mathscr{N}}$ and network state $\mathscr{S}(t)$ at the beginning of each time slot $t$. Then following the approach of opportunistically minimizing an expectation, it takes a control action to minimize (118) subject to the constraints (104c)–(104g) in Step 2. Note that the objective function of (118) follows from (117) because i) the variables of the optimization problem are $\{p_{k,n}(t),\rho_{k,n}(t)\}_{k\in\mathscr{K},n\in\mathscr{N}}$ and $\{b_k(t)\}_{k\in\mathscr{K}}$ and thus, the second term of the upper bound (117) is neglected as it does not depend on the optimization variables and ii) the opportunistically minimizing an expectation approach minimizes (117) by ignoring the expectations in each slot. In Step 3, according to the solution of (118), the virtual queue and AoI of each sensor are updated by using (107) and (115), respectively.

[4]To make the concept of opportunistically minimizing an expectation clear, consider the following. A system sees a random variable $w$ with some (possibly unknown) probability distribution and we need to choose a control action $a$ from an action set $\mathscr{A}_w$ to minimize the expectation of a general cost function $C(a,w)$, i.e., $\mathbb{E}[C(a,w)]$, where the expectation is taken with respect to the distribution of $w$ and the distribution of our action $a$ that possibly depends on $w$. Assume for simplicity that, for any given outcome $w$, there is at least one action $a_w^{\min}$ that minimizes the function $C(a,w)$ over all $a\in\mathscr{A}_w$. According to the approach of opportunistically minimizing an expectation, the policy that minimizes $\mathbb{E}[C(a,w)]$ is the one that observes $w$ and selects action $a_w^{\min}$ [100, Page 13]. In the considered system model, the channel coefficients $\{h_{k,n}(t)\}_{k\in\mathscr{K},n\in\mathscr{N}}$ play the role of random variable $w$; the sampling action, power allocation, and sub-channel assignment variables $\{b_k(t)\}_{k\in\mathscr{K}}$, $\{p_{k,n}(t),\rho_{k,n}(t)\}_{k\in\mathscr{K},n\in\mathscr{N}}$ play the role of control action $a$; and the objective function of the per-slot optimization problem, i.e., $\mathbb{E}\left[V\sum_{k\in\mathscr{K}}\sum_{n\in\mathscr{N}}p_{k,n}(t)+\frac{1}{2}\sum_{k\in\mathscr{K}}b_k(t)\big(1-(\delta_k(t)+1)^2-2Q_k(t)\delta_k(t)\big)\Big|\mathscr{S}(t)\right]$, plays the role of cost function $\mathbb{E}[C(a,w)]$.

**Algorithm 1** Proposed dynamic control algorithm for problem (104)

Step 1. **Initialization**: set $t = 0$, set $V$, and initialize $\{Q_k(0) = 0, \delta_k(0) = 0\}_{k\in\mathscr{K}}$
**for** each time slot $t$ **do**
Step 2. **Sampling action, transmit power, and sub-channel assignment**: obtain $\{p_{k,n}(t), \rho_{k,n}(t)\}_{k\in\mathscr{K},n\in\mathscr{N}}$ and $\{b_k(t)\}_{k\in\mathscr{K}}$ by solving the following optimization problem

$$\begin{aligned} &\text{minimize} \quad V\sum_{k\in\mathscr{K}}\sum_{n\in\mathscr{N}} p_{k,n}(t) + \frac{1}{2}\sum_{k\in\mathscr{K}} b_k(t)\left[1-(\delta_k(t)+1)^2 - 2Q_k(t)\delta_k(t)\right] \\ &\text{subject to} \quad (104c)-(104g), \end{aligned} \tag{118}$$

with variables $\{p_{k,n}(t), \rho_{k,n}(t)\}_{k\in\mathscr{K},n\in\mathscr{N}}$ and $\{b_k(t)\}_{k\in\mathscr{K}}$
Step 3. **Queue update**: update $\{Q_k(t+1), \delta_k(t+1)\}_{k\in\mathscr{K}}$ using (107) and (115)
Set $t = t+1$, and go to Step 2
**end for**

It is worth noting that the optimization problem (118) is a mixed integer non-convex optimization problem containing both integer (i.e., sub-channel assignment and sampling action) and continuous (i.e., power allocation) variables. One way to find the optimal solution of problem (118) is to use an exhaustive search method. However, it suffers from high computational complexity which increases exponentially with the number of variables in the system. Therefore, in Section 4.4, a sub-optimal solution for the optimization problem (118) is proposed. Before that, the optimality of the proposed dynamic algorithm is analyzed which is carried out in the next section.

### 4.3 Optimality analysis of the solution

In this section, the performance of the proposed Lyapunov drift-plus-penalty method (i.e., Algorithm 1) used to solve problem (104) is studied. In particular, the main result of our analysis will be stated in Theorem 7 which characterizes the trade-off between the optimality of the objective function (i.e., the average total transmit power) and average backlogs of the virtual queues in (107).

First, an important property of the AoI evolution under the proposed dynamic control algorithm is noted: the Lyapunov drift-plus-penalty Algorithm 1 ensures that the AoI of sensors are *bounded*, i.e., there is a constant $\delta^{\max} < \infty$ such that $\delta_k(t) \leq \delta^{\max}, \forall k \in \mathscr{K}, t$. Recall that the main goal of Algorithm 1 is to minimize the objective function of (118) in each slot. The objective function of (118) can be written as a form $\sum_{k=1}^{K} f(b_k(t), \delta_k(t))$, where $f(b_k(t), \delta_k(t)) = V\sum_{n\in\mathscr{N}} p_{k,n}(t) - 1/2 b_k(t)\left[-1+(\delta_k(t)+1)^2 + 2Q_k(t)\delta_k(t)\right]$. The maximum value of $f(b_k(t), \delta_k(t))$ for each sensor $k$ is zero and it is achieved when the sensor does not take a sample in slot $t$,

i.e., $b_k(t) = 0$. However, if sensor $k$ does not take a sample, its AoI increases by one after each slot, and thus, after some slots the term $1/2\left[-1+(\delta_k(t)+1)^2+2Q_k(t)\delta_k(t)\right]$ of $f(b_k(t),\delta_k(t))$ becomes greater than the first term $V\sum_{n\in\mathcal{N}} p_{k,n}(t)$; in this case, it is optimal for sensor $k$ to take a sample since it makes $f(b_k(t),\delta_k(t))$ negative. Thus, it can be concluded that each sensor takes a sample in a finite number of time slots, and this implies that there is a constant $\delta^{\max} < \infty$ such that $\delta_k(t) \leq \delta^{\max}, \forall k \in \mathcal{K}, t$.

Next, Lemma 5 is presented which shows that if problem (104) is feasible, we can get arbitrarily close to the optimal solution by channel-only policies. This lemma is used to prove Theorem 7.

**Lemma 5.** Under the assumption that each channel is a stationary process and i.i.d over slots, if problem (104) is feasible, then for any $\nu > 0$, there is a channel-only policy that satisfies in each slot

$$\sum_{k\in\mathcal{K}}\sum_{n\in\mathcal{N}} \mathbb{E}\left[p^*_{k,n}(t)\right] \leq G^{\text{opt}} + \nu, \tag{119}$$

$$\mathbb{E}[\delta^*_k(t)] - \nu \leq \Delta^{\max}_k, \ \forall k \in \mathcal{K}, \tag{120}$$

where $G^{\text{opt}}$ denotes the optimal value of the average total transmit power (i.e., the optimal value of the objective function of problem (104)), and $p^*_{k,n}(t)$ and $\delta^*_k(t)$ denote the allocated power to sensor $k$ over sub-channel $n$ and the value of the AoI of sensor $k$ determined by the channel-only policy, respectively.

*Proof.* See proof of Theorem 4.5 in [100, Appendix 4.A]. □

Next, Theorem 7 is presented which characterizes a trade-off between the optimality of the objective function of problem (104) and the average backlogs of the virtual queues in the system.

**Theorem 7.** Suppose that problem (104) is feasible and $L(\mathbf{Q}(0)) < \infty$. Then, for any values of parameter $V > 0$, Algorithm 1 satisfies the average AoI constraints in (104b). Further, let $\bar{p}_{k,n}(t)$ denote the allocated power to sensor $k$ over sub-channel $n$ in slot $t$ as determined by Algorithm 1, and $\bar{Q}_k(t)$ denote the virtual queue of sensor $k$ in slot $t$ as determined by Algorithm 1. Then, we have the following upper bounds for the average total transmit power and the average backlogs of the virtual queues in the system:

$$\lim_{T\to\infty} \frac{1}{T}\sum_{t=0}^{T-1}\sum_{k\in\mathcal{K}}\sum_{n\in\mathcal{N}} \mathbb{E}[\bar{p}_{k,n}(t)] \leq \frac{B}{V} + G^{\text{opt}}, \tag{121}$$

$$\lim_{T\to\infty}\frac{1}{T}\sum_{t=0}^{T-1}\sum_{k\in\mathscr{K}}\mathbb{E}[\bar{Q}_k(t)]\leq\frac{B+V\hat{G}(\varepsilon)}{\varepsilon}, \tag{122}$$

where $\hat{G}(\varepsilon)$ with $\varepsilon>0$ is specified by Assumption 1 (i.e., (105) and (106)), and constant $B$ is determined as follows

$$B=\frac{1}{2}\sum_{k\in\mathscr{K}}\Big((\Delta_k^{\max})^2+(\delta^{\max})^2\Big). \tag{123}$$

Before proving Theorem 7, the following remark is presented.

**Remark 4.** Inequality (122) implies the strong stability of the virtual queues $\{Q_k(t)\}_{k\in\mathscr{K}}$ which, in turn, implies that the average AoI constraints in (104b) are satisfied. In addition, from inequality (122), we can see that the upper bound of the average backlogs of the virtual queues is an increasing linear function of parameter $V$. Moreover, inequality (121) shows that the value of $V$ can be chosen so that $\frac{B}{V}$ is arbitrarily small, and thus, the average total transmit power achieved by Algorithm 1 becomes arbitrarily close to the optimal value $G^{\text{opt}}$. Consequently, parameter $V$ provides a trade-off between the optimality of the objective function (i.e., the average total transmit power) and average backlogs of the virtual queues in the system.

Next, Theorem 7 is proved.

*Proof.* Let $\bar{\delta}_k(t+1)$ and $\bar{\alpha}(\mathscr{S}(t))$ denote the value of the AoI of sensor $k$ and the conditional Lyapunov drift as determined by Algorithm 1 in slot $t$, respectively. Then, by using the bound in (114) and Lemma 5, we have

$$\begin{aligned}
&\bar{\alpha}(\mathscr{S}(t))+V\sum_{k\in\mathscr{K}}\sum_{n\in\mathscr{N}}\mathbb{E}[\bar{p}_{k,n}(t)\mid\mathscr{S}(t)]\overset{(a)}{\leq}V\sum_{k\in\mathscr{K}}\sum_{n\in\mathscr{N}}\mathbb{E}[\bar{p}_{k,n}(t)\mid\mathscr{S}(t)]+ \\
&\frac{1}{2}\sum_{k\in\mathscr{K}}\Big((\Delta_k^{\max})^2+\mathbb{E}[(\bar{\delta}_k(t+1))^2\mid\mathscr{S}(t)]+2Q_k(t)\big(\mathbb{E}[\bar{\delta}_k(t+1)\mid\mathscr{S}(t)]-\Delta_k^{\max}\big)\Big) \\
&\overset{(b)}{\leq}V\mathbb{E}\sum_{k\in\mathscr{K}}\sum_{n\in\mathscr{N}}\big[p_{k,n}^*(t)\big|\mathscr{S}(t)\big]+\frac{1}{2}\sum_{k\in\mathscr{K}}\Big((\Delta_k^{\max})^2+\mathbb{E}[(\delta_k^*(t+1))^2\mid\mathscr{S}(t)]+ \\
&2\bar{Q}_k(t)\big(\mathbb{E}[\delta_k^*(t+1)\mid\mathscr{S}(t)]-\Delta_k^{\max}\big)\Big)\overset{(c)}{\leq}V(G^{\text{opt}}+\nu)+\frac{1}{2}\sum_{k\in\mathscr{K}}\Big((\Delta_k^{\max})^2+(\delta^{\max})^2 \\
&+2\bar{Q}_k(t)\nu\Big),
\end{aligned} \tag{124}$$

where, as defined earlier, $p_{k,n}^*(t)$ and $\delta_k^*(t+1)$ denote the allocated power to sensor $k$ over sub-channel $n$ and the value of the AoI of sensor $k$ determined by the channel-

only policy that yields (119) and (120) for a fixed $\nu > 0$. Inequality $(a)$ comes from the upper bound in (114). Inequality $(b)$ follows because i) Algorithm 1 minimizes the left-hand side of inequality $(b)$ over all possible policies (not only channel-only policies) by using the opportunistically minimizing an expectation method [100, Sect. 1.8] and ii) the considered channel-only policy that yields (119) and (120) is a particular policy among all the policies. Inequality $(c)$ follows because i) we have $\mathbb{E}[(\delta_k^*(t+1))^2 \mid \mathscr{S}(t)] \leq (\delta^{\max})^2$, and ii) the considered channel-only policy that yields (119) and (120) is independent of the network state $\mathscr{S}(t)$. Thus, we have

$$\sum_{k\in\mathscr{K}}\sum_{n\in\mathscr{N}} \mathbb{E}\left[p_{k,n}^*(t)\middle|\mathscr{S}(t)\right] = \sum_{k\in\mathscr{K}}\sum_{n\in\mathscr{N}} \mathbb{E}\left[p_{k,n}^*(t)\right] \leq G^{\text{opt}} + \nu, \tag{125}$$

$$\mathbb{E}[\delta_k^*(t+1) \mid \mathscr{S}(t)] - \Delta_k^{\max} = \mathbb{E}[\delta_k^*(t+1)] - \nu \leq \Delta_k^{\max},\ \forall k \in \mathscr{K}. \tag{126}$$

By taking $\nu \to 0$, (124) results in the following inequality

$$\bar{\alpha}(\mathscr{S}(t)) + V \sum_{k\in\mathscr{K}}\sum_{n\in\mathscr{N}} \mathbb{E}[\bar{p}_{k,n}(t) \mid \mathscr{S}(t)] \leq B + VG^{\text{opt}}, \tag{127}$$

where $B$ is the constant defined in (123), i.e., $B = 1/2\sum_{k\in\mathscr{K}}\left((\Delta_k^{\max})^2 + (\delta^{\max})^2\right)$.

Taking expectations over randomness of the network state on both sides of (127) and using the law of iterated expectations, we have

$$\mathbb{E}\left[L\left(\bar{\mathbf{Q}}(t+1)\right)\right] - \mathbb{E}\left[L\left(\bar{\mathbf{Q}}(t)\right)\right] + V \sum_{k\in\mathscr{K}}\sum_{n\in\mathscr{N}} \mathbb{E}[\bar{p}_{k,n}(t)] \leq B + VG^{\text{opt}}, \tag{128}$$

where $\bar{\mathbf{Q}}(t)$ denotes a vector containing all the virtual queues in slot $t$ under Algorithm 1. By summing over $t \in \{0, \ldots, T-1\}$ and using the law of telescoping sums, we have

$$\mathbb{E}\left[L\left(\bar{\mathbf{Q}}(T)\right)\right] - \mathbb{E}\left[L\left(\bar{\mathbf{Q}}(0)\right)\right] + V \sum_{t=0}^{T-1}\sum_{k\in\mathscr{K}}\sum_{n\in\mathscr{N}} \mathbb{E}[\bar{p}_{k,n}(t)] \leq TB + TVG^{\text{opt}}. \tag{129}$$

Now we are ready to prove the bound of the average total transmit power in (121). In this regard, (129) is rewritten as follows

$$V \sum_{t=0}^{T-1}\sum_{k\in\mathscr{K}}\sum_{n\in\mathscr{N}} \mathbb{E}[\bar{p}_{k,n}(t)] \leq -\mathbb{E}\left[L\left(\bar{\mathbf{Q}}(T)\right)\right] + \mathbb{E}\left[L\left(\bar{\mathbf{Q}}(0)\right)\right] + TB + TVG^{\text{opt}} \overset{(a)}{\leq} \tag{130}$$
$$TB + TVG^{\text{opt}} + \mathbb{E}\left[L\left(\bar{\mathbf{Q}}(0)\right)\right],$$

where inequality $(a)$ follows because the negative term on the right-hand side of the first inequality was neglected. Dividing (130) by $TV$, we have

$$\frac{1}{T}\sum_{t=0}^{T-1}\sum_{k\in\mathscr{K}}\sum_{n\in\mathscr{N}}\mathbb{E}[\bar{p}_{k,n}(t)] \leq \frac{B}{V}+G^{\text{opt}}+\frac{\mathbb{E}\left[L\left(\bar{\mathbf{Q}}(0)\right)\right]}{TV}. \tag{131}$$

Since $\mathbb{E}\left[L\left(\bar{\mathbf{Q}}(0)\right)\right]$ has a finite value, taking the limit $T\to\infty$ in (131) proves the bound of the average total transmit power in (121).

To prove the bound of the average backlogs of the virtual queues in (122), it is assumed that the Slater's condition presented in Assumption 1 holds. In other words, it is assumed that there is a channel-only policy so that the virtual queues are strongly stable. Thus, by using the bound in (114), we have (cf. (124))

$$\begin{aligned}
&\bar{\alpha}(\mathscr{S}(t))+V\sum_{k\in\mathscr{K}}\sum_{n\in\mathscr{N}}\mathbb{E}[\bar{p}_{k,n}(t)\mid\mathscr{S}(t)] \overset{(a)}{\leq} V\sum_{k\in\mathscr{K}}\sum_{n\in\mathscr{N}}\mathbb{E}[\bar{p}_{k,n}(t)\mid\mathscr{S}(t)]+ \qquad (132)\\
&\frac{1}{2}\sum_{k\in\mathscr{K}}\left((\Delta_k^{\max})^2+\mathbb{E}[(\bar{\delta}_k(t+1))^2\mid\mathscr{S}(t)]+2\bar{Q}_k(t)\left(\mathbb{E}[\bar{\delta}_k(t+1)\mid\mathscr{S}(t)]-\Delta_k^{\max}\right)\right)\\
&\overset{(b)}{\leq} V\sum_{k\in\mathscr{K}}\sum_{n\in\mathscr{N}}\mathbb{E}\left[\hat{p}_{k,n}(t)\middle|\mathscr{S}(t)\right]+\frac{1}{2}\sum_{k\in\mathscr{K}}\left((\Delta_k^{\max})^2+\mathbb{E}[(\hat{\delta}_k(t+1))^2\mid\mathscr{S}(t)]+\right.\\
&\left.2\bar{Q}_k(t)\left(\mathbb{E}[\hat{\delta}_k(t+1)\mid\mathscr{S}(t)]-\Delta_k^{\max}\right)\right)\overset{(c)}{\leq} V\hat{G}(\varepsilon)+B-\varepsilon\sum_{k\in\mathscr{K}}\bar{Q}_k(t),
\end{aligned}$$

where, as defined earlier, $\hat{p}_{k,n}(t)$ and $\hat{\delta}_k(t+1)$ denote the allocated power to sensor $k$ over sub-channel $n$ and the value of the AoI of sensor $k$ determined by the channel-only policy that yields (105) and (106) in the Slater's condition, respectively. Inequality $(a)$ comes from the upper bound in (114). Inequality $(b)$ follows because i) Algorithm 1 minimizes the left-hand side of inequality $(b)$ over all possible policies (not only channel-only policies) by using the opportunistically minimizing an expectation method and ii) the considered channel-only policy that yields (105) and (106) in the Slater's condition is a particular policy among all the policies. Inequality $(c)$ follows because i) we have $\mathbb{E}[(\hat{\delta}_k(t+1))^2\mid\mathscr{S}(t)]\leq(\delta^{\max})^2$, ii) constant $B$ is given by (123), and iii) the channel-only policy that yields (105) and (106) is independent of the network state $\mathscr{S}(t)$. Thus, we have

$$\sum_{k\in\mathscr{K}}\sum_{n\in\mathscr{N}}\mathbb{E}\left[\hat{p}_{k,n}(t)\mid\mathscr{S}(t)\right]=\sum_{k\in\mathscr{K}}\sum_{n\in\mathscr{N}}\mathbb{E}\left[\hat{p}_{k,n}(t)\right]=\hat{G}(\varepsilon), \tag{133}$$

$$\mathbb{E}[\hat{\delta}_k(t+1)\mid\mathscr{S}(t)]+\varepsilon=\mathbb{E}[\hat{\delta}_k(t+1)]+\varepsilon\leq\Delta_k^{\max},\ \forall k\in\mathscr{K}. \tag{134}$$

Taking expectations over randomness of the network state on both sides of the resulting inequality in (132) and using the law of iterated expectations, we have

$$\mathbb{E}\left[L\left(\bar{\mathbf{Q}}(t+1)\right)\right]-\mathbb{E}\left[L\left(\bar{\mathbf{Q}}(t)\right)\right]+V\sum_{k\in\mathscr{K}}\sum_{n\in\mathscr{N}}\mathbb{E}[\bar{p}_{k,n}(t)]\leq \tag{135}$$
$$B-\varepsilon\sum_{k\in\mathscr{K}}\mathbb{E}[\bar{Q}_k(t)]+V\hat{G}(\varepsilon).$$

By summing over $t\in\{0,\ldots,T-1\}$ and using the law of telescoping sums, we have

$$\mathbb{E}\left[L\left(\bar{\mathbf{Q}}(T)\right)\right]-\mathbb{E}\left[L\left(\bar{\mathbf{Q}}(0)\right)\right]+V\sum_{t=0}^{T-1}\sum_{k\in\mathscr{K}}\sum_{n\in\mathscr{N}}\mathbb{E}[\bar{p}_{k,n}(t)]\leq \tag{136}$$
$$TB-\varepsilon\sum_{t=0}^{T-1}\sum_{k\in\mathscr{K}}\mathbb{E}[\bar{Q}_k(t)]+TV\hat{G}(\varepsilon).$$

To prove the bound in (122), the inequality (136) is rewritten as follows

$$\varepsilon\sum_{t=0}^{T-1}\sum_{k\in\mathscr{K}}\mathbb{E}[\bar{Q}_k(t)]\leq-\mathbb{E}\left[L\left(\bar{\mathbf{Q}}(T)\right)\right]+\mathbb{E}\left[L\left(\bar{\mathbf{Q}}(0)\right)\right]- \tag{137}$$
$$V\sum_{t=0}^{T-1}\sum_{k\in\mathscr{K}}\sum_{n\in\mathscr{N}}\mathbb{E}[\bar{p}_{k,n}(t)]+TB+TV\hat{G}(\varepsilon)\overset{(a)}{\leq}TB+TV\hat{G}(\varepsilon)+\mathbb{E}\left[L\left(\bar{\mathbf{Q}}(0)\right)\right],$$

where inequality $(a)$ follows because the negative terms on the right-hand side of the first inequality was neglected. By dividing (137) by $T\varepsilon$, we have

$$\frac{1}{T}\sum_{t=0}^{T-1}\sum_{k\in\mathscr{K}}\mathbb{E}[\bar{Q}_k(t)]\leq\frac{B+V\hat{G}(\varepsilon)}{\varepsilon}+\frac{\mathbb{E}\left[L\left(\bar{\mathbf{Q}}(0)\right)\right]}{T\varepsilon}. \tag{138}$$

Since $\mathbb{E}\left[L\left(\bar{\mathbf{Q}}(0)\right)\right]$ has a finite value, taking the limit $T\to\infty$ in (138) proves the bound of the average backlogs of the virtual queues in (122). □

### 4.4 A sub-optimal solution for the per-slot problem (118)

As discussed in Section 4.2, we need to solve an instance of the optimization problem (118) in each slot (see Algorithm 1). Problem (118) is a mixed integer non-convex optimization problem containing both integer (i.e., sub-channel assignment and sampling action) and continuous (i.e., power allocation) variables. Thus, finding its optimal solution is not trivial and conventional methods for solving convex optimization problems cannot directly be used. The optimal solution of problem (118) can be found by an

exhaustive search method that requires searching over all possible combinations of the binary variables, i.e., the sub-channel assignment and sampling action variables, and solving a (simple) power allocation problem for each such combination. However, the computational complexity of this method increases exponentially with the number of sampling action and sub-channel assignment variables in the system (i.e., $KN$). Thus, finding an appropriate sub-optimal solution with low computational complexity is necessary for the optimization problem (118). Next, in Section 4.4.1, the proposed sub-optimal solution is presented. Then, in Section 4.4.2, complexity analysis of the sub-optimal solution is presented.

### 4.4.1 Solution algorithm

The main idea behind the proposed sub-optimal solution is to reduce the computational complexity from that of the full exhaustive search method described above. To this end, we search only over all possible combinations of sampling action variables $b_k(t)$, $\forall k \in \mathscr{K}$; for each such combination, a low-complexity two-stage optimization strategy is proposed to find a sub-optimal solution to the joint power allocation and sub-channel assignment problem. Then, among all the solutions, the best one is selected as the sub-optimal solution to problem (118). Note that if the number of sub-channels $N$ is less than the number of sensors $K$ (i.e., $N < K$) we do not search over all possible combinations of sampling action variables because the maximum number of sensors that can take a sample in each slot is $N$.

Let $\mathbf{b}(t) = [b_1(t), \ldots, b_K(t)]$ denote a vector containing all binary sampling action variables in slot $t$. Further, let $\mathscr{B}$ denote the set of all possible values of binary vector $\mathbf{b}(t)$ with cardinality $|\mathscr{B}| = 2^K$. In addition, let $\tilde{\mathscr{B}} \subseteq \mathscr{B}$ denote the set of all possible values of such binary vectors $\mathbf{b}(t)$ for which the number of sensors that have a sample to transmit is less than or equal to the number of sub-channels $N$, i.e., $\tilde{\mathscr{B}} = \{\mathbf{b}(t) \mid \mathbf{b}(t) \in \mathscr{B}, \|\mathbf{b}(t)\|_0 \leq N\}$, where $\|\cdot\|_0$ counts the number of non-zero elements in a vector. Note that for $K \leq N$, the set $\tilde{\mathscr{B}}$ is equal to set $\mathscr{B}$, i.e., $\tilde{\mathscr{B}} = \mathscr{B}$.

The steps of the proposed sub-optimal solution are summarized in Algorithm 2. Step 2 performs exhaustive search over feasible sampling actions $\mathbf{b}(t) \in \tilde{\mathscr{B}}$: for each such $\mathbf{b}(t)$ a sub-optimal power allocation and sub-channel assignment is obtained by finding an approximate solution for the mixed integer non-convex problem (118) with variables $\{\rho_{k,n}(t), p_{k,n}(t)\}_{k\in\mathscr{K},n\in\mathscr{N}}$ (i.e., problem (139)) which is presented in the next subsections. Step 3 returns a sub-optimal solution to problem (118).

The power allocation and sub-channel assignment problem (139) is a mixed integer non-convex optimization problem. Thus, a two-stage sequential optimization method is

**Algorithm 2** Proposed sub-optimal solution algorithm to problem (118)

Step 1. **Initialization**: set $O=0$, $\{\tilde{b}_k(t)=0\}_{k\in\mathscr{K}}$, $\{\tilde{p}_{k,n}(t)=0\}_{k\in\mathscr{K},n\in\mathscr{N}}$, and $\{\tilde{\rho}_{k,n}(t)=0\}_{k\in\mathscr{K},n\in\mathscr{N}}$

Step 2. For each $\mathbf{b}(t)\in\tilde{\mathscr{B}}$ **do**

A. Find a sub-optimal solution for the following joint power allocation and sub-channel assignment problem

$$\begin{aligned}&\text{minimize} \quad V\sum_{k\in\mathscr{K}}\sum_{n\in\mathscr{N}}p_{k,n}(t)+\frac{1}{2}\sum_{k\in\mathscr{K}}b_k(t)\left[1-(\delta_k(t)+1)^2-2Q_k(t)\delta_k(t)\right]\\&\text{subject to} \quad (104c)-(104f),\end{aligned} \tag{139}$$

with variables $\{\rho_{k,n}(t),p_{k,n}(t)\}_{k\in\mathscr{K},n\in\mathscr{N}}$

B. Denote the obtained solution by $\{\dot{p}_{k,n}(t)\}_{k\in\mathscr{K},n\in\mathscr{N}}$, $\{\dot{\rho}_{k,n}(t)\}_{k\in\mathscr{K},n\in\mathscr{N}}$, and $\{\dot{b}_k(t)\}_{k\in\mathscr{K}}$

C. If $V\sum_{k\in\mathscr{K}}\sum_{n\in\mathscr{N}}\dot{p}_{k,n}(t)+\frac{1}{2}\sum_{k\in\mathscr{K}}\dot{b}_k(t)\left[1-(\delta_k(t)+1)^2-2Q_k(t)\delta_k(t)\right]\leq O$:

I. Set $\{\tilde{p}_{k,n}(t)=\dot{p}_{k,n}(t)\}_{k\in\mathscr{K},n\in\mathscr{N}}$, $\{\tilde{\rho}_{k,n}(t)=\dot{\rho}_{k,n}(t)\}_{k\in\mathscr{K},n\in\mathscr{N}}$, $\{\tilde{b}_k(t)=\dot{b}_k(t)\}_{k\in\mathscr{K}}$

II. Set $O=V\sum_{k\in\mathscr{K}}\sum_{n\in\mathscr{N}}\tilde{p}_{k,n}(t)+\frac{1}{2}\sum_{k\in\mathscr{K}}\tilde{b}_k(t)\left[1-(\delta_k(t)+1)^2-2Q_k(t)\delta_k(t)\right]$

Step 3. Return $\{\tilde{\rho}_{k,n}(t)\}_{k\in\mathscr{K},n\in\mathscr{N}}$, $\{\tilde{\rho}_{k,n}(t)\}_{k\in\mathscr{K},n\in\mathscr{N}}$, and $\{\tilde{b}_k(t)\}_{k\in\mathscr{K}}$ as a sub-optimal solution to problem (118)

proposed to find a sub-optimal solution to (139). The method performs first a greedy sub-channel assignment, which is followed by power allocation.

### *Sub-channel assignment*

The proposed greedy algorithm to assign the sub-channels is presented in Algorithm 3. The main idea is to find the strongest sub-channel among all the sensors that have a sample to transmit, and assign this sub-channel greedily to that sensor (Step 1). This assigned sub-channel is then removed from the set of available sub-channels because each sub-channel can be assigned to at most one sensor (Step 2). For fairness, the sensor that was just assigned the sub-channel is removed from the set of competing sensors guaranteeing that this sensor cannot get more sub-channels until the other sensors get the same number of sub-channels (Step 3). This procedure is repeated until all the sub-channels are assigned to the sensors.

### *Power allocation*

Given that the sub-channels have been assigned, power allocation for each sensor that has a sample to transmit can be determined separately. Let $\mathscr{N}_k\subseteq\mathscr{N}$ denote the set of

**Algorithm 3** Sub-Channel Assignment

**Initialization:** a) initialize sets $\mathscr{K}' = \{k \mid k \in \mathscr{K}, b_k(t) = 1\}$, and $\mathscr{N}' = \mathscr{N}$, b) initialize $\{\rho_{k,n}(t) = 0\}_{k\in\mathscr{K},n\in\mathscr{N}}$, and c) set $i = 1$
**While** $i \leq N$ **do**
Step 1. Set $\rho_{k,n}(t) = 1$ where $(k,n) = \arg\max_{k\in\mathscr{K}',n\in\mathscr{N}'} |h_{k,n}(t)|^2$
Step 2. $\mathscr{N}' = \mathscr{N}' \setminus \{n\}$
Step 3. If $\mathscr{K}' \setminus \{k\} = \emptyset$, set $\mathscr{K}' = \mathscr{K}$; otherwise, set $\mathscr{K}' = \mathscr{K}' \setminus \{k\}$
Step 4. $i = i + 1$
**End while**

sub-channels assigned to sensor $k$. Thus, for each sensor $k$ that has a sample to transmit (i.e., $b_k(t) = 1$), the following optimization problem needs to be solved

$$\begin{aligned} \text{minimize} \quad & \textstyle\sum_{n\in\mathscr{N}_k} p_{k,n}(t) \\ \text{subject to} \quad & \textstyle\sum_{n\in\mathscr{N}_k} \rho_{k,n}(t)\underline{W}\log_2\left(1+\frac{p_{k,n}(t)|h_{k,n}(t)|^2}{\underline{W}N_0}\right) = \underline{\eta} \\ & p_{k,n}(t) \geq 0, \ \forall n \in \mathscr{N}_k, \end{aligned} \tag{140}$$

with variables $\{p_{k,n}(t)\}_{n\in\mathscr{N}_k}$. The optimization problem (140) can be solved by the water-filling approach [102, Proposition 2.1].

### 4.4.2 Complexity of the sub-optimal solution

In this section, the complexity of the sub-optimal solution for problem (118) is investigated and it is compared with that of the full exhaustive search method. The proposed sub-optimal solution presented in Algorithm 2 has three main steps, namely, i) determining the sampling actions which is solved by searching over all feasible sampling action combinations, ii) sub-channel assignment which is solved by the proposed greedy algorithm presented in Algorithm 3, and iii) power allocation which is solved by the water-filling approach. The computational complexity of the search over feasible sampling actions is equal to the cardinality of $\tilde{\mathscr{B}}$, i.e., $|\tilde{\mathscr{B}}|$ which is less than or equal to $2^K$ (recall that since $\tilde{\mathscr{B}} \subseteq \mathscr{B}$, we have $|\tilde{\mathscr{B}}| \leq |\mathscr{B}| = 2^K$). Since the proposed greedy algorithm to solve the sub-channel assignment (i.e., Algorithm 3) has $N$ iterations, its computational complexity is $N$. Since the water-filling approach needs at most $N$ iterations, its worst-case computational complexity is $N$ [102]. Thus, since for each possible sampling action combination, a sub-channel assignment and a power allocation problem with complexity $2N$ is solved, the computational complexity of the proposed sub-optimal solution presented in Algorithm 2 is $2N|\tilde{\mathscr{B}}|$. Next, the

computational complexity of the exhaustive search method to solve problem (118) is investigated.

The exhaustive search method searches over all feasible binary sampling action and sub-channel assignment variables. For each such combination, a convex power allocation problem is solved. Since the computational complexity of the search over sampling actions is $|\tilde{\mathscr{B}}|$ and there are $NK$ binary sub-channel assignment variables, computational complexity of the binary search is $|\tilde{\mathscr{B}}|2^{KN}$. Assuming that the water-filling approach presented in [102, Proposition 2.1] is used to solve the power allocation problem, the worst-case computational complexity of the power allocation is $N$. Thus, the computational complexity of the exhaustive search method to solve problem (118) is $N|\tilde{\mathscr{B}}|2^{KN}$.

Considering the discussion above, it can be seen that as compared to the full exhaustive search method, the computational complexity of the proposed sub-optimal solution reduces by a factor that is exponential in $KN$.

## 4.5 Numerical and simulation results

In this section, the performance of the proposed dynamic control algorithm presented in Algorithm 1 is evaluated in terms of transmit power consumption and AoI of the sensors. In addition, the optimality gap of the sub-optimal solution applied to solve problem (118) presented in Algorithm 2 is evaluated.

### *4.5.1 Simulation setup*

Consider a WSN depicted in Fig. 23, where the sink is located in the center and $K = 10$ sensors are randomly placed in a two-dimensional plane. Sensors are indexed according to their distance to the sink in such a way that sensor 1 is the nearest sensor to the sink and sensor 10 is the farthest. The channel coefficient from sensor $k$ to the sink over sub-channel $n$ in slot $t$ is modeled as $h_{k,n}(t) = (d_k/d_0)^{\underline{\xi}} c_{k,n}(t)$, where $d_k$ is the distance from sensor $k$ to the sink, $d_0$ is the far field reference distance, $\underline{\xi}$ is the path loss exponent, and $c_{k,n}(t)$ is a Rayleigh distributed random coefficient. Accordingly, $(d_k/d_0)^{\underline{\xi}}$ represents large-scale fading and the term $c_{k,n}(t)$ represents small-scale Rayleigh fading. The path loss exponent and the far field reference distance are set as $\underline{\xi} = -3$ and $d_0 = 1$, respectively, and the parameter of Rayleigh distribution is set as 0.5. The bandwidth of each sub-channel is $\underline{W} = 180$ kHz. The size of each packet is $\underline{\eta} = 600$ Bytes. The same maximum acceptable average AoI is considered for all the sensors, i.e., $\Delta_k^{\max} = \Delta^{\max}, \forall k$.

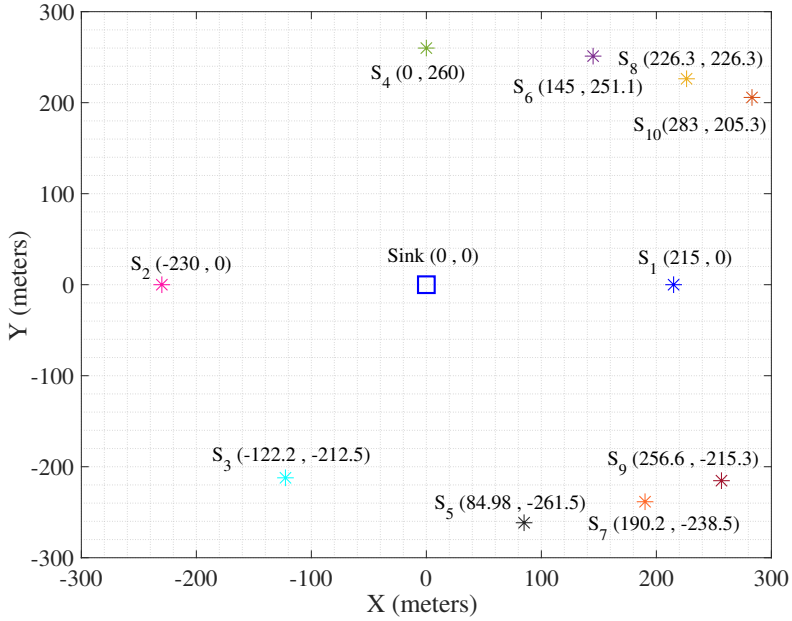


**Fig. 23. The considered WSN where the sink is located in the center and $K = 10$ sensors are randomly placed. The coordinates of sensor $k$ is shown by $S_k(x_k, y_k)$.**

### *4.5.2 Performance of the dynamic control algorithm*

In this section, the performance of the dynamic control algorithm (i.e., Algorithm 1) is evaluated in terms of transmit power consumption and average AoI of the sensors. To solve the optimization problem (118), Algorithm 2 is used.

Fig. 24 illustrates the evolution of the average total transmit power for different values of parameter $V$ with maximum acceptable average AoI of sensors $\Delta^{\max} = 4$ and $N = 10$ sub-channels. The figure shows that when $V$ increases, the average total transmit power decreases. This is because when $V$ increases, more emphasis is on minimizing the total transmit power in the objective function of optimization problem (118).

In addition, for the benchmarking, a baseline policy that has a fixed sampling rate is considered. The sampling rate is set as $1/7$, so that resulting average AoI of each sensor is equal to the maximum acceptable average AoI $\Delta_k = \Delta^{\max} = 4, \forall k \in \mathscr{K}$. The sampling schedule of the considered baseline method is presented in Table 8. For this baseline policy, the sub-channel assignment and transmit power allocation are determined by the proposed methods in Section 4.4.1. As can be seen in Fig. 24, the proposed dynamic control algorithm achieves more than 60 % saving in the average

**Table 8. Sampling schedule of the considered fixed rate sampling policy of rate $1/7$.**

| Time slot $t$ | 1 | 2 | 3 | 4 | 5 | 6 | 7 | 8 | 9 | 10 | 11 |
|---|---|---|---|---|---|---|---|---|---|---|---|
| Sensor $k$ with $b_k(t) = 1$ | 1 | 2 | 3 | 4 | 5, 6 | 7, 8 | 9, 10 | 1 | 2 | 3 | $\cdots$ |

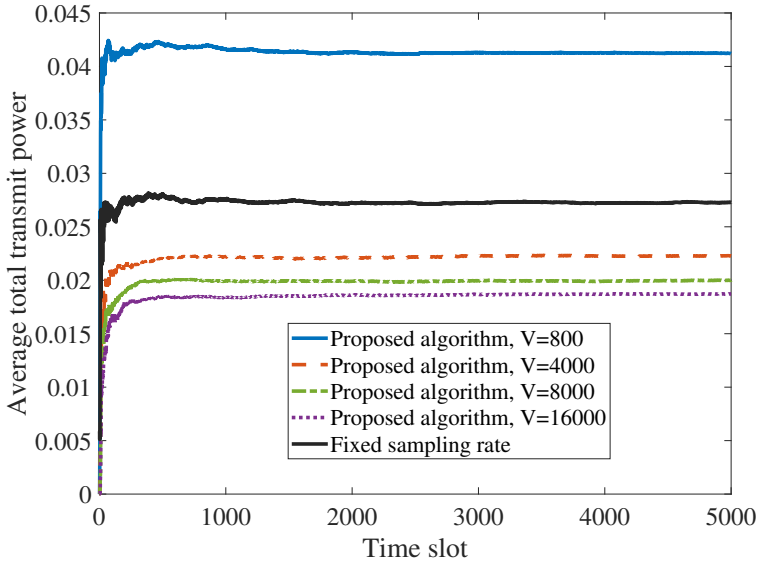


**Fig. 24. Evolution of the average total transmit power of the sensors for different values of $V$ with $\Delta^{\max} = 4$ and $N = 10$. For comparison, a control policy with a fixed sampling rate is included as a baseline method.**

total transmit power compared to the baseline policy. This shows the advantage of the proposed dynamic control algorithm in optimizing the sampling process in contrast to relying on a pre-defined sampling schedule which enforces a sensor to transmit a status update even under a bad channel situation.

Fig. 25 illustrates the trade-off between the average total transmit power and average backlogs of the virtual queues as a function of $V$ for $\Delta^{\max} = 4$ and $N = 10$ sub-channels. As can be seen, by increasing $V$ the average backlogs of the virtual queues increase and the average total transmit power decreases. This shows the inherent trade-off provided by the drift-plus-penalty method which was shown in Theorem 7. Moreover, the figure demonstrates that when $V$ is sufficiently large, increasing it further does not significantly reduce the power. This is visible in Fig. 24 as well.

Fig. 26 illustrates the evolution of the average total transmit power for different numbers of sub-channels $N$ with $\Delta^{\max} = 4$ and $V = 8000$. The figure shows that when $N$ increases, the average total transmit power decreases, as expected. This is because

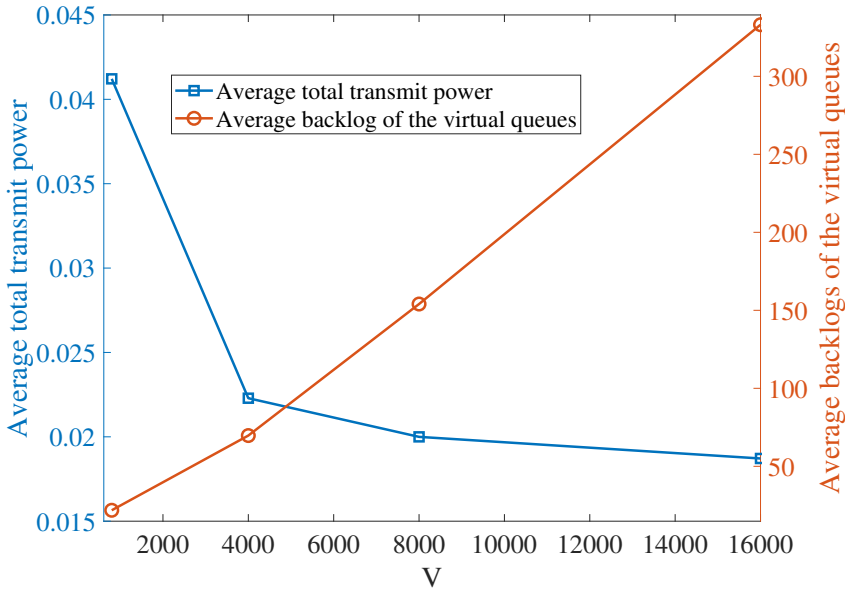


**Fig. 25. Trade-off between the average total transmit power of the sensors and average backlogs of the virtual queues as a function of $V$.**

when $N$ increases, more sub-channels can be assigned to each sensor, and thus, one packet can be transmitted with less power. In addition, we can see that the effect of increasing the number of sub-channels from $N = 6$ to $N = 8$, and further to $N = 10$, is more profound. This is because when there are fewer sub-channels than sensors, due to the orthogonality of the sub-channel assignment, all the sensors cannot be served in every slot and some sensors can get a sub-channel only after a few slots. Note that in order to meet the AoI constraint, the sensors may be enforced to transmit their sample even if the power consumption is excessive. On the other hand, increasing the number of sub-channels from $N = 10$ to $N = 12$ yields only negligible gain. This is because the greedy sub-channel assignment policy guarantees that each sensor will be assigned at least one sub-channel.

Fig. 27 illustrates the evolution of the average total transmit power for different values of maximum AoI $\Delta^{\max}$ with $N = 10$ sub-channels and $V = 8000$. The figure shows that when $\Delta^{\max}$ decreases, the average total transmit power increases. This is because when $\Delta^{\max}$ decreases, each sensor needs to take samples more frequently to satisfy constraint (104b).

Fig. 28 depicts the average AoI for individual sensors as a function of $V$ for $\Delta^{\max} = 4$ and $N = 10$ sub-channels. According to this figure, when $V$ increases, the average AoI

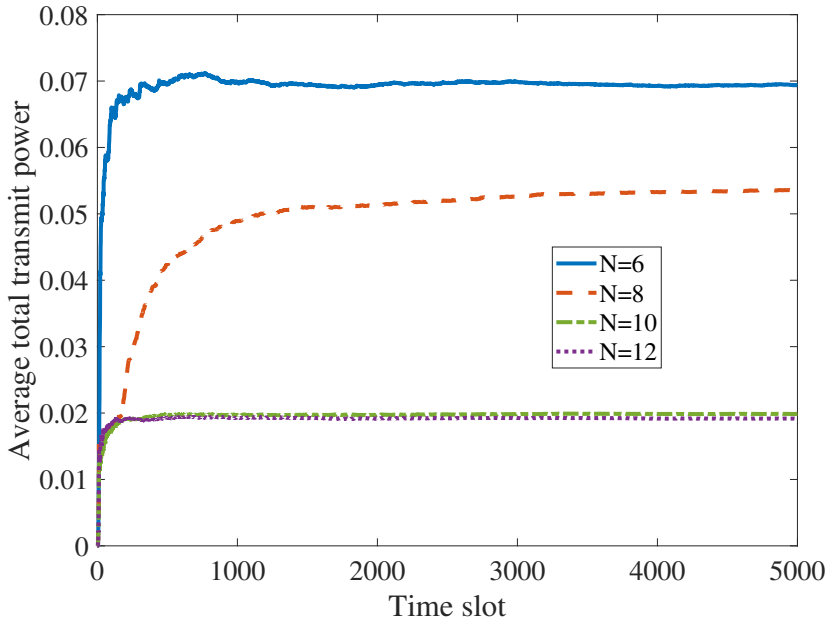


**Fig. 26. Evolution of the average total transmit power of the sensors for different numbers of sub-channels $N$ with $\Delta^{\max} = 4$ and $V = 8000$.**

of each sensor increases as well. This is because when $V$ increases, the backlogs of the virtual queues associated with the average AoI constraint (104b) increase. We can also observe that the average AoI of each sensor is always smaller than the maximum acceptable average AoI $\Delta^{\max}$. This validates that the drift-plus-penalty method is able to meet the average constraint through enforcing the virtual queue stability. Moreover, we can see that a sensor that has a longer distance to the sink has higher average AoI. This is because a sensor far away from the sink must compensate for the large-scale fading by using more power, and thus, it rarely samples.

### *4.5.3 Performance of the sub-optimal solution*

To evaluate the optimality gap of the sub-optimal solution for (118) presented in Algorithm 2, the results obtained by the sub-optimal solution are compared to those of the optimal solution calculated by the full exhaustive search method. In this regard, a small setup with $K = 5$ sensors $\{S_1, \ldots, S_5\}$ (see Fig. 23) and $N = 5$ sub-channels is considered. The maximum acceptable average AoI of sensors is $\Delta^{\max} = 4$.

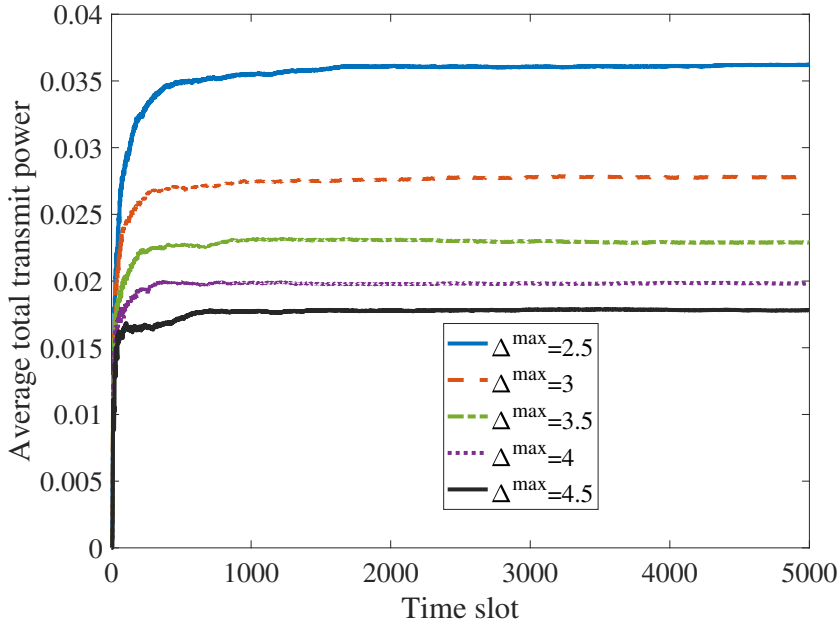


**Fig. 27. Evolution of the average total transmit power of the sensors for different values of $\Delta^{\max}$ with $N = 10$ and $V = 8000$.**

Fig. 29 illustrates the evolution of the average total transmit power for different values of $V$. Fig. 30 illustrates the trade-off between the average total transmit power of the sensors and average backlogs of the virtual queues as a function of $V$. Fig. 31 depicts the average AoI of different sensors as a function of $V$. Fig. 32 depicts the evolution of the average AoI of different sensors for $V = 8000$. From these figures, it can be seen that the proposed sub-optimal solution provides a near-optimal solution for the optimization problem (118).

### 4.6 Summary and discussion

A status update system consisting of a set of sensors and one sink was considered. A controller controls the sampling process and decides for each sensor whether it takes a sample or not at the beginning of each slot. The status update packets of the sensors are transmitted by sharing a set of orthogonal sub-channels in each slot. The problem of minimizing the average total transmit power of sensors under the average AoI constraint for each sensor was formulated. To solve the problem, the Lyapunov drift-plus-penalty method was used and the optimality analysis was conducted. In the numerical results

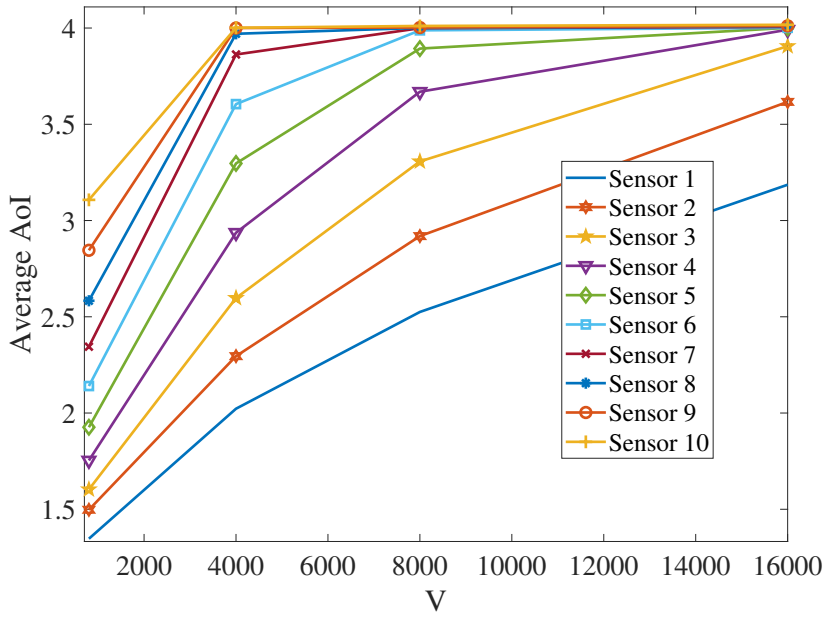


**Fig. 28. The average AoI of different sensors as a function of $V$ for $\Delta^{\max} = 4$ and $N = 10$.**

section, the performance of the proposed dynamic solution algorithm was shown in terms of transmit power consumption and AoI of sensors. The results showed that by using the proposed dynamic control algorithm more than 60 % saving in the average total transmit power can be achieved compared to a baseline policy. In addition, it was shown that the sub-optimal solution for the per-slot optimization problems provides a near-optimal solution.

The numerical results illustrated the inherent trade-off between the average AoI of the sensors and the average total transmit power that the Lyapunov drift-plus-penalty method brings in the system. This trade-off is adjusted by the penalty parameter $V$. A high value of $V$ is beneficial in that it enforces smaller transmit powers, yet at the cost of increasing the average AoI of each sensor. The results validated that, regardless of the value of $V$, the proposed drift-plus-penalty method met the time average AoI constraints through successfully enforcing the virtual queue stability. Regarding the selection of parameter $V$ in practice, it was observed that when $V$ is sufficiently large, increasing it further does not significantly reduce the power.

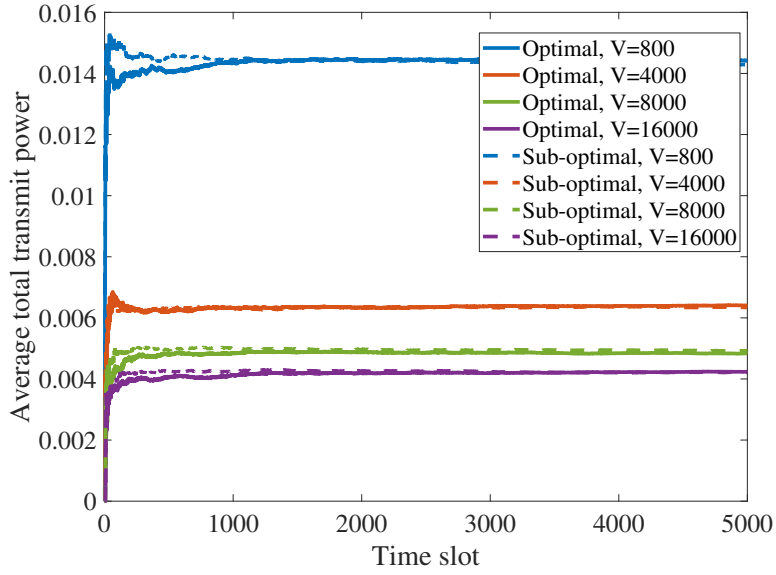


**Fig. 29. Evolution of the average total transmit power of the sensors for different values of $V$.**

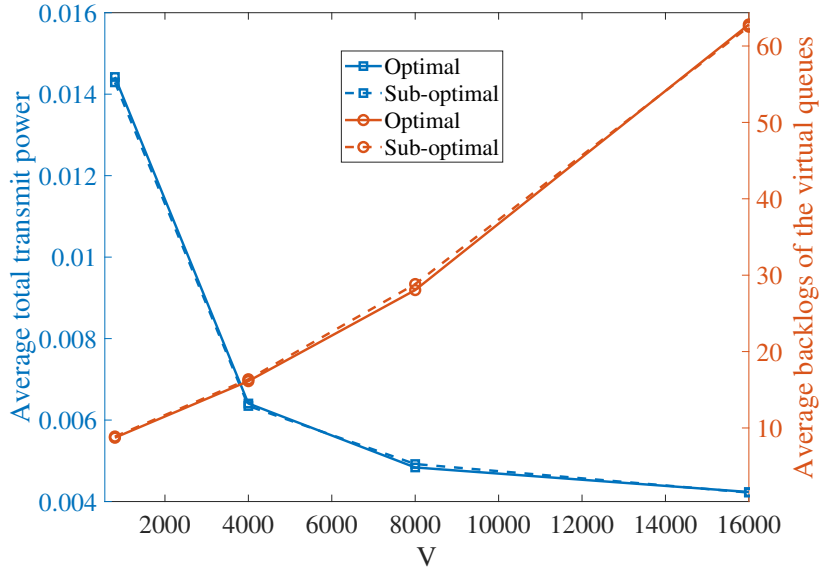


**Fig. 30. Trade-off between the average total transmit power and average backlogs of the virtual queues as a function of $V$.**

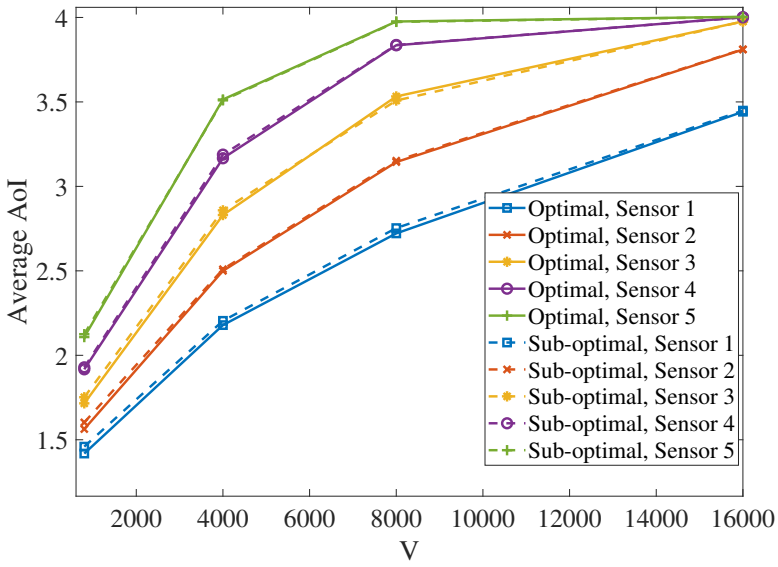


**Fig. 31. The average AoI of different sensors as a function of $V$.**

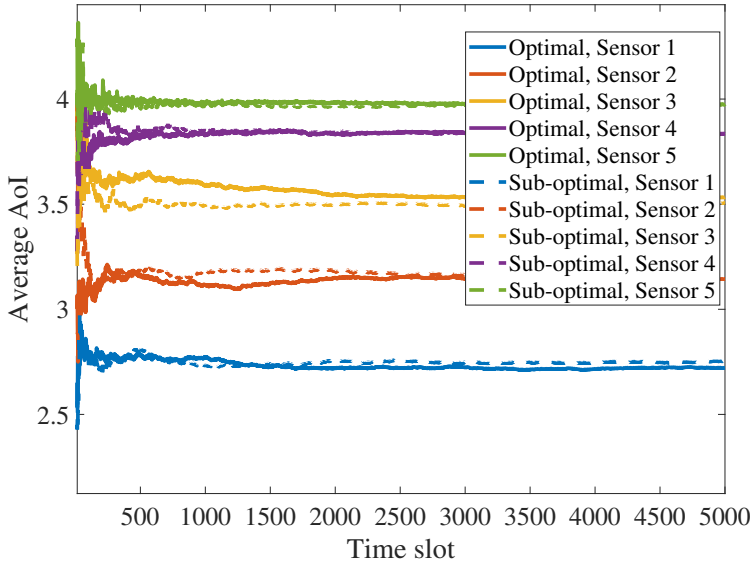


**Fig. 32. Evolution of the average AoI of different sensors for $V = 8000$.**

# 5 AoI in wireless sensor networks: A multi-access channel

Due to the scarcity of radio spectrum and the simplicity of devices in WSNs, it is critical to implement an appropriate channel access protocol to efficiently send the status update packets from the sensors to the destination over a shared channel. CSMA/CA is the most simple and practical contention-based access technique in wireless networks. CSMA/CA is a distributed channel access scheme that allows each sensor to initiate transmissions without any admission whenever a sensor has a data packet to transmit.

In this chapter, an application of the derived results for the AoI analysis in M/G/1 queueing models in Chapter 2 is studied. The worst case average AoI and average peak AoI of a sensor in a simplified CSMA/CA-based WSN under the FCFS policy are derived. The worst case analysis is carried out by considering that when a sensor contends for the channel to transmit its status update packet, all the other sensors have a packet to transmit and thus, the probability of collisions has the highest value.

The remainder of this chapter is organized as follows. Section 5.1 presents the system model and the AoI metrics. The worst case average AoI and average peak AoI of the simplified CSMA/CA-based system are derived in Section 5.2. Numerical results are presented in Section 5.3 and conclusions are drawn in Section 5.4.

## 5.1 System model and AoI metrics

Consider a simplified CSMA/CA-based WSN consisting of $K$ sensors, denoted by $\mathscr{K} = \{1, \ldots, K\}$. Each sensor is assigned to send status update packets of a random process to a destination. The AoI of one sensor, $k$, in a worst case scenario where all the other sensors $k' \in \mathscr{K} \setminus \{k\}$ always have a packet to transmit is studied, i.e., the other $K-1$ sensors have saturated queues. In this scenario, the probability of collisions for sensor $k$ has the highest value. It is assumed that the packet arrival rate of sensor $k$ follows the Poisson process with rate $\lambda$, and the server of sensor $k$ works according to the FCFS policy. In the following, a simplified CSMA/CA technique and the AoI metrics are presented.

### 5.1.1 CSMA/CA mechanism

Here, the main concept of the standard CSMA/CA technique, standardized by IEEE 802.11, is briefly presented. When sensor $k$ has a packet to transmit, it monitors the shared channel. If the channel is idle for a predetermined period of time named distributed interframe space (DIFS), the sensor transmits. Otherwise, if the channel is sensed busy, the sensor persists to monitor the channel until it is found idle for a DIFS period, denoted by $T_{\mathrm{DIFS}}$. The time immediately following an idle DIFS period is *slotted*. At this point, the sensor generates a random number $w$ according to the discrete uniform distribution taking values in $\{1,\ldots,\bar{C}\}$ and sets a back-off counter to the generated number, where $\bar{C}$ is a fixed contention window size. After choosing the random number, the back-off time counter of the sensor decrements at the beginning of each *slot*. Thus, a slot represents the time interval between two consecutive back-off counter states. When there is no transmission by the other sensors, the back-off counter state decrements after a fixed time interval denoted by $T_{\mathrm{F}}$. When a transmission is detected, the counter is frozen; when the channel is sensed idle for $T_{\mathrm{DIFS}}$, the counter is reactivated. The sensor starts to transmit its data when the counter reaches zero. After transmitting the data, the transmitter senses the channel to detect the acknowledgment (ACK) message from the destination. If the transmitter does not receive an ACK within a predetermined time, or it detects the signal of other sensors in the channel, it reschedules the packet transmission according to the random back-off rule. After a successful transmission, if the sensor has the next packet in its buffer, the transmission process is started from the random back-off rule.

### 5.1.2 Average AoI and peak AoI

The considered status update system for sensor $k$ is identical to an M/G/1 queueing model. Let $S$ denote the service time. Then, the average AoI $\Delta$ and the average peak AoI $A$ of sensor $k$ is calculated by (see equations (65) and (67))

$$\Delta = \mathbb{E}[S] + \frac{\lambda \mathbb{E}[S^2]}{2(1-\lambda \mathbb{E}[S])} + \frac{1-\lambda \mathbb{E}[S]}{\lambda L_S(\lambda)}, \tag{141}$$

$$A = \frac{1}{\lambda} + \frac{\lambda \mathbb{E}[S^2]}{2(1-\lambda \mathbb{E}[S])} + \mathbb{E}[S], \tag{142}$$

where $\mathbb{E}[S]$ is the expectation of the service time[5], $\mathbb{E}[S^2]$ is the second moment of the service time, and $L_S(\lambda) = \mathbb{E}[e^{-\lambda S}]$ is the Laplace transform of the PDF of the service time at the packet arrival rate $\lambda$.

In general, the calculation of (1) and (2) requires finding closed-form expressions of the service time parameters $\mathbb{E}[S]$, $\mathbb{E}[S^2]$, and $L_S(\lambda)$ for the standard CSMA/CA-based system. This, however, is intractable due to the intricate nature of the contention mechanism which results in a dependency of the transmissions of the different sensors. In this regard, the approximations introduced in [103] are used as follows. It is assumed that the probability of a collision in each slot for each sensor has a fixed value which thus disregards the dependencies of the transmission states of other sensors as well as the influence of the number of retransmissions. It is worth noting that when we are evaluating the system from the viewpoint of sensor $k$, the main analysis intrinsically focuses on the behavior of the system when sensor $k$ has a packet to transmit. On the other hand, the other sensors always have a packet to transmit. Thus, conditioned on the transmission stage of sensor $k$, each of the $K$ sensors in the network sees $K-1$ sensors that have a packet to transmit. Moreover, it is assumed that a packet transmission process is started by the random back-off rule and that the ACK message is instantaneous and error-free.

## 5.2 Worst case average AoI and average peak AoI of the simplified CSMA/CA-based system

To calculate the average AoI and average peak AoI in (141) and (142), respectively, the three required quantities $\mathbb{E}[S]$, $\mathbb{E}[S^2]$, and $L_S(\lambda)$ are derived. Let $M$ denote a discrete random variable that represents the number of (channel access) attempts sensor $k$ uses to successfully transmit a data packet. Let $S_m$ denote a random variable that represents the service time conditioned on the event that the number of attempts is $M = m$, i.e., the first $m-1$ attempts are failed and the $m^{\text{th}}$ attempt is successful. Accordingly, $S_m$ is expressed as

$$S_m = \sum_{j=1}^{m-1} \zeta_j + \xi_m, \tag{143}$$

where $\zeta_j$ is a random variable that represents the elapsed time of an unsuccessful transmission of sensor $k$ at the $j$th attempt and $\xi_m$ is a random variable that represents the elapsed time of a successful transmission of sensor $k$ at the $m$th attempt.

[5]Note that in Chapter 2, expectation of the service time $\mathbb{E}[S]$ was shown as $1/\mu$, i.e., $\mathbb{E}[S] = 1/\mu$.

By using the law of iterated expectations, the expectation $\mathbb{E}[S]$, second moment $\mathbb{E}[S^2]$, and Laplace transform $\mathbb{E}[e^{-\lambda S}]$ are calculated as follows:

$$\begin{aligned}
\mathbb{E}[S] &= \mathbb{E}_M\big[\mathbb{E}[S|M]\big] = \sum_{m=1}^{\infty} \mathbb{E}[S_m]\Pr(M=m), \\
\mathbb{E}[S^2] &= \mathbb{E}_M\big[\mathbb{E}[S^2|M]\big] = \sum_{m=1}^{\infty} \mathbb{E}[S_m^2]\Pr(M=m), \\
\mathbb{E}[e^{-\lambda S}] &= \mathbb{E}_M\big[\mathbb{E}[e^{-\lambda S}|M]\big] = \sum_{m=1}^{\infty} \mathbb{E}\big[e^{-\lambda S_m}\big]\Pr(M=m),
\end{aligned} \tag{144}$$

where $\Pr(M=m)$ is the probability of the event that $m-1$ attempts are failed and the $m$th attempt is successful. It can seen from (144) that to calculate the expectations $\mathbb{E}[S]$, $\mathbb{E}[S^2]$, and $\mathbb{E}[e^{-\lambda S}]$, we need to calculate the quantities $\mathbb{E}[S_m]$, $\mathbb{E}[S_m^2]$, $\mathbb{E}[e^{-\lambda S_m}]$, and $\Pr(M=m)$. These are derived in the following subsections.

### 5.2.1 Calculation of the first moment of $S_m$

By using (143), $\mathbb{E}[S_m]$ in (144) is written as follows:

$$\mathbb{E}[S_m] = \sum_{j=1}^{m-1} \mathbb{E}[\zeta_j] + \mathbb{E}[\xi_m]. \tag{145}$$

First, the expectation $\mathbb{E}[\xi_m]$ is derived. Let a discrete random variable $\bar{W}$ represent the random number generated by sensor $k$ in the back-off rule. Let $\xi_{j,w}$ denote the elapsed time of a successful transmission of sensor $k$ at the $j$th attempt conditioned on the event that the generated number is $\bar{W}=w$. Then, by using the law of iterated expectations, $\mathbb{E}[\xi_j]$ can be calculated as follows:

$$\begin{aligned}
\mathbb{E}[\xi_j] &= \mathbb{E}_{\bar{W}}\big[\mathbb{E}[\xi_j|\bar{W}]\big] \\
&= \sum_{w=1}^{C} \mathbb{E}[\xi_{j,w}]\Pr(\bar{W}=w) \\
&\overset{(a)}{=} \sum_{w=1}^{\bar{C}} \frac{\mathbb{E}[\xi_{j,w}]}{\bar{C}},
\end{aligned} \tag{146}$$

where equality $(a)$ follows because the random number $\bar{W}$ is selected according to the uniform distribution, i.e., $\Pr(\bar{W}=w) = 1/\bar{C}$.

By the definition of a successful transmission, $\xi_{j,w}$ in (146) is equal to the summation of the elapsed time until the back-off time counter reaches zero and the required time to transmit a packet, i.e.,

$$\xi_{j,w} = \sum_{i=1}^{w} \bar{T}_{j,i} + T_{\mathrm{P}}, \tag{147}$$

where $\bar{T}_{j,i}$ is a random variable that represents the time interval between two consecutive back-off counter states $i$ and $i-1$ at the $j$th attempt and $T_{\mathrm{P}}$ is the required time to transmit a data packet (which is determined according to the channel rate, data packet size etc.). By substituting (147) in (146), we have

$$\mathbb{E}[\xi_j] = \frac{1}{\bar{C}} \sum_{w=1}^{\bar{C}} \left( \sum_{i=1}^{w} \mathbb{E}[\bar{T}_{j,i}] + T_{\mathrm{P}} \right). \tag{148}$$

Similarly as for $\mathbb{E}[\xi_j]$, the expectation $\mathbb{E}[\zeta_j]$ is derived by introducing a random variable $\zeta_{j,w}$ to describe the elapsed time of an unsuccessful transmission of sensor $k$ at the $j$th attempt conditioned on the event that the generated number in the back-off rule is $\bar{W} = w$. Thus, $\mathbb{E}[\zeta_j]$ can be calculated as follows:

$$\begin{aligned} \mathbb{E}[\zeta_j] &= \mathbb{E}_{\bar{W}} \left[ \mathbb{E}[\zeta_j | \bar{W}] \right] \\ &= \sum_{w=1}^{C} \mathbb{E}[\zeta_{j,w}] \Pr(\bar{W} = w) \\ &= \sum_{w=1}^{\bar{C}} \frac{\mathbb{E}[\zeta_{j,w}]}{\bar{C}}. \end{aligned} \tag{149}$$

The random variable $\zeta_{j,w}$ is equal to the summation of the elapsed time until the back-off time counter reaches zero and the required time to transmit a packet, i.e.,

$$\zeta_{j,w} = \sum_{i=1}^{w} \bar{T}_{j,i} + T_{\mathrm{P}}. \tag{150}$$

By substituting (150) in (149), we have

$$\mathbb{E}[\zeta_j] = \frac{1}{\bar{C}} \sum_{w=1}^{\bar{C}} \left( \sum_{i=1}^{w} \mathbb{E}[\bar{T}_{j,i}] + T_{\mathrm{P}} \right). \tag{151}$$

To calculate $\mathbb{E}[\xi_j]$ in (148) and $\mathbb{E}[\zeta_j]$ in (151), we need to calculate $\mathbb{E}[\bar{T}_{j,i}]$. The random variable $\bar{T}_{j,i}$ can be defined based on two events: 1) when there is no transmission by the other sensors $k' \in \mathscr{K} \setminus \{k\}$ between two back-off counter states $i$ and $i-1$, we

have $\bar{T}_{j,i} = T_{\mathrm{F}}$, where $T_{\mathrm{F}}$ is the maximum duration that the sensor persists to sense the idle channel before decrementing the back-off counter; 2) when there is at least one transmission (successful or unsuccessful) of the other sensors $k' \in \mathscr{K} \setminus \{k\}$ between two consecutive back-off counter states $i$ and $i-1$, the time between states $i$ and $i-1$ is equal to the summation of the required time to transmit a packet $T_{\mathrm{P}}$, the DIFS period $T_{\mathrm{DIFS}}$, and a fraction of the slot size $T_{\mathrm{F}}$ (i.e., the time interval between the time instant that the back-off counter state is decremented to $i$ and the time instant that sensor $k$ detects a transmission of the other sensors). However, similarly as in the analysis in [103], this fraction of the slot size is neglected in computing $\bar{T}_{j,i}$, and thus, we have $\bar{T}_{j,i} = T_{\mathrm{P}} + T_{\mathrm{DIFS}}$. It is worth to note that in a CSMA/CA-based system, $T_{\mathrm{F}}$ is significantly smaller than the time period $T_{\mathrm{P}} + T_{\mathrm{DIFS}}$. For example, with the considered parameters in the numerical results in Section 5.3, $T_{\mathrm{F}}$ is less than 2 % of $T_{\mathrm{P}} + T_{\mathrm{DIFS}}$. Let $P^{\mathrm{tr}}_{j,i}$ denote the probability of having at least one transmission by the other sensors between two consecutive back-off counter states $i$ and $i-1$ at $j$th attempt. Thus, $\mathbb{E}[\bar{T}_{j,i}]$ is given by

$$\mathbb{E}[\bar{T}_{j,i}] = P^{\mathrm{tr}}_{j,i}(T_{\mathrm{P}} + T_{\mathrm{DIFS}}) + (1 - P^{\mathrm{tr}}_{j,i})T_{\mathrm{F}}. \tag{152}$$

Due to the considered assumptions, the probability of having at least one transmission by the other sensors between each two consecutive back-off counter states at each attempt has a fixed value and we have [103, Eq. (9)]

$$P^{\mathrm{tr}}_{j,i} = P^{\mathrm{tr}} = 1 - \left(\frac{\bar{C}-1}{\bar{C}+1}\right)^{K-1}, \forall i, j. \tag{153}$$

Therefore, (152) becomes

$$\mathbb{E}[\bar{T}_{j,i}] = \mathbb{E}[\bar{T}] = (1 - P^{\mathrm{tr}})T_{\mathrm{F}} + P^{\mathrm{tr}}(T_{\mathrm{P}} + T_{\mathrm{DIFS}}), \forall i, j. \tag{154}$$

Considering (154) and the expressions for $\mathbb{E}[\xi_j]$ and $\mathbb{E}[\zeta_j]$ in (148) and (151), respectively, we have:

$$\mathbb{E}[\xi_j] = \mathbb{E}[\zeta_{j'}] \triangleq \bar{\xi}_1, \ \forall j, j', \tag{155}$$

where, by substituting (154) in (148), $\bar{\xi}_1$ is calculated as

$$\bar{\xi}_1 = \frac{(\bar{C}+1)\mathbb{E}[\bar{T}]}{2} + T_{\mathrm{P}}. \tag{156}$$

Finally, by using (155) in (145), we have

$$\mathbb{E}[S_m] = m\bar{\xi}_1. \tag{157}$$

### 5.2.2 Calculation of the second moment of $S_m$

By using (143), $\mathbb{E}[S_m^2]$ in (144) is calculated as follows:

$$\begin{aligned}\mathbb{E}[S_m^2] &= \mathbb{E}\left[\left(\sum_{j=1}^{m-1}\zeta_j + \xi_m\right)^2\right] = \mathbb{E}\left[\sum_{j=1}^{m-1}\zeta_j^2\right] \\ &+ 2\mathbb{E}\left[\sum_{j=1}^{m-1}\sum_{j'=1,j'\neq j}^{m-1}\zeta_j\zeta_{j'}\right] + \mathbb{E}\left[\xi_m^2\right] + 2\mathbb{E}\left[\xi_m\sum_{j=1}^{m-1}\zeta_j\right].\end{aligned} \tag{158}$$

Since the elapsed time of each channel access attempt is independent of the elapsed time of the other attempts, we have

$$\begin{aligned}\mathbb{E}[\zeta_j\zeta_{j'}] &= \mathbb{E}[\zeta_j]\mathbb{E}[\zeta_{j'}], \forall j, j',\ j \neq j' \\ \mathbb{E}[\zeta_j\xi_{j'}] &= \mathbb{E}[\zeta_j]\mathbb{E}[\xi_{j'}], \forall j, j',\ j \neq j'.\end{aligned} \tag{159}$$

By means of (159), $\mathbb{E}[S_m^2]$ in (158) can be presented as a function of $\bar{\xi}_1$ in (156), $\mathbb{E}[\xi_m^2]$, and $\mathbb{E}[\zeta_j^2], j = \{1,\ldots,m-1\}$. By following steps similar to (146)–(155) for $\mathbb{E}[\xi_j^2]$ and $\mathbb{E}[\zeta_j^2]$, it is easy to show that

$$\mathbb{E}[\xi_j^2] = \mathbb{E}[\zeta_{j'}^2] \triangleq \bar{\xi}_2,\ \forall j, j', \tag{160}$$

where $\bar{\xi}_2$ is calculated using the steps similar as for $\bar{\xi}_1$, resulting in

$$\begin{aligned}\bar{\xi}_2 &= \frac{1}{\bar{C}}\sum_{w=1}^{\bar{C}}\left(2w\mathbb{E}[\bar{T}]T_{\mathrm{P}} + T_{\mathrm{P}}^2 + w\mathbb{E}[\bar{T}^2] + w(w-1)\mathbb{E}[\bar{T}]^2\right) \\ &\overset{(a)}{=} T_{\mathrm{P}}^2 + (\bar{C}+1)\left[\frac{(2\mathbb{E}[\bar{T}]T_{\mathrm{P}} + \mathbb{E}[\bar{T}^2] - \mathbb{E}[\bar{T}]^2)}{2} + \frac{(2\bar{C}+1)\mathbb{E}[\bar{T}]^2}{6}\right],\end{aligned} \tag{161}$$

where equality $(a)$ follows from the following feature of the finite series [90, Sect. 1.5]

$$\sum_{u=1}^{\bar{U}} u^2 = \frac{\bar{U}(\bar{U}+1)(2\bar{U}+1)}{6},$$

$\mathbb{E}[\bar{T}]$ is calculated by (154), and $\mathbb{E}[\bar{T}^2]$ is given by

$$\mathbb{E}[\bar{T}^2] = (1-P^{\mathrm{tr}})T_{\mathrm{F}}^2 + P^{\mathrm{tr}}(T_{\mathrm{P}} + T_{\mathrm{DIFS}})^2. \tag{162}$$

Finally, by applying (155), (159), and (160), (158) is written by

$$\mathbb{E}[S_m^2] = m\bar{\xi}_2 + m(m-1)\bar{\xi}_1^2. \tag{163}$$

### 5.2.3 Calculation of the Laplace transform of $S_m$ at $\lambda$

By substituting (143) in $\mathbb{E}[e^{-\lambda S_m}]$, we have

$$\mathbb{E}[e^{-\lambda S_m}] = \mathbb{E}\big[\textstyle\prod_{j=1}^{m-1} e^{-\lambda\zeta_j} e^{-\lambda\xi_m}\big]. \tag{164}$$

Due to the fact that elapsed time of different attempts are independent of each other, we have

$$\begin{aligned}
\mathbb{E}[e^{-\lambda\zeta_j} e^{-\lambda\zeta_{j'}}] &= \mathbb{E}[e^{-\lambda\zeta_j}]\mathbb{E}[e^{-\lambda\zeta_{j'}}], \forall j, j',\ j \neq j' \\
\mathbb{E}[e^{-\lambda\zeta_j} e^{-\lambda\xi_{j'}}] &= \mathbb{E}[e^{-\lambda\zeta_j}]\mathbb{E}[e^{-\lambda\xi_{j'}}], \forall j, j',\ j \neq j'.
\end{aligned} \tag{165}$$

By applying (165), (164) is written as follows:

$$\mathbb{E}[e^{-\lambda S_m}] = \textstyle\prod_{j=1}^{m-1} \mathbb{E}\big[e^{-\lambda\zeta_j}\big]\mathbb{E}\big[e^{-\lambda\xi_m}\big]. \tag{166}$$

By following steps similar to (146)–(155) for $\mathbb{E}[e^{-\lambda\zeta_j}]$ and $\mathbb{E}[e^{-\lambda\xi_j}]$, it can be shown that

$$\mathbb{E}[e^{-\lambda\zeta_j}] = \mathbb{E}[e^{-\lambda\xi_{j'}}] \triangleq \bar{\xi}_3,\ \forall j, j', \tag{167}$$

where $\bar{\xi}_3$ is given as

$$\begin{aligned}
\bar{\xi}_3 &= \frac{1}{\bar{C}} \sum_{w=1}^{\bar{C}} \left(\mathbb{E}[e^{-\lambda\bar{T}}]^w e^{-\lambda T_{\mathrm{P}}}\right) \\
&\overset{(a)}{=} \frac{e^{-\lambda T_{\mathrm{P}}}\mathbb{E}[e^{-\lambda\bar{T}}](1-\mathbb{E}[e^{-\lambda\bar{T}}]^{\bar{C}})}{\bar{C}(1-\mathbb{E}[e^{-\lambda\bar{T}}])},
\end{aligned} \tag{168}$$

where equality $(a)$ follows from the following feature of the finite series [90, Sect. 1.5]

$$\sum_{u=1}^{\bar{U}} \bar{\alpha}^u = \frac{\bar{\alpha}(1-\bar{\alpha}^{\bar{U}})}{1-\bar{\alpha}},$$

and $\mathbb{E}[e^{-\lambda \bar{T}}]$ is given by

$$\mathbb{E}[e^{-\lambda \bar{T}}] = (1-P^{\mathrm{tr}})e^{-\lambda T_{\mathrm{F}}} + P^{\mathrm{tr}} e^{-\lambda (T_{\mathrm{P}}+T_{\mathrm{DIFS}})}. \tag{169}$$

Finally, using (167), $\mathbb{E}[e^{-\lambda S_m}]$ in (166) is written as

$$\mathbb{E}[e^{-\lambda S_m}] = \bar{\xi}_3^m. \tag{170}$$

### 5.2.4 Calculation of probability $\Pr(M=m)$

Due to the considered assumptions, the probability of a successful transmission in each attempt has a fixed value which is denoted by $P_{\mathrm{S}}$. Therefore, $\Pr(M=m)$ is given by

$$\Pr(M=m) = P_{\mathrm{S}}(1-P_{\mathrm{S}})^{m-1}. \tag{171}$$

Since there are $\bar{C}$ slots in each contention interval, the probability of success in each contention interval is equal to

$$P_{\mathrm{S}} = \sum_{w=1}^{\bar{C}} P_w^{\mathrm{suc}} \Pr(\bar{W}=w), \tag{172}$$

where $P_w^{\mathrm{suc}}$ is the probability of successful transmission of sensor $k$ in slot $w$. When sensor $k$ chooses to transmit in slot $w$, probability of having a successful transmission is equal to the probability that the other $K-1$ sensors do not transmit in slot $w$ which is given by [103, Eq. (9)]

$$P_w^{\mathrm{suc}} = \Big(\frac{\bar{C}-1}{\bar{C}+1}\Big)^{K-1}. \tag{173}$$

Substituting (173) into (172) we have

$$P_{\mathrm{S}} = \left(\frac{\bar{C}-1}{\bar{C}+1}\right)^{K-1}. \tag{174}$$

*Final expressions for $\mathbb{E}[S]$, $\mathbb{E}[S^2]$, and $L_S(\lambda)$ in* (144)

Substituting (157), (163), (170), and (171) in (144), we have

$$\begin{aligned}
\mathbb{E}[S] &= \sum_{m=1}^{\infty} m\bar{\xi}_1 P_{\mathrm{S}}(1-P_{\mathrm{S}})^{m-1},\\
\mathbb{E}[S^2] &= \sum_{m=1}^{\infty} \left(m\bar{\xi}_2 + m(m-1)\bar{\xi}_1^2\right) P_{\mathrm{S}}(1-P_{\mathrm{S}})^{m-1},\\
\mathbb{E}[e^{-\lambda S}] &= \sum_{m=1}^{\infty} \bar{\xi}_3^m P_{\mathrm{S}}(1-P_{\mathrm{S}})^{m-1}.
\end{aligned} \tag{175}$$

According to the feature of the series, for each $0 \leq \bar{\alpha} < 1$, we have [90, Sect. 8.6]

$$\begin{aligned}
\sum_{u=1}^{\infty} u\bar{\alpha}^u &= \frac{\bar{\alpha}}{(1-\bar{\alpha})^2},\\
\sum_{u=1}^{\infty} u^2\bar{\alpha}^u &= \frac{\bar{\alpha}(1+\bar{\alpha})}{(1-\bar{\alpha})^3}.
\end{aligned} \tag{176}$$

Thus, by applying (176) in (175), $\mathbb{E}[S]$, $\mathbb{E}[S^2]$, and $\mathbb{E}[e^{-\lambda S}]$ are calculated as follows:

$$\begin{aligned}
\mathbb{E}[S] &= \frac{\bar{\xi}_1}{P_{\mathrm{S}}},\\
\mathbb{E}[S^2] &= \frac{\bar{\xi}_2}{P_{\mathrm{S}}} + \frac{\bar{\xi}_1^2(2-2P_{\mathrm{S}})}{P_{\mathrm{S}}^2},\\
L_S(\lambda) &= \begin{cases} \dfrac{\bar{\xi}_3 P_{\mathrm{S}}}{1-\bar{\xi}_3+\bar{\xi}_3 P_{\mathrm{S}}}, & \bar{\xi}_3(1-P_{\mathrm{S}}) < 1,\\ \infty, & \text{Otherwise,} \end{cases}
\end{aligned} \tag{177}$$

with $\bar{\xi}_1$, $\bar{\xi}_2$, and $\bar{\xi}_3$ given in (156), (161), and (168), respectively. As the outcome, the expressions in (177) can be used to calculate the average AoI in (141) and the average peak AoI in (142) in the considered model.

### 5.3 Numerical results

In this section, numerical results are presented to show the behavior of the AoI for different system parameters. The system parameters are set as $T_{\mathrm{DIFS}} = 128\,\mu$s, $T_{\mathrm{F}} = 50\,\mu$s, channel bit rate 1 Mbit/s, and packet size 300 Bytes.

Figs. 33 and 34 depict the average AoI and average peak AoI of sensor $k$ as a function of the packet arrival rate $\lambda$ for different number of sensors with contention window sizes $\bar{C} = \{100, 800\}$, respectively. When the number of sensors $K$ increases, the average AoI and average peak AoI dramatically increase because the probability of collisions in the system increases. It is worth noting that when $K$ increases, the values of the packet arrival rate $\lambda$ that minimize the average AoI and average peak AoI both decrease. In addition, the curvatures demonstrate that the range of values of $\lambda$ that result in near-optimal AoI becomes narrower for the increasing values of $K$. This emphasizes the importance of implementing an optimal generation policy of status update packets in WSNs with a shared-access channel.

Fig. 35 illustrates the average AoI of sensor $k$ as a function of $\lambda$ for different contention window sizes with a fixed number of sensors $K = 100$. According to this figure, naively increasing (or decreasing) the contention window size does not minimize the average AoI and average peak AoI. Namely, $\bar{C} = 1000$ leads to a smaller average AoI than both $\bar{C} = 500$ and $\bar{C} = 1500$. However, for all larger contention window sizes $\bar{C} = \{500, 1000, 1500\}$, the AoI is not very sensitive to the packet arrival rate $\lambda$ in the sense that a wide range of values of $\lambda$ results in relatively low values of the average AoI.

Fig. 36 illustrates the optimal value of the contention window size $\bar{C}$ as a function of the number of sensors $K$ and the arrival rate $\lambda$. According to this figure, when the number of sensors increases, the optimal contention window size $\bar{C}$ increases. This is because when $\bar{C}$ increases, the probability of a collision decreases. In other words, increasing the size of the contention window mitigates the effect of an increased number of sensors on the probability of a collision. However, $\bar{C}$ can not be set to an arbitrary large number because it results in a high value of the average AoI. In addition, the curve shows that for the small number of sensors, when the packet arrival rate $\lambda$ increases, the optimal $\bar{C}$ increases smoothly. Moreover, the figure illustrates that for a large number of sensors, when $\lambda$ increases, the optimal $\bar{C}$ first increases and then decreases. This represents the trade-off between the effect of the probability of a collision and the delay imposed by the contention window size on the average AoI.

### 5.4 Summary and discussion

The worst case average AoI and average peak AoI of a simplified CSMA/CA-based system were analytically evaluated. The worst case analysis was carried out by considering a scenario in which the probability of collisions for one considered sensor has the highest value. According to the numerical results, the number of contending sensors significantly affects the AoI due to network congestion. The experiments

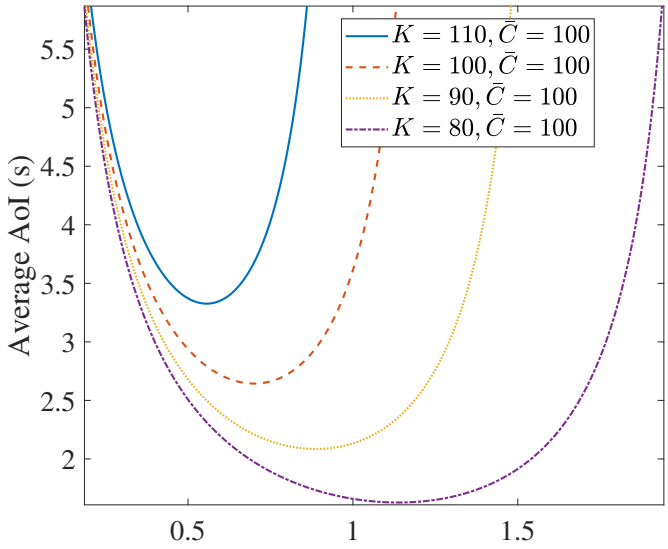


**Fig. 33. The average AoI of sensor $k$ as a function of $\lambda$ for different number of sensors with a fixed contention window size $\bar{C} = 100$ (Reprinted by permission [23] © 2020, IEEE).**

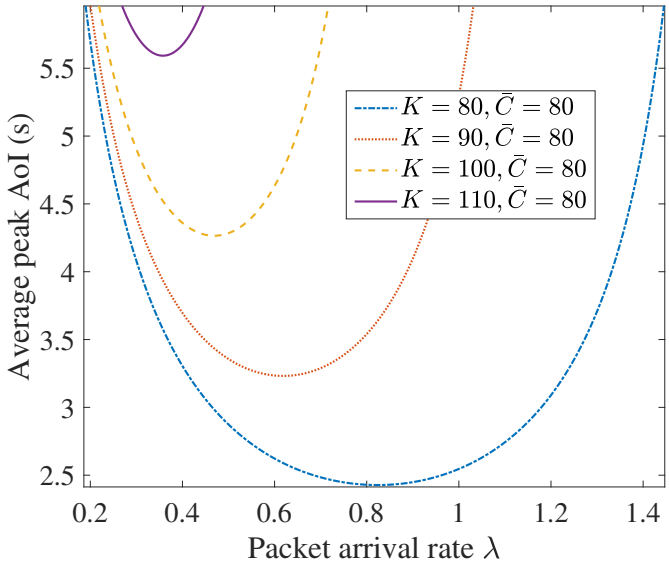


**Fig. 34. The average peak AoI of sensor $k$ as a function of $\lambda$ for different number of sensors with $\bar{C} = 80$ (Reprinted by permission [23] © 2020, IEEE).**

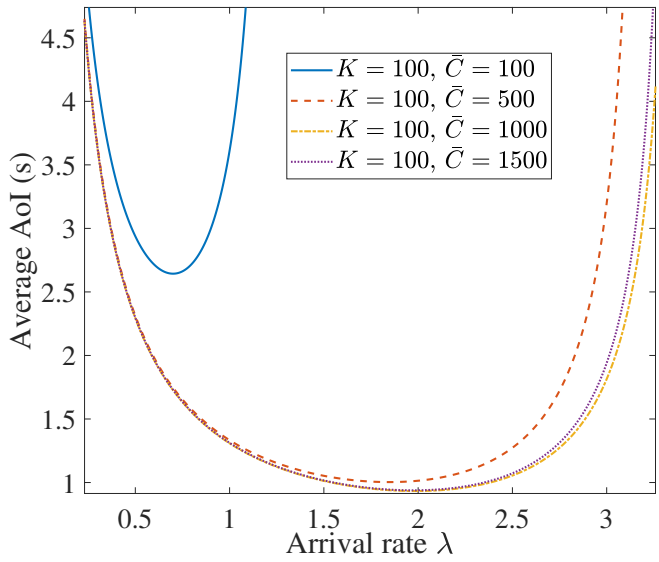


**Fig. 35. The average AoI of sensor $k$ as a function of $\lambda$ for different contention window sizes with a fixed number of sensors $K = 100$ (Reprinted by permission [23] © 2020, IEEE).**

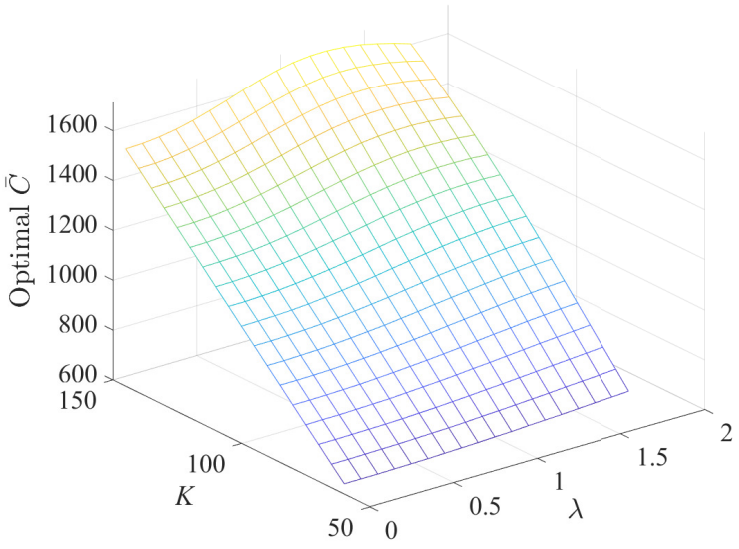


**Fig. 36. The optimal value of the contention window size $\bar{C}$ as a function of the number of sensors $K$ and arrival rate $\lambda$ (Reprinted by permission [23] © 2020, IEEE).**

illustrated that optimizing the contention window size and the packet arrival rate can significantly improve the freshness of status updates in the considered system.

The presented analysis confined to simplifications of CSMA/CA by omitting the dependencies of sensors' queues. Analyzing a CSMA/CA-based system where all sensors have bursty arrivals instead of saturated queues is most likely analytically intractable. This is true even in a simplified homogeneous scenario, where all sensors have equal packet arrival rates. This comes from the fact that in CSMA/CA-based systems, there are complex interactions of queues which result in having highly correlated queues in various sensors [104, 105].

# 6 Conclusions and future work

This chapter summarizes the thesis, discusses the contributions and their insights, and presents the conclusions. Finally, several future directions are provided.

## 6.1 Conclusions

The objective of this thesis was to analyze the information freshness and propose various methods to improve it in future networks and cyber-physical systems. To this end, the AoI was used as a metric to measure the information freshness. Two different approaches were investigated: i) analyzing the AoI when we cannot control the sampling process in the system where the AoI characterization for various queueing modes and packet management polices was provided; ii) optimizing the AoI when we can control the sampling process in the system where a dynamic control algorithm to optimize radio resource allocation and sampling action was provided.

In Chapter 2, a single-server multi-source FCFS queueing model with Poisson arrivals was considered and the average AoI of each source was analyzed for the M/M/1 and M/G/1 cases. For the M/M/1 case, an exact expression for the average AoI was derived and for the M/G/1 case, three approximate expressions for the average AoI were derived. The simulation results showed that the approximate expressions for the average AoI are relatively accurate for different service time distributions. In addition, they showed that the delay does not fully capture the information freshness, i.e., minimizing the average system delay does not necessarily lead to good performance in terms of AoI and, reciprocally, minimizing the average AoI does not minimize the average system delay.

In Chapter 3, the effectiveness of applying various packet management policies in a status update system was studied. A status update system consisting of two independent sources, one server, and one sink was considered. Three source-aware packet management policies were introduced and their AoI performance was analyzed. According to the source-aware policies, a packet in the system can be preempted only by a packet with the same source index. The average AoI and MGF of the AoI for each source under the proposed policies were derived. The numerical results showed that in general the proposed source-aware policies result in higher fairness in the system than that of the existing policies. Moreover, the results showed that to have a reliable status update system, higher moments of the AoI need to be taken into account.

From Chapters 2 and 3, it can be concluded that when there is a possibility to manage the packets in the system and it is not necessary to deliver all the packets to the destination, an appropriate packet management policy can significantly improve the information freshness and the fairness among sources in a multi-source queueing model.

Chapter 4 considered a system where the sampling process can be controlled. A status update system consisting of a set of sensors and one sink was considered. The status update packets from the sensors are transmitted by sharing a set of orthogonal sub-channels in each slot. The problem of average total transmit power minimization subject to an average AoI constraint for each sensor was studied. To solve the proposed problem, the Lyapunov drift-plus-penalty method was used. The optimality analysis of the proposed solution was conducted. In the numerical results section, the trade-off between the average total transmit power and the average AoI of the sensors was shown. In addition, the performance of the solution algorithm was illustrated.

In Chapter 5, an application of the derived average AoI and average peak AoI expressions in Chapter 2 was studied. A simplified CSMA/CA-based WSN was considered and the worst case average AoI and average peak AoI were derived. The worst case analysis was carried out by considering that when a sensor contends for the channel to transmit its status update packet, all the other sensors have a packet to transmit. Therefore, the probability of collisions has the highest value. The experiments illustrated that optimizing the contention window size and the packet arrival rate can significantly improve the freshness of status updates in the considered system.

## 6.2 Future work

Since the AoI is a relatively new metric to analyze the information freshness, there are many interesting future works to be considered. Some of the possible research directions are listed in the following.

Chapter 3 opens several research directions for future study. It would be interesting to extend the results for more than two sources. As stated earlier, the same methodology as used in Chapter 3 can be applied for more than two sources; however, the complexity of the calculations increases exponentially with the number of sources. Another interesting future work includes calculating the stationary distribution of the AoI in a computation-intensive multi-source status update system where the information of a transmitted packet is not available until being processed by the sink. In other words, in addition to having a queueing system on the transmitter side, we have a queueing system at the sink side as well. Consequently, different packet management policies can be considered on both transmitter and sink sides.

The proposed system model in Chapter 4 could be made more realistic by considering different types of sensors with various service requirements. More specifically, the sensors could be divided into two non-overlapping groups: i) a set of AoI-sensitive sensors and ii) a set of throughput-sensitive sensors. Here, the sink needs the information gathered by each throughput-sensitive sensor during all the slots, i.e., the throughput-sensitive sensors have data to transmit in each slot. An interesting future work would be to study the trade-off between the average AoI of the AoI-sensitive sensors and the throughput of the throughput-sensitive sensors. In this regard, one can formulate an optimization problem with an objective to minimize sum average AoI of the AoI-sensitive sensors subject to minimum throughput requirement for the throughput-sensitive sensors.

As discussed in Chapter 3, considering higher moments of the AoI is essential to be taken into account in the system design. The proposed optimization problem in Chapter 4 can be improved by considering the second moment of the AoI as an additional constraint in the optimization problem. Alternatively, a multi-objective optimization problem can be considered with the first and second moments of the AoI as the objectives of the problem.

Another interesting future work would be to address a more realistic setup in a CSMA/CA-based system, where all sensors have bursty arrivals instead of saturated queues. However, due to the complex interactions of queues, an exact analysis is most likely analytically intractable and thus, one may need to resort on numerical simulations. In addition, machine learning approaches could be used to analyze and improve the performance of such a system.

# References


[1] P. Corke, T. Wark, R. Jurdak, W. Hu, P. Valencia, and D. Moore, "Environmental wireless sensor networks," *Proc. IEEE*, vol. 98, no. 11, pp. 1903–1917, Nov. 2010.

[2] P. Papadimitratos, A. D. L. Fortelle, K. Evenssen, R. Brignolo, and S. Cosenza, "Vehicular communication systems: Enabling technologies, applications, and future outlook on intelligent transportation," *IEEE Commun. Mag.*, vol. 47, no. 11, pp. 84–95, Nov. 2009.

[3] M. Xiong and K. Ramamritham, "Deriving deadlines and periods for real-time update transactions," in *Proc. IEEE Real. Time. Sys. Symp.*, Phoenix, AZ, USA, Dec. 1–3, 1999, pp. 32–43.

[4] Y.-C. Hu and D. B. Johnson, "Ensuring cache freshness in on-demand ad hoc network routing protocols," in *Proc. IEEE Princ. of Mobile. Comp.*, Toulouse, France, Oct. 30–31, 2002, pp. 25–30.

[5] R. D. Yates, Y. Sun, D. R. B. III, S. K. Kaul, E. Modiano, and S. Ulukus, "Age of information: An introduction and survey," https://arxiv.org/abs/2007.08564.2020.

[6] Y. Sun, I. Kadota, R. Talak, and E. Modiano, *Age of Information: A New Metric For Information Freshness*. Synthesis Lectures on Communication Networks, 2019, vol. 12, no. 2.

[7] A. Kosta, N. Pappas, and V. Angelakis, "Age of information: A new concept, metric, and tool," *Foun. and Trends in Net.*, vol. 12, no. 3, pp. 162–259, 2017.

[8] S. Kaul, R. Yates, and M. Gruteser, "Real-time status: How often should one update?" in *Proc. IEEE Int. Conf. on Computer. Commun. (INFOCOM)*, Orlando, FL, USA, Mar. 25–30, 2012, pp. 2731–2735.

[9] R. D. Yates and S. K. Kaul, "The age of information: Real-time status updating by multiple sources," *IEEE Trans. Inform. Theory*, vol. 65, no. 3, pp. 1807–1827, Mar. 2019.

[10] S. Kaul, M. Gruteser, V. Rai, and J. Kenney, "Minimizing age of information in vehicular networks," in *Proc. Commun. Society. Conf. on Sensor, Mesh and Ad Hoc Commun. and Net.*, Salt Lake City, UT, USA, Jun. 27–30, 2011, pp. 350–358.

[11] V. Raghunathan, C. Schurgers, S. Park, and M. B. Srivastava, "Energy-aware wireless microsensor networks," *IEEE Signal Processing Mag.*, vol. 19, no. 2, pp. 40–50, Mar. 2002.

[12] G. Anastasi, M. Conti, M. D. Francesco, and A. Passarella, "Energy conservation in wireless sensor networks: A survey," *Ad Hoc Netw.*, vol. 7, no. 3, pp. 537–568, May 2009.

[13] M. Moltafet, M. Leinonen, and M. Codreanu, "On the age of information in multi-source queueing models," *IEEE Trans. Commun.*, vol. 68, no. 8, pp. 5003–5017, May 2020.

[14] ——, "An exact expression for the average AoI in a multi-source M/M/1 queueing model," in *Proc. IEEE Int. Symp. Pers., Indoor, Mobile Radio Commun.*, London, United Kingdom, Sep. 1–3, 2020, pp. 1–6.

[15] ——, "An approximate expression for the average AoI in a multi-source M/G/1 queueing model," in *Proc. IEEE 6G Wireless Summit (6G SUMMIT)*, Levi, Finland, Mar. 17–20, 2020, pp. 1–5.

[16] M. Moltafet, M. Leinonen, and M. Codreanu, "Average AoI in multi-source systems with source-aware packet management," *IEEE Trans. Commun.*, vol. 69, no. 2, pp. 1121–1133, Feb. 2021.

[17] ——, "Moment generating function of the AoI in a two-source system with packet management," *IEEE Wireless Commun. Lett.*, vol. 10, no. 4, pp. 882–886, Apr. 2021.

[18] M. Moltafet, M. Leinonen, and M. Codreanu, "Average age of information for a multi-source M/M/1 queueing model with packet management," in *Proc. IEEE Int. Symp. Inform. Theory*, Los Angeles, CA, USA, Jun. 21–26, 2020, pp. 1765–1769.

[19] ——, "Average age of information in a multi-source M/M/1 queueing model with LCFS prioritized packet management," in *Proc. IEEE Int. Conf. on Computer. Commun. (INFOCOM) Workshop*, Toronto, Canada, Jul. 6–9, 2020, pp. 303–308.

[20] ——, "Average age of information for a multi-source M/M/1 queueing model with packet management and self-preemption in service," in *Proc. Int. Symp. Modeling and Optimization in Mobile, Ad Hoc and Wireless Net.*, Volos, Greece, Jun. 15–19 2020, pp. 1–5.

[21] M. Moltafet, M. Leinonen, M. Codreanu, and N. Pappas, "Power minimization for AoI of information constrained dynamic control in wireless sensor networks," *IEEE Trans. Commun.*, (Under Revision) [Online]:https://arxiv.org/pdf/2007.05364.pdf, 2020.

[22] ——, "Power minimization in wireless sensor networks with constrained AoI using stochastic optimization," in *Proc. Annual Asilomar Conf. Signals, Syst., Comp.*, Pacific Grove, USA, Nov. 3–6, 2019, pp. 406–410.

[23] M. Moltafet, M. Leinonen, and M. Codreanu, "Worst case age of information in wireless sensor networks: A multi-access channel," *IEEE Wireless Commun. Lett.*, vol. 9, no. 3, pp. 321–325, Mar. 2020.

[24] ——, "Worst case analysis of age of information in a shared-access channel," in *Proc. Int. Symp. Wireless Commun. Systems*, Oulu, Finland, Aug. 27–30, 2019, pp. 613–617.

[25] A. M. Bedewy, Y. Sun, and N. B. Shroff, "Age-optimal information updates in multihop networks," in *Proc. IEEE Int. Symp. Inform. Theory*, Aachen, Germany, Jun. 25–30, 2017, pp. 576–580.

[26] M. Costa, M. Codreanu, and A. Ephremides, "Age of information with packet management," in *Proc. IEEE Int. Symp. Inform. Theory*, Honolulu, HI, USA, Jun. 20–23, 2014, pp. 1583–1587.

[27] ——, "On the age of information in status update systems with packet management," *IEEE Trans. Inform. Theory*, vol. 62, no. 4, pp. 1897–1910, Apr. 2016.

[28] R. D. Yates and S. Kaul, "Real-time status updating: Multiple sources," in *Proc. IEEE Int. Symp. Inform. Theory*, Cambridge, MA, USA, Jul. 1–6, 2012, pp. 2666–2670.

[29] D. G. Kendall, "Stochastic processes occurring in the theory of queues and their analysis by the method of the imbedded Markov chain," *The Annals of Mathematical Statistics*, vol. 24, no. 3, pp. 338–354, 1953.

[30] N. Akar, O. Dogan, and E. U. Atay, "Finding the exact distribution of (peak) age of information for queues of PH/PH/1/1 and M/PH/1/2 type," *IEEE Trans. Commun.*, vol. 68, no. 9, pp. 5661–5672, Jun. 2020.

[31] K. Chen and L. Huang, "Age-of-information in the presence of error," in *Proc. IEEE Int. Symp. Inform. Theory*, Barcelona, Spain, Jul. 10–15, 2016, pp. 2579–2583.

[32] S. K. Kaul, R. D. Yates, and M. Gruteser, "Status updates through queues," in *Proc. Conf. Inform. Sciences Syst. (CISS)*, Princeton, NJ, USA, Mar. 21–23, 2012, pp. 1–6.

[33] A. Soysal and S. Ulukus, "Age of information in G/G/1/1 systems," in *Proc. Annual Asilomar Conf. Signals, Syst., Comp.*, Pacific Grove, CA, USA, Nov. 3–6, 2019, pp. 2022–2027.

[34] C. Kam, S. Kompella, G. D. Nguyen, and A. Ephremides, "Effect of message transmission path diversity on status age," *IEEE Trans. Inform. Theory*, vol. 62, no. 3, pp. 1360–1374, Dec. 2016.

[35] J. P. Champati, H. Al-Zubaidy, and J. Gross, "Statistical guarantee optimization for age of information for the D/G/1 queue," in *Proc. IEEE Int. Conf. on Computer. Commun. (INFOCOM) Workshop*, Honolulu, HI, USA, Apr. 15–19, 2018, pp. 130–135.

[36] E. Najm, R. Yates, and E. Soljanin, "Status updates through M/G/1/1 queues with HARQ," in *Proc. IEEE Int. Symp. Inform. Theory*, Aachen, Germany, Jun. 25–30, 2017, pp. 131–135.

[37] Y. Inoue, H. Masuyama, T. Takine, and T. Tanaka, "A general formula for the stationary distribution of the age of information and its application to single-server queues," *IEEE Trans. Inform. Theory*, vol. 65, no. 12, pp. 8305–8324, Aug. 2019.

[38] Y. Inoue, H. Masuyama, T. Takine, and T. Tanaka, "The stationary distribution of the age of information in FCFS single-server queues," in *Proc. IEEE Int. Symp. Inform. Theory*, Aachen, Germany, Jun. 25–30, 2017, pp. 571–575.

[39] E. Najm and R. Nasser, "Age of information: The gamma awakening," in *Proc. IEEE Int. Symp. Inform. Theory*, Barcelona, Spain, Jul. 10–16, 2016, pp. 2574–2578.

[40] A. Soysal and S. Ulukus, "Age of information in G/G/1/1 systems: Age expressions, bounds, special cases, and optimization," [Online]: https://arxiv.org/abs/1905.13743, 2019.

[41] B. Buyukates, A. Soysal, and S. Ulukus, "Age of information in multicast networks with multiple update streams," in *Proc. Annual Asilomar Conf. Signals, Syst., Comp.*, Pacific Grove, CA, USA,, Nov. 3–6 2019, pp. 1977–1981.

[42] L. Huang and E. Modiano, "Optimizing age-of-information in a multi-class queueing system," in *Proc. IEEE Int. Symp. Inform. Theory*, Hong Kong, China, Jun. 14–19, 2015, pp. 1681–1685.

[43] E. Najm and E. Telatar, "Status updates in a multi-stream M/G/1/1 preemptive queue," in *Proc. IEEE Int. Conf. on Computer. Commun. (INFOCOM)*, Honolulu, HI, USA, Apr. 15–19, 2018, pp. 124–129.

[44] E. Najm, R. Nasser, and E. Telatar, "Content based status updates," *IEEE Trans. Inform. Theory*, vol. 66, no. 6, pp. 3846–3863, Oct. 2020.

[45] R. D. Yates, "The age of information in networks: Moments, distributions, and sampling," *IEEE Trans. Inform. Theory*, vol. 66, no. 9, pp. 5712–5728, May 2020.

[46] ——, "Age of information in a network of preemptive servers," in *Proc. IEEE Int. Conf. on Computer. Commun. (INFOCOM)*, Honolulu, HI, USA, Apr. 15–19 2018, pp. 118–123.

[47] ——, "Status updates through networks of parallel servers," in *Proc. IEEE Int. Symp. Inform. Theory*, Vail, CO, USA, Jun. 17–22, 2018, pp. 2281–2285.

[48] S. K. Kaul and R. D. Yates, "Age of information: Updates with priority," in *Proc. IEEE Int. Symp. Inform. Theory*, Vail, CO, USA, Jun. 17–22, 2018, pp. 2644–2648.

[49] A. Javani, M. Zorgui, and Z. Wang, "Age of information in multiple sensing," in *Proc. IEEE Global Telecommun. Conf.*, Waikoloa, HI, USA, Dec. 9–13, 2019.

[50] S. Farazi, A. G. Klein, and D. Richard Brown, "Average age of information in multi-source self-preemptive status update systems with packet delivery errors," in *Proc. Annual Asilomar Conf. Signals, Syst., Comp.*, Pacific Grove, CA, USA, 2019.

[51] S. K. Kaul and R. D. Yates, "Timely updates by multiple sources: The M/M/1 queue revisited," in *Proc. Conf. Inform. Sciences Syst. (CISS)*, Princeton, NJ, USA, Mar. 18–20, 2020.

[52] R. D. Yates and S. K. Kaul, "Age of information in uncoordinated unslotted updating," in *Proc. IEEE Int. Symp. Inform. Theory*, Los Angeles, CA, USA, Jun. 21–26, 2020.

[53] A. Maatouk, M. Assaad, and A. Ephremides, "On the age of information in a CSMA environment," *IEEE/ACM Trans. Net.*, vol. 28, no. 2, pp. 818–831, Feb. 2020.

[54] D. Qiao and M. C. Gursoy, "Age-optimal power control for status update systems with packet-based transmissions," *IEEE Wireless Commun. Lett.*, vol. 8, no. 6, pp. 1604–1607, Jul. 2019.

[55] R. V. Bhat, R. Vaze, and M. Motani, "Throughput maximization with an average age of information constraint in fading channels," [Online]. https://arxiv.org/pdf/1911.07499.pdf, 2019.

[56] B. T. Bacinoglu, Y. Sun, E. Uysal Bivikoglu, and V. Mutlu, "Achieving the age-energy tradeoff with a finite-battery energy harvesting source," in *Proc. IEEE Int. Symp. Inform. Theory*, Vail, CO, USA, Jun. 17–22, 2018.

[57] X. Wu, J. Yang, and J. Wu, "Optimal status update for age of information minimization with an energy harvesting source," *IEEE Trans. Green Commun. Net.*, vol. 2, no. 1, pp. 193–204, Mar. 2018.

[58] M. K. Abdel-Aziz, C. Liu, S. Samarakoon, M. Bennis, and W. Saad, "Ultra-reliable low-latency vehicular networks: Taming the age of information tail," in *Proc. IEEE Global Telecommun. Conf.*, Abu Dhabi, United Arab Emirates, Dec. 9–13 2018, pp. 1–7.

[59] M. K. Abdel-Aziz, S. Samarakoon, C. Liu, M. Bennis, and W. Saad, "Optimized age of information tail for ultra-reliable low-latency communications in vehicular networks," *IEEE Trans. Commun.*, vol. 68, no. 3, pp. 1911–1924, Dec. 2020.

[60] I. Krikidis, "Average age of information in wireless powered sensor networks," *IEEE Wireless Commun. Lett.*, vol. 8, no. 2, pp. 628–631, Apr. 2019.

[61] R. Talak, S. Karaman, and E. Modiano, "Optimizing information freshness in wireless networks under general interference constraints," *IEEE/ACM Trans. Net.*, vol. 28, no. 1, pp. 15–28, Dec. 2019.

[62] R. Talak, I. Kadota, S. Karaman, and E. Modiano, "Scheduling policies for age minimization in wireless networks with unknown channel state," in *Proc. IEEE Int. Symp. Inform. Theory*, Vail, CO, USA, Jun. 17–22 2018, pp. 2564–2568.

[63] B. Yu, Y. Cai, and D. Wu, "Joint access control and resource allocation for short-packet-based mMTC in status update systems," *IEEE J. Select. Areas Commun.*, Early Access, 2020.

[64] A. E. Kalor and P. Popovski, "Minimizing the age of information from sensors with common observations," *IEEE Wireless Commun. Lett.*, vol. 8, no. 5, pp. 1390–1393, May 2019.

[65] Y. Gu, Q. Wang, H. Chen, Y. Li, and B. Vucetic, "Optimizing information freshness in two-hop status update systems under a resource constraint," https://arxiv.org/abs/2007.02531, 2020.

[66] Z. Qian, F. Wu, J. Pan, K. Srinivasan, and N. B. Shroff, "Minimizing age of information in multi-channel time-sensitive information update systems," in *Proc. IEEE Int. Conf. on Computer. Commun. (INFOCOM)*, Toronto, ON, Canada,, Jul. 6–9 2020, pp. 446–455.

[67] Y. Sun and B. Cyr, "Information aging through queues: A mutual information perspective," in *Proc. IEEE Works. on Sign. Proc. Adv. in Wirel. Comms.*, Kalamata, Greece, Jun. 25–28, 2018, pp. 1–5.

[68] ——, "Sampling for data freshness optimization: Non-linear age functions," *IEEE J. Commun. Net.*, vol. 21, no. 3, pp. 204–219, Jul. 2019.

[69] B. T. Bacinoglu and E. Uysal-Biyikoglu, "Scheduling status updates to minimize age of information with an energy harvesting sensor," in *Proc. IEEE Int. Symp. Inform. Theory*, Aachen, Germany, Jun. 25–30, 2017.

[70] A. M. Bedewy, Y. Sun, S. Kompella, and N. B. Shroff, "Age-optimal sampling and transmission scheduling in multi-source systems," https://arxiv.org/abs/1812.09463, 2019.

[71] ——, "Optimal sampling and scheduling for timely status updates in multi-source networks," https://arxiv.org/abs/2001.09863, 2020.

[72] Z. Chen, N. Pappas, E. Björnson, and E. G. Larsson, "Optimal control of status updates in a multiple access channel with stability constraints," [Online]. https://arxiv.org/abs/1910.05144, 2019.

[73] S. Feng and J. Yang, "Optimal status updating for an energy harvesting sensor with a noisy channel," in *Proc. IEEE Int. Conf. on Computer. Commun. (INFOCOM) Workshop*, Honolulu, HI, USA, Apr. 15–19 2018, pp. 348–353.

[74] M. Hatami, M. Leinonen, and M. Codreanu, "AoI minimization in status update control with energy harvesting sensors," https://arxiv.org/abs/2009.04224, 2020.

[75] M. Hatami, M. Jahandideh, M. Leinonen, and M. Codreanu, "Age-aware status update control for energy harvesting IoT sensors via reinforcement learning," in *Proc. IEEE Int. Symp. Pers., Indoor, Mobile Radio Commun.*, London, UK, Aug. 31–Sep. 3 2020, pp. 1–5.

[76] E. T. Ceran, D. Gunduz, and A. Gyorgy, "Average age of information with hybrid ARQ under a resource constraint," in *Proc. IEEE Wireless Commun. and Networking Conf.*, Barcelona, Spain, Apr. 15–18 2018, pp. 1–6.

[77] ——, "Average age of information with hybrid ARQ under a resource constraint," *IEEE Trans. Wireless Commun.*, vol. 18, no. 3, pp. 1900–1913, Feb. 2019.

[78] ——, "Reinforcement learning to minimize age of information with an energy harvesting sensor with HARQ and sensing cost," in *Proc. IEEE Int. Conf. on Computer. Commun. (INFOCOM) Workshop*, Paris, France, Apr. 1–2 2019, pp. 656–661.

[79] A. Arafa, J. Yang, and S. Ulukus, "Age-minimal online policies for energy harvesting sensors with random battery recharges," in *Proc. IEEE Int. Conf. Commun.*, Kansas City, MO, USA, May 20–24, 2018, pp. 1–6.

[80] A. Arafa, J. Yang, S. Ulukus, and H. V. Poor, "Age-minimal transmission for energy harvesting sensors with finite batteries: Online policies," *IEEE Trans. Inform. Theory*, vol. 66, no. 1, pp. 534–556, Sep. 2020.

[81] A. Kosta, N. Pappas, A. Ephremides, and V. Angelakis, "Age of information and throughput in a shared access network with heterogeneous traffic," in *Proc. IEEE Global Telecommun. Conf.*, Abu Dhabi, United Arab Emirates, Dec. 9–13, 2018, pp. 1–6.

[82] R. D. Yates and S. K. Kaul, "Status updates over unreliable multiaccess channels," in *Proc. IEEE Int. Symp. Inform. Theory*, Aachen, Germany, Jun. 25–30, 2017, pp. 331–335.

[83] X. Chen, K. Gatsis, H. Hassani, and S. S. Bidokhti, "Age of information in random access channels," in *Proc. IEEE Int. Symp. Inform. Theory*, 2020.

[84] A. Kosta, N. Pappas, A. Ephremides, and V. Angelakis, "Age of information performance of multiaccess strategies with packet management," *J. Commun. Netw.*, vol. 21, no. 3, pp. 244–255, Jul. 2019.

[85] I. Kadota, A. Sinha, and E. Modiano, "Scheduling algorithms for optimizing age of information in wireless networks with throughput constraints," *IEEE/ACM Trans. Networking*, vol. 27, no. 4, pp. 1359–1372, Jun. 2019.

[86] I. Kadota, E. Uysal-Biyikoglu, R. Singh, and E. Modiano, "Minimizing the age of information in broadcast wireless networks," in *Proc. Annual Allerton Conf. Commun., Contr., Computing*, Monticello, IL, USA, Sep. 27–30 2016, pp. 844–851.

[87] Y. Hsu, E. Modiano, and L. Duan, "Age of information: Design and analysis of optimal scheduling algorithms," in *Proc. IEEE Int. Symp. Inform. Theory*, Aachen, Germany, Jun. 25–30 2017, pp. 561–565.

[88] I. Kadota and E. Modiano, "Minimizing the age of information in wireless networks with stochastic arrivals," *IEEE Trans. Mobile Comput.*, Early Access, 2019.

[89] E. Fountoulakis, N. Pappas, M. Codreanu, and A. Ephremides, "Optimal sampling cost in wireless networks with age of information constraints," in *Proc. IEEE Int. Conf. on*

*Computer. Commun. (INFOCOM) Workshop*, Toronto, ON, Canada,, Jul. 6–9, 2020, pp. 918–923.

[90] L. Rade and B. Westergren, *Mathematics Handbook for Science and Engineering*. Berlin, Germany: Springer, 2005.

[91] R. Sheldon M, *Introduction to Probability Models*. California: Academic press, 2010.

[92] L. Takacs, "Investigation of waiting time problems by reduction to Markov processes," *Acta Math. Hung.*, vol. 6, pp. 101–129, 1955.

[93] L. Kleinrock, *Queueing Systems, Volume 1: Theory*. New York: John Wiley and Sons, 1995.

[94] P. Cantrell, "Computation of the transient M/M/1 queue cdf, pdf, and mean with generalized Q-functions," *IEEE Trans. Commun.*, vol. 34, no. 8, pp. 814–817, Aug. 1986.

[95] D. Bertsekas and R. Gallager, *Data Networks*. Englewood Cliffs, New Jersey: Prentice-Hall International, 1992.

[96] J. N. Daigle, *Queueing Theory with Applications to Packet Telecommunication*. New York: Springer Science, 2005.

[97] A. B. Sediq, R. H. Gohary, R. Schoenen, and H. Yanikomeroglu, "Optimal tradeoff between sum-rate efficiency and Jain's fairness index in resource allocation," *IEEE Trans. Wireless Commun.*, vol. 12, no. 7, pp. 3496–3509, Jul. 2013.

[98] R. Jain, D. Chiu, and W. Hawe, "A quantitative measure of fairness and discrimination for resource allocation in shared systems," *Digital Equipment Corporation, DEC-TR-301, Tech. Rep., 1984*, available: http://www1.cse.wustl.edu/ jain/papers/ftp/fairness.pdf.

[99] I. Kadota, A. Sinha, and E. Modiano, "Optimizing age of information in wireless networks with throughput constraints," in *Proc. IEEE Int. Conf. on Computer. Commun. (INFOCOM)*, Honolulu, HI, USA, Apr. 15–19, 2018, pp. 1844–1852.

[100] M. J. Neely, *Stochastic Network Optimization With Application to Communication and Queueing Systems*. Belmont, MA, USA: Morgan and Claypool, 2010.

[101] L. Georgiadis, M. J. Neely, and L. Tassiulas, "Resource allocation and cross-layer control in wireless networks," *Found. Trends Netw.*, vol. 1, no. 1, pp. 1–144, Apr. 2006.

[102] P. He and L. Zhao, "Generalized water-filling for sum power minimization with peak power constraints," in *Proc. Int. Conf. Wireless Commun. and Sign. Proc.*, Nanjing, China, Oct. 15–17, 2015, pp. 1–5.

[103] G. Bianchi, "Performance analysis of the IEEE 802.11 distributed coordination function," *IEEE Trans. Appl. Superconduct.*, vol. 18, no. 3, pp. 535–547, Mar. 2000.

[104] R. R. Rao and A. Ephremides, "On the stability of interacting queues in a multiple-access system," *IEEE Trans. Inform. Theory*, vol. 34, no. 5, pp. 918–930, Sep. 1988.

[105] Wei Luo and A. Ephremides, "Stability of n interacting queues in random-access systems," *IEEE Trans. Inform. Theory*, vol. 45, no. 5, pp. 1579–1587, Jul. 1999.

[106] A. Papoulis, *Probability, Random Variables, and Stochastic Processes*. New York: McGraw-Hill, 1984.

# Appendix 1

## 1.1 Proof of Lemma 1, 2, and 3

### 1.1.1 Proof of Lemma 1

Using the facts that $T_{1,i-1}$ and $X_{1,i}$ are independent and the PDF of $X_{1,i}$ is $f_{X_{1,i}}(x) = \lambda_1 e^{-\lambda_1 x}$, $P(E_{1,i}^{\mathrm{B}})$ can be written as

$$\begin{aligned} P(E_{1,i}^{\mathrm{B}}) &= \int_0^\infty P(T_{1,i-1} \geq X_{1,i} | T_{1,i-1} = t) f_{T_{1,i-1}}(t) \mathrm{d}t \\ &= 1 - \int_0^\infty e^{-\lambda_1 t} f_{T_{1,i-1}}(t) \mathrm{d}t \\ &\overset{(a)}{=} 1 - L_T(\lambda_1), \end{aligned} \tag{178}$$

where equality (a) follows because the system times of different packets are stochastically identical, i.e., $T_{1,i} =^{\mathrm{st}} T_{2,i} =^{\mathrm{st}} T$, $\forall i$ [7, 28]; and $L_T(\lambda_1)$ denotes the Laplace transform of the PDF of the system time $T$ at $\lambda_1$. Because $E_{1,i}^{\mathrm{L}}$ is the complementary event of $E_{1,i}^{\mathrm{B}}$, we have

$$P(E_{1,i}^{\mathrm{L}}) = 1 - P(E_{1,i}^{\mathrm{B}}) = L_T(\lambda_1). \tag{179}$$

The relation between the Laplace transforms of the PDFs of the system time $T$ and service time $S$ is given as [96, Sect. 5.1.2]

$$L_T(a) = \frac{\big(1-\rho\big) a L_S(a)}{a - \lambda\big(1 - L_S(a)\big)}. \tag{180}$$

Finally, substituting (180) in (178) and (179) results in the expressions (21) and (22), respectively.

### 1.1.2 Proof of Lemma 2

The proof of Lemma 2 follows from the fact that for random variables $Y_1$ and $Y_2$ and a certain event $\underline{A}$, the conditional PDF $f_{Y_1,Y_2|\underline{A}}(y_1, y_2)$ is given by [106, Sect. 4.4]

$$f_{Y_1,Y_2|\underline{A}}(y_1,y_2) = \begin{cases} \dfrac{f_{Y_1,Y_2}(y_1,y_2)}{P(\underline{A})} & (y_1,y_2) \in \underline{A} \\ 0 & \text{otherwise.} \end{cases} \tag{181}$$

In Lemma 2, $Y_1$ and $Y_2$ are $X_{1,i}$ and $T_{1,i-1}$, respectively, which are two independent random variables, and event $\underline{A}$ is $E^{\mathrm{B}}_{1,i}$.

### 1.1.3 Proof of Lemma 3

According to the feature of the Laplace transform, for any function $f(y), y \geq 0$, we have [90, Sect. 13.5]:

$$L_{\int_0^y f(b)\mathrm{d}b}(a) = \frac{L_{f(y)}(a)}{a}. \tag{182}$$

Therefore, using (27) and (182), we have

$$\begin{aligned} L_{x^2 F_{T_1}(x)}(a)\Big|_{a=\lambda_1} &= L_{x^2 \int_0^x f_{T_1}(b)\mathrm{d}b}(a)\Big|_{a=\lambda_1} \\ &= \frac{\mathrm{d}^2\left(\frac{L_T(a)}{a}\right)}{\mathrm{d}a^2}\Big|_{a=\lambda_1} \\ &= \frac{aL''_T(a) - 2L'_T(a)}{a^2} + \frac{2L_T(a)}{a^3}\Big|_{a=\lambda_1} \\ &= \frac{\lambda_1 L''_T(\lambda_1) - 2L'_T(\lambda_1)}{\lambda_1^2} + \frac{2L_T(\lambda_1)}{\lambda_1^3}. \end{aligned} \tag{183}$$

## 1.2 Values of $\bar{v}_{q0}$, $\forall q \in \mathscr{Q}$, for Policy 1

$$\bar{v}_{00} = \frac{3\rho_1^4 + \rho_1^3(5\rho_2+9) + \rho_1^2(2\rho_2^2+11\rho_2+10) + \rho_1(4\rho_2^2+6\rho_2+5) + \rho_2^2+\rho_2+1}{\mu\rho_1(1+\rho_1)^2\big((\rho+1)^2-\rho_2\big)\big(\rho^2+\rho(2\rho_1\rho_2+1)+1\big)}, \tag{184}$$

$$\bar{v}_{10} = \frac{\rho_2^5 + 3\rho_2^4 + 4\rho_2^3 + 3\rho_2^2 + \rho_2 + \sum_{k=1}^{7}\rho_1^k\gamma_{1,k}}{\mu\rho_1(1+\rho)(1+\rho_2)(1+\rho_1)^2\big((\rho+1)^2-\rho_2\big)\big(\rho^2+\rho(2\rho_1\rho_2+1)+1\big)}, \tag{185}$$

where

$$\begin{aligned}
\gamma_{1,1} &= 4\rho_2^5 + 16\rho_2^4 + 26\rho_2^3 + 22\rho_2^2 + 9\rho_2 + 1,\\
\gamma_{1,2} &= 2\rho_2^5 + 25\rho_2^4 + 64\rho_2^3 + 70\rho_2^2 + 35\rho_2 + 6,\\
\gamma_{1,3} &= 11\rho_2^4 + 62\rho_2^3 + 107\rho_2^2 + 72\rho_2 + 16,\\
\gamma_{1,4} &= \rho_2^4 + 23\rho_2^3 + 75\rho_2^2 + 77\rho_2 + 23,\\
\gamma_{1,5} &= 3\rho_2^3 + 23\rho_2^2 + 41\rho_2 + 18,\\
\gamma_{1,6} &= 3\rho_2^2 + 10\rho_2 + 7,\\
\gamma_{1,7} &= \rho_2^2 + 10\rho_2 + 1.
\end{aligned}$$

$$\bar{v}_{20} = \frac{\rho_2^6 + 4\rho_2^5 + 7\rho_2^4 + 7\rho_2^3 + 4\rho_2^2 + \rho_2 + \sum_{k=1}^{7} \rho_1^k \gamma_{2,k}}{\mu(1+\rho)(1+\rho_1)^2(1+\rho_2)^2\big((\rho+1)^2 - \rho_2\big)\big(\rho^2 + \rho(2\rho_1\rho_2+1)+1\big)}, \quad (186)$$

where

$$\begin{aligned}
\gamma_{2,1} &= 5\rho_2^6 + 23\rho_2^5 + 46\rho_2^4 + 51\rho_2^3 + 32\rho_2^2 + 10\rho_2 + 1,\\
\gamma_{2,2} &= 4\rho_2^6 + 36\rho_2^5 + 108\rho_2^4 + 156\rho_2^3 + 119\rho_2^2 + 46\rho_2 + 7,\\
\gamma_{2,3} &= \rho_2^6 + 2\rho_2^5 + 100\rho_2^4 + 213\rho_2^3 + 222\rho_2^2 + 111\rho_2 + 21,\\
\gamma_{2,4} &= 4\rho_2^5 + 40\rho_2^4 + 134\rho_2^3 + 202\rho_2^2 + 138 + 33,\\
\gamma_{2,5} &= 6\rho_2^4 + 39\rho_2^3 + 89\rho_2^2 + 87\rho_2 + 28,\\
\gamma_{2,6} &= 4\rho_2^3 + 18\rho_2^2 + 26\rho_2 + 12,\\
\gamma_{2,7} &= \rho_2^2 + 3\rho_2 + 2.
\end{aligned}$$

$$\bar{v}_{30} = \frac{\rho_2^6 + 3\rho_2^5 + 4\rho_2^4 + 3\rho_2^3 + \rho_2^2 + \sum_{k=1}^{7} \rho_1^k \gamma_{3,k}}{\mu\rho_1(1+\rho)(1+\rho_2)(1+\rho_1)^2\big((\rho+1)^2 - \rho_2\big)\big(\rho^2 + \rho(2\rho_1\rho_2+1)+1\big)}, \quad (187)$$

where

$$\begin{aligned}
\gamma_{3,1} &= 5\rho_2^6 + 19\rho_2^5 + 30\rho_2^4 + 25\rho_2^3 + 10\rho_2^2 + \rho_2,\\
\gamma_{3,2} &= 5\rho_2^6 + 37\rho_2^5 + 84\rho_2^4 + 87\rho_2^3 + 41\rho_2^2 + 6\rho_2,\\
\gamma_{3,3} &= 2\rho_2^6 + 27\rho_2^5 + 101\rho_2^4 + 149\rho_2^3 + 91\rho_2^2 + 18\rho_2,\\
\gamma_{3,4} &= 8\rho_2^5 + 55\rho_2^4 + 126\rho_2^3 + 110\rho_2^2 + 30\rho_2,\\
\gamma_{3,5} &= 12\rho_2^4 + 51\rho_2^3 + 69\rho_2^2 + 27\rho_2,\\
\gamma_{3,6} &= 8\rho_2^3 + 20\rho_2^2 + 12\rho_2,\\
\gamma_{3,7} &= 2\rho_2^2 + 2\rho_2.
\end{aligned}$$

$$\bar{\nu}_{40} = \frac{\rho_2^7 + 4\rho_2^6 + 7\rho_2^5 + 7\rho_2^4 + 4\rho_2^3 + \rho_2^2 + \sum_{k=1}^{7} \rho_1^k \gamma_{4,k}}{\mu(1+\rho)(1+\rho_2)^2(1+\rho_1)^2\big((\rho+1)^2-\rho_2\big)\big(\rho^2+\rho(2\rho_1\rho_2+1)+1\big)}, \quad (188)$$

where

$$\begin{aligned}
\gamma_{4,1} &= 6\rho_2^7 + 27\rho_2^6 + 53\rho_2^5 + 58\rho_2^4 + 36\rho_2^3 + 11\rho_2^2 + \rho_2,\\
\gamma_{4,2} &= 6\rho_2^7 + 48\rho_2^6 + 137\rho_2^5 + 193\rho_2^4 + 145\rho_2^3 + 55\rho_2^2 + 8\rho_2,\\
\gamma_{4,3} &= 2\rho_2^7 + 32\rho_2^6 + 143\rho_2^5 + 286\rho_2^4 + 287\rho_2^3 + 140\rho_2^2 + 26\rho_2,\\
\gamma_{4,4} &= 8\rho_2^6 + 67\rho_2^5 + 201\rho_2^4 + 281\rho_2^3 + 183\rho_2^2 + 43\rho_2,\\
\gamma_{4,5} &= 12\rho_2^5 + 67\rho_2^4 + 137\rho_2^3 + 123\rho_2^2 + 38\rho_2,\\
\gamma_{4,6} &= 8\rho_2^4 + 31\rho_2^3 + 40\rho_2^2 + 14\rho_2,\\
\gamma_{4,7} &= 2\rho_2^3 + 5\rho_2^2 + 3\rho_2.
\end{aligned}$$

$$\bar{\nu}_{50} = \frac{\rho_2^6 + 3\rho_2^5 + 4\rho_2^4 + 3\rho_2^3 + \rho_2^2 + \sum_{k=1}^{7} \rho_1^k \gamma_{5,k}}{\mu(1+\rho)(1+\rho_2)(1+\rho_1)^2\big((\rho+1)^2-\rho_2\big)\big(\rho^2+\rho(2\rho_1\rho_2+1)+1\big)}, \quad (189)$$

where

$$\gamma_{5,1} = 6\rho_2^6 + 22\rho_2^5 + 34\rho_2^4 + 28\rho_2^3 + 11\rho_2^2 + \rho_2,$$
$$\gamma_{5,2} = 7\rho_2^6 + 47\rho_2^5 + 103\rho_2^4 + 105\rho_2^3 + 49\rho_2^2 + 7\rho_2,$$
$$\gamma_{5,3} = 3\rho_2^6 + 38\rho_2^5 + 133\rho_2^4 + 190\rho_2^3 + 115\rho_2^2 + 23\rho_2,$$
$$\gamma_{5,4} = 12\rho_2^5 + 78\rho_2^4 + 170\rho_2^3 + 145\rho_2^2 + 40\rho_2,$$
$$\gamma_{5,5} = 18\rho_2^4 + 73\rho_2^3 + 95\rho_2^2 + 37\rho_2,$$
$$\gamma_{5,6} = 12\rho_2^3 + 29\rho_2^2 + 17\rho_2,$$
$$\gamma_{5,7} = 3\rho_2^2 + 3\rho_2.$$

### 1.3 Values of $\bar{v}^s_{q0}$ for Policy 2

$$\bar{v}^s_{00} = \frac{\rho_1}{2\rho_1\rho_2 + \rho + 1}\Big[\frac{(1-\bar{s})^2 + \rho_2}{(\rho_1 - \bar{s})(1+\rho_1-\bar{s})^2(1+\rho-\bar{s})^2} + \frac{\rho_1^3 + \rho_1^2(3 - 2\bar{s} + \rho_2) + \rho_1((2-\bar{s})^2 + \rho_2(2-\bar{s}) - 1)}{(\rho_1 - \bar{s})(1+\rho_1-\bar{s})^2(1+\rho-\bar{s})^2}\Big].$$

$$\bar{v}^s_{10} = \frac{\rho_1^2}{2\rho_1\rho_2 + \rho + 1}\Big[\frac{\rho_1^3(\rho_2 + 1 - \bar{s}) + \rho_1^2\alpha_{1,1} + \rho_1\alpha_{1,2} + (1-\bar{s})^3}{(1-\bar{s})(\rho_1-\bar{s})(1+\rho_1-\bar{s})^2(1+\rho_2-\bar{s})(1+\rho-\bar{s})} + \frac{(\rho_2+1)^2 - 3\rho_2\bar{s} - 1}{(1-\bar{s})(\rho_1-\bar{s})(1+\rho_1-\bar{s})^2(1+\rho_2-\bar{s})(1+\rho-\bar{s})}\Big],$$

where

$$\alpha_{1,1} = (\rho_2+2)^2 + 2(\bar{s}-2)^2 + 3(1-\rho_2) - 9,$$
$$\alpha_{1,2} = \rho_2^2(2-\bar{s}) + \rho_2(5 - 6\bar{s} + 2\bar{s}^2) + 3 - 7\bar{s} + 5\bar{s}^2 - \bar{s}^3.$$

$$\bar{v}^s_{20} = \frac{\rho_1\rho_2}{2\rho_1\rho_2 + \rho + 1}\Big[\frac{1 - 2\bar{s} + \rho_2}{(\rho_1 - \bar{s})(1+\rho_1-\bar{s})^2(1+\rho-\bar{s})} + \frac{\rho_1^3 + \rho_1^2(3 - 2\bar{s} + \rho_2) + \rho_1(3(1-\bar{s}) + \bar{s}^2 + (2-\bar{s}))}{(\rho_1 - \bar{s})(1+\rho_1-\bar{s})^2(1+\rho-\bar{s})}\Big].$$

$$\bar{v}^s_{30} = \frac{\rho_1^2\rho_2}{2\rho_1\rho_2+\rho+1}\Big[\frac{\rho_1^3(\rho_2+1-\bar{s})+\rho_1^2\alpha_{3,1}+\rho_1\alpha_{3,2}+(\rho_2+1)^2}{(\rho_1-\bar{s})(1-\bar{s})^2(1+\rho_1-\bar{s})^2(1+\rho_2-\bar{s})(1+\rho-\bar{s})}+ \frac{(1-\bar{s})^3-3\rho_2\bar{s}-1}{(\rho_1-\bar{s})(1-\bar{s})^2(1+\rho_1-\bar{s})^2(1+\rho_2-\bar{s})(1+\rho-\bar{s})}\Big],$$

where

$$\alpha_{3,1} = (\rho_2+2)^2+2(\bar{s}-1)^2-\bar{s}(3\rho_2+1)-3,$$
$$\alpha_{3,2} = \rho_2^2(2-\bar{s})+\rho_2(5-6\bar{s}+2\bar{s}^2)+3-7\bar{s}+5\bar{s}^2-\bar{s}^3.$$

$$\bar{v}^s_{40} = \frac{\rho_1^2\rho_2}{2\rho_1\rho_2+\rho+1}\Big[\frac{\rho_1^3+\rho_1^2(3-2\bar{s}+\rho_2)+\rho_1(3(1-\bar{s})}{(\rho_1-\bar{s})(1-\bar{s})(1+\rho_1-\bar{s})^2(1+\rho-\bar{s})} + \frac{\rho_2(2-\bar{s})+\bar{s}^2+1)+1-2\bar{s}+\rho_2}{(\rho_1-\bar{s})(1-\bar{s})(1+\rho_1-\bar{s})^2(1+\rho-\bar{s})}\Big].$$

### 1.4 Values of $\bar{v}^s_{q0}$ for Policy 3

$$\bar{v}^s_{00} = \frac{\rho_1}{2\rho_1\rho_2+\rho+1}\Big[\frac{\rho_1^2(1-\bar{s})(1+\rho_2)+\rho_1\bar{\alpha}_{0,1}+(1+\rho_2)^2}{(\rho_1-\bar{s})(1-\bar{s})(1+\rho_1-\bar{s})(1+\rho_2-\bar{s})(1+\rho-\bar{s})}+ \frac{\rho_2\bar{s}(\bar{s}-3)+(1-\bar{s})^3-1}{(\rho_1-\bar{s})(1-\bar{s})(1+\rho_1-\bar{s})(1+\rho_2-\bar{s})(1+\rho-\bar{s})}\Big],$$

where

$$\bar{\alpha}_{0,1} = \rho_2(\rho_2+3)+\rho_2\bar{s}(\bar{s}-3)+2(1-\bar{s}).$$

$$\bar{v}^s_{10} = \frac{\rho_1^2}{2\rho_1\rho_2+\rho+1}\Big[\frac{\rho_1^2\bar{\alpha}_{1,1}+\rho_1\bar{\alpha}_{1,2}+\rho_2^3+\rho_2^2(3-4\bar{s})}{(\rho_1-\bar{s})(1-\bar{s})^2(1+\rho_1-\bar{s})(1+\rho_2-\bar{s})^2(1+\rho-\bar{s})}+ \frac{\rho_2(3-8\bar{s}+6\bar{s}^2-\bar{s}^3)+(1-\bar{s})^4}{(\rho_1-\bar{s})(1-\bar{s})^2(1+\rho_1-\bar{s})(1+\rho_2-\bar{s})^2(1+\rho-\bar{s})}\Big],$$

where

$$\bar{\alpha}_{1,1} = (\rho_2+1)^2+\rho_2\bar{s}(\bar{s}-2)+(1-\bar{s})^2-1,$$
$$\bar{\alpha}_{1,2} = \rho_2^3+\rho_2^2(4-3\bar{s})+\rho_2(5-9\bar{s}+4\bar{s}^2-\bar{s}^3)+2(1-\bar{s})^3.$$

$$\bar{v}^s_{20} = \frac{\rho_1\rho_2}{2\rho_1\rho_2+\rho+1}\Big[\frac{\rho_1^2(\rho_2+1)+\rho_1(\rho_2^2+3\rho_2+2-\bar{s}(2\rho_2+3))+\rho_2^2}{(\rho_1-\bar{s})(1-\bar{s})(1+\rho_1-\bar{s})(1+\rho_2-\bar{s})(1+\rho-\bar{s})}+$$
$$\frac{\rho_2(2-3\bar{s})+1-3\bar{s}+2\bar{s}^2}{(\rho_1-\bar{s})(1-\bar{s})(1+\rho_1-\bar{s})(1+\rho_2-\bar{s})(1+\rho-\bar{s})}\Big],$$

$$\bar{v}^s_{30} = \frac{\rho_1^2\rho_2}{2\rho_1\rho_2+\rho+1}\Big[\frac{\rho_1^2\bar{\alpha}_{3,1}+\rho_1\bar{\alpha}_{3,2}+\rho_2^3+\rho_2^2(3-4\bar{s})}{(\rho_1-\bar{s})(1-\bar{s})^3(1+\rho_1-\bar{s})(1+\rho_2-\bar{s})^2(1+\rho-\bar{s})}+$$
$$\frac{\rho_2(3-8\bar{s}+6\bar{s}^2-\bar{s}^3)+(1-\bar{s})^2}{(\rho_1-\bar{s})(1-\bar{s})^3(1+\rho_1-\bar{s})(1+\rho_2-\bar{s})^2(1+\rho-\bar{s})}\Big],$$

where

$$\bar{\alpha}_{3,1} = (\rho_2+1)^2+\rho_2\bar{s}(\bar{s}-2)+(1-\bar{s})^2-1,$$
$$\bar{\alpha}_{3,2} = \rho_2^3+\rho_2^2(4-3\bar{s})+\rho_2(5-9\bar{s}+4\bar{s}^2-\bar{s}^3)+2(1-\bar{s})^3.$$

$$\bar{v}^s_{40} = \frac{\rho_1^2\rho_2}{2\rho_1\rho_2+\rho+1}\Big[\frac{\rho_1^2(\rho_2+1)+\rho_1(\rho_2^2+3\rho_2+2-\bar{s}(2\rho_2+3))}{(\rho_1-\bar{s})(1-\bar{s})^2(1+\rho_1-\bar{s})(1+\rho_2-\bar{s})(1+\rho-\bar{s})}+$$
$$\frac{(\rho_2+1)^2+3\rho_2-3\bar{s}+2\bar{s}^2}{(\rho_1-\bar{s})(1-\bar{s})^2(1+\rho_1-\bar{s})(1+\rho_2-\bar{s})(1+\rho-\bar{s})}\Big].$$

775. Ramesh Babu, Shashank (2021) The onset of martensite and auto-tempering in low-alloy martensitic steels

776. Kekkonen, Päivi (2021) Several actors, one workplace : development of collaboration of several actors inside and between the organisations

777. Vuolio, Tero (2021) Model-based identification and analysis of hot metal desulphurisation

778. Selkälä, Tuula (2021) Cellulose nanomaterials and their hybrid structures in the removal of aqueous micropollutants

779. Vilmi, Pauliina (2021) Component fabrication by printing methods for optics and electronics applications

780. Zhang, Kaitao (2021) Interfacial complexation of nanocellulose into functional filaments and their potential applications

781. Asgharimoghaddam, Hossein (2021) Resource management in large-scale wireless networks via random matrix methods

782. Kekkonen, Jere (2021) Performance of a 16×256 time-resolved CMOS single-photon avalanche diode line sensor in Raman spectroscopy applications

783. Borovkova, Mariia (2021) Polarization and terahertz imaging for functional characterization of biological tissues

784. de Castro Tomé, Mauricio (2021) Advanced electricity metering based on event-driven approaches

785. Järvenpää, Esko (2021) Yläpuolisen siltakaaren optimaalinen muoto

786. Lindholm, Maria (2021) Insights into undesired load factors at work now and tomorrow : findings from different professions and working conditions

787. Miettinen, Jyrki & Visuri, Ville-Valtteri & Fabritius, Timo (2021) Carbon-containing thermodynamic descriptions of the Fe–Cr–Cu–Mo–Ni–C system for modeling the solidification of steels

788. Tavakolian, Mohammad (2021) Efficient spatiotemporal representation learning for pain intensity estimation from facial expressions

789. Longi, Henna (2021) Regional innovation systems and company engagement in the Arctic context

Book orders:
Virtual book store
http://verkkokauppa.juvenesprint.fi

UNIVERSITY OF OULU P.O. Box 8000 FI-90014 UNIVERSITY OF OULU FINLAND

# ACTA UNIVERSITATIS OULUENSIS



ISBN 978-952-62-2990-4 (Paperback)
ISBN 978-952-62-2991-1 (PDF)
ISSN 0355-3213 (Print)
ISSN 1796-2226 (Online)

UNIVERSITY OF OULU